U.S.NRC
United States Nuclear Regulatory Commission
Protecting People and the Environment

NUREG/CR-7206
PNNL-23701

Spent Fuel Transportation Package Response to the MacArthur Maze Fire Scenario

Draft Report for Comment

Office of Nuclear Material Safety and Safeguards

AVAILABILITY OF REFERENCE MATERIALS IN NRC PUBLICATIONS

NRC Reference Material

As of November 1999, you may electronically access NUREG-series publications and other NRC records at NRC's Library at www.nrc.gov/reading-rm.html. Publicly released records include, to name a few, NUREG-series publications; *Federal Register* notices; applicant, licensee, and vendor documents and correspondence; NRC correspondence and internal memoranda; bulletins and information notices; inspection and investigative reports; licensee event reports; and Commission papers and their attachments.

NRC publications in the NUREG series, NRC regulations, and Title 10, "Energy," in the *Code of Federal Regulations* may also be purchased from one of these two sources.

1. **The Superintendent of Documents**
   U.S. Government Publishing Office
   Mail Stop IDCC
   Washington, DC 20402-0001
   Internet: bookstore.gpo.gov
   Telephone: (202) 512-1800
   Fax: (202) 512-2104

2. **The National Technical Information Service**
   5301 Shawnee Rd., Alexandria, VA 22312-0002
   www.ntis.gov
   1-800-553-6847 or, locally, (703) 605-6000

A single copy of each NRC draft report for comment is available free, to the extent of supply, upon written request as follows:

Address: **U.S. Nuclear Regulatory Commission**
Office of Administration
Publications Branch
Washington, DC 20555-0001
E-mail: distribution.resource@nrc.gov
Facsimile: (301) 415-2289

Some publications in the NUREG series that are posted at NRC's Web site address www.nrc.gov/reading-rm/doc-collections/nuregs are updated periodically and may differ from the last printed version. Although references to material found on a Web site bear the date the material was accessed, the material available on the date cited may subsequently be removed from the site.

Non-NRC Reference Material

Documents available from public and special technical libraries include all open literature items, such as books, journal articles, transactions, *Federal Register* notices, Federal and State legislation, and congressional reports. Such documents as theses, dissertations, foreign reports and translations, and non-NRC conference proceedings may be purchased from their sponsoring organization.

Copies of industry codes and standards used in a substantive manner in the NRC regulatory process are maintained at—

The NRC Technical Library
Two White Flint North
11545 Rockville Pike
Rockville, MD 20852-2738

These standards are available in the library for reference use by the public. Codes and standards are usually copyrighted and may be purchased from the originating organization or, if they are American National Standards, from—

American National Standards Institute
11 West 42nd Street
New York, NY 10036-8002
www.ansi.org
(212) 642-4900

Legally binding regulatory requirements are stated only in laws; NRC regulations; licenses, including technical specifications; or orders, not in NUREG-series publications. The views expressed in contractorprepared publications in this series are not necessarily those of the NRC.

The NUREG series comprises (1) technical and administrative reports and books prepared by the staff (NUREG–XXXX) or agency contractors (NUREG/CR–XXXX), (2) proceedings of conferences (NUREG/CP–XXXX), (3) reports resulting from international agreements (NUREG/IA–XXXX), (4) brochures (NUREG/BR–XXXX), and (5) compilations of legal decisions and orders of the Commission and Atomic and Safety Licensing Boards and of Directors' decisions under Section 2.206 of NRC's regulations (NUREG–0750).

DISCLAIMER: This report was prepared as an account of work sponsored by an agency of the U.S. Government. Neither the U.S. Government nor any agency thereof, nor any employee, makes any warranty, expressed or implied, or assumes any legal liability or responsibility for any third party's use, or the results of such use, of any information, apparatus, product, or process disclosed in this publication, or represents that its use by such third party would not infringe privately owned rights.

U.S.NRC
United States Nuclear Regulatory Commission
Protecting People and the Environment

NUREG/CR-7206
PNNL-23701

Spent Fuel Transportation Package Response to the MacArthur Maze Fire Scenario

Draft Report for Comment

Manuscript Completed: August 2015
Date Published: December 2015

Prepared by:
H. E. Adkins, Jr.[1], J. M. Cuta[1], N. A. Klymyshyn[1],
S. R. Suffield[1], C. S. Bajwa[2], K. B. McGrattan[3],
C. E. Beyer[1], and A. Sotomayor-Rivera[4]

[1]Pacific Northwest National Laboratory
P. O. Box 999
Richland, WA 99352

[2]International Atomic Energy Agency
Vienna International Centre
P.O. Box 100
A-1400 Vienna, Austria

[3]National Institute of Standards and Technology
Engineering Laboratory
100 Bureau Drive, Stop 8600
Gaithersburg, MD 20899-8600

[4]U.S. Nuclear Regulatory Commission

J. Piotter, NRC Project Manager

NRC Job Code J5710

Office of Nuclear Material Safety and Safeguards

COMMENTS ON DRAFT REPORT

Any interested party may submit comments on this report for consideration by the NRC staff. Comments may be accompanied by additional relevant information or supporting data. Please specify the report number **NUREG-7206** in your comments, and send them by the end of the comment period specified in the *Federal Register* notice announcing the availability of this report.

Addresses: You may submit comments by any one of the following methods. Please include Docket ID **NRC-2015-0207** in the subject line of your comments. Comments submitted in writing or in electronic form will be posted on the NRC website and on the Federal rulemaking website http://www.regulations.gov.

Federal Rulemaking Website: Go to http://www.regulations.gov and search for documents filed under Docket ID **NRC-2015-0207**. Address questions about NRC dockets to Carol Gallagher at 301-415-3463 or by e-mail at Carol.Gallagher@nrc.gov.

Mail comments to: Cindy Bladey, Chief, Rules, Announcements, and Directives Branch (RADB), Division of Administrative Services, Office of Administration, Mail Stop: OWFN-12-H08, U.S. Nuclear Regulatory Commission, Washington, DC 20555-0001.

For any questions about the material in this report, please contact: Joseph Borowsky, Thermal Engineer, 301-415-7507 or by e-mail at Joseph.Borowsky@nrc.gov.

Please be aware that any comments that you submit to the NRC will be considered a public record and entered into the Agencywide Documents Access and Management System (ADAMS). Do not provide information you would not want to be publicly available.

ABSTRACT

The U.S. Nuclear Regulatory Commission has established requirements for packaging and transportation of spent nuclear fuel assemblies under normal conditions of transport and for hypothetical accident conditions. Real-world accidents of greater severity are possible, but are of much lower probability, and the probability of such an accident involving a spent nuclear fuel (SNF) package is even lower. However, because of the potential consequences, the U.S. Nuclear Regulatory Commission has undertaken the examination of specific accidents to determine the potential consequences to an SNF package. The MacArthur Maze accident of April 2007, which did not involve SNF, was selected for evaluation because of the severity of the fire and the unusual structural consequences, in which the heat from the fire caused the overhead roadway segments to collapse onto the roadway where the fire was burning.

The General Atomics GA-4 legal weight truck transportation package was selected for this investigation. Based on fire modeling with the Fire Dynamics Simulator code, and physical examination of material samples obtained onsite, a bounding fire scenario was defined for this accident. The complex and dynamic fire conditions are represented as a fully engulfing pool fire at 2012°F (1100°C) prior to the overhead roadway collapse, and as a smaller and less severe fully engulfing pool fire at 1652°F (900°C) afterward.

Thermal models of the GA-4 package were constructed for the ANSYS and COBRA-SFS codes, to determine the response of the package to the fire scenario, including the long post-fire cooldown transient. Additional detailed structural and thermal-structural models were developed using ANSYS and LS-DYNA for the roadway and package, which showed that the falling overhead segments could impose only relatively innocuous loads on the stainless steel body and DU gamma shield, compared to the hypothetical accident conditions structural loading that the package is designed to withstand.

Thermal evaluations of the package response to this fire scenario predict that the peak cladding temperature would exceed the short-term limit of 1058°F (570°C) long before the end of the fire. Maximum cladding temperatures on all rods in the package are predicted to exceed this temperature limit in the course of the transient, and remain above this limit for several hours. The maximum peak cladding temperature in the transient is predicted to be in the range of 1350-1400°F (732-760°C), and occurs approximately 3 hours after the end of the postulated fire accident. Temperatures in the regions of the package seals exceed the seal material limits for most of the fire duration.

The FRAPTRAN-1.4 code was used to estimate a fuel rod burst rupture temperature of 1097°F (592°C). Together with the temperature histories of the fuel, this suggests that there is the potential for all rods in the package to rupture in this fire scenario. The package seals are assumed to fail. However, a detailed thermo-structural model showed that the lid closure bolts maintain a positive clamping force throughout the transient, thus limiting the release. Using conservative and bounding modeling assumptions, the total possible release was estimated at approximately one-fourth of the mixture A2. Since the regulatory limit is specified as an A2 quantity per week for accident conditions, the estimated release is below the prescribed limit for safety. Therefore this very conservative estimate indicates that the potential release from this package, were it to be involved in a fire accident as severe as the MacArthur Maze fire scenario, would not pose a risk to public health and safety.

TABLE OF CONTENTS

LIST OF FIGURES

LIST OF TABLES

EXECUTIVE SUMMARY

The U.S. Nuclear Regulatory Commission (NRC) has established requirements for packaging and transportation of spent nuclear fuel (SNF) assemblies under normal conditions of transport (NCT) and for hypothetical accident conditions (HAC). These requirements (10 CFR 71) conservatively bound fire conditions that an SNF package might credibly encounter. However, real-world accidents of greater severity are certainly possible, and the NRC has undertaken the examination of such accidents, to determine what the potential consequences might be for a spent nuclear fuel package. Two previous studies of transportation accidents, one resulting in a fire in a railroad tunnel (NUREG/CR-6886 2009) and one in a highway tunnel (NUREG/CR-6894 2007) were undertaken with three different SNF package designs. Based on conservative scenarios constructed from these real-world fire conditions, the results of these studies have shown that the design basis for SNF packages is sufficiently robust for them to survive such beyond-design-basis conditions without adverse consequences to public safety. In all cases evaluated, the modeling results showed that the various SNF packages would be expected to maintain required shielding for ionizing radiation, and also would maintain the integrity of the containment boundary sufficiently to limit potential release of radioactive material from the packages to within regulatory bounds for accident conditions.

The MacArthur Maze accident of April 29, 2007 was selected as a third study in this series of evaluations of real-world accidents because of the severity of the fire and the unusual structural consequences, in which the heat from the fire caused the overhead roadway segments to collapse onto the lower roadway where the fire was burning. Since this was a highway accident, the only type of SNF package that could potentially be involved would be a legal weight truck (LWT) package. The General Atomics GA-4 LWT transportation package was selected for this investigation, mainly because it can carry a relatively large payload for an over-the-road transportation package, and therefore the potential consequences of package failure could be more severe than for packages with smaller payload capacities. The GA-4 package is designed to transport up to four intact pressurized water reactor spent fuel assemblies, with a maximum total package decay heat load of 2.5 kW.

The MacArthur Maze accident involved a gasoline tanker truck and trailer that overturned and caught fire on the I-880 connector of the MacArthur Maze interchange in Oakland, CA. The fire lasted approximately 108 minutes, consuming the tanker's entire load of 8,600 gallons of gasoline. The heat from the fire caused two sections of the overhead I-580 freeway to collapse onto the lower roadway, the first falling at approximately 17 minutes into the fire, the second collapsing on only one end, and reaching its final configuration by about 37 minutes. Figure S.1 shows an image of the fire just prior to the collapse of the first overhead roadway section to fall. Figure S.2 shows the configuration of the collapsed roadway, in an image taken in daylight the next day, after the fire was out. (Note that these images were captured from opposite sides of the freeway, and therefore the left-right orientation of the sections of roadway is reversed in the two images.)

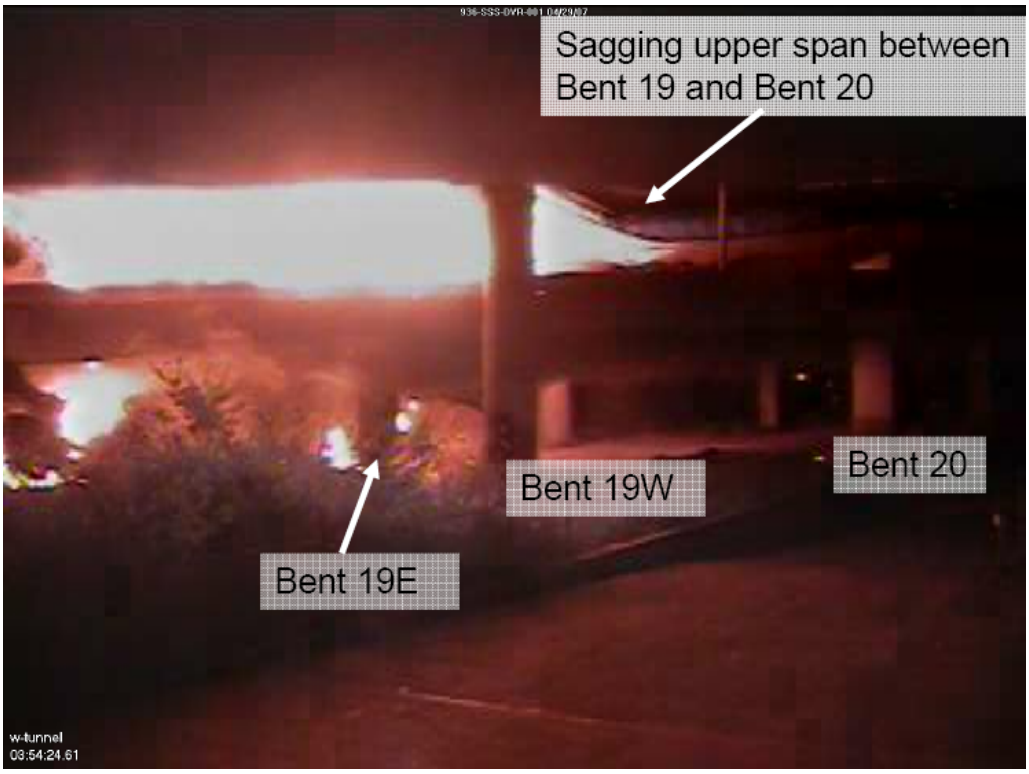

Figure S.1. MacArthur Maze Fire at +16.7 Minutes (WTP Video Image at 03:54:24.61 PDT, photo from MAIT Report, CHP 2007, reprinted with permission.)

Figure S.2. Roadway Configuration after the MacArthur Maze Fire (photo from MAIT Report, CHP 2007, reprinted with permission.)

Based on fire modeling with the Fire Dynamics Simulator (FDS) code, and physical examination of material samples obtained from the damaged highway girders and the remnants of the tanker truck, a bounding fire scenario was defined for the thermal and structural evaluations of the potential effects of this fire on an SNF package. The complex and dynamic fire conditions are represented as a fully engulfing pool fire at 2012°F (1100°C) prior to the overhead roadway collapse, and as a slightly smaller and less severe fully engulfing pool fire at 1652°F (900°C) after the roadway collapse. These temperatures represent conservative bounding values for open pool hydrocarbon fires for any possible configuration of both the pre-collapse and post-collapse fire pools in this accident.

As an additional simplifying conservatism in the definition of the scenario, it is assumed that the pre-collapse pool fire (at 2012°F [1100°C]) lasts for the full 37 minutes required for the completion of the collapse of the overhead segments. The smaller fire size is assumed as a step change to 1652°F (900°C), after 37 minutes, and this smaller pool fire is assumed to persist unchanged until the end of the fire, at 108 minutes. The fire scenario for modeling purposes also assumes that in the post-fire configuration, the fallen overhead roadway segment completely covers the SNF package, resulting in an additional barrier to heat transfer from the package during the cooldown phase of the transient.

Thermal and Structural Modeling Approach and Summary of Results

Detailed thermal models of the GA-4 package were constructed for the ANSYS and COBRA-SFS codes, for transient evaluations to determine the temperature response of the package to the fire scenario, including the long post-fire cooldown transient. Figure S.3 shows an exploded view of the GA-4 package, illustrating its main design features. Figure S.4 shows an axial cross-sectional diagram of the ANSYS model of the package.

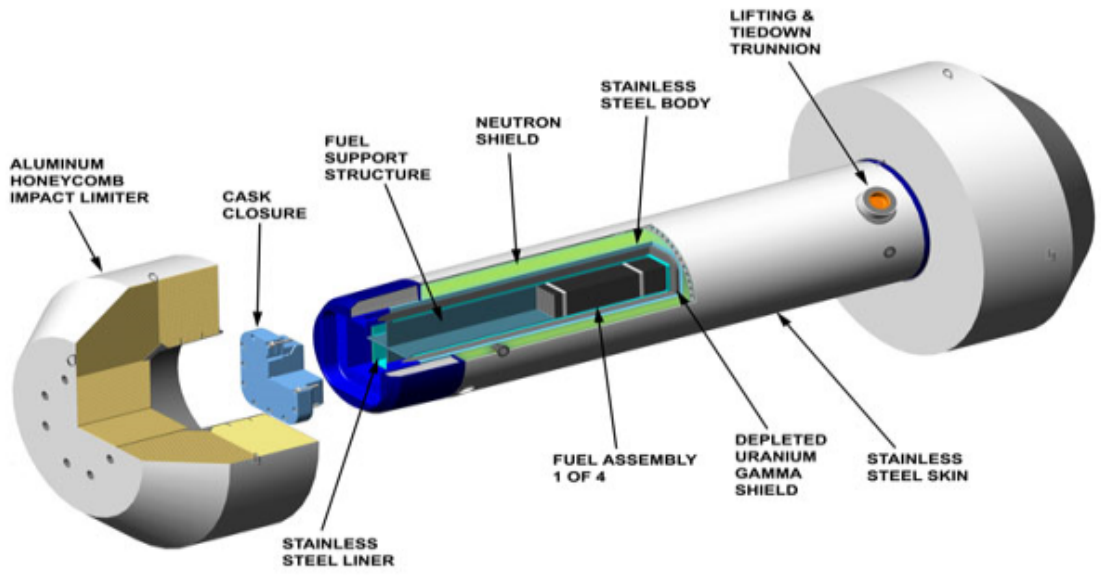

Figure S.3. GA-4 Package: Exploded View

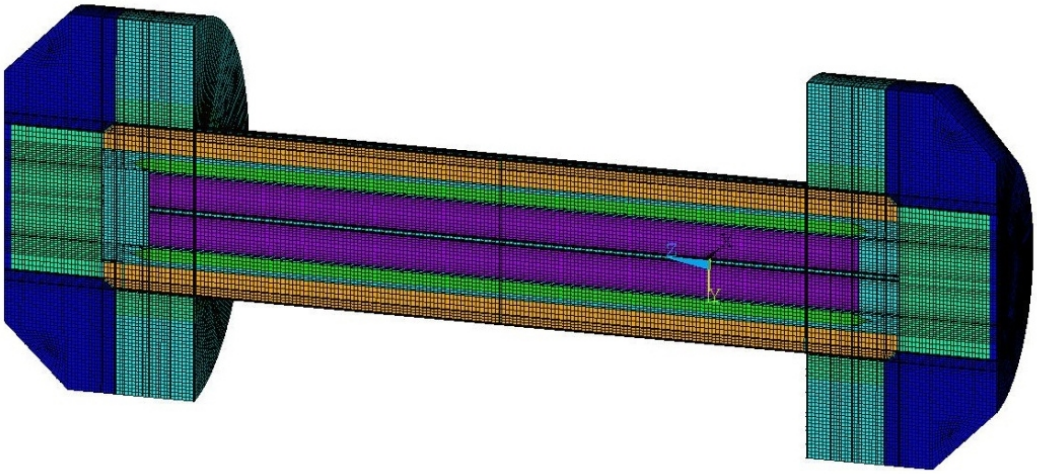

Figure S.4. Axial Cross-Section of ANSYS Model of GA-4 Package

Figure S.5 shows a cross-sectional diagram of the COBRA-SFS model of the package. The initial condition of the package at the start of the fire scenario was defined as steady-state NCT. Additional detailed structural and thermal-structural models were also developed using ANSYS and LS-DYNA for the roadway and package, for evaluation of the package response to the effect of the roadway falling on it.

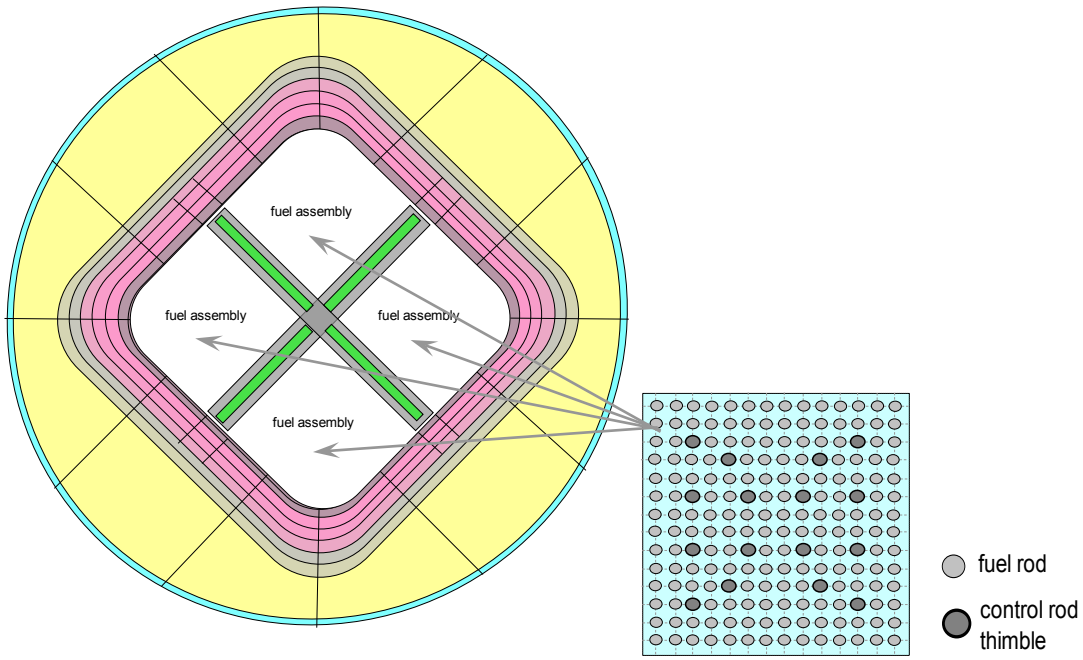

Figure S.5. Cross-Section of COBRA-SFS Model of GA-4 Package

Considerable effort was given to defining bounding and conservative estimates of the possible configurations of the package on the roadway that could produce the “worst case” structural loading of the SNF package due to the overhead roadway spans falling on it. However, the results of these evaluations clearly showed that the most adverse possible impacts of the overhead spans imposed relatively innocuous loads on the stainless steel body and depleted uranium (DU) gamma shield of the package, compared to the HAC structural loading that the package is designed to withstand. At a nominal fully loaded weight of approximately 55,000 lb (nearly 28 tons), the package itself falling from a height of 30 ft (9 meters) – the HAC package drop scenario (see 10 CFR 71) – would be expected to do far more damage, even with the added impact of the projecting “blades” of the steel girders.

The only real challenge of the overhead roadway drop in the fire scenario is that the impact is postulated to occur with the package at higher temperatures than are typically assumed in the structural analyses for HAC scenarios. (The HAC drop is postulated to occur before the HAC fire [10 CFR 71]). This could potentially make the package more vulnerable to structural damage, due to the reduction in the strength of steel with increasing temperatures. However, the steel girders of the overhead span suffer more from this effect, and the weight of the overhead roadway concrete is not sufficient to impart significant loading to damage the package in any way. Figure S.6 (a) and (b) illustrates the results of the most severe case of dropping the overhead roadway span onto the GA-4 package, and the resulting plastic strain in the package body wall.

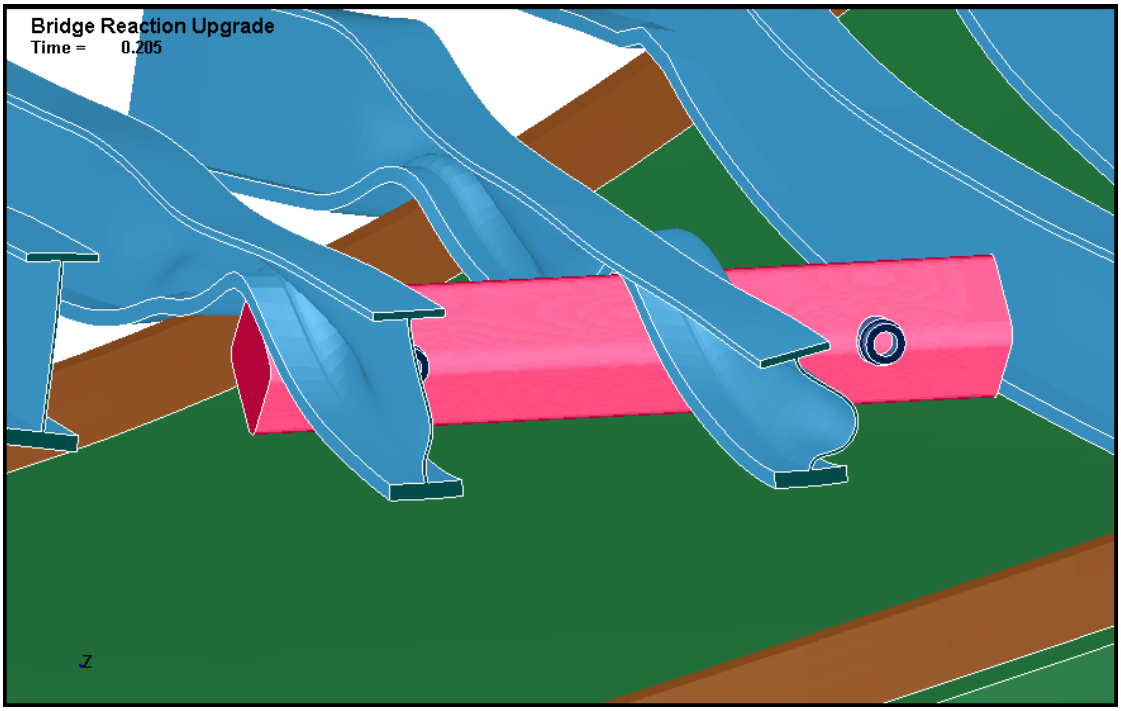

(a)

(Note: image of upper roadway shows girders only; concrete roadway omitted from image for clarity.)

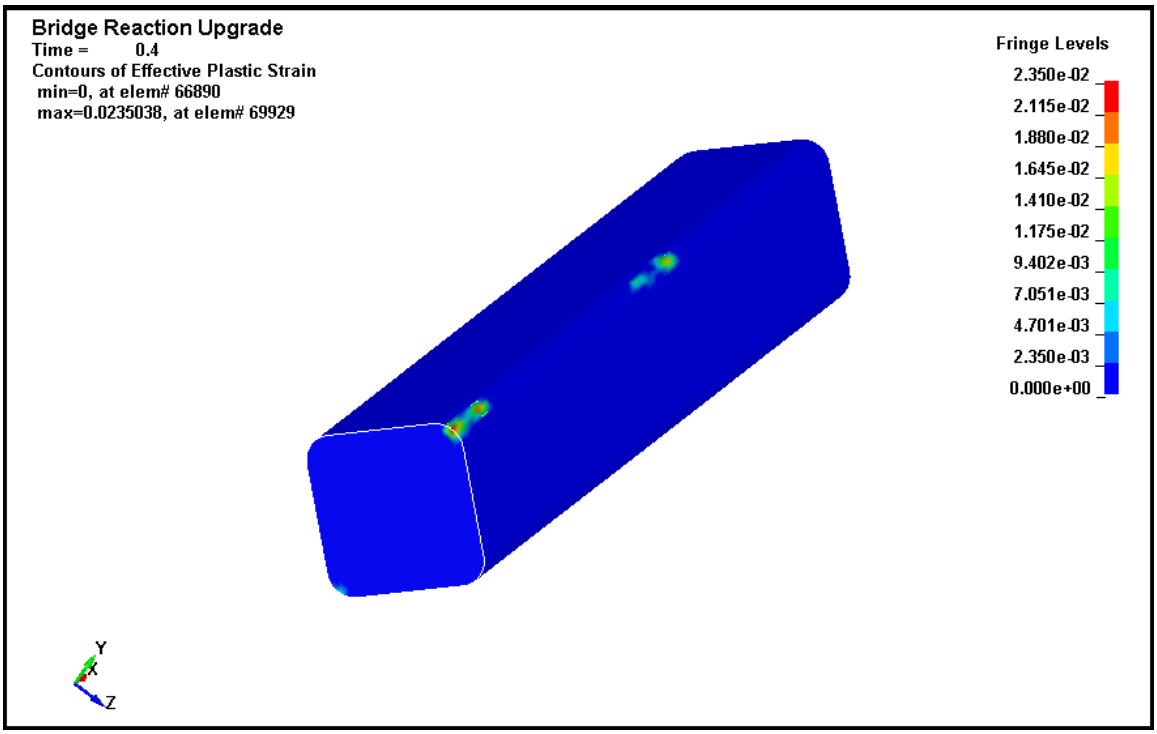

(b)

Figure S.6. Deformation of I-580 Span after Impact with Package Body, (a) Predicted Deformation Due To Impact of Upper Roadway on GA-4 Stainless Steel Body, and (b) Predicted Effective Plastic Strain in Package Body Wall

Much more interesting structural analyses were undertaken to investigate in detail the response of the bolts attaching the impact limiters to the package, and the package lid closure bolts. Complete evaluation of bolt performance was further complicated by the use of thread inserts in all bolt attachments in the package, in which helical coils of Type 304 stainless steel fill the interface between the bolt threads and the threaded holes in the package body. Differential thermal expansion of the Inconel bolts relative to the XM-19 stainless steel package body, and different strength-versus-temperature properties of the three metals involved, results in a time-and-temperature dependent history of force on the bolts that raised the possibility that the impact limiters might detach from the package. These material issues also raised the possibility that there could be a loss of clamping force between the lid and the package body during the post-fire cooldown. Figure S.7 illustrates the finite element analysis (FEA) model meshes constructed for detailed modeling of the impact limiter bolts and for the closure lid, flange and bolt structure, including thread inserts.

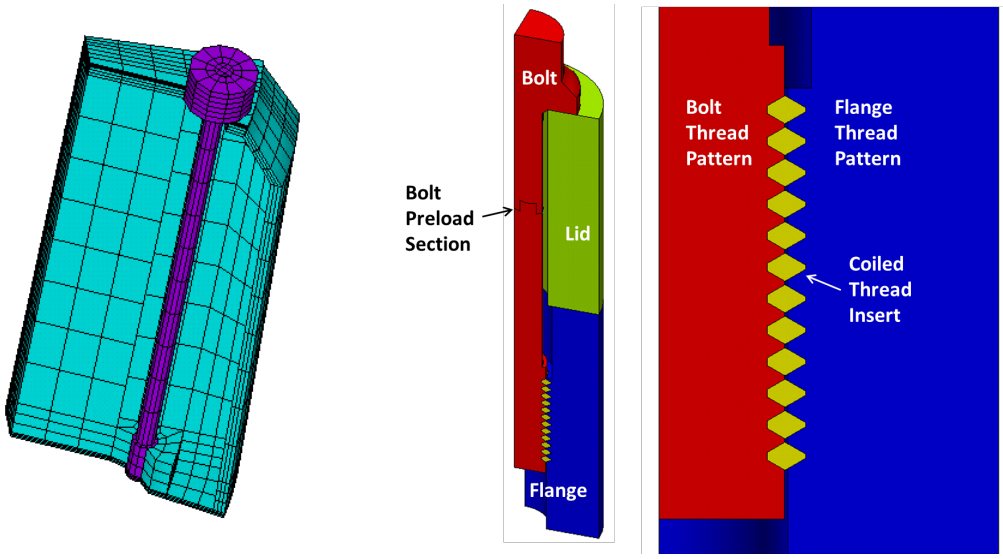

(a) (b)

Figure S.7. Detailed Model Mesh Diagrams for (a) Impact Limiter Bolt Evaluations with ANSYS and (b) Closure Lid Bolt Evaluations with LS-DYNA

Detailed evaluations of the structural and thermal response of the impact limiter bolts to the conditions of the MacArthur Maze fire scenario with FEA modeling using ANSYS show definitively that the impact limiter bolts will not fail under these conservative and bounding thermal and structural loading conditions. Loss of the impact limiters is not a credible consequence of this fire scenario for the GA-4 package. Additional detailed evaluations of the response of the lid closure bolts to the fire scenario undertaken with LS DYNA show unambiguously that the lid closure bolts maintain a positive clamping force between the package lid and body flange during all phases of the fire scenario, including the fire duration (108 minutes) and the very long cooldown period of approximately 400 hours, back to post-fire steady-state ambient conditions. This means that there is at all times forced metal-to-metal contact between the lid and the package body. This is particularly important to assessing the response of the GA-4 package to this fire scenario, because the thermal evaluations show that the seals exceed their rated temperature limits within the first hour or so of the transient. The metal-to-metal contact with positive clamping force constitutes the main containment boundary of the package in this scenario.

Thermal evaluations of the package response to this fire scenario predict that the peak cladding temperature would be expected to exceed the short-term limit of 1058°F (570°C) long before the end of the fire. Maximum cladding temperatures on all rods in the package are predicted to exceed this temperature limit in the course of the transient, and remain above this limit for several hours. In addition, the thermal inertia of the package and the insulating effect of the fallen overhead roadway, which is assumed to blanket the package during the post-fire cooldown means that fuel cladding temperatures continue to rise for many hours after the end of the fire. The insulating effect of the impact limiters, which shield the package ends from direct heating by the fire, results in the cooler ends of the rods continuing to heat up for several hours after the end of the fire, as heat in the hot central region of the rods redistributes throughout the package. Figure S.8 illustrates the thermal response of the package from the end of the fire to approximately 12 hours into the cooldown transient, which at that point is far from over.

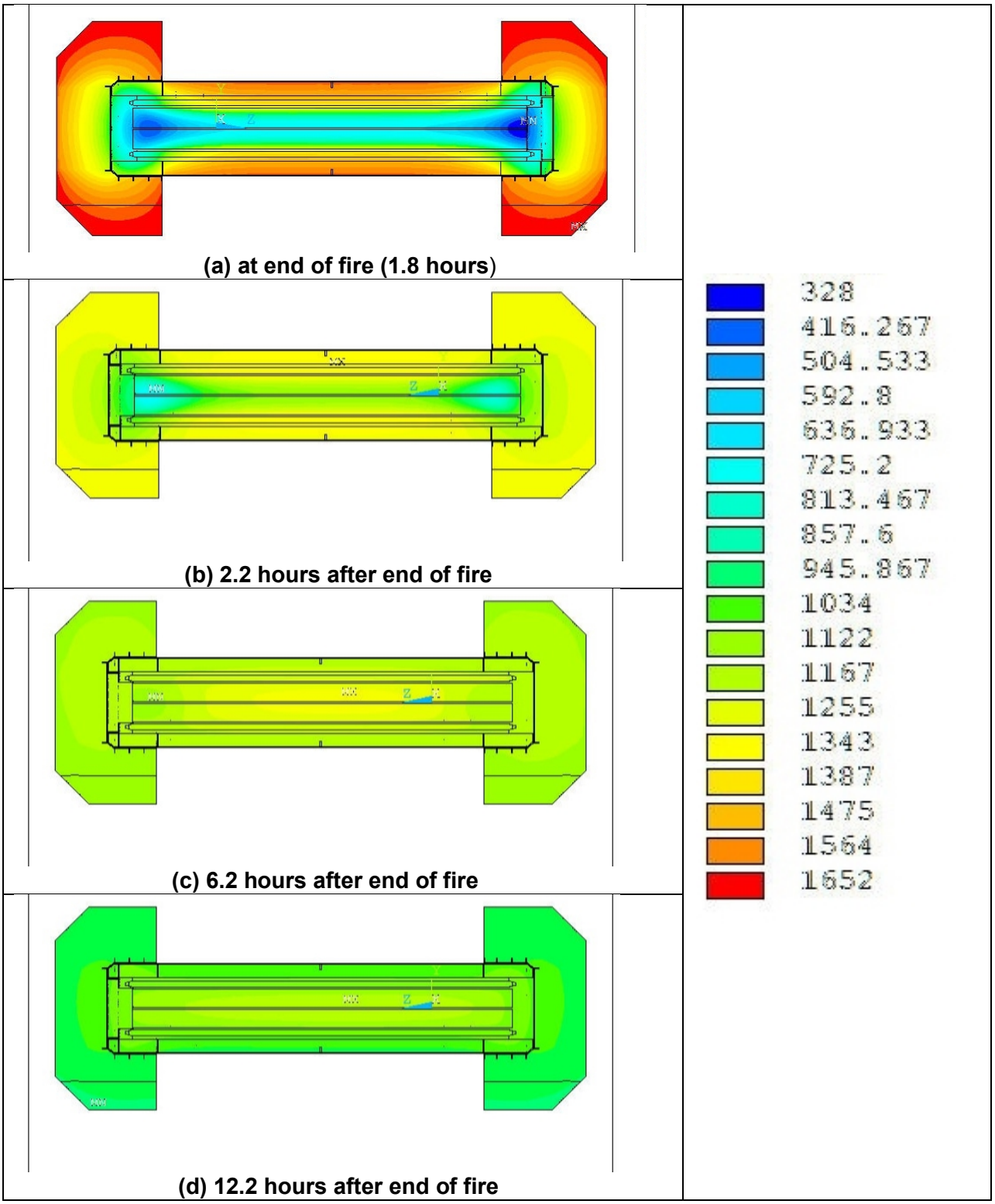

Figure S.8. ANSYS Model Predictions of Temperature Distributions (°F) in GA-4 Package during Post-fire Cooldown

The maximum peak cladding temperature in the transient is predicted to be in the range of 1350-1400°F (732-760°C), and occurs approximately 3 hours after the end of the fire. Based on the predicted fuel cladding temperatures from the COBRA-SFS modeling of the complete MacArthur Maze fire scenario, fuel performance was evaluated by direct comparison to fuel rod burst data as a function of cladding hoop stress and temperature. In addition to comparison to relevant data, predicted fuel rod rupture temperatures were obtained using the burst rupture model in the FRAPTRAN-1.4 code (NUREG/CR-7023 2011). Creep rupture is considered a possible alternative mechanism of failure for spent fuel rods. To evaluate this possibility, a separate analysis was performed with a creep rupture model, using the FRAPCON-3.4 code (NUREG/CR-7022 2011) in conjunction with the DATING code (Simonen and Gilbert 1988; Gilbert et al. 2002).

Fuel performance analyses for peak temperatures on the hottest rod in the MacArthur Maze fire scenario as predicted with the COBRA-SFS model, predict cladding rupture temperatures of 1097°F (592°C) using LOCA burst strain modeling (FRAPTRAN) and 1229°F (665°C) using creep rupture modeling (FRAPCON/DATING). Applicable experimental data (NUREG/CR-0344) yields measured rupture temperatures in the range 1205-1256°F (652-680°C). The burst rupture and creep rupture models both predict that the hottest fuel rod would rupture if subjected to the temperatures predicted in this fire scenario. Furthermore, the peak temperature on the hottest rod at the time of rupture is eventually exceeded by all rods in the package during the transient, which suggests that there is the potential for all rods in the package to rupture in this fire scenario.

Potential Radiological Consequences

Neutron and gamma radiation dose rates from the GA-4 package as a result of the postulated conditions of the MacArthur Maze fire scenario would not exceed the design basis of the package, which is well within the regulatory limits for hypothetical accident conditions. The neutron shielding is lost very early in the transient, but loss of the neutron shield tank is a design-basis assumption for this package in all HAC analyses. The more severe conditions of the MacArthur Maze fire can do no more damage to the GA-4 package neutron shield than is assumed *a priori* in the HAC analyses. The gamma shielding for the GA-4 is provided by a layer of DU within the stainless steel package body. The shielding function of this material is not affected by the higher temperature it is predicted to reach in the MacArthur Maze fire scenario. There is no credible scenario in this fire accident that could result in neutron and gamma dose rates from the design-basis GA-4 package exceeding the regulatory limits for accident conditions.

Loss of the package seals due to exceeding seal material thermal limits means that there is the potential for radioactive material to escape from the package. Rupture of all rods in the package, as is predicted by the fuel performance analyses, based on the calculated thermal response of the fuel, means that fission gases and fuel particulate would be released to the package cavity. In addition, the assumption of 100% spalling of CRUD from the external surfaces of the fuel rods is assumed for all accident conditions for SNF packages, per NRC guidance. Therefore, it must be assumed that there is material available in the package cavity that could be released through the failed seals. But because the lid closure bolts maintain positive clamping force throughout the transient, it is not physically possible for very much of it to actually escape. Conservative and bounding modeling assumptions yield an estimate of the

maximum possible release as 0.24 of the mixture A_2 quantity[1] determined for the design basis contents of the package. The HAC regulatory limit specifies a maximum allowable release *rate* of an A_2 per week. The estimated value is for the total potential release from the package in this scenario. This predicted release estimate is below the prescribed limit, and indicates that the potential release from this package in the MacArthur Maze fire scenario would not pose a risk to public health and safety.

[1] An A_2 quantity is defined in 49 CFR 173.403 as the maximum activity of a Class 7 (radioactive) material permitted in a Type A package, which does not require an accident resistant design. The amount of material that constitutes an A_2 quantity depends on its specific activity and other radiological properties. Appendix A of 10 CFR 71 specifies the specific A_2 quantities for a large number of radioactive materials, and defines methods for calculating values for materials not listed in the table. Spent nuclear fuel requires a Type B package, which can carry more than an A_2 quantity of radioactive material, but must retain the integrity of containment and shielding under normal conditions of transport (as per 49 CFR 173) and meet the release limits of less than an A_2 per week for hypothetical accident conditions.

ACKNOWLEGMENTS

This evaluation of the potential thermal and structural consequences to an SNF package of a transportation accident of the severity of the MacArthur Maze fire and highway collapse has been the work of many contributors over several years. The successful completion of this work has been due in large measure to Chris Bajwa, the NRC Project Manager initially guiding this effort, and who has continued to support and encourage the work after leaving NRC to work with the IAEA. The work of Kevin McGrattan (NIST), was an invaluable contribution, providing realistic assessment of the behavior of the fire itself, and defining the bounding fire scenario used in the analysis. The California Highway Patrol (CHP), in particular the members of the Multi-Disciplinary Accident Investigation Team (MAIT), provided invaluable assistance and detailed information, through personal communications and also in the detailed and comprehensive MAIT Report published by CHP describing the accident. CHP officers personally assisted the NRC in obtaining physical samples of fire-damaged girders, concrete, and truck remnants, used to provide direct estimates of temperatures reached in the fire. The work of Carl Beyer of PNNL, and his expertise related to nuclear fuel and cladding behavior under severe thermal and mechanical stresses that could lead to burst rupture was vital to the assessment of the potential consequences of exposing spent nuclear fuel to an accident of the severity of the MacArthur Maze scenario. The efforts of technical editors Colleen Winters, Cornelia Brim, and Susan Tackett were absolutely essential to making this work accessible, readable, and understandable to the wide audience for which it has been prepared.

ABBREVIATIONS AND ACRONYMS

ASME	American Society of Mechanical Engineers
AST	adiabatic surface temperature
ASTM	American Society of Mechanical Engineers
BCL	Battelle Columbus Laboratory
CFD	computational fluid dynamics
CG	center of gravity
CHP	California Highway Patrol
CNWRA	Center for Nuclear Waste Regulatory Analyses
CRUD	Chalk River Unknown Deposit, a generic term for corrosion and wear products (rust particles, etc.) that become radioactive (i.e., activated) when exposed to radiation.
DU	depleted uranium
FDS	Fire Dynamics Simulator
FEA	finite element analysis
FSS	fuel support structure
HAC	hypothetical accident conditions
I-580	Interstate 580
I-880	Interstate 880
IAEA	International Atomic Energy Agency
ILSS	impact limiter support structure
LOCA	loss-of-coolant accident
LWT	legal weight truck
MAIT	Multi-Disciplinary Accident Investigation Team
NCT	normal conditions of transport
NIST	National Institute of Standards and Technology
NRC	U.S. Nuclear Regulatory Commission
NS	neutron shield
ORNL	Oak Ridge National Laboratory
PWR	pressurized water reactor
SAR	safety analysis report
SARP	Safety Analysis Report for Packaging
SFST	Spent Fuel Storage and Transportation
SNF	spent nuclear fuel
TBq	Terabecquerel (SI unit for radioactivity; equal to 27 Curies (Ci))
WTP	East Bay Municipal Utility District Wastewater Treatment Plant

1.0 INTRODUCTION

Current U.S. Nuclear Regulatory Commission (NRC) regulations specify that spent nuclear fuel (SNF) transportation packages must be designed to survive exposure to a fully engulfing fire accident lasting no less than 30 minutes with an average flame temperature of "no less than 1475°F (800°C)" (10 CFR 71). The package[1] must maintain containment, shielding, and criticality functions throughout the fire event and post-fire cooldown in order to meet NRC requirements. The performance of spent fuel packages in severe accidents has been examined in previous studies by the NRC, as documented in NUREG-0170 (*Final Environmental Statement on the Transportation of Radioactive Material by Air and Other Modes*), NUREG/CR-4829 (*Shipping Container Response to Severe Highway and Railway Accident Conditions*, also known as the "Modal Study"), and NUREG/CR-6672 (*Re-examination of Spent Fuel Shipment Risk Estimates*). These studies evaluated a broad range of hypothetical transportation accidents involving collisions, fires, and collisions followed by fires. However, these studies did not specifically examine the effects of an actual transportation accident involving a severe fire that included a roadway collapse.

NRC has undertaken the examination of real-world accidents of greater severity than postulated in the hypothetical accident conditions (HAC) fire, to determine what the potential consequences might be, were such an accident ever to involve an SNF package. Two previous studies of transportation accidents have been performed; the first was of the 2001 fire in the Howard Street railroad tunnel in Baltimore, MD (NUREG/CR-6886 2009) and the second was of the 1982 fire in the Caldecott Tunnel on California State Route 24 near Oakland, California (NUREG/CR-6894 2007). Based on conservative scenarios constructed from these real-world fire conditions, the results of these studies have shown that the design basis for SNF packages is sufficiently robust for them to survive such beyond-design-basis conditions without adverse consequences to public safety. In all cases evaluated, the modeling results showed that the various SNF packages would be expected to maintain required shielding for ionizing radiation, and also would maintain the integrity of the containment boundary sufficiently to limit potential release of radioactive material from the packages to within regulatory bounds for accident conditions.

The MacArthur Maze accident of April 29, 2007 was selected as a third study in this series of evaluations of real-world accidents because of the severity of the fire and the unusual structural consequences, in which the heat from the fire caused the overhead roadway spans to collapse onto the roadway where the fire was burning. On April 29, 2007 at approximately 3:37 a.m., a tanker truck and trailer carrying 8,600 gallons (32,554 liters) of gasoline overturned and caught fire on the Interstate 880 (I-880) connector of the MacArthur Maze interchange located in Oakland, California. The intense heat from the fire weakened the steel girders of the Interstate 580 (I-580) roadway above the fire, collapsing two adjacent spans (approximately 156 feet [47.55 m]) of the elevated roadway onto the section of freeway below. A surveillance camera from the monitoring system of the East Bay Municipal Utility District Wastewater Treatment Plant (WTP) adjacent to the roadway captured a video of almost the entire fire duration. This video shows the first I-580 roadway span beginning to sag by about 10 minutes into the fire and collapsing completely at approximately 17 minutes. The video also shows a second span of the I-580 roadway descending slowly to the lower (I-880) roadway, beginning at about 17 minutes and reaching its final (partially collapsed) configuration by about 37 minutes. The video shows that the collapse of the second span greatly reduced the size of the fire, but it continued to burn

[1] The term "package" refers collectively to the contents (in this case spent nuclear fuel), and the protective enclosure into which the contents are placed.

intensely until about 102 minutes. As a fire management decision, the first responders on the scene allowed the fire to burn unchecked until the hydrocarbon fuel was fully consumed. At that point, the fire began to noticeably decrease in brightness, diminishing to a small glowing spot by approximately 108 minutes after the start of the fire. On the video, there is no visible glow from the fire after about 120 minutes.

Figure 1.1 shows a post-fire aerial view of the collapsed spans, extracted from the California Highway Patrol Multi-Discipline Accident Investigation Team (MAIT) report (CHP 2007). The staff of the NRC Division of Spent Fuel Storage and Transportation (SFST) undertook an investigation of the fire and roadway collapse to determine what impact this event might have on the risk associated with SNF transportation on public roadways. This evaluation included an assessment of the fire exposure temperatures of the upper roadway girders and tanker truck (NRC 2008), computational fluid dynamics (CFD) modeling of the open pool (pre-collapse) portion of the fire, and an analytical evaluation of the response of a representative NRC certified SNF transportation package to boundary conditions simulating temperatures predicted for the MacArthur Maze fire.

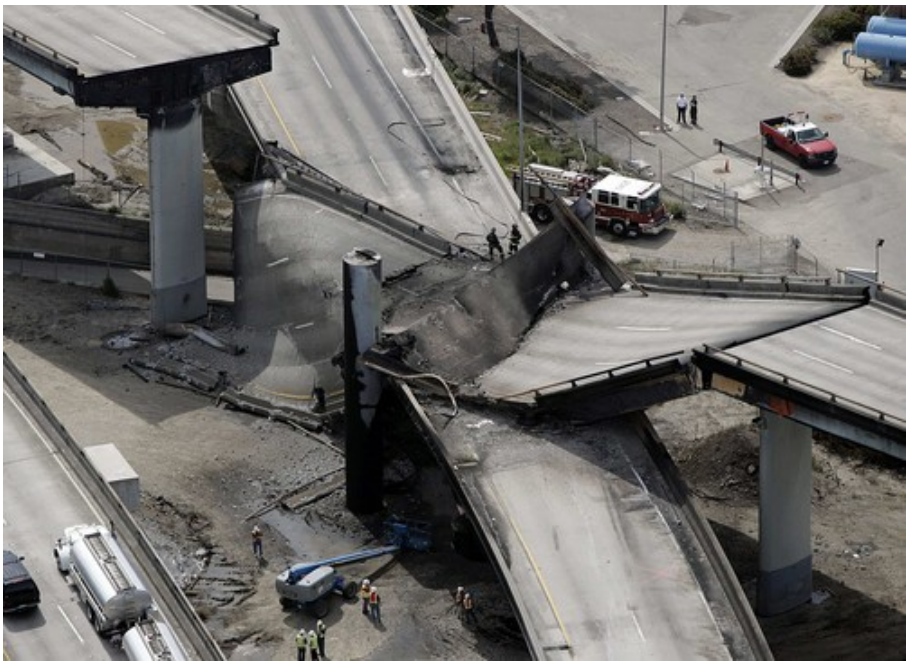

Figure 1.1. Roadway Configuration after the MacArthur Maze Fire (photo from MAIT Report, CHP 2007, reprinted with permission.)

This report provides a description of the analytical evaluation of the transportation package response and a detailed presentation of the results of the evaluation. Section 2.0 contains a summary description of the MacArthur Maze fire, and Section 3.0 describes the numerical modeling of the fire. Section 4.0 describes the fire scenario developed for this evaluation in detail, based on the known accident conditions and the numerical modeling of the fire. Analytical models of the SNF transportation package are described in Section 5.0. Section 6.0 presents the analytical approach, including detailed description of modeling assumptions. Analysis results are presented in Section 7.0. Section 8.0 addresses potential consequences of the fire scenario, with respect to the SNF transportation package. Results and conclusions of this study are summarized in Section 9.0, and references are listed in Section 10.0.

2.0 THE MACARTHUR MAZE FIRE

This section presents a detailed description of the fire and summarizes the results of analyses of material samples obtained to characterize temperatures reached by structures in or near the fire. Section 2.1 contains the fire description. Section 2.2 summarizes the analyses undertaken to determine estimates of peak temperatures reached in sampled materials from the roadway and tanker truck exposed to the fire.

2.1 Description of the MacArthur Maze Fire

Documentation of the MacArthur Maze fire is unusual in that nearly the entire fire duration was captured on video by the surveillance camera system of the nearby East Bay Municipal Utility WTP. The WTP video shows the rapid development of a large, openly burning fire on the I-880 roadway, ignition of ground fires below the roadway, the collapse of the overhead I-580 spans, and the post-collapse fire near Bent[1] 19. Key points in the fire duration are illustrated with video-capture images in Figure 2.1 through Figure 2.7.

Figure 2.1. MacArthur Maze Fire at +39 Seconds (WTP video image at 03:38:22.93 PDT, photo from MAIT Report, CHP 2007, reprinted with permission.)

[1] The term “bent” is used by the California highway authority (CalTrans) to refer to the structures consisting of a horizontal beam supported by two pillars, used to hold up elevated freeway segments.

The image in Figure 2.1 shows that the fire developed extremely rapidly, attaining nearly full size within minutes of a sudden bright flash from the direction of the freeway, which was captured in the video footage and occurs at 3:37 a.m. By the time the camera was turned to view the fire, approximately 10 seconds later, flame extended for nearly the full length of the lower roadway segment between Bent 18 and Bent 19, as shown in the video capture image in Figure 2.1. The east pillar of Bent 19 appears to be engulfed in flame below the level of the I-880 roadway, indicating that fuel is spilling off the roadway through the bridge scuppers for rainwater run-off near this location.

By approximately 7 minutes, the fire had reached full size, as illustrated in Figure 2.2. At this point, flame entirely fills the space between the upper and lower roadway and is impinging on the girders on the underside of I-580. In this image, brush on the ground below the roadway is burning vigorously, but the flames around the Bent 19E pillar have self-extinguished. The video shows that the fire configuration illustrated in Figure 2.2 persisted with little significant change until the collapse of the overhead roadway spans.

Figure 2.2. MacArthur Maze Fire at +6.8 Minutes (WTP video image at 03:44:31.96 PDT, photo from MAIT Report, CHP 2007, reprinted with permission.)

The sag in the span between Bent 19 and Bent 20[2] begins to be discernable in the video at about 9.3 minutes. Figure 2.3 shows the deep sag in the span at 16.7 minutes, moments before total collapse. (This image shows a rare glimpse of Bent 20, illuminated by the ground fires.)

[2] Bent 20 is generally not visible in the video images, mainly because of the camera angle; it is located to the right of Bent 19, from the perspective of the WTP.

Figure 2.3. MacArthur Maze Fire at +16.7 Minutes (WTP video image at 03:54:24.61 PDT, photo from MAIT Report, CHP 2007, reprinted with permission.)

Moments after the complete collapse of the span between Bent 19 and Bent 20, the roadway span between Bent 18 and Bent 19 was also visibly sagging, as can be seen in Figure 2.4. In this image, fire is no longer visible to the right of Bent 19 in the region of the fallen roadway. To the left of Bent 19, the sagging portion of the span between Bent 18 and Bent 19 is intruding into the fire, significantly affecting flame shape and distribution.

Figure 2.4. MacArthur Maze Fire at +19.8 Minutes (WTP video image at 03:57:33.19 PDT, photo from MAIT Report, CHP 2007, reprinted with permission.)

The slow gradual descent of the Bent 19 end of the second I-580 span to the lower roadway is clearly shown in the WTP video. The partial collapse of this span appears to be complete by 37.3 minutes into the fire, as illustrated in Figure 2.5. This image shows that the fire has self-extinguished in the region between Bent 18 and the point where the upper span contacts the roadway. The fire is confined to a relatively narrow region near Bent 19, between the ends of the two fallen I-580 spans.

Figure 2.5. MacArthur Maze Fire at +37.3 Minutes (WTP video image at 04:15:00.02 PDT, photo from MAIT Report, CHP 2007, reprinted with permission.)

The remainder of the WTP video shows that after the two upper roadway spans reached their final collapsed configurations, the fire continued to burn until the available fuel supply was consumed. Figure 2.6 shows an image of the fire at +72.3 minutes, and there is almost no change in brightness or configuration of the fire compared to the image in Figure 2.5 at +37.3 minutes. This behavior is observed on the WTP video until essentially the end of the fire. Figure 2.7 shows the relatively abrupt end of the fire, with an image captured at approximately +107 minutes.

Figure 2.6. MacArthur Maze Fire at +72.3 Minutes (WTP video image at 04:50:00.33 PDT, photo from MAIT Report, CHP 2007, reprinted with permission.)

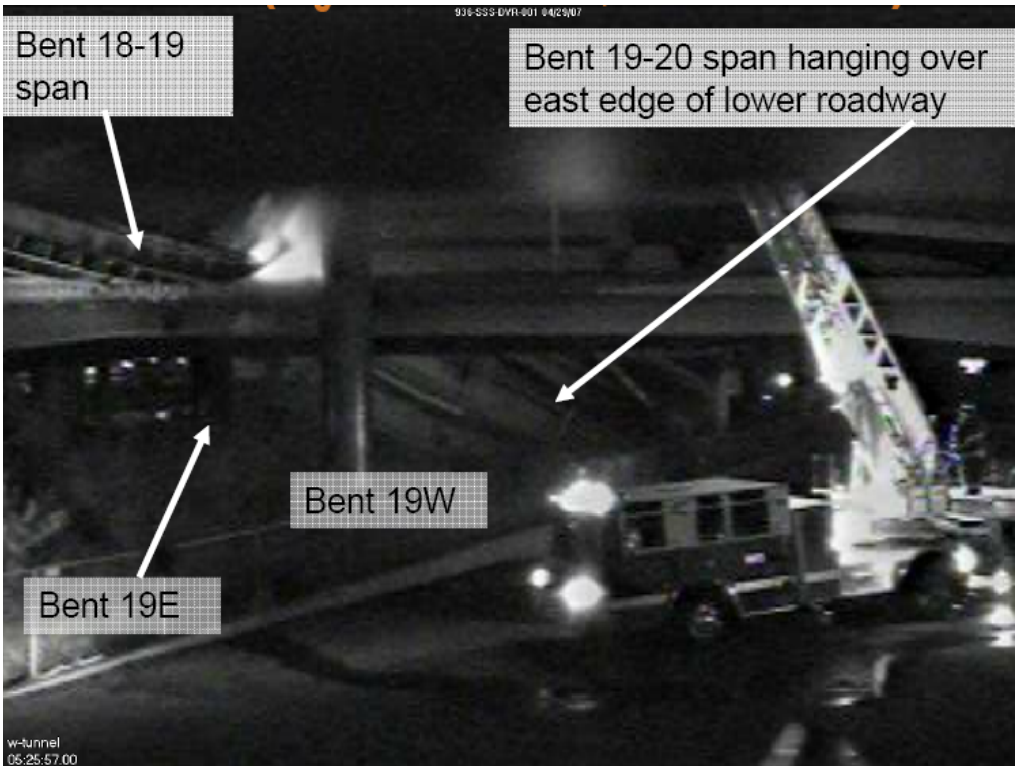

Figure 2.7. MacArthur Maze Fire at +107.3 Minutes (WTP video image at 05:25:57.00 PDT, photo from MAIT Report, CHP 2007, reprinted with permission.)

The WTP video shows that the fire characteristics changed significantly over the duration of the fire. Initially, there was a large, intense, openly burning fire because of the fuel spill. The relatively straightforward “open pool” nature of this portion of the fire was complicated by the presence of the I-580 roadway overhead, which partially confined and channeled the hot fire gases rising from the fire along the steel support girders on the underside of the upper roadway. This caused the fire to behave more like a very well ventilated tunnel fire than a classic open pool fire, and probably led to higher fire temperatures than would typically be obtained in an open pool fire of similar size.

The complete collapse of the overhead span between Bent 19 and Bent 20 at approximately 17 minutes, and the protracted partial collapse of the span between Bent 18 and Bent 19, beginning at about 18 minutes, resulted in a significant reduction in the overall fire size, while also substantially changing the configuration of the steel and concrete structures affected by the fire. By +18 minutes, the fire was extinguished on the I-880 roadway past Bent 19 in the direction of Bent 20, because of the fallen I-580 span. Beyond the contact point of the second partially fallen I-580 span, in the direction of Bent 18, the fire on the lower roadway was greatly reduced in size and intensity, and was completely extinguished in this region by +37 minutes into the fire. From that point on, the fire was confined to a narrow strip approximately 12-13 ft (5 m) wide along the roadway between the Bent 19 East and West pillars.

The WTP video shows very clearly what happened during the fire and provides evidence that can be used to bound specific features of the fire, but it cannot provide the detailed temperature information needed for analytical evaluations of the potential consequences of the fire. The following section discusses the results of evaluations to determine the temperatures reached by materials exposed to the MacArthur Maze fire.

2.2 Maximum Material Temperatures in the MacArthur Maze Fire

The dramatic failure of the steel girders supporting the upper I-580 roadway spans in the MacArthur Maze fire prompted early speculation in the media that the fire could have produced temperatures in excess of 3000°F (1650°C), the melting point of steel. This speculation failed to take into account two crucial factors: the maximum temperatures achievable in an open hydrocarbon-fueled pool fire, and the temperature-dependent nature of the strength of structural steel. Although there was considerable evidence of fire damage to the roadway structures in the post-fire investigations and clean-up, no evidence of melting of steel was found at any location.

Based on experimental and analytical evaluations of large pool fires (Society of Fire Protection Engineers 2008), a consistent estimate of the bounding flame temperature for these types of fires is approximately 1832°F (1000°C). Higher temperatures may be achievable if the fire is confined in a manner that does not restrict the flow of oxygen to the fire or remove significant heat from the fire by means of conduction or evaporation. However, the upper limit is only about 2462°F (1350°C), based on tunnel fire testing (Brekelmans et al. 2008; NFPA 2008). Section 3.0 presents a discussion of the results of modeling the open pool, pre-collapse portion of the MacArthur Maze fire using CFD with the Fire Dynamics Simulator (FDS) code (McGrattan et al. 2008), developed at the National Institute of Standards and Technology (NIST). The FDS analysis (as discussed in Section 3.4) predicts fire temperatures in the range 1472-1922°F (800-1050°C), with an overall peak of 1994°F (1090°C), at a location 3.3 ft (1 m) above the lower roadway surface and fully engulfed in the fire. These results show that a bounding value of 2012°F (1100°C) is a reasonable and conservative estimate of the flame temperature for the

open burning portion of the MacArthur Maze fire. Temperature estimates based on evaluation and testing of material samples obtained from the damaged roadway structures are somewhat lower than this bounding value.

These physically based bounding values for the fire temperatures show that the steel girders could not have melted at any point during the fire, and no evidence of melted steel was found in the post-fire evaluation and clean-up. An estimate of the approximate range of temperatures that the structures of the highway spans and the tanker truck were exposed to was obtained by evaluation of physical samples taken from the accident site (NRC 2008). These included samples of the structural steel girders, welds, surface paint and paint flakes, and selected materials from the remains of the tanker truck. Figure 2.8 illustrates the locations on the fallen roadway spans where physical samples were obtained for this evaluation. (Sample numbers correspond to numbering in Table 2.1.) Figure 2.9 shows the remains of the tanker truck at the accident site, labeling some of the few recognizable components from which material samples could be obtained.

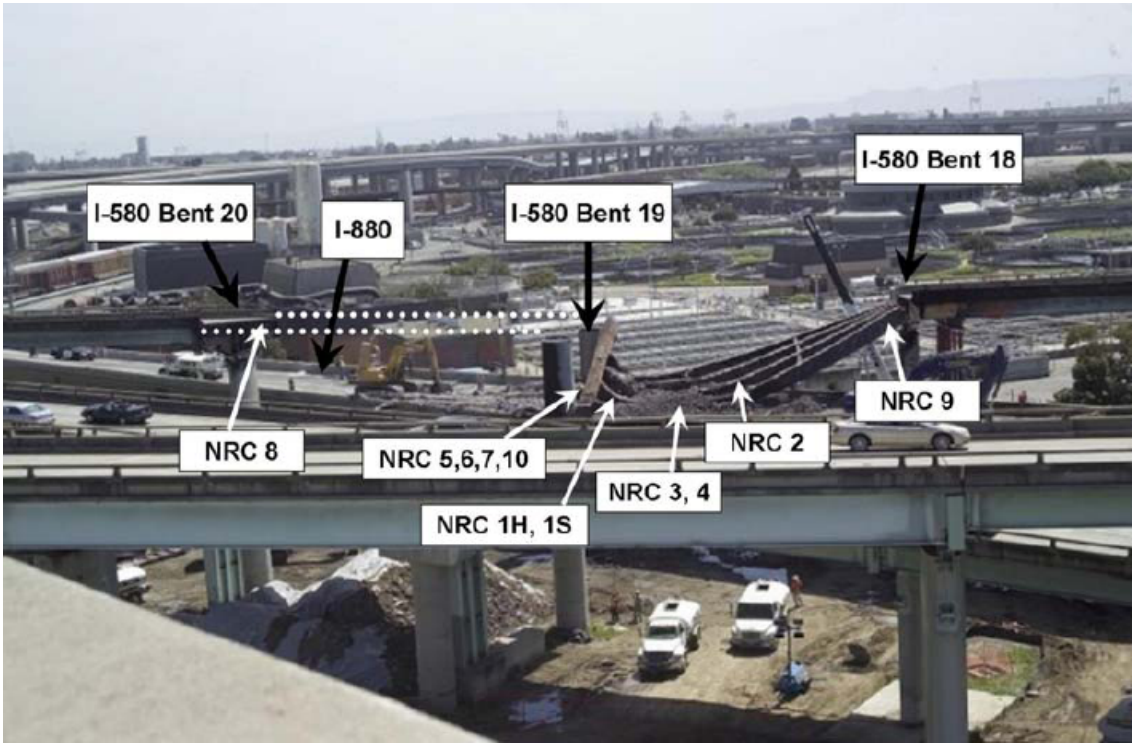

Figure 2.8. Approximate Locations of Collected Specimens for Materials Evaluation of Effects of MacArthur Maze Fire (photo from MAIT Report, CHP 2007, reprinted with permission.)

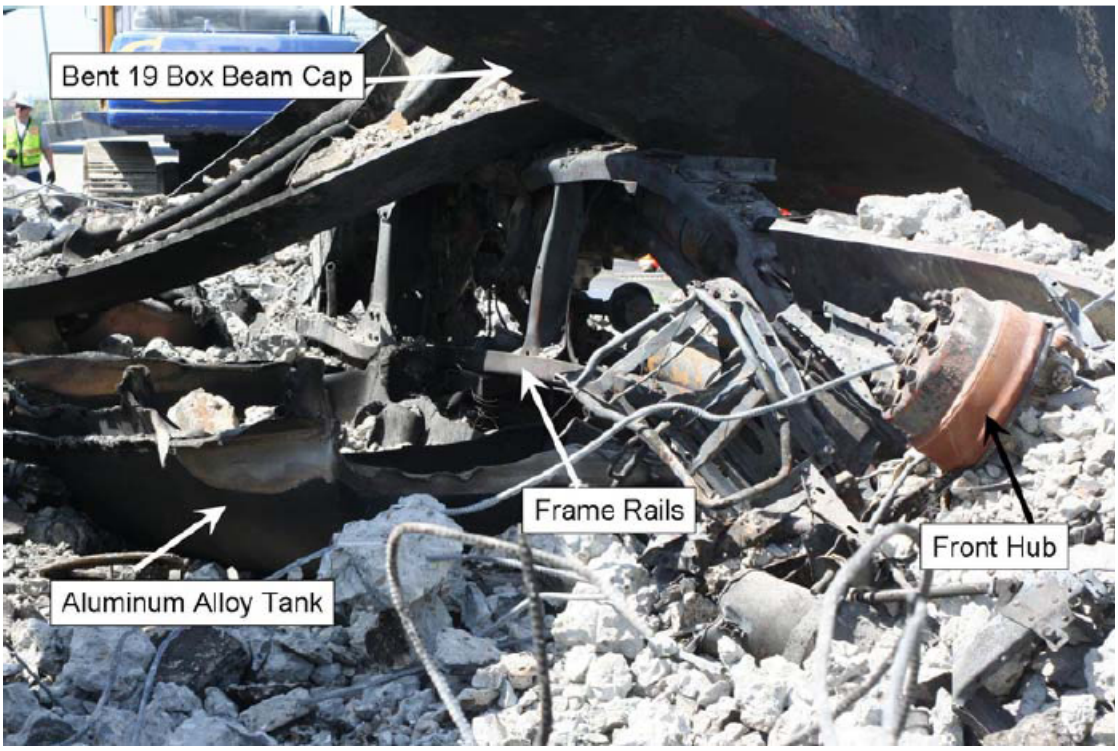

Figure 2.9. Approximate Locations of Collected Specimens Obtained from the Remains of the Tanker Truck Following the MacArthur Maze Fire (photo from MAIT Report, CHP 2007, reprinted with permission.)

Based on analysis of temperature-dependent physical changes in the materials examined, the maximum steel temperatures were estimated to be in the range 1796-1868°F (980-1020°C). Table 2.1 lists temperatures estimated from the condition of specific samples. These results indicate that material temperatures were generally below 1832°F (1000°C), and varied significantly with location in the fire. For example, there were unmelted segments of the tanker's aluminum tank, and only partial melting of at least one of the truck's aluminum wheels.

Table 2.1. Material Temperatures Estimated from Evaluation of Samples

Sample ID	Estimated Fire Exposure Temperature (°F)	Estimated Fire Exposure Temperature (°C)	Description of Sample Location
NRC 9	392	200	plate girder 12 with stiffener, near Bent 18 (no evidence of overheating)
	1292	700	from paint damage 10 ft from NRC-9
NRC 3	1652	900	Girder 5 (showing significant distortion of stiffener plate)
NRC 4	1562	850	Girder 5 (minimum temperature for sample)
NRC 5	572	300	Box Girder 7 lower plate with side and weld (portion of beam that fell on tanker truck)
NRC 7	752	400	rivet head in Box Girder 8; orange discoloration of paint
NRC 1S	1472	800	Plate Girder 3 with stiffener near Bent 19; with welds
NRC 10	752	400	flakes peeled off plate girder angles on Box Beam Cap 8
Truck S-13	1328	720	radiator (aluminum screen)

Table 2.1. (continued)

Sample ID	Estimated Fire Exposure Temperature (°F)	(°C)	Description of Sample Location
Truck S-6	1382	750	3 large bolts on frame near engine
Truck S-11	1292	700	brass fitting on engine
Truck S-12	1657	903	bolt on engine, passenger side (includes steel wire and melted aluminum)
Truck S-8, 9, 10	1094	590	copper (grounding strap on frame, battery cable, electrical system)
Truck S-17	1000	538	stainless steel mirror support bracket
Truck S-7	932	500	bolt on frame
Truck S-15	1328	720	aluminum tank section
	1058	570	unmelted tank segments

The material evaluations suggest that the steel girders experienced maximum temperatures in the range of 1472-1652°F (800-900°C) at locations where flames directly impinged on the girders. This is not sufficient to melt steel, but exposure to these temperatures would significantly reduce the strength of the load-bearing girders. Figure 2.10 shows the extremely rapid drop in yield strength beginning at about 800°F (427°C) for A36 steel (equivalent to the type of steel in the girders[3] supporting the I-580 roadway). The yield strength of this material at the estimated maximum temperatures experienced during the fire is less than 20% of its normal room-temperature value. With such a reduction in strength, the girders could not support the overhead spans.

[3] According to Caltrans reports *580 Damage – Preliminary Report (5-3-07)* and *580 Damage – Supplementary Report (5-15-07)*, (Caltrans tracking number CAL0422, from the Office of Structural Materials), as-built plans from the seismic retrofit project in 1994 indicate that the steel girders are ASTM A709 (Grade 50). The original as-built plans from 1953 specify ASTM A7. OSM tested girder samples to "ASTM A7 Spec." The ASTM web site (www.astm.org) shows A7 as "withdrawn 1967, replaced with A36/A36M."

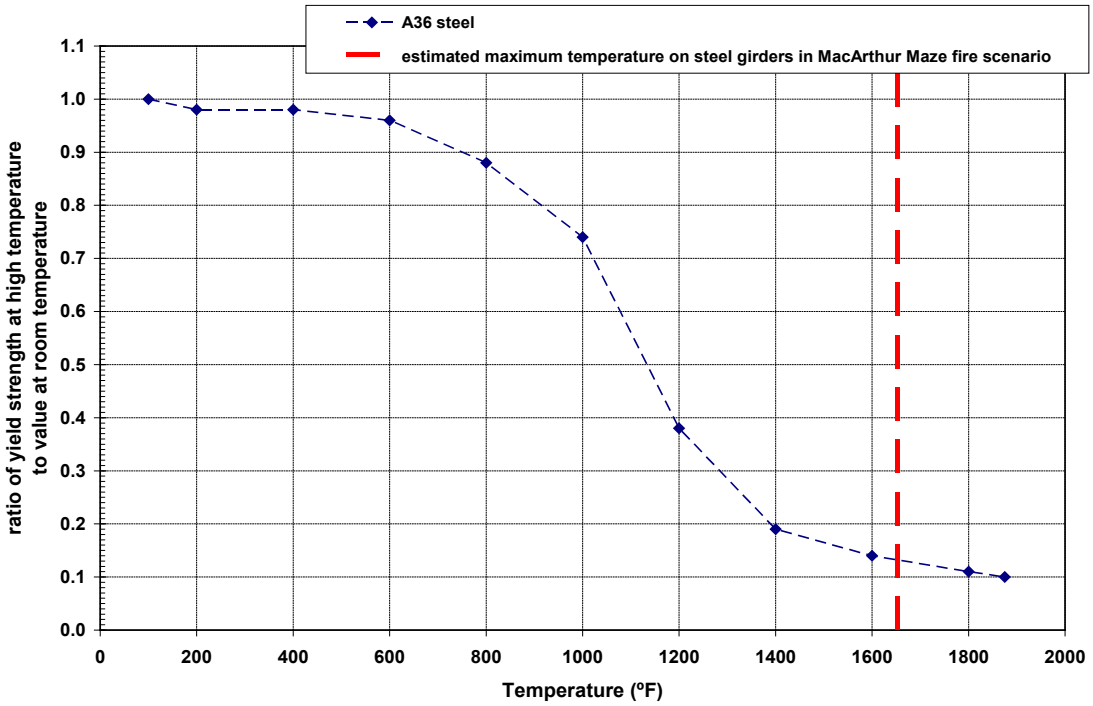

Figure 2.10. Typical Structural Steel Yield Strength Variation with Temperature (plot based on data from Brockenbrough and Merritt 1999.)

3.0 NUMERICAL MODELING OF THE MACARTHUR MAZE FIRE

This section describes numerical simulations of the MacArthur Maze fire using the FDS code, a computational fluid dynamics model developed specifically to study fire behavior (McGrattan et al. 2008). Various versions of the software were used during the development of the model. The final calculations were performed with FDS version 5.4.3.

A preliminary model of this fire was developed for NRC at the Center for Nuclear Waste Regulatory Analyses (CNWRA), Southwest Research Institute, San Antonio, Texas under contract NRC-02-07-006, and provided an initial scoping analysis of the fire. The model was then refined and final calculations were performed by NIST.

3.1 FDS Model Geometry

The computational domain of the model was initially defined as 131 ft wide by 197 ft long by 59 ft high (40 m by 60 m by 18 m). In subsequent refinement of the model, the height was doubled to 118 ft (36 m). Eight mesh blocks consisting of square cells 1.64 ft (0.5 m) or 0.82 ft (0.25 m) on a side divide the volume into uniform sub-volumes. Figure 3.1 shows the overall geometry of the model, in relation to the roadway configuration. Figure 3.2 and Figure 3.3 illustrate the simplified representation of structural components, including the roadways.

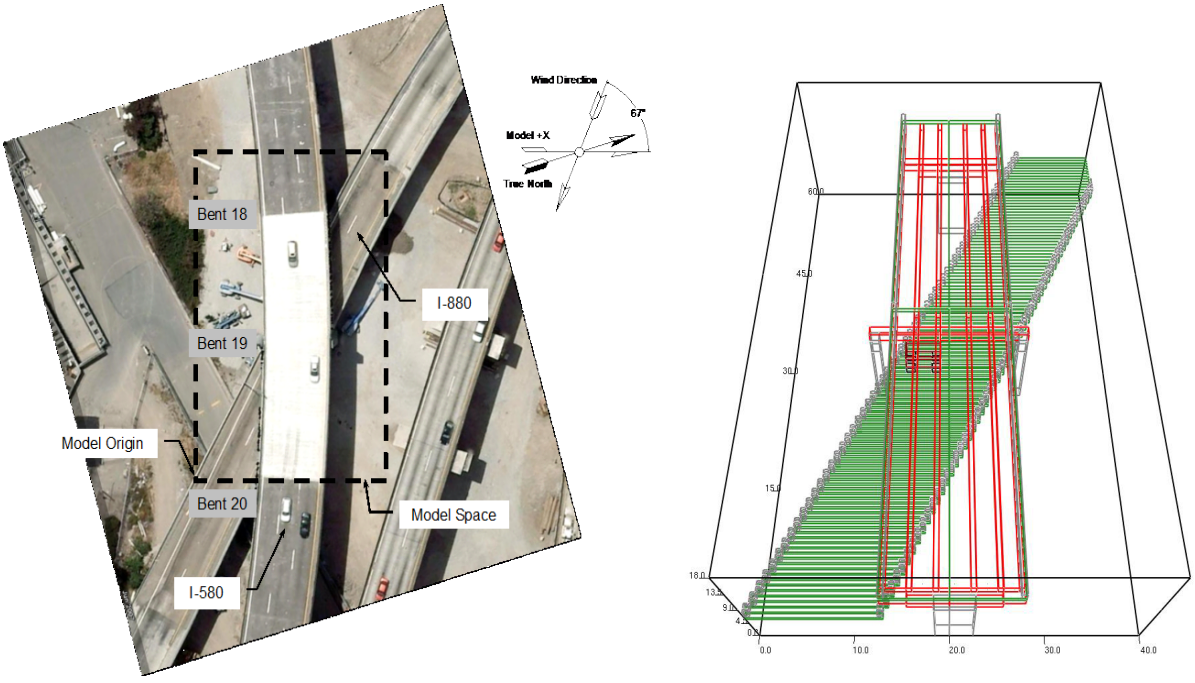

Figure 3.1. Simplified Model Geometry (photo from MAIT Report, CHP 2007, reprinted with permission.)

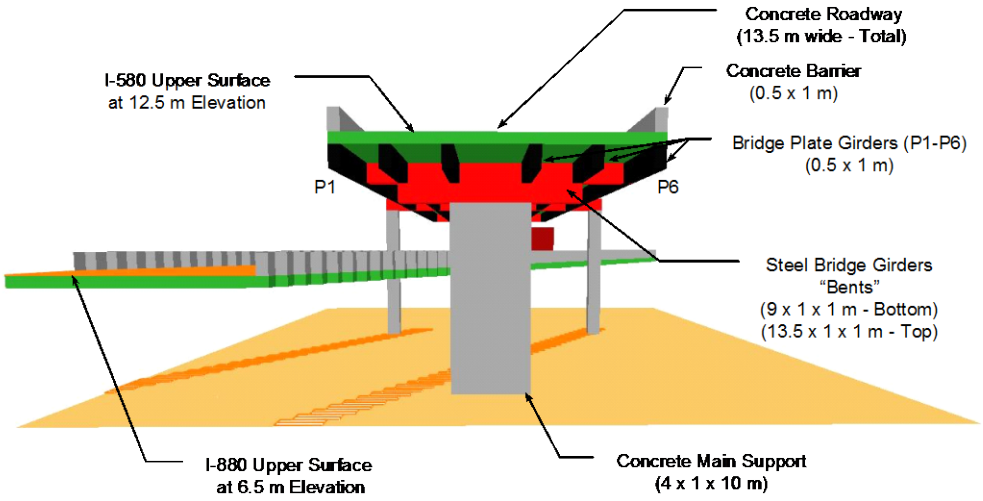

Figure 3.2. Transverse View of Model Geometry

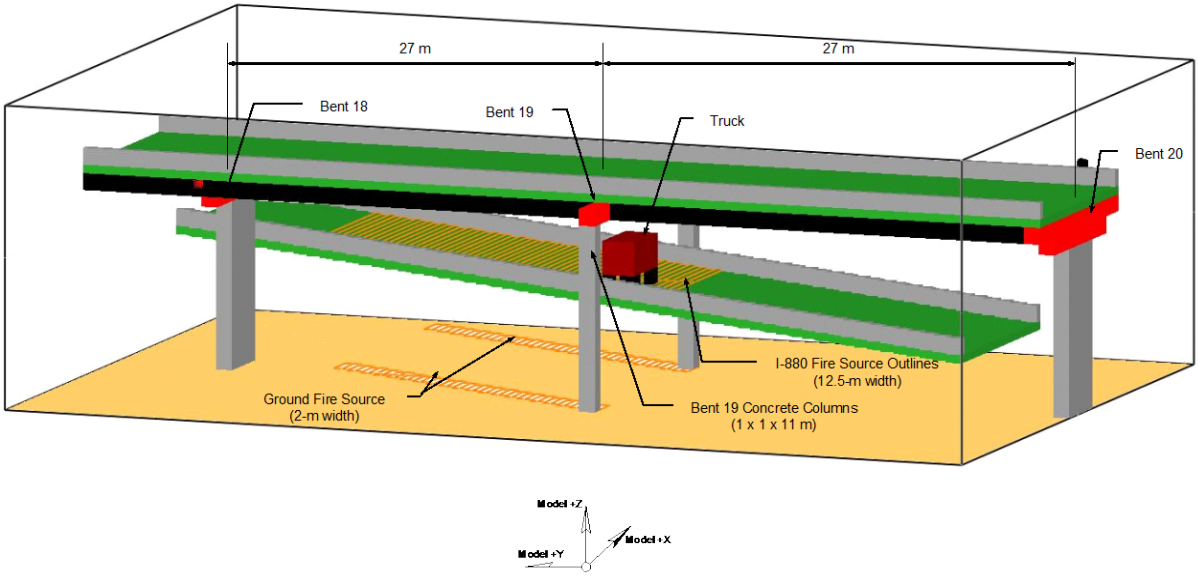

Figure 3.3. Longitudinal Views of Model Geometry

The location and size of the major structural components (e.g., girders and columns) were based on a review of documentary photographs and drawings, primarily from the MAIT report (CHP 2007). The dimensions of the roadway components were approximated to within 1.64 ft (0.5 m), due to of the relatively coarse numerical grid used in the model to solve the governing flow equations. The base model used 1.64 ft (0.5 m) resolution, and sensitivity studies were performed with a mesh resolution of 0.82 ft (0.25 m). All of the steel structural components were modeled with a 0.4 inch (1 cm) thickness at the surface, to allow the FDS code to provide estimates of surface temperatures of these components. As a conservatism in the fire modeling, the FDS code does not evaluate heat transfer within the structural interior of these structures, and therefore does not remove heat from the fire that would in reality be absorbed by them. A more detailed heat conduction calculation for the steel girders was performed with a finite-element model, as part of the development of appropriate boundary conditions for analysis of the structural collapse of the overhead spans. This analysis is discussed in Section 6.4.1.

The concrete roadways were represented in the FDS model as slabs 1.64 ft (0.5 m) thick. Each roadway included concrete side barriers modeled as 3.3 ft (1 m) high by 1.64 ft (0.5 m) thick. The tanker truck shown in the model diagrams was represented as a simple obstruction. The contribution to the fire of its combustible interior was considered negligible in comparison to that of the spilled gasoline, and was not included explicitly in the total heat release. In the model simulation, the fire was started by assuming that the truck was initially burning and radiating thermal energy to the road surface, which was covered with gasoline over the area defining the fuel pool. The fuel was assumed to begin burning when the local roadway temperature reached a specified threshold value of 140°F (60°C). This resulted in the fire spreading radially from the truck location, and encompassing the entire pool area in approximately 3 minutes. This gives a reasonable and conservative estimate of the development of the fire, since the WTP video shows that the fire reached full size within approximately 6 minutes.

3.2 FDS Model Fire

The WTP video shows that the fire was located mainly between Bent 18 and Bent 19, and extended some distance beyond Bent 19 in the direction of Bent 20. The extent of the fire across the width of the roadway could not be determined from the video, but post-fire examination of the I-880 roadway surface (Wiss, Janney, Elstner Associates, Inc. 2007) suggests that the fire probably spanned much of the width of the deck, as indicated by extensive spalling of the surface concrete. This is shown on the roadway diagram in Figure 3.4(a). Based on the spalling patterns and the video images, the modeled fire was assumed to span the full width of the roadway and extend from Marker 4 to Marker 12, as illustrated in Figure 3.4(b).

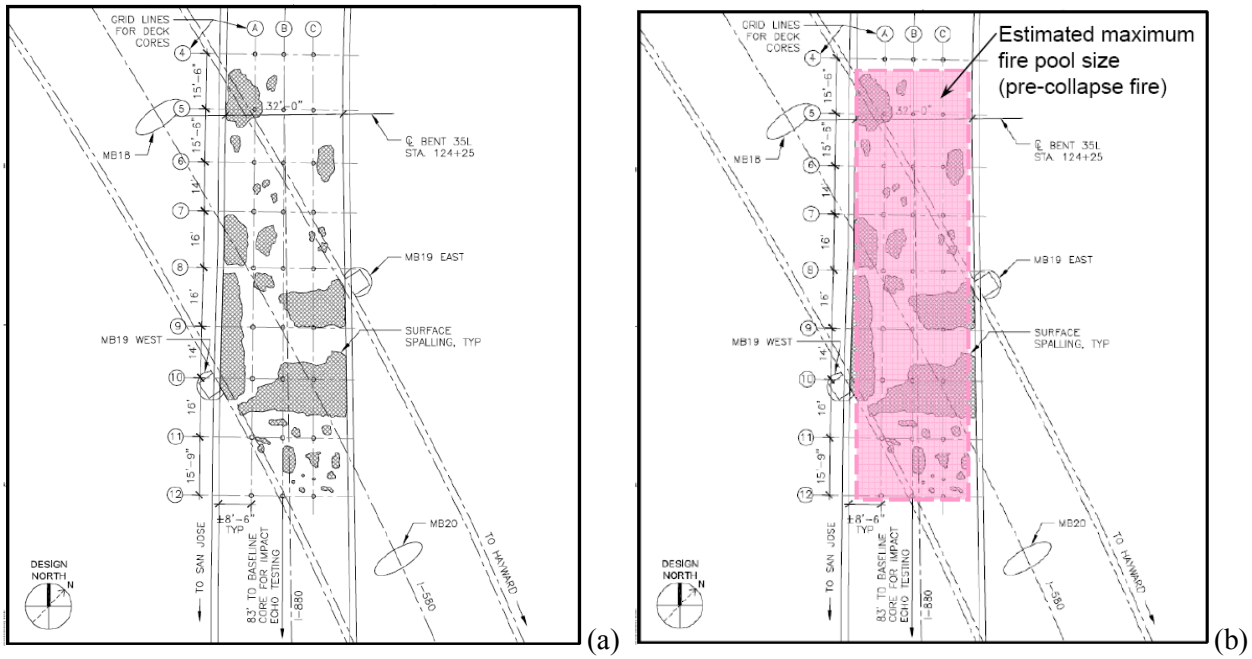

Figure 3.4. Maximum Fire Pool Size, Based on Areas of Concrete Spalling on I-880 Surface (Wiss, Janney, Elstner Associates, Inc. 2007, photo from MAIT Report, CHP 2007, reprinted with permission.)

Sensitivity studies were performed in which the area of the fire was increased to twice the estimated maximum size, and then decreased to half of this value. Depending on the specified burning rate, variations in the fire area changed the overall heat release rate of the fire, but

within the burning region, there was essentially no change in the predicted fire temperatures. In all cases, the calculations predicted that the upper roadway would be exposed to direct flame impingement during the pre-collapse portion of the fire. The results of these analyses indicate that within the range of uncertainty in the actual fire area, the characteristic temperatures do not change significantly with assumed fire size.

The total heat release rate for a fire is a function of the burning rate (i.e., mass loss rate, which is also a function of the availability of oxygen), fuel properties (including heat of combustion and density), and the geometry of the fire. Although the total amount of fuel consumed in the MacArthur Maze fire is known, the actual distribution of the fuel during the various phases of the fire is not known. Some fraction poured out over the I-880 roadway to create the large pool fire, some burned within the partially destroyed tanks of the truck and trailer, and some spilled off the roadway through the bridge scuppers to feed the ground fires. The ground fires burned vigorously and for much of the total fire duration, resulting in a considerable amount of spalling at the base of Column 35L supporting the I-880 roadway (Wiss, Janney, Elstner Associates, Inc. 2007), which is elevated approximately 6.5 m (21.3 ft) above the ground. The burning rate would have varied significantly with location, and it is therefore impossible to directly calculate the heat release rate for this fire.

The burning rate of the gasoline fire was estimated based on evaluations of burning rate for pools formed by realistic fuel spills on concrete[1] (Society of Fire Protection Engineers 2008), rather than prepared fuel pools in test tanks. The burning rate, or mass loss rate, can be as high as 0.045 kg/m^2/s to 0.065 kg/m^2/s for a deep gasoline pool fire larger than a few meters in diameter, but the depth of the fire pool is an important parameter. Shallow pools formed by liquid fuels spilled on concrete burn at approximately 0.01 kg/m^2/s, which is significantly lower than the burn rate of a deep pool carefully prepared for a fire experiment. During the MacArthur Maze fire, the depth as well as the extent of the pool formed by the gasoline spilling from the tanker varied both with location and time, and in addition, some amount of fuel was lost from the pool on the roadway as it spilled through the scupper drains.

Because of these unknowns, the heat release rate for the MacArthur Maze fire can only be approximated based on an average burning rate over the known fire duration and estimated fuel supply. Table 3.1 summarizes heat release rates for a range of burning rate values corresponding to different assumptions about the fire pool configuration. The heat release rates are calculated assuming a nominal effective heat of combustion of 43,700 kJ/kg (Society of Fire Protection Engineers 2002) for gasoline, which typically has a density of 760 kg/m^3. A value of 1000 kW/m^2 was chosen for the heat release rate specified in the final FDS calculations representing the initial 17-minute phase of the fire. This was based on the assumption that the depth of the spilled gasoline would have been relatively shallow over most of the roadway. Near the truck, however, the spill could have been deeper, resulting in a local burning rate for the gasoline that may have been greater than that of the rest of the pool. The value of 1000 kW/m^2 represents a conservative estimate for a large pool that could have deep spots, but for the most part is relatively shallow.

[1] Specifically, the chapter "Liquid Fuel Fires", by D.T. Gottuk and D.A. White, in *SFPE Handbook of Fire Protection Engineering*, 4th ed.

Table 3.1. Summary of Heat Release Rates for Large Pool Fires

Burning Rate	Heat Release Rate	Pool Characteristics
0.010 kg/m^2/s	437 kW/m^2	shallow pool; spill on concrete
0.0229 kg/m^2/s	1000 kW/m^2	estimated average for shallow pool with some deep spots
0.045 kg/m^2/s	2404 kW/m^2	deep pool; lower bound for burning rate
0.065 kg/m^2/s	2840 kW/m^2	deep pool; upper bound for burning rate

The assumed average burning rate of 0.0229 kg/m^2/s for the maximum estimated pool size was used for the entire fire duration of 108 minutes in the FDS simulation. This is a conservative assumption, since the fire would have consumed the entire 8,600 gallons of gasoline in about 54 minutes at this burning rate. In addition, the pre-collapse pool fire would have consumed about 5,900 gallons, or approximately 68% of the gasoline fuel supply, in the first 37 minutes (assuming no change in the pool size), leaving only 32% of the fuel for the remaining two-thirds of the total fire duration. This indicates that the average burning rate of 0.0229 kg/m^2/s, extended over the entire 108 minutes of the fire duration, is a conservative estimate of the average burning rate for the MacArthur Maze fire.

3.3 FDS Fire Model Output

The primary purpose of performing the FDS simulations was to determine appropriate temperature boundary conditions for evaluating the potential effect of the MacArthur Maze fire scenario on an SNF transportation package. A significant output of the fire model for this purpose is the quantity referred to as the adiabatic surface temperature (AST). This is a potentially misleading term, since the surface in this context is a virtual surface, not an actual physical surface in the model. The surface referred to in this term is a hypothetical thermal concept defined in fire temperature measurement calculations to represent a perfect, non-intrusive measurement at a specific location within the fire. An AST defines the source temperature at a given location in the fire for thermal radiation and convective heat transfer from flames and hot gases to actual solid surfaces that see the fire. An AST can be obtained for any point in the fire, and is determined in the manner described below.

The net total heat flux seen by an actual surface exposed to fire is composed of two components; thermal radiation and convection. This can be defined simply as:

$$q''_{tot} = q''_{rad} + q''_{con} \qquad (3\text{-}1)$$

where

q''_{tot} = net total local heat flux
q''_{rad} = local heat flux due to thermal radiation
q''_{con} = local heat flux due to convection

The thermal radiation term in Equation (3-1) is the difference between the absorbed incident thermal radiation and that emitted from the surface. The heat transmitted through the surface is neglected, and the absorptivity and emissivity are assumed equal, neglecting any dependence on wavelength. With these simplifications, the net heat received by the surface as thermal radiation can be written as:

$$q''_{rad} = \varepsilon (q''_{inc} - \sigma T_s^4) \tag{3-2}$$

where

q''_{inc} = incident thermal radiation heat flux
ε = emissivity of the surface
σ = Stefan Boltzmann constant
T_s = local surface temperature

The emissivity (or absorptivity) is a material property of the surface that can be determined by measurement. However, in most cases of structural materials exposed to fire, it can be assumed that the initial emissivity will change rapidly to a very high value due to sooting of the surface. A conservative estimate is 0.9 for highly sooted surfaces. A minimum value of 0.8 for absorptivity of exterior surfaces of an SNF package in the HAC fire is specified in 10 CFR 71.

Because fires are characterized by widely varying temperature distributions in space and time, the incident thermal radiation heat flux should ideally include all contributions from nearby flames, hot gases, and other surfaces. The incident thermal radiation may therefore be written as the sum of the contributions from all of the radiating sources:

$$q''_{inc} = \sum_i \varepsilon_i F_i \sigma T_i^4 \tag{3-3}$$

where

q''_{inc} = total local incident thermal radiation heat flux on a given surface from all sources
ε_i = emissivity of the i^{th} source surface
σ = Stefan-Boltzmann constant
F_i = dimensionless geometric viewfactor between the local surface and the i^{th} source surface
T_i = local surface temperature of the i^{th} source

FDS includes an algorithm for calculating the incident thermal radiation heat flux using Eq. (3-3), based on the local surface temperatures and the geometry of the mesh.

The convective heat flux depends on the difference between the surrounding gas temperature and the surface temperature, and on local fluid dynamics. The relationship between heat flux and temperature difference is generally characterized with a heat transfer coefficient, which is determined from an empirical heat transfer correlation, such that:

$$q''_{con} = h(T_g - T_s) \tag{3-4}$$

where

h = local heat transfer coefficient
T_g = gas temperature adjacent to the exposed surface
T_s = local surface temperature

Substituting Eq. (3-2) and Eq. (3-4) into Eq. (3-1), the total net heat flux to a surface can therefore be expressed as

$$q''_{tot} = \varepsilon(q''_{inc} - \sigma T_s^4) + h(T_g - T_s) \tag{3-5}$$

The relationship in Eq. (3-5) can be used to determine the AST at the location of an actual surface in the model. The "virtual" surface at this (and any other) location is by definition a perfect insulator, and since the total net heat flux to this idealized perfect insulator "surface" is by definition zero, Eq. (3-5) reduces to

$$\varepsilon(q''_{inc} - \sigma T_{AST}^4) + h(T_g - T_{AST}) = 0 \tag{3-6}$$

Numerically, the adiabatic surface temperature is a very useful quantity because it provides a natural interface between models that represent fire behavior and models that represent thermal and mechanical behavior of structures. A fire model in this context is any calculation method used to predict the temperature and species concentrations of a fire-driven flow. A structural model is any calculation method used to predict temperatures or stress/strain responses in an object exposed to the fire. The fire model may compute the evolving temperature of the bounding surfaces out of necessity, but it does not generally include a detailed representation of the thermal response of solid objects. Even a computational fluid dynamics model may only approximate a bounding solid as an infinitely thick slab for the purpose of estimating its surface temperature.

If the results of the fire model are to be used to perform a more detailed heat transfer calculation of the thermal response of a solid object within or near the fire, then some sort of interface is required to transfer information at the gas-solid interface. The most obvious quantity for this purpose is the heat flux at the surface, but in practice, this leads to major computational difficulties. The net heat flux to a surface computed by the fire model is dependent on the corresponding surface temperature, which is also computed by the fire model. Depending on the model, this surface temperature might not be of the desired accuracy. In addition, it is common in many popular solid phase heat transfer programs to input a prescribed thermal boundary based on external gas temperature and calculated surface temperature (as in Eq. 3-9) rather than as a prescribed heat flux. Both of these problems can be circumvented by using the adiabatic surface temperature T_{AST} as the intermediary between the fire and structural models.

The interface is fairly simple. At every surface point at which the fire model computes an incident thermal radiation heat flux and a corresponding gas temperature adjacent to that surface, the following implicit equation can be solved for the adiabatic surface temperature, assuming that the emissivity and convective heat transfer coefficient are effectively constant at that location.

$$\varepsilon(q''_{inc,FM} - \sigma T_{AST}^4) + h(T_{g,FM} - T_{AST}) = 0 \tag{3-7}$$

where

$q''_{inc,FM}$ = incident thermal radiation heat flux computed by the fire model at the exposed surface
$T_{g,FM}$ = gas temperature computed by the fire model adjacent to the exposed surface
T_{AST} = adiabatic surface temperature computed by the fire model

A key feature of Equation (3-7) is that the fire model does not require any assumptions to compute the incident thermal radiation heat flux. This equation merely serves as the definition of the adiabatic surface temperature, but it does not imply that the fire model calculates the heat flux in any particular way. Most importantly, it does not imply that the fire model uses a fixed heat transfer coefficient, *h*. The values of T_{AST} for any location in the fire model can be stored in a file according to a user-specified time interval and length increment appropriate for the application.

For the structural model, the heat flux to an object's surface and its temperature due to the fire conditions computed by the fire model can be calculated by the relationship:

$$q''_{tot,SM} = \varepsilon(q''_{inc,FM} - \sigma T_{s,SM}^4) + h(T_{g,FM} - T_{s,SM}) \quad (3\text{-}8)$$

Subtracting Eq. (3-8) from Eq. (3-7) yields the total net heat flux to the surface of an object as:

$$q''_{tot,SM} = \varepsilon\sigma(T_{AST}^4 - T_{s,SM}^4) + h(T_{AST} - T_{s,SM}) \quad (3\text{-}9)$$

where

$q''_{inc,FM}$ = incident thermal radiation heat flux computed by the structural model at the exposed surface
$T_{g,FM}$ = gas temperature computed by the structural model adjacent to the exposed surface
T_{AST} = adiabatic surface temperature computed by the fire model

The AST is interpreted by the structural model as an effective black body radiation temperature for the purpose of computing the incident thermal radiation at an actual surface in the structural model, and as a gas temperature for the purpose of computing the convective heat flux at the given surface. The advantage of this approach is that it requires transfer of only one quantity, the AST, from a fire model to a structural model, rather than bringing over a heat flux, surface temperature, and convective heat transfer coefficient. A side benefit is that the structural model need not be reconfigured to accept a heat flux as its boundary condition. It needs only to be modified to accept a temporally and spatially varying "exposing" temperature (i.e., the AST), which it can use to calculate the heat flux based on that temperature and the surface temperature calculated in the structural model. Most models of this type are already configured to accept a time-varying "exposing" temperature curve as an external boundary condition.

3.4 Fire Model Results for Pre-Collapse Configuration

The FDS analysis using the model described in Sections 3.1 and 3.2 was used to determine the fire behavior during the pre-collapse phase of the fire, which lasted approximately 17 minutes. This was the hottest and most intense portion of the fire, and would be expected to produce the most severe conditions for the thermal analysis of the effect of the fire on a SNF transportation package. The upper bound on the peak predicted temperatures from the FDS model during the first phase of the fire is in the neighborhood of 2012°F (1100°C). This is illustrated in Figure 3.5 with the predicted ASTs for a "target" object located 3.3 ft (1 m) above the roadway at a point in the fire near the final position of the tanker truck. The target is a rectangular block consisting of surfaces facing up, down, north, south, east, and west, and the temperature exposure for a given surface on this hypothetical object depends on orientation. The different curves of the plot are labeled in reference to the direction the surface faces. Figure 3.6 shows a similar plot of AST values for the same location at a higher elevation, approximately 3.3 ft (1 m) below the overhead girders.

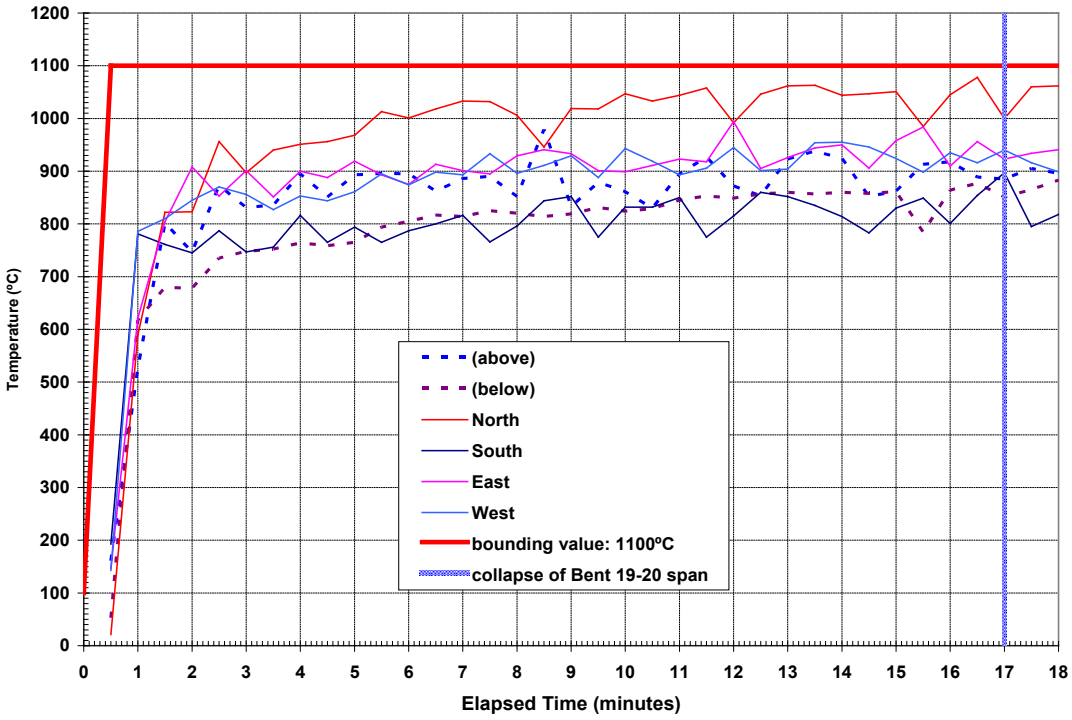

Figure 3.5. Predicted AST Values 1 Meter above the Lower Roadway Surface

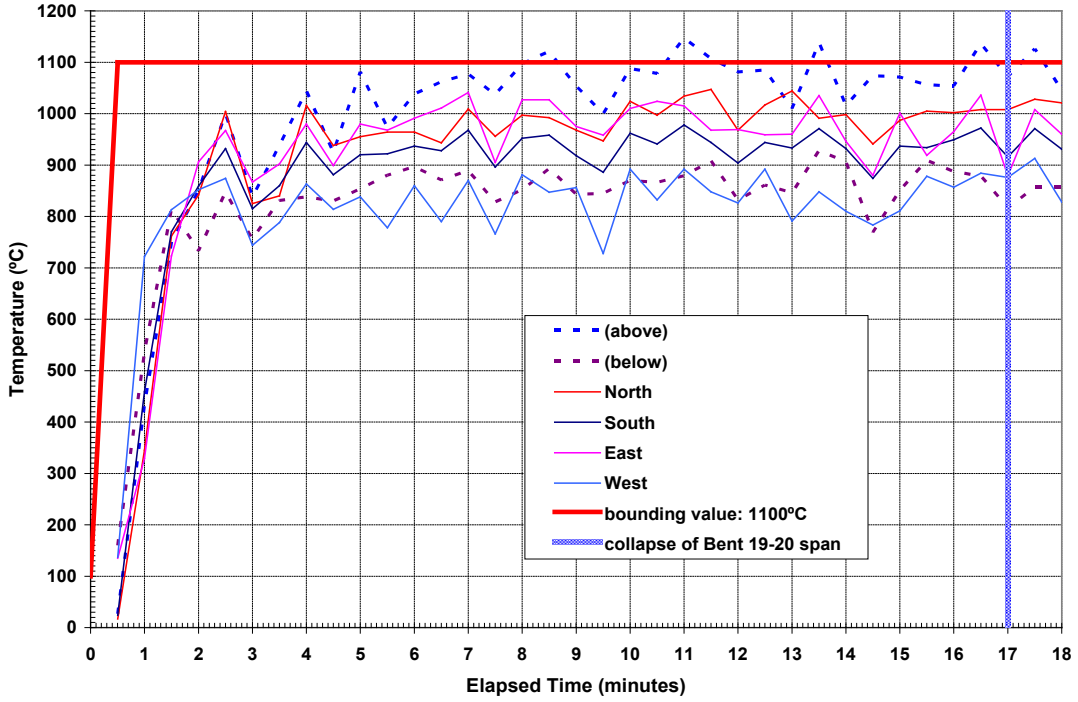

Figure 3.6. Predicted AST Values 3 Meters above the Lower Roadway Surface (1 meter below the Upper Roadway)

Based on these CFD analysis results and on material analyses of physical samples taken from the steel girders, roadway concrete, and remains of the destroyed tanker truck, (see discussion in Section 2.1), the initial portion the fire transient is conservatively bounded by a fully engulfing fire with uniform flame temperature of 2012°F (1100°C). The fire emissivity is assumed to be 0.9, which is characteristic of a sooty, optically dense hydrocarbon pool fire.

3.5 Bounding Assumptions for Post-Collapse Fire

In the MacArthur Maze fire, the collapse of the overhead spans greatly reduced the size and intensity of the fire. The abrupt fall of the span between Bent 19 and Bent 20 effectively extinguished the portion of the fire extending to the right of Bent 19. The slow descent of the Bent 19 end of the second span, which occurred over approximately 20 minutes, introduced this structure into the middle of the large pool fire on the lower roadway. The I-580 span eventually made contact with the lower roadway surface along a line extending approximately the full width of the roadway, at a distance of about 5 m (15 ft) from Bent 19. The effect of this intrusion was a fairly rapid decrease in the extent of the fire in the region beneath the descending roadway span. Within approximately 20 minutes (from 17 to 37 minutes after ignition), the fire was completely extinguished in the direction of Bent 18, and the extent of the fire was reduced to the gap between the fallen roadway spans near Bent 19. An estimate of the maximum fire area during this second phase is illustrated in Figure 3.7.

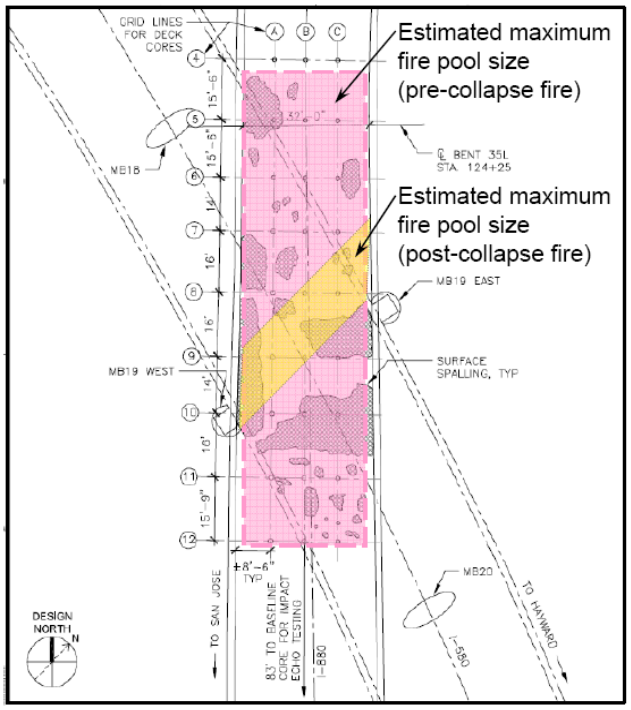

Figure 3.7. Estimated Fire Pool for Post-collapse Portion of the MacArthur Maze Fire

The area of this region is about one-fifth of the estimated maximum area of the first phase of the fire. CFD codes such as FDS generally do not have the capability to significantly alter the geometry of the physical structure of the fire environment or make large changes in the physical extent of the fire (other than changes caused by consuming available fuel.) The FDS analysis is not able to track the changing fire conditions during this portion of the fire, and estimates of the bounding fire temperature must rely on alternative methods.

The intrusion of the partially fallen span into the post-collapse fire would have the effect of wicking heat out of the fire, thereby reducing the flame temperature. In addition, the reduction in physical extent of the fire is sufficient to categorize this portion of the fire as only partially engulfing, which means that a large object (on the order of the size of a small automobile) would not be completely immersed in flames. In the parlance of thermal radiation heat transfer, it would "see" the colder surroundings. Experimental work has shown (Society of Fire Protection Engineers 2002)[1] that partially engulfing fires typically range from 1472°F (800°C) to 1652°F (900°C).

The post-collapse portion of the MacArthur Maze fire, therefore, is conservatively bounded by assuming a flame temperature of 1652°F (900°C). A further level of conservatism is added if the fire is assumed to be fully engulfing for a SNF transportation package. This approach neglects the effect of heat absorbed from the fire by the structural mass of the concrete roadways, and is a conservative and bounding representation of the fire behavior in this portion of the transient.

[1] Specifically, the chapter "Fire Hazard Calculations for Large, Open Hydrocarbon Fires," by Beyler, in *SFPE Handbook of Fire Protection Engineering*, 2nd ed.

The appropriate bounding temperature for the fire during the 20-minute transition from a large pool fire at 2012°F (1100°C) to a smaller pool fire at 1652°F (900°C) is not readily apparent from the information available on the MacArthur Maze fire. As a conservative simplification, this transition interval is modeled as if the large open pool fire had persisted for the full 20 minutes required for the partial collapse of the Bent 18-19 span, out to 37 minutes of the fire duration. At 37 minutes, the boundary temperature representing the fire is abruptly reduced from 2012°F (1100°C) to 1652°F (900°C), and remains at this value out to 108 minutes, to conservatively bound the end of the fire duration. These bounding fire temperatures are illustrated in Figure 3.8.

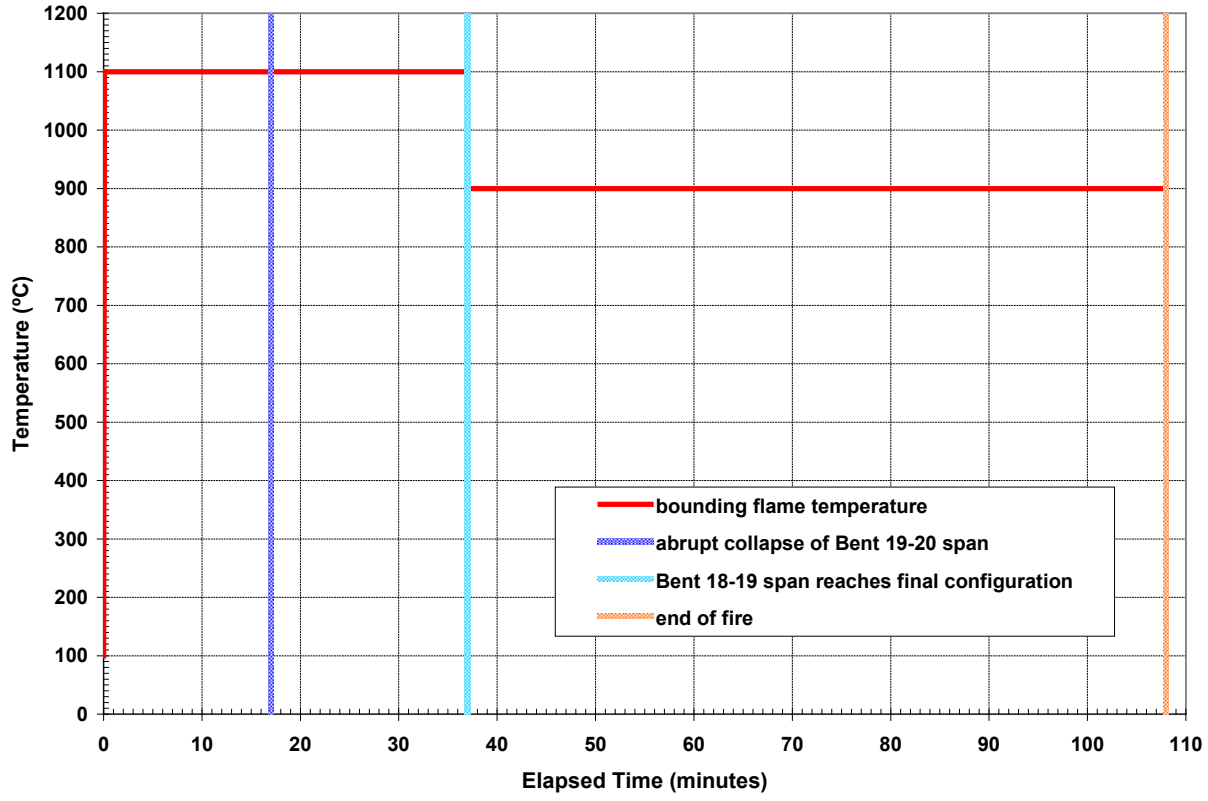

Figure 3.8. Estimated Bounding Maximum Fire Temperatures for the MacArthur Maze Fire

4.0 THE MACARTHUR MAZE FIRE SCENARIO

There are several different aspects of the MacArthur Maze fire that could expose an SNF transportation package to conditions potentially more severe than the HAC fire specified in 10 CFR 71. These can be summarized as follows:

1. exposure of the package to the large fully engulfing fire prior to the collapse of the overhead I-580 roadway span between Bent 19 and Bent 20, which is at a higher engulfing flame temperature and longer duration than the HAC fire
2. subsequent exposure of the package to the relatively long duration of the fire following the collapse of the overhead spans, which is also at a higher engulfing flame temperature and significantly longer duration than the HAC fire
3. physical impact of a collapsing overhead span on the package
4. post-fire cooldown with the package assumed to be covered by the concrete “blanket” of a collapsed overhead span.

As the above list shows, this fire scenario subjects the SNF package to both structural and thermal conditions that could adversely affect its performance. To assure that bounding conditions were considered for all aspects of this complex scenario, the thermal and structural analyses were performed separately. To conservatively bound the worst that the MacArthur Maze fire and roadway collapse could do to the SNF package, the scenario selected for analysis evaluated the most adverse thermal conditions and the most adverse structural configuration. The package was assumed to be positioned in the most adverse location for the different portions of the thermal analyses and the structural analyses, without realistic constraints on how the package could possibly relocate from one place to another during the fire scenario.

The thermal analyses for this fire scenario, which cover items 1, 2, and 4 of the above list, are discussed in Section 4.1. The structural analyses (item 3 above) are discussed Section 4.2.

4.1 Thermal Conditions in MacArthur Maze Fire Scenario

The thermal analyses were performed assuming that the SNF package would be fully engulfed in the fire for the full 108 minutes of the total fire duration. The effects of the physical impact of the collapsing span(s) were ignored for this portion of the analysis, for two specific reasons. First, the impact of the overhead span on the SNF package would completely smother the fire (if the package had been located beneath the first span to fall) or greatly decrease the intensity of the fire in the vicinity of the package (if it had been located beneath the second span to fall). In the first case, the fire would have lasted less than 20 minutes; in the second case, the fire would no longer be fully engulfing after approximately 25 minutes, and the concrete roadway of the fallen span would absorb a significant portion of the energy from the fire. In either case, the potential thermal load on the package would be greatly diminished.

For the thermal analysis, the package is assumed to be in the following locations:

- the package is on the lower I-880 roadway, fully engulfed in fire for 37 minutes, exposed to a flame temperature of 2012°F (1100°C)

- after 37 minutes, the package is still on the lower I-880 roadway, fully engulfed in fire, but the flame temperature is assumed to drop to 1652°F (900°C) for the remaining 71 minutes of the smaller post-collapse fire, resulting in a total fire exposure duration of 108 minutes

- after 108 minutes of fire exposure, the package is still on the lower I-880 roadway, but is enclosed in a concrete 'tunnel' simulating the collapsed roadway, which is cooled only by natural convection from the exposed concrete surfaces of the upper and lower roadways.

4.2 Structural Loads in MacArthur Maze Fire Scenario

The primary structural load considered in the MacArthur Maze fire scenario is the impact of a section of the upper roadway falling onto the package. If a tractor-trailer rig carrying a legal weight truck (LWT) SNF package were to be involved in an accident of the severity of the MacArthur Maze fire scenario, the package could be subjected to additional impact loads, such as collisions with other vehicles caught in the fire or impact with road barriers or debris. Potential scenario-dependent impact loads of this nature are not considered in this study. Regardless of the path the package might have to take to reach the postulated locations within the MacArthur Maze fire scenario, the loads it would be subjected to are assumed to be minor and within the realm of regulatory accident scenarios that provide the design bases for all SNF transportation packages.

SNF transportation packages are designed to survive and maintain containment under severe impact scenarios. The HAC drop scenario, as specified in 10 CFR 71, is a 30-ft drop onto an unyielding surface, with the package impact occurring at the most adverse orientation. The large mass[1] of a typical SNF package leads to a relatively large amount of kinetic energy at impact, which would be much greater than the kinetic energy that could be imparted to the package by the falling overhead section. On that basis alone, the falling overpass section would not be expected to be a more damaging scenario than the HAC drop scenario. However, the falling overhead section impact is postulated to occur at elevated temperatures, which reduce the package material strength, compared to the assumptions for the HAC drop scenario (which is assumed to occur at normal operating conditions). To evaluate the package performance in the more challenging thermal environment of the MacArthur Maze fire scenario, a range of postulated package locations and orientations on the lower roadway beneath the falling overhead section were selected for analysis. The goal was to select a limited number of analyses that would bound potential package response in this scenario.

A realistic location for the package to receive the maximum impact force from the collapsing overhead span would be near the edge of the large pool fire, or possibly outside the fire pool entirely. That is, a location that would result in maximum impact loading and post-fire blanketing by the fallen overhead roadway would be a location likely to receive minimum fire exposure. Conversely, if the package were positioned to receive maximum fire exposure (i.e., fully engulfed for both the pre-collapse and post-collapse fire conditions) it would have to be located near the middle of the area encompassed by the smaller post-collapse fire pool (see Figure 3.7), where it could not be struck at all by either of the two collapsed spans.

As a bounding assumption, the peak temperatures predicted in the thermal analysis for the fully engulfing 2012°F (1100°C) fire conditions (see Section 4.1 above) were imposed on the package in the structural analysis. The package was positioned at a location where it would receive the maximum force of impact from the collapse of the I-580 overhead span between

[1] Total weight of the GA-4 package when fully loaded is 55,000 lb (27.5 T).

Bent 19 and Bent 20. As a further conservatism, the package was positioned on the lower roadway, rather than on the truck conveyance transporting it. There is no credible means in this accident for the package to have become separated from its conveyance, but the I-880 roadway provides the stiffest possible platform for the package when it receives the impact force of the collapsing overhead span. If the package were on the conveyance, much of the force of the impact would be absorbed by the compliance of the overall system. In addition, the impact forces would be smaller than those obtained with the package on the roadway, since the free-fall distance of the collapsing span before impact with the package on the conveyance would be reduced by about 30%.

The package is assumed to be at the maximum temperature obtained from the thermal analysis after 37 minutes of exposure to the fire. The temperature of the descending roadway span (in particular, the temperature of the steel girders) is estimated from a separate thermal analysis of the upper roadway response to the fire, and corresponds to the conditions at 18 minutes into the fire. This disparity between the time-stamp for the package and the roadway girders is to obtain conservatively bounding values for each component. For the package, the hotter it is at the time of impact, the more vulnerable the steel and other material would be to deformation or damage. It is therefore assumed that the package has the longest possible time to heat up (i.e., 37 minutes) before the overhead span falls on it. For the roadway girders, the cooler they are at the time of impact, the stiffer they would be, and the more damage they could potentially do to the package. It is therefore assumed that the falling roadway has the shortest possible time to heat up (i.e., 18 minutes) before falling on the package. This timing difference could not occur in reality, but as a modeling assumption, it yields a conservative bound for the possible range of behavior for both components.

The orientation of the SNF package with respect to the falling roadway determines how many of the girders actually strike the package, where they strike, and at what angle, and therefore has a significant effect on the potential consequences of the impact. The spacing of the girders relative to the length of the package is such that no more than two girders could strike the package in any given configuration. Possible orientations include:

- a single girder striking along the full axial length of the package
- a single girder striking across the package, perpendicular to the long axis
- two girders striking across the package at an angle, with one impact near the package lid.

It is not obvious which impact orientation could do the most damage to the package, and the analysis considers the full range of possibilities, including impacts on the package lid flange region. The analysis also evaluated the effect of a girder striking directly onto one of the package lifting trunnions, which would impart an extremely localized load to the package body. This requires the highly improbable configuration of the package standing on the roadway on one side pair of its lifting trunnions, to obtain a geometry in which such an impact could actually occur.

The assumptions defining components of the package model can affect the magnitude of the loads that are imparted to the package by the accident scenario. To maximize the impact load on the stainless steel body of the package, the effect of impact limiters was neglected in all cases, even though the impact limiters are not expected to detach from the package during the accident. Similarly, the thin outer shell and liquid contents of the neutron shield are neglected, on the assumption that the liquid would be gone by the time the overpass collapsed and that the thin steel plates of the neutron shield would absorb only a negligible amount of impact energy through deformation. In addition to conservatively neglecting energy absorption mechanisms,

modeling choices were made to simplify the impact model and reduce the computational cost as much as reasonably possible. These modeling choices result in the falling overpass structure making direct contact with the stainless steel body of the package or its trunnions, rather than being first intercepted by the impact limiters and neutron shield tank. Detailed descriptions of the overpass and package structural models are presented in Section 5.4.1 and Section 5.4.2, respectively. Section 6.4 describes the assumptions and analysis method in more detail.

In addition to the overpass and package impact modeling, structural evaluations were performed for key package bolts under thermal expansion loading. The differences in thermal expansion coefficients of the package structural materials and the fastener bolts lead to increased bolt tension, even under uniform temperature loading. Temperature results from the thermal models were used to develop temperature load histories for the bolts and surrounding material. These bolt evaluations are assumed to be independent of the impact events. In all credible load cases, the key temperature states occur much later in the transient than the overpass collapse at 37 minutes. Section 5.4.3 discusses the bolt thermal expansion models in more detail.

5.0 ANALYTICAL MODELS FOR THE MACARTHUR MAZE FIRE SCENARIO

This section describes the analytical models developed to investigate the potential effects of the MacArthur Maze fire scenario on a typical over-the-road spent fuel transportation package design. This analysis evaluates the transient thermal response of the package and roadway structure from the initial steady-state conditions through the fire scenario, and many hours into the post-fire cooldown. The models appropriately capture the thermal inertia of the SNF package and the transient temperature response of the system.

Because of the severity and complexity of this fire scenario, multiple thermal and structural models were developed. This included two independent thermal modeling approaches using the finite element analysis (FEA) code ANSYS and the finite difference thermal-hydraulics code COBRA-SFS and structural models using ANSYS and LS-DYNA. The ANSYS thermal model represented the complete package, including the impact limiters. The COBRA-SFS thermal model was developed to evaluate the potential effects of loss of the impact limiters, and to provide a detailed, best-estimate evaluation of the thermal response of the fuel rod cladding to this fire scenario. The structural models were used to evaluate the potential effects of the impact of the falling overhead span on the package, and assumed a range of possible orientations of the package on the lower roadway. Additional detailed models of the bolted lid and flange were also developed, to evaluate potential effects on the package containment boundary as a consequence of the thermal and structural loading imposed by this fire scenario.

The basic design of the package selected for this analysis is described in Section 5.1. The models representing this package for analysis with ANSYS and COBRA-SFS are presented in Sections 5.2 and 5.3, respectively. Structural models developed using LS-DYNA and ANSYS are presented in Section 5.4.

5.1 GA-4 Legal Weight Truck Spent Fuel Shipping Package

The General Atomics GA-4 LWT transportation package was selected for this investigation to evaluate the potential effects of an accident of the magnitude and severity of the MacArthur Maze fire on an NRC-certified SNF transportation package. This package can carry a relatively large payload for an over-the-road transportation package, and therefore the potential consequences of package failure could be more severe than for packages with smaller payload capacities. The GA-4 package is designed to transport up to four intact pressurized water reactor (PWR) spent fuel assemblies with a maximum decay heat load of 2105.4 Btu/hr (0.617 kW) per assembly, for a total package decay heat load of 8423 Btu/hr (2.468 kW).

The GA-4 can carry zircaloy-clad UO_2 fuel with maximum initial enrichment of 3.15% ^{235}U, in 14x14 assemblies with maximum average burnup of 35 GWd/MTU (minimum cooling time of 10 years), or 15x15 assemblies with maximum average burnup of 45 GWd/MTU (minimum cooling time of 15 years). This package is not licensed to carry high burnup fuel (i.e., fuel with average burnup greater than 45 GWd/MTU). There are packages permitted to carry high

burnup fuel pins, but their contents are less than a complete fuel assembly. In addition, transportation of high burnup fuel (>45 GWd/MTU) by road is currently evaluated on a case-by-case basis, pending development of general guidance[1].

For the purpose of this analysis, the package was assumed to contain four WE 14x14 PWR spent nuclear fuel assemblies at the maximum decay heat load. This is the limiting design basis configuration for thermal analysis of the package. Figure 5.1 shows an exploded view of the package, illustrating the main design features. The payload capacity is 6648 lb (3015 kg), and the fully loaded package weighs approximately 55,000 lb (24,948 kg). The package containment boundary is provided by the following structures:

- stainless steel package body wall
- stainless steel bottom plate
- stainless steel package closure lid secured by Inconel fasteners
- dual O-ring seals for the closure lid, gas sample port, and drain valve.

The stainless steel package body encloses the gamma shield, which consists of an inner shell of depleted uranium. Neutron shielding is provided by a stainless steel neutron shield tank external to the package body, containing a water/propylene glycol mixture. Aluminum honeycomb impact limiters, completely enclosed in a thin stainless steel outer skin and inner housing, are attached to each end of the package. Configuration details, including design drawings, are provided in the safety analysis report (SAR) for this transport package (General Atomics 1998).

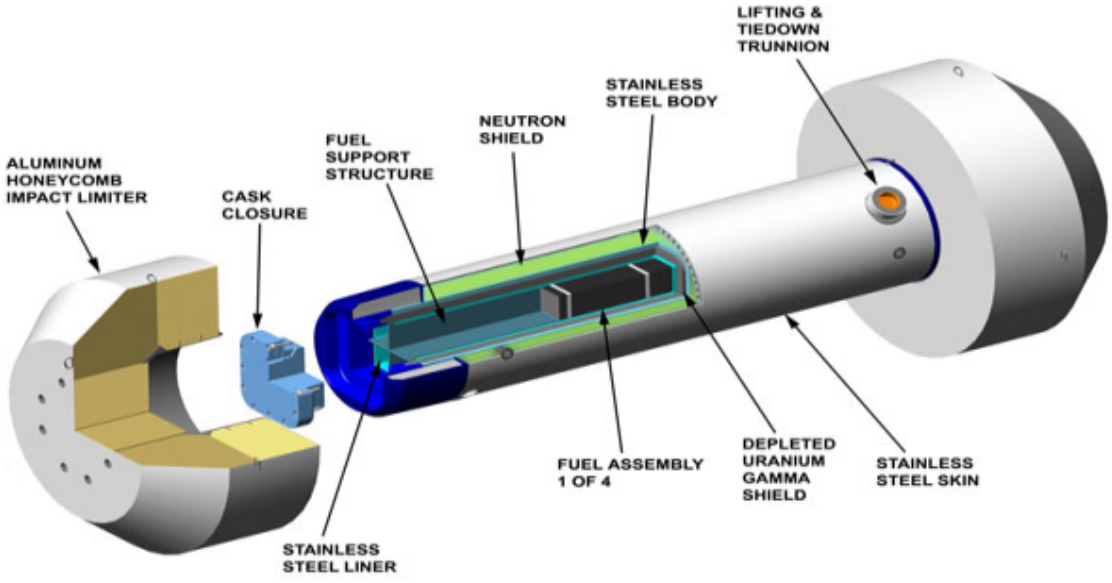

Figure 5.1. GA-4 Package: Exploded View

[1] Transportation of high-burnup fuel is specifically addressed in Revision 2 of NRC Interim Staff Guidance 11 (ISG-11, Rev. 2). A summary of current status of this issue is provided in the Electric Power Research Institute (EPRI) report *Transportation of Commercial Spent Nuclear Fuel, Regulatory Issues Resolution*, EPRI, Palo Alto, CA. 2010. 1016637.

5.2 ANSYS Model of GA-4 Package

A detailed three-dimensional representation of the GA-4 package was constructed using ANSYS® (ANSYS 2003). To simulate the effects of the different segments of the MacArthur Maze fire scenario (as described in Section 4.0), the ANSYS model also includes elements representing a segment of the lower roadway beneath the package and the collapsed upper roadway, which is assumed to cover the package at 37 minutes into the fire scenario. However, the model conservatively neglects the thermal effect of direct contact between the package and the roadway. During the fire, the package is treated as fully engulfed in flame. The model considers forced convection due to the hot fire gases flowing past the package, and thermal radiation to the optically dense fire environment. During the post-fire cooldown, the model includes thermal radiation from the outer surfaces of the package to the roadway surfaces, and conduction-only heat transfer to the surrounding air. The roadway surfaces were included to evaluate the potential effect of the collapsed roadway on the rate of cooldown of the package after the end of the fire. (A detailed description of the thermal boundary conditions for this multi-step scenario is presented in Section 6.3.)

Section 5.2.1 describes the detailed ANSYS model of the GA-4 package. Section 5.2.2 describes the approach used to represent the package buried under the collapsed roadway in the post-fire analysis. Section 5.2.3 presents the material properties used to represent the different elements of the package in the fire and post-fire cooldown transients.

5.2.1 GA-4 Package Representation

The package is assumed to be oriented horizontally throughout the fire scenario, including the actual fire duration, for maximum heat input into the package from the fire. The horizontal orientation of the package beneath the fallen roadway also represents the most adverse conditions for heat removal from the package in the post-collapse fire environment. The conveyance carrying the package is omitted from the model as a conservative representation for both the thermal and structural modeling of this fire scenario. In the thermal model, the fire is treated as fully engulfing, such that the package is subjected to a uniform bounding flame temperature in all directions. In effect, the package is treated as suspended in the fire, and thermal effects of contact with the surface of the road (e.g., heat conduction losses and potential thermal shielding of portions of the package) are neglected. Including the conveyance in a realistic manner would have the effect of partially shielding the package from the fire burning on the roadway below. These assumptions constitute a significant conservatism in the overall modeling approach, since the conveyance and the roadway beneath the package could provide substantial limitations on the rate of heat deposition to the package in this fire scenario.

The model geometry was developed from engineering drawings provided in the SAR for the GA-4 package (General Atomics 1998). Table 5.1 summarizes the ANSYS model element types used for the various components of the package and surrounding roadway. The structure of the package is represented in fine detail, including the lifting trunnions and impact limiters. Convection and thermal radiation heat transfer is represented for specific interior and exterior surfaces, including thermal radiation between the outer surfaces of the package and the external environment. During the fully engulfing fire scenario, the package sees only the bounding fire temperature. During the post-fire cooldown, thermal radiation exchange is calculated between the package and the enclosing roadway concrete. Surface elements were

also generated along the exterior of the package to account for solar insolation loads to calculate the normal conditions of transport, which defines the initial temperature distribution for the package.

Table 5.1. Summary of Elements in ANSYS Model of GA-4

Number of Elements	Element Type	Modeled Structure(s) or Connections
1,851,067	SOLID70 8-node brick elements	fuel assembly, fuel spacer, fuel support structure (FSS) inner frame, helium gap, FSS liner, DU gamma shield, package body, neutron shield, stiffener ring, impact limiter support structure, outer shell, trunnion assembly, closure assembly, and honeycomb structure of the impact limiters
45,240	SHELL57 4-node quadrilateral thermal elements	exterior surface of the impact limiters
761	LINK33 3-D conduction bar elements	package closure bolts; impact limiter attachment bolts
25,331	CONTA173 contact elements	connecting impact limiters, closure assembly, and lifting trunnions to appropriate package assembly surfaces
27,893	TARGE170 contact elements	
232,980	SURF152 elements	convective heat transfer and solar insolation loads at the outer surfaces of the package
218	MATRIX50 elements	radiative heat exchange between internal package surfaces, and between the external surfaces of the package and the environment

A cross-sectional view of the ANSYS model is shown in Figure 5.2, with the major components of the GA-4 package indicated. All components illustrated in Figure 5.2 were modeled using brick elements. The square blocks shown in red are homogeneous regions representing the four fuel assemblies within the package. The fuel assemblies are contained within the cruciform stainless steel fuel support structure (FSS) and FSS liner. The helium gas in the gaps between the homogenized fuel assembly regions and the FSS plates was explicitly modeled with solid elements. The model includes a composite representation of the layers of the cruciform inner frame of the FSS, which consists of thin sheets of stainless steel enclosing boron carbide rods. The thin steel of the FSS liner is represented with a single layer of nodes (illustrated in light blue in the diagram in Figure 5.2).

The GA-4 gamma shield (represented by three layers of elements illustrated in multiple colors in Figure 5.2), consisting of a rectangular tube of depleted uranium (DU), encloses the FSS liner. The DU gamma shield is in non-loadbearing contact with the square cross-section of the FSS liner, and has rounded outer corners, in order to fit within the cross-sectional geometry of the steel package body. The rectangular stainless steel package body forms the inner surface of the liquid neutron shield (NS) tank. The liquid neutron shield tank contains a 56% propylene glycol/water mixture that is modeled as a solid material using the elements shown between the steel package body and the outer wall of the tank. The outer wall of the NS tank is a thin cylindrical stainless steel shell, and is represented in the model as a single layer of elements, as shown in Figure 5.2. This layer constitutes the outer surface of the package assembly.

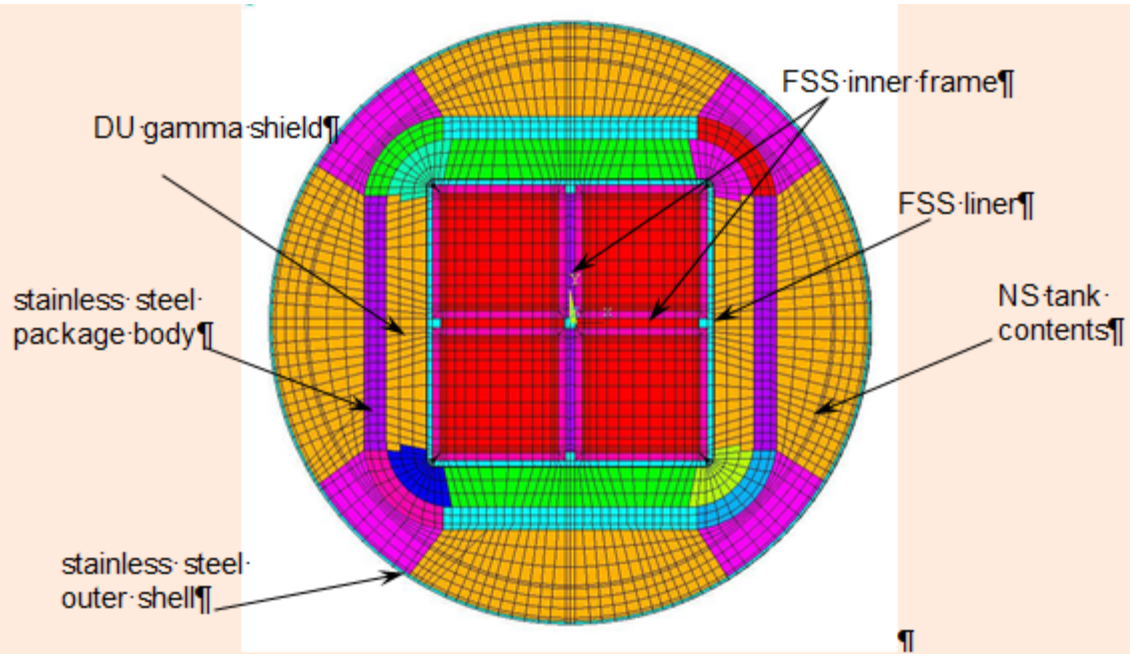

Figure 5.2. Cross Section of ANSYS® Model of GA-4 Package Near Midplane

The diagram in Figure 5.2 shows a cross-section of the package near the center of the axial length of the cask cavity. In this region, there is only liquid in the region between the cask body and the NS tank outer shell. At either end of the package, in the regions covered by the impact limiters, the NS tank is structurally supported by 36 radially distributed stainless steel ribs designated as the impact limiter support structure (ILSS). These ribs extend radially from the thick steel shell of the package body to the thin outer stainless steel shell, and provide additional pathways for conduction heat transfer from the cask body to the NS tank outer shell, in addition to structural support. This region is explicitly modeled in detail in the ANSYS model, but for clarity is omitted from the diagram in Figure 5.2.

A slice through the long axis of the model is illustrated in the diagram in Figure 5.3, and shows the modeling of the ends of the package, including the impact limiters, which consist of an internal aluminum honeycomb structure enclosed within a stainless steel skin. The stainless steel shell of each impact limiter was modeled with shell elements. All other components were modeled using brick elements. A detailed representation of the model in the region of the top impact limiter and package closure is illustrated in Figure 5.4. This diagram shows the impact limiter stainless steel skin and a thin air gap between the impact limiter and the external surface of the package. This gap, which conservatively accounts for the tolerance of the fit of the impact limiter onto the package, was represented in the model geometry using SOLID70 brick elements.

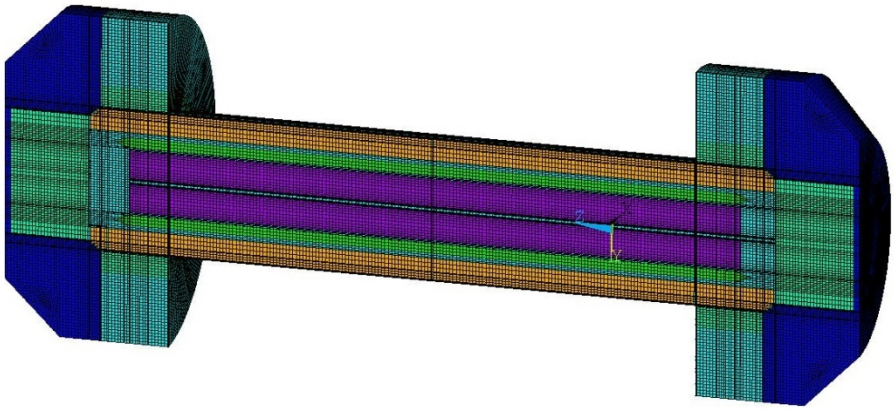

Figure 5.3. GA-4 Package Geometry, Including Impact Limiters

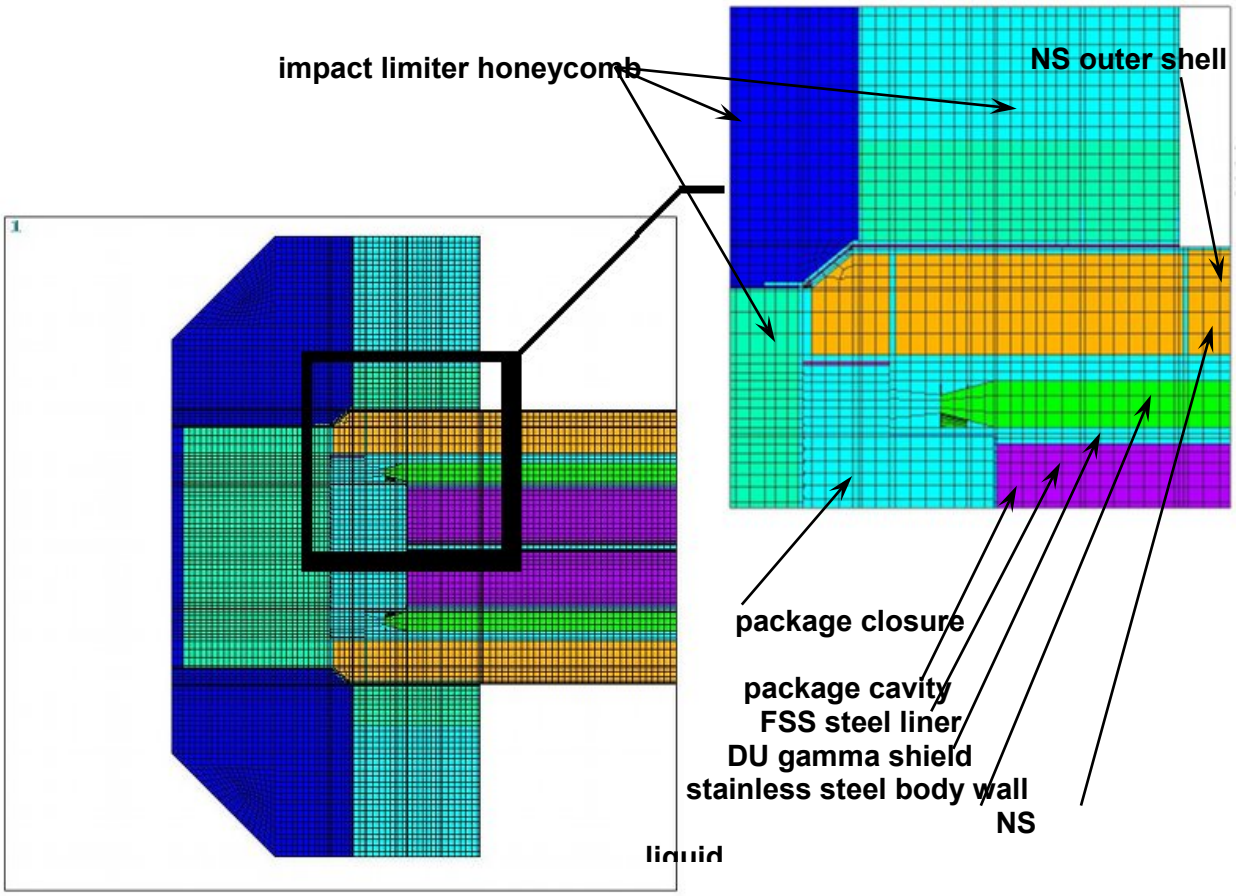

Figure 5.4. GA-4 Package Geometry Model: Impact Limiter Details

For this analysis, the air gap between the closure lid and the impact limiter steel liner was assumed to remain open during the fire and in the post-fire cooldown, even though deformation

or warping of the impact limiter in response to the fire conditions could potentially reduce or eliminate this gap. During the fire, this assumption would tend to slow the rate of heat input to the package through the impact limiters, but because very little heat from the fire can enter the package through the highly insulating material of the impact limiters, this assumption would be expected to have a negligible effect on the thermal response of the package. In the post-fire cooldown, however, this assumption would tend to slow the rate of heat removal from the package, by increasing the insulating effect of the impact limiters.

The thermal inertia of an SNF package can result in significantly higher temperatures being reached on some components in the post-fire cooldown, compared to temperatures reached during the fire, particularly for temperatures in nominally cooler regions of the package. It was therefore deemed more important to capture the effect of retaining the air gap throughout the fire scenario, particularly since heat transfer in the package end regions would not be expected to affect the peak component temperatures during the fire, which occur near the package midplane, due to direct heat input from the fire.

The lower end of the package consists of a thick stainless steel bottom plate welded to the steel inner and outer walls of the package. The upper end of the package is sealed with a stainless steel closure assembly that attaches to a stainless steel flange on the steel body wall. Figure 5.5 shows the detailed representation of the closure assembly developed for this model. Helium-filled gaps between the closure assembly and the FSS, and between the stainless steel flange and the closure assembly, were included in the model geometry. These gaps were represented with solid brick elements.

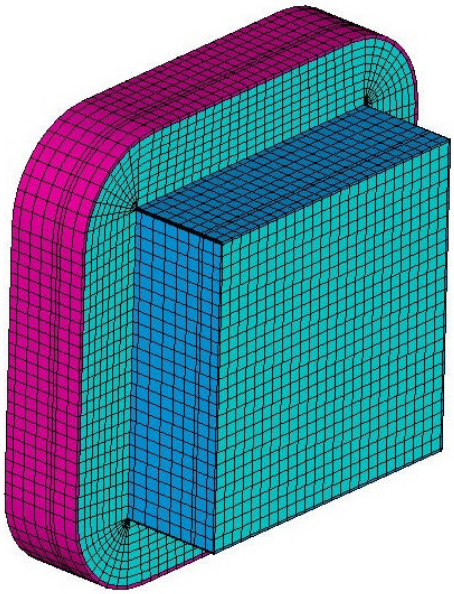

Figure 5.5. GA-4 Package Geometry Model: Closure Assembly Details

Sections 6.2 and 6.3 provide detailed discussions of the modeling assumptions and boundary conditions for the fire analysis. The detailed representation of the package internals was designed to capture all three possible modes of heat transfer (i.e., conduction, convection, and thermal radiation) between all of the components of the model. Conduction is handled inherently in ANSYS by the elements and corresponding material properties representing each component, but convective and radiative mechanisms must be carefully implemented to

properly capture the physical behavior of the system. The representation of the fuel assemblies is particularly important in appropriately modeling the thermal response of the fuel rods and predicting the peak cladding temperature. Heat transfer within the fuel assemblies is primarily by conduction and thermal radiation, with convection only a relatively minor contributor.

The fuel assemblies were modeled as homogeneous regions with an effective radial conductivity determined using an effective conductivity model (Bahney and Lotz 1996) that is widely used in the nuclear industry in safety analysis for SNF packages. In this model, the combined effect of thermal radiation and conduction is characterized using an effective conductivity that is a function of assembly geometry and decay heat. The application of the fuel effective conductivity model developed for this analysis introduces a modification to more accurately account for the temperature gradient between the outermost row of rods in the assembly and the enclosing wall. This is accomplished by including a helium gap between the homogenized material region representing the fuel assembly and the wall of the enclosing basket (in this case the FSS cruciform and liner, as shown in the diagram in Figure 5.2), rather than extending the homogenous region to the wall, as is the approach normally used in the effective conductivity model. An additional feature of this modified representation is that it more directly takes into account the effect of the non-uniform wall temperature distribution around the fuel assembly, which can be of particular significance in modeling fire scenarios.

Axial conduction within the fuel assembly region was modeled only in the fuel cladding and backfill gas, to be consistent with typical applications of the fuel effective conductivity model, conservatively neglecting axial conduction in the uranium oxide fuel. The axial effective conductivity was determined with a cross-sectional area weighting scheme based on the total cross-sectional area of the assembly. However, to appropriately capture the thermal inertia of the fuel assemblies for the transient response in the fire scenario, the effective density and heat capacity for the fuel region was defined based on volumetric averages of the corresponding properties of the helium gas, fuel rod cladding, and uranium oxide fuel pellets.

An average volumetric heat generation of 2105 Btu/hr (617 W) was applied over the active fuel length for each fuel assembly. The axial distribution of decay heat was represented by dividing the active fuel length into 16 separate zones, and the local heat load was determined by multiplying the average by an appropriate peaking factor for that particular zone. The peaking factor was determined based on the bounding axial power profile presented in the SAR, which has a normalized peaking factor of 1.1.

The helium gas filling the 0.5075-inch gap between the nominal fuel assembly cross-section and FSS was modeled with solid elements and used standard helium thermal properties for conduction, density, and specific heat. Convection across the gap was accounted for by multiplying the local gas conduction values by an empirically derived[1] Nusselt number of 3.66. Thermal radiation exchange across the gap was modeled with MATRIX50 super elements. These were created by using SHELL57 elements to designate the discrete enclosure. The AUX-12 hidden ray-tracing method was used to compute view factors for each element within the super-element. All other gaps in the package assembly, such as between the closure assembly and FSS, or the impact limiters and package skin were modeled in a similar manner, which included thermal radiation and conduction across surfaces but assumed negligible convection.

[1] This value is based on thermal measurements in full-scale spent fuel storage systems. See Michener et al. (1995) and Creer et al. (1987).

Other potential gaps not explicitly modeled within the geometry, such as between the gamma shield and package FSS, and between the gamma shield and stainless steel wall were accounted for by modifying the material properties of the adjacent materials to include the calculated effective properties for the material and gap. For very small gaps, the calculations were based on the following assumptions:

- the thermal radiation view factor is specified as 1.0 (gap completely enclosed)
- the temperature difference across the gap is small
- convection heat transfer across the gap can be neglected.

For the pre-fire steady-state and post-fire transient cooldown analyses, nominal gap distances were used to determine the effective thermal conductivity. During the fire transient, the gaps were assumed to close due to thermal expansion of the package materials, such that the calculated effective thermal conductivity across a gap reduced to the thermal conductivity of the adjacent solid material without the gap. This ensured a conservative approach with respect to the effect of heat transfer across the gaps throughout the entire analysis.

The impact limiter attachment bolts and the closure assembly bolts were represented as line elements within the model. Small variations in the overall length of individual bolts were accounted for by calculating an equivalent cross-sectional area, which was specified in the real constant properties for the line elements.

5.2.2 GA-4 Package beneath Collapsed Roadway

The location of the package and configuration of the concrete roadway overlay, as represented in the fire scenario modeling, is defined to maximize coverage of the package, within the physical geometry of the collapsed structures. The overall length of the GA-4 package without impact limiters is 15.65 ft (4.77 m), and the outer diameter is 3.3 ft (1 m). With impact limiters, the overall length is 19.5 ft (5.94 m) and the maximum diameter is 7.5 ft (3.39 m). Figure 5.6 shows block “footprints” of the package (with impact limiters) approximately to scale in the locations where an object of that size could be completely covered by the fallen roadway spans. The conveyance is not considered in this evaluation, as noted in Section 5.2.1 as a modeling conservatism for the fire exposure. It is also a conservative assumption for consideration of the effect of the roadway collapsing onto the package. Due to the size of the package and the conveyance, it would be virtually impossible to completely cover them both with the fallen roadway in this accident scenario.

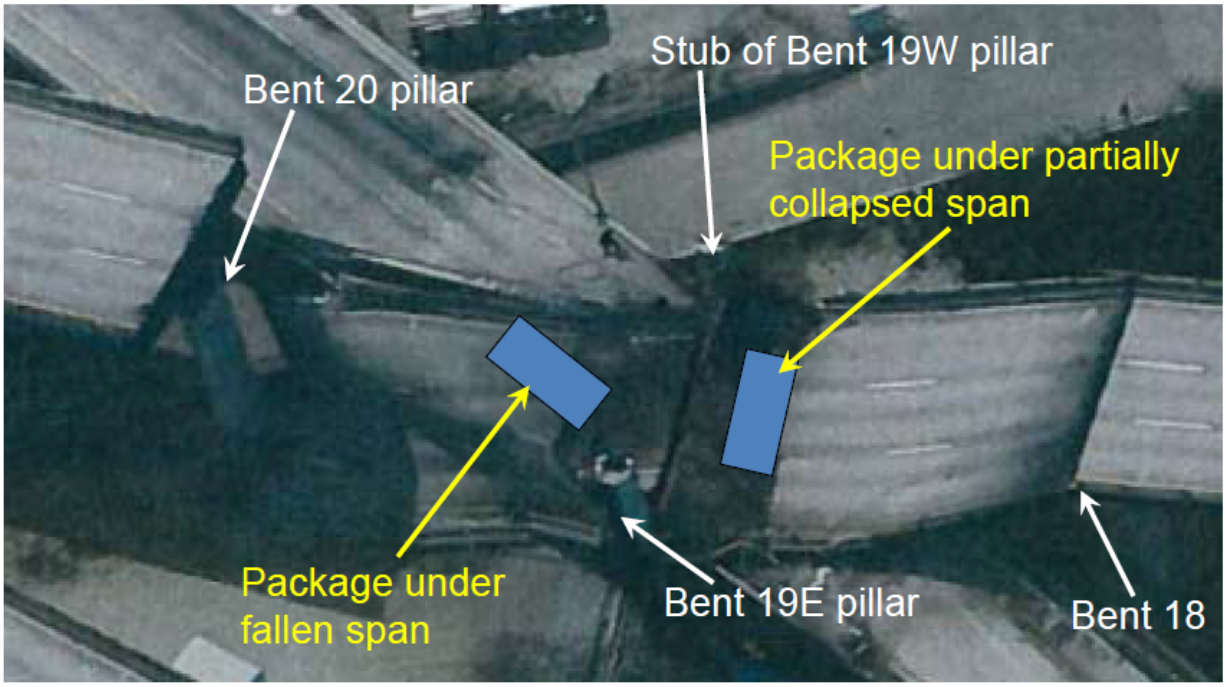

Figure 5.6. Locations Where an SNF Package Could be Covered by Collapsed I-580 Spans (photo from MAIT Report, CHP 2007, reprinted with permission)

Modeling of the structural response of the package due to the collapse of the roadway spans is discussed in Section 5.4. From the standpoint of thermal performance of the GA-4 package, the important effect of the collapse is the additional thermal barrier imposed by a concrete "blanket" over the package in the post-fire cooldown. Of the two possible locations where the package would be completely covered by a fallen span, the location beneath the fully collapsed Bent 19-20 span clearly imposes the more severe conditions. At the location beneath the partially collapsed Bent 18-19 span, only the top of the package would be covered, due to the limited area of contact between the upper span and the lower roadway. Beneath the completely collapsed Bent 19-20 span, the package would be entirely covered by the fallen roadway.

Figure 5.7 shows a cross-section diagram of the assumed configuration for the GA-4 package beneath the collapsed I-580 span. As a conservative simplification, it is assumed that the package is not actually in physical contact with the concrete structure enclosing it, and the neutron shield tank outer shell is not deformed by contact with the fallen span. This preserves the air gap of the evacuated shield tank, which insulates the package body during cooldown. The crushed girders on the underside of the fallen overhead span are assumed to hold the roadway 9.4 inches (0.24 m) away from the package body. This distance is estimated from the collapsed height of the severely deformed girders of the actual roadway structure that were exposed to the intense heat of the large pool fire. In addition, the package is assumed to stand on its lifting trunnions, so that there is a 5-inch (0.13-m) gap between the package body and the lower roadway. A similar gap is assumed between the package outer shell and the surface of the concrete edge barrier. The touch-point of the fallen I-580 span on the I-880 roadway is assumed to be approximately one-quarter of the lower roadway width, at 4.66 ft (1.42 m) from the package centerline. Given the stiffness of the concrete-and-steel roadbed, it is reasonable to suppose that the presence of the package would tend to hold the upper span away from contact with the lower roadway over much of its width, which makes this an extremely conservative assumption.

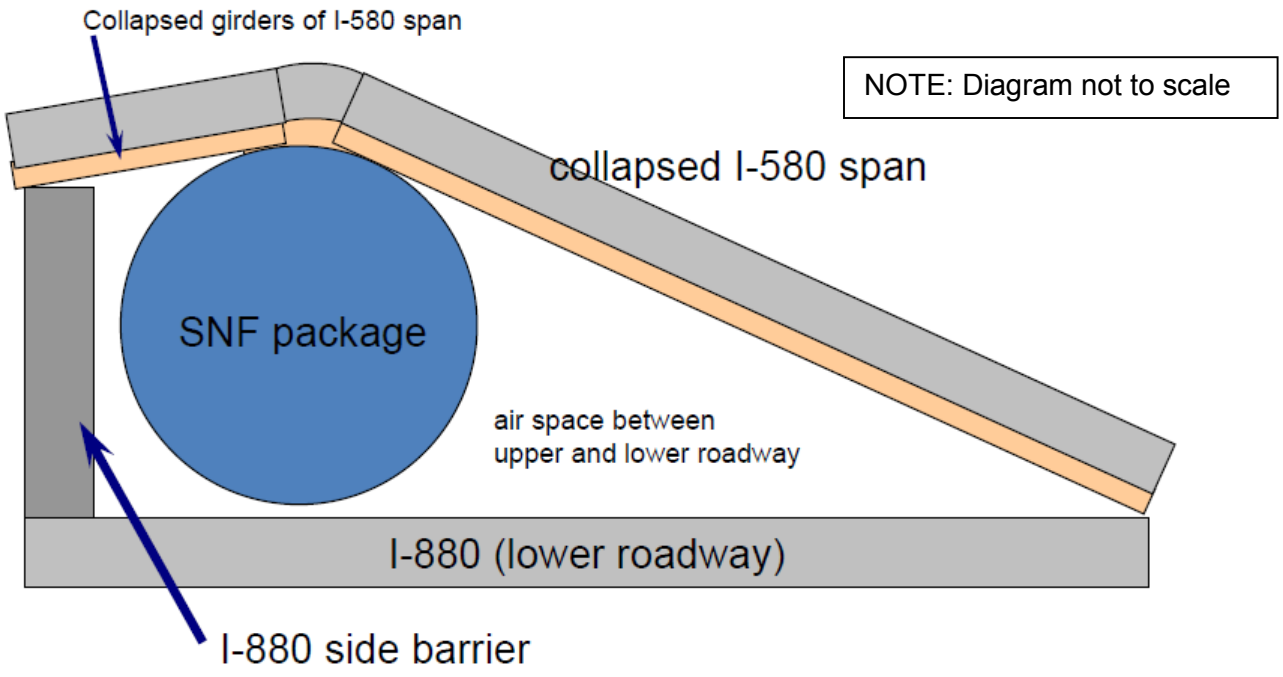

Figure 5.7. Diagram of Collapsed Roadway Configuration over SNF Package

In the ANSYS model, the configuration shown in Figure 5.7 is represented by enclosing the entire SNF package within a simplified structure representing the external environment, as illustrated in Figure 5.8. During the fire, this structure provides boundary conditions for the thermal analysis simulating a fully engulfing fire surrounding the package. (See Section 6.4 for discussion of the modeling of the structural response of the package in this fire scenario.) After the end of the fire, the surrounding enclosure models the configuration of the package positioned on the lower I-880 roadway adjacent to the side barrier, beneath the fallen upper I-580 roadway. Heat transfer between the package and the enclosing concrete was assumed to consist of conduction and convection through the surrounding air within the enclosure, and thermal radiation exchange between the package external surfaces and the concrete surfaces representing the roadway above and below. This provides a conservative representation of the postulated package configuration during the post-fire cooldown.

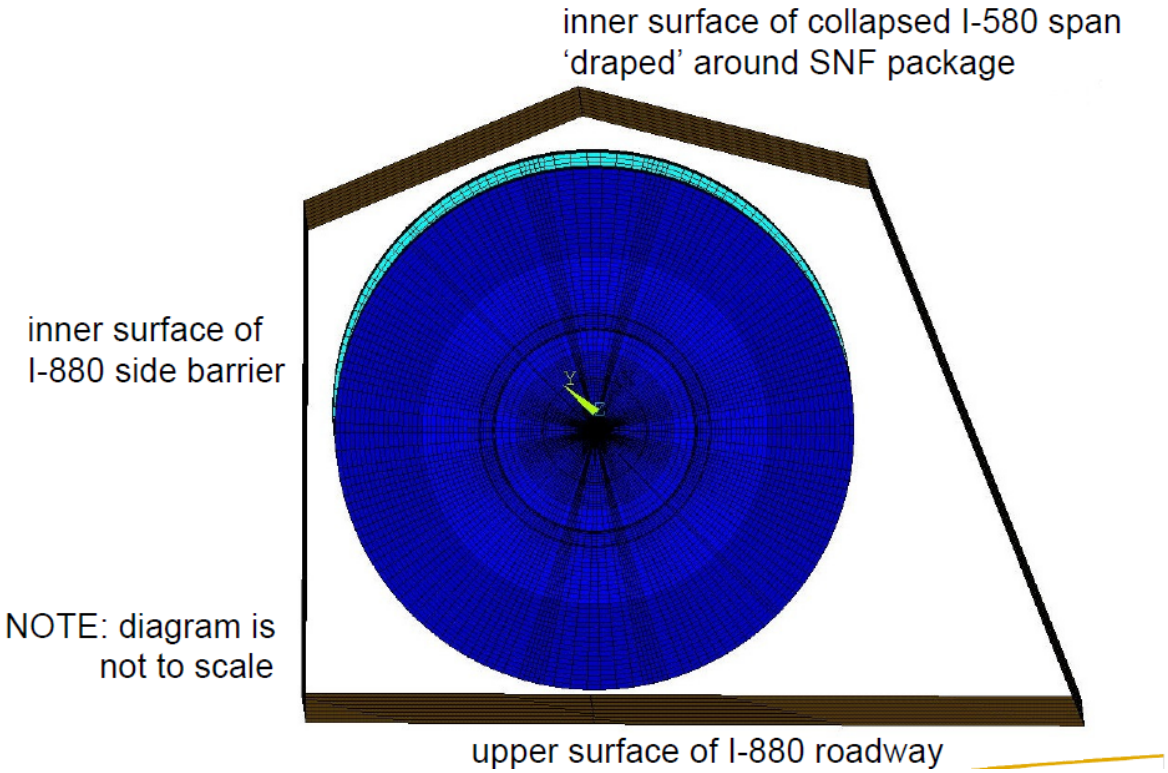

Figure 5.8. ANSYS Analysis of GA-4 Package: Model Element Plot (Axial View)

Thermal radiation interaction between the package and concrete roadway surfaces was defined by coating the exterior surfaces with SHELL57 elements having appropriately specified emissive material properties. The SHELL57 elements were then used to produce highly structured AUX-12 generated MATRIX50 super elements. A total of twenty-four MATRIX50 super elements were defined to capture the radiation interaction between the package and roadway surfaces. The twenty-four MATRIX50 super elements represent two sets of thermal radiation conditions; half of the super elements represented pre-fire thermal radiation emissivities, and the other half represented the fire and post-fire emissivities. Only one set of external MATRIX50 super-elements was active at a time during the calculation, depending on the stage of the analysis (i.e., pre-fire, fire, or post-fire).

The concrete enclosure is essentially the same for the ANSYS and the COBRA-SFS models, except for the dimensions assumed for the post-collapse structure. For the ANSYS model, the size of the enclosure is expanded to accommodate the impact limiters, while in the COBRA-SFS model, the concrete overlays the package body (as described in Section 5.3). In reality, of course, the falling roadway would crush the impact limiters against the package body, but this was conservatively neglected in the ANSYS model. Accounting for the effect on thermal behavior due to crushing of the impact limiters would add unnecessary complication to model, and in addition, would be a less conservative approach, as it would tend to enhance conduction heat transfer from the package. Assuming the stainless steel shells of the impact limiters retain their original configuration imposes a conservative representation of the insulating barrier these structures present to heat transfer from the package during the cooldown phase of the transient.

Convection heat transfer on the external surfaces of the package was determined using empirical correlations, which are described in Section 6.3. Free convection was assumed before and after the fire, while forced convection was assumed during the fire. Convection was implemented using SURF152 elements. These elements are placed on the exterior surface of a body and communicate with the designated sink temperature assigned to a single node (called the "space node") to compute the heat flux. Figure 5.9 shows a representation of a space node relative to the package assembly.

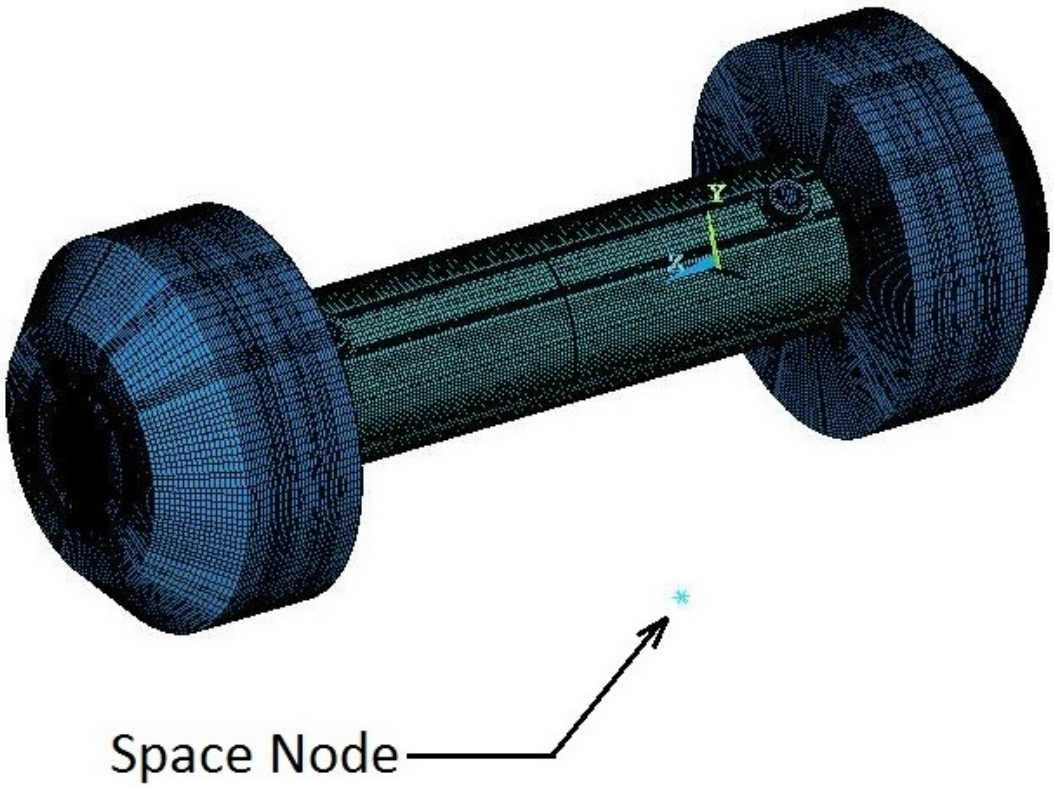

Figure 5.9. Space Node for Convection Heat Transfer

In order to represent variation in convection heat transfer over different regions of the package surface, due to variation in the surface geometry, the external surfaces were partitioned into axial and radial zones. The package was divided into four different zones along the exposed outer surfaces, corresponding to the top, bottom, and left and right sides of the horizontal package, as illustrated by the colored segments in Figure 5.10, to appropriately model variations in convection along the exterior of the package. On the package body, these zones correspond to the radial positions of the four fuel assemblies within the package. The outer surfaces of the impact limiters were also split into four zones in the same manner as the package body, as illustrated in Figure 5.10. In addition, the four lifting trunnions were split into two different zones each, with two located along the top package boundary and the remaining two located along the bottom boundary of the package. Within each zone different heat transfer coefficient correlations were used, corresponding to the geometry of the surface (e.g., vertical flat surface, horizontal curved surface), by defining subzones within each zone. A sink node was defined for each zone and subzone, which defines the ambient air temperature seen by the package in that zone or subzone, and is used to calculate the local convection coefficient at the package surface.

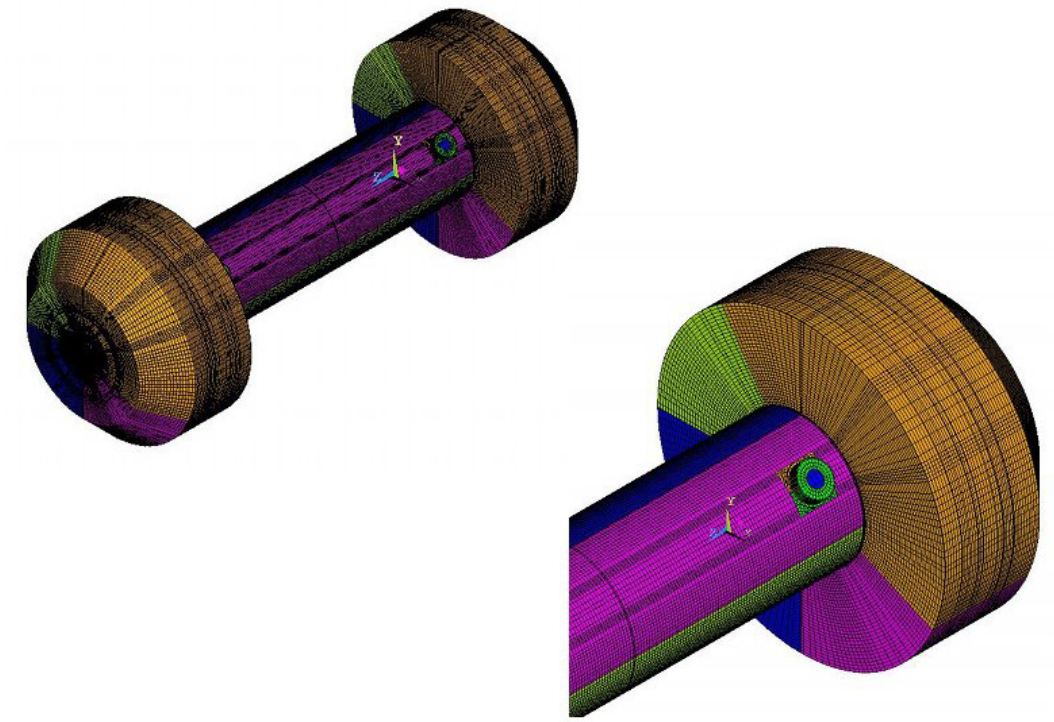

Figure 5.10. Zones for Convection Computations for Package Assembly Surfaces

The external environment was split into eight different zones corresponding to the upper roadway and lower roadway, with the ends open to the ambient, as illustrated in Figure 5.11. (As shown in Figure 5.11, these modeling structures are tilted and rotated for clarity; when properly oriented, the cross-section of the defined zones match the cross-section of the model diagram shown in Figure 5.8.) The convective heat transfer coefficient is assigned to the package and external elements based on the temperature difference between the surface and sink temperature, and on the surface geometry, as described in Section 6.0. The heat exchange between these surfaces and the space node is then computed by ANSYS as part of the overall solution for a given time-step in the transient.

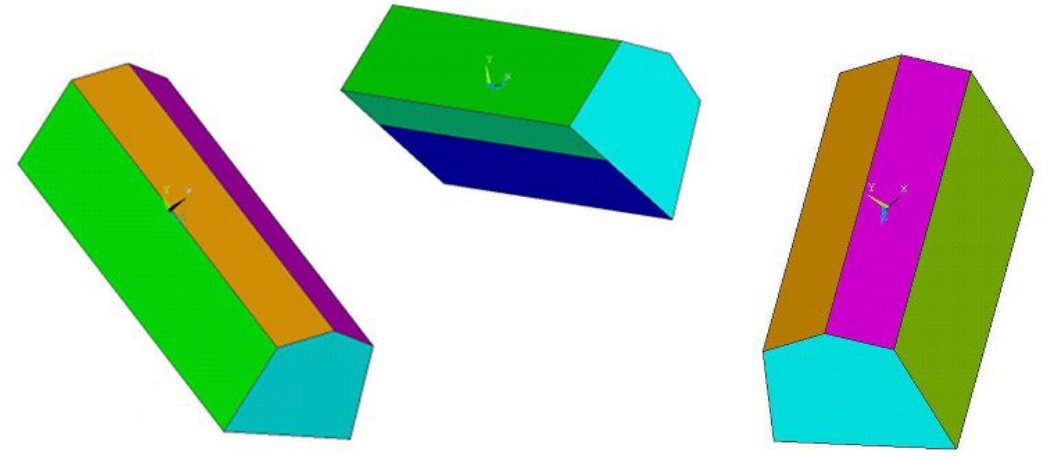

Figure 5.11. Zones for External Heat Transfer from Roadways and External Environment

During the fire, the sink node temperature for the SURF152 elements is set to the bounding flame temperature representing the fully engulfing fire. The external convection coefficient is computed using a forced convection relation derived from gas temperatures and velocities predicted in the fire simulation with the FDS code (as discussed in detail in Section 3.3). These boundary conditions are provided for the top, sides, and bottom of the enclosure, corresponding to the four zones on the package, as shown in Figure 5.10. During the fire, the nodes representing the external environment are also set to the bounding flame temperature.

5.2.3 Material Properties for GA-4 Package in ANSYS Model

The specific thermal material properties used to represent the components of the GA-4 package and roadway structures in the ANSYS model are listed in detail in Appendices A and B. For elements of the model representing the major components of the package, the specified properties are those of the single material comprising that component. However, for efficiency of meshing, the thin plates of the FSS and enclosed neutron absorber rods, the complex honeycomb structures of the impact limiters, and the fuel assemblies are represented using effective thermal properties defined specifically for the overall region. In addition, the effect of the fire on the integrity of the liquid-filled neutron shield tank was also explicitly modeled with changes in material properties in the transient calculation.

The neutron absorber plates of the FSS are composed of boron carbide rods sandwiched between thin stainless steel (XM-19) panels, with helium surrounding the boron carbide rods. Homogeneous material properties were defined for the elements representing the FSS plates, based on volumetric averaging of the material properties for XM-19 stainless steel, boron carbide, and helium. It was assumed that convection in the helium gas would be negligible in the narrow enclosed space within the FSS plates, and the effective thermal conductivity was calculated based on conduction and thermal radiation heat transfer only. Anisotropic properties were defined for this material, assuming conduction only along the axial length of the FSS, with conduction and thermal radiation through the thickness of the composite plate. Thermal radiation was modeled assuming that the helium-filled space between the boron carbide rods and the enclosing steel plates was very small, completely enclosed within the stainless steel panels, with a very small temperature difference between them.

The stainless steel inner support structure and outer shell of the impact limiters was explicitly modeled using elements with properties of XM-19 stainless steel. Composite material properties were used to model the aluminum honeycomb material enclosed within the steel shell. The design of the impact limiters is defined in the package SAR (General Atomics 1998) as a standard non-reinforced hexagonal aluminum structure, and includes specific regions with differing densities, which are bonded together and to the stainless steel shell with adhesive foam. Effective properties for these regions were determined based on material data for aluminum honeycomb from HEXEL Composites (1999), using a volumetric averaging scheme. This approach included the properties of the adhesive foam as well as the air-filled aluminum honeycomb. The effective thermal conductivity values for the honeycomb regions were calculated assuming the material was isotropic within a region, as indicated by the HEXEL Composites data for the honeycomb.

In the course of the transient calculation, the material properties of the impact limiters were modified to account for structural configuration changes and effects of the fire. Portions of the aluminum honeycomb in the impact limiters are assumed to melt during the fire, due to the extremely high temperatures predicted in this transient. For the aluminum honeycomb material in the impact limiters, local melting would be expected to significantly increase in the void (air)

volume compared to the intact honeycomb material. This would tend to increase the insulating effect of the impact limiters, reducing the rate of heat transfer through this material. During the fire portion of the transient, the impact limiters were conservatively assumed to remain intact, allowing the maximum heat transfer to the package through these components during the fire. However, the assumption of intact impact limiters is no longer conservative in the post-fire cooldown portion of the transient. With larger air regions within the impact limiter structure due to local melting of the honeycomb, the damaged impact limiters would tend to further slow the rate of heat removal from the package during the cooldown transient, compared to the effect of intact impact limiters. The material properties of elements in the ANSYS model representing the honeycomb material were therefore modified in the post-fire portion of the calculation to account for the effects of melting.

Fire damage to the impact limiters was determined from the predicted temperature distribution within these regions at the end of the fire. The percentage of honeycomb nodes above the melting point of the aluminum alloy (approximately 1100°F [593°C]) was used to calculate the total volume of melted aluminum, and the volume of "lost" honeycomb. It was assumed that the molten aluminum would flow due to gravity to the lowest point on the horizontal side of the impact limiters. Therefore, elements in this region encompassing a volume corresponding to the volume of melted aluminum were modified to have the properties of aluminum alloy, rather than the honeycomb mesh. The remaining volume of the impact limiter was assumed to be a mixture of air (corresponding to the volume of the melted mesh) and unmelted intact honeycomb. The thermal conductivity of the elements representing this volume within the impact limiters was modified using an effective thermal conductivity calculated based on volume-averaging of the thermal properties of air and the unmelted honeycomb mesh material.

The effect of the fire on the material properties of the liquid neutron shield was also explicitly represented in the transient calculation. The neutron shield liquid temperature is calculated to exceed its boiling point very early in the fire transient. Prior to rupture, heat transfer through the liquid in the tank is represented with an effective conductivity relationship based on an empirical correlation (Guyer and Brownell 1989) for convection and conduction heat transfer across a gap between two long, horizontal concentric cylinders at different temperatures. The fluid thermal conductivity used in this relationship was determined based on material property data for propylene glycol and water mixtures provided in the GA-4 SAR (General Atomics 1998). (Appendix B contains a detailed description of this correlation, and verification of its applicability to the geometry of the GA-4 neutron shield tank.)

The neutron shield tank is assumed to rupture when the peak temperature in the liquid is predicted to exceed the boiling point of the water-glycol mixture. After rupture, the neutron shield tank contents are assumed to consist only of air, with heat transfer by conduction and convection. Thermal radiation between the inner walls of the empty tank is also accounted for, by direct calculation between the elements on the inner surface of the tank outer shell and the outer surface of the package body.

The effective conductivity of the material within the neutron shield tank was determined as a function of the average tank temperature and the radial temperature difference between the tank inner and outer surfaces. The radial temperature difference was calculated separately along the flats and corners of the neutron shield, to account for the effect of the non-uniform gap due to the square cross-section of the tank inner surface within the circular outer tank shell. Material properties for the tank were updated between each time step during the transient solution. The affected nodes were assumed to consist of a 56% propylene glycol solution up to the point where the maximum temperature reached the mixture's boiling point of 276°F (136°C).

The boiling point for the tank contents, and hence the time of assumed tank rupture, was calculated based on the maximum normal operating pressure of the neutron shield tank (General Atomics 1998), and data for vapor pressure versus temperature of aqueous solutions of propylene glycol (Dow Chemical Company 2003). When the maximum temperature in the tank exceeded the boiling point, it was assumed that rupture had occurred and all the liquid in the tank instantly vaporized. The effective conductivity was then computed using dry air as the medium. This calculation extended through the remainder of the fire and was also continued during the cooldown period. This approach conservatively neglects energy absorbed by the phase change (i.e., the heat of vaporization for the liquid), but this is mainly as a matter of convenience, since this would constitute a very small deduction from the total energy imparted to the package.

5.3 COBRA-SFS Model of GA-4 Package

The GA-4 package was also analyzed with COBRA-SFS (Michener et al. 1995), a thermal-hydraulic code developed for analysis of multi-assembly spent fuel storage and transportation systems. The code uses a lumped-parameter finite-difference approach for predicting flow and temperature distributions in spent fuel transfer, storage, and transportation systems, and fuel assemblies under forced and natural circulation flow conditions. It is applicable to both steady-state and transient conditions in single-phase gas-cooled spent fuel packages with thermal radiation, convection, and conduction heat transfer.

The COBRA-SFS model was developed to provide detailed temperature distributions on the individual fuel rods within the package in this fire scenario. In addition, the COBRA-SFS model was used to investigate the potential effects on the package if it is assumed that the impact limiters have detached from the package in the accident prior to the fire. The impact limiters have a very large effect on the thermal response of the package internals to fire conditions, since these structures act as thermal shields on the package ends. The impact limiters are designed to remain attached to the package during design-basis accident scenarios, but the MacArthur Maze fire involves fire temperatures exceeding that of the HAC fire defined in 10 CFR 71. In addition, this scenario includes structural impacts due to the collapse of the overhead highway spans after the fire exposure, which is the reverse of the impact-then-fire scenario prescribed for hypothetical accidents in 10 CFR 71. It is unlikely that the impact limiters would come off, even in this extraordinary scenario, but if it were to happen, it would significantly influence the thermal behavior of the package. The effect of the loss of the impact limiters on the package response to this fire is therefore included in this analysis.

As in the evaluations with the ANSYS model, evaluations with COBRA-SFS consider two configurations for the package during the fire scenario. Prior to and during the collapse of the two overhead roadway spans (as discussed in Section 2.1), the package is assumed to be in a fully engulfing fire at 2012°F (1100°C), and sees a uniform bounding fire temperature in all directions. After the collapse, the package is assumed to be exposed to a fully engulfing 1652°F (900°C) fire. In a separate independent calculation, the concrete structure of the collapsed roadway configuration is exposed to these fully engulfing fire conditions, in preparation for the post-fire cooldown calculation. The concrete surface temperatures obtained in this calculation are used as boundary conditions for both the ANSYS model and the COBRA-SFS model evaluations of the post-fire cooldown conditions. For the post-fire analysis with COBRA-SFS, the model includes the GA-4 package, the lower roadway, side barrier, collapsed upper roadway, and the air space between the package and the concrete structures. The

model of the package is described in Section 5.3.1. The package-under-concrete configuration for the post-fire scenario is discussed in Section 5.3.2.

5.3.1 COBRA-SFS Model of GA-4 Package in Fully Engulfing Pool Fire

The GA-4 package was modeled for the COBRA-SFS calculations in sufficient detail to capture the thermal response of the system components in the radial and axial directions. Material properties used in the model are listed in Appendix A. The four fuel assemblies within the basket are each modeled as rod and subchannel arrays (Michener et al. 1995), for appropriate representation of thermal radiation heat transfer as well as conduction and convection. The basket separating and containing the fuel assemblies is represented using multiple layers of solid conduction nodes, to capture the effect of the B_4C poison rods stacked within the steel plates forming the arms of the cruciform structure.

The steel inner liner, DU gamma shield, and steel package body are also represented with multiple layers of solid conduction nodes, to appropriately resolve the temperature gradients through these relatively thick components. In addition, these structures are also divided radially, to capture the effects of non-uniform external conditions surrounding the package. A cross-section diagram illustrating the noding for the COBRA-SFS model is shown in Figure 5.12.

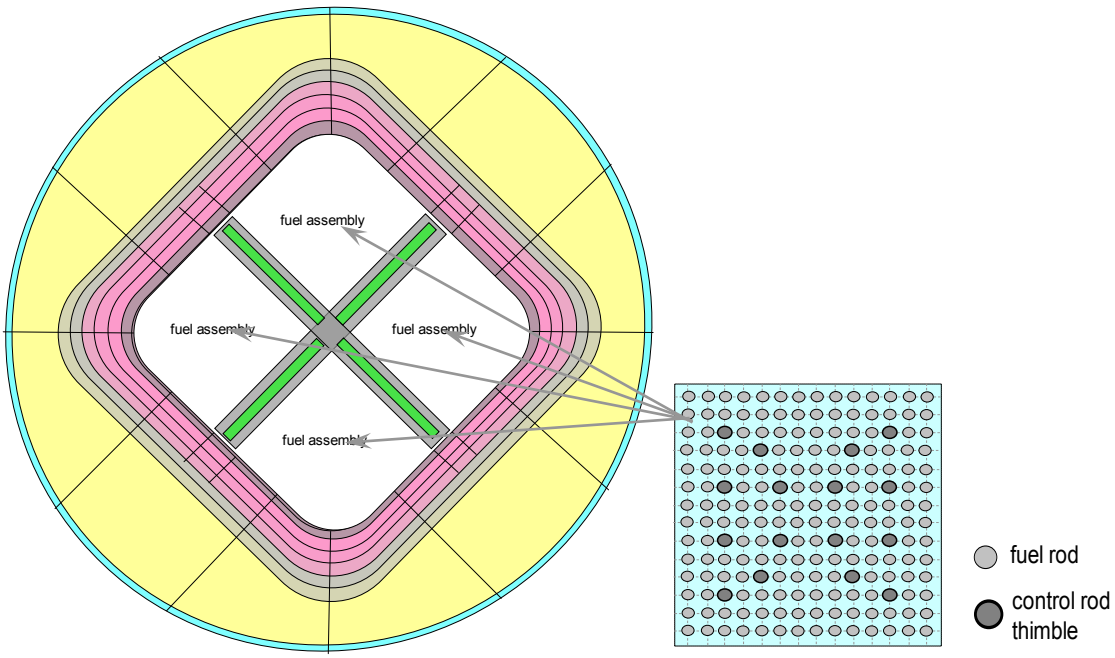

Figure 5.12. Cross-section of COBRA-SFS Model of GA-4 Package, Including Fuel Assemblies, Basket, Package Body, and Neutron Shield

The impact limiters on the package ends are assumed lost, and are not included in the COBRA-SFS model of the GA-4. The impact limiters are designed to remain in place through the sequence of accidents specified in 10 CFR 71 for HAC; however the MacArthur Maze fire scenario involves fire temperatures exceeding that of the HAC fire. Although it is unlikely that the impact limiters would detach from the package even in this severe accident scenario, the

impact limiters would be expected to suffer severe degradation, due to the long fire duration and the postulated impact of the overhead span on the package. The impact limiters provide significant thermal shielding for this package in any fire scenario, and therefore can have a large effect on the response of the system to the fire. Therefore, this assumption is included in the COBRA-SFS model, for completeness in the overall analysis of the effects on the package of the MacArthur Maze fire scenario. However, evaluation results shown in Section 7.3.6.1 show that the impact limiters would remain attached to the GA-4 package. Results obtained with the COBRA-SFS model assuming loss of the impact limiters are therefore bounding and conservative.

The neutron shield tank initially contains a liquid 56% propylene glycol/water mixture with maximum design pressure of 150 psig (1.135 MPa), which gives a boiling temperature of 276°F (135.6°C). However, the tank is not an ASME pressure vessel, and in the SAR analyses for the HAC fire at 1472°F (800°C), it is conservatively assumed that in the initial steady-state, the tank has already ruptured and contains only air. In the COBRA-SFS analysis, the tank is assumed to remain intact up to the point in the transient where the maximum temperature in the neutron shield region exceeds the boiling point of the glycol/water mixture. Heat transfer across the neutron shield tank is treated in the same manner as in the ANSYS analysis, described in Section 5.2.3, with an effective conductivity correlation defined for the neutron shield tank contents.

The maximum temperature in the region modeling the tank contents is predicted to occur within sixty seconds of the initiation of the fire transient in this scenario, at which point the medium within the tank is assumed to be dry air, and thermal radiation between the tank inner surfaces is added to the model. The internal surfaces of the shield tank are specified with a uniform emissivity 0.9 after the assumed loss of liquid contents, to conservatively represent the effect of sooting, on the assumption that highly sooted fire gas could enter the ruptured and fully vented tank. Additional package modeling details related to boundary conditions and assumptions are included in Section 6.3.

5.3.2 COBRA-SFS Model of GA-4 Package beneath Collapsed Upper Roadway

The representation of the GA-4 package for the post-fire cooldown with the package beneath the collapsed upper roadway is the same as the model developed for the fully engulfing fire portion of the scenario. For the post-fire cooldown, the model is expanded beyond the package exterior shell to include additional nodes representing the concrete of the upper and lower roadways in relation to the package. The location of the package and configuration of the concrete covering it is defined to maximize coverage of the package, within the physical geometry of the collapsed structures in this fire scenario, as discussed in Section 5.2.2 and illustrated by Figure 5.7. The concrete enclosure is essentially the same for the ANSYS and the COBRA-SFS models, except for the interior dimensions of the post-collapse structure. For the ANSYS model, the size of the enclosure is expanded to accommodate the diameter of the impact limiters, while in the COBRA-SFS model, the concrete overlays the package body.

As illustrated in Figure 5.7, the space between the package and the concrete structure is modeled as an air channel, roughly analogous to the air flow pathway in a ventilated concrete storage module. The main differences are that the orientation is horizontal, and the geometry of the concrete “annulus” is decidedly irregular. Heat transfer to the environment is modeled as free convection from the exposed surfaces of the concrete roadways and side barrier. For simplicity, the cross-section geometry shown in Figure 5.7 is assumed to extend uniformly over the axial length of the package, and the “edge” of the model where the upper span touches the

lower roadway is treated as an adiabatic boundary. Both assumptions are conservative, as they limit or eliminate potential paths for heat to be transferred from the package by conduction through the concrete.

5.4 Structural Models for the MacArthur Maze Fire Scenario

The structural evaluations undertaken to determine the potential consequences of the MacArthur Maze fire scenario focus on two main issues. The first issue is to evaluate the effect of dropping a section of the I-580 roadway onto a SNF package that has been subjected to a fully engulfing fire. This accident scenario differs significantly from the HAC drop scenarios postulated in 10 CFR 71, and it is necessary to determine whether or not this real-life accident scenario is bounded by the postulated accidents defined in the regulations. The second issue is the structural response of the package to the extraordinary thermal load imposed on the package closure lid bolts and on the impact limiter attachment bolts in this fire scenario. The severity and duration of the MacArthur Maze fire scenario exceed the postulated HAC fire in 10 CFR 71. Retention of the impact limiters on the package body and the response of the closure lid bolts greatly affect the potential consequences of this fire scenario, if an SNF package were to be subjected to such severe conditions.

Evaluation of these two important issues requires modeling approaches on two different scales. The drop scenario evaluations require large-scale modeling of the package and roadway structures. These models are described in detail in Sections 5.4.1, and include both the roadway and the SNF package. The bolt response evaluations require detailed modeling of the regions of the package containing the impact limiter attachment bolts and the lid closure bolts. These evaluations use two independent approaches to evaluate this issue, initially using classical bolt modeling studies, and then developing detailed FEA modeling of these structures in the GA-4, with boundary conditions provided from the thermal modeling of the package. The classical modeling and preliminary FEA modeling is described in Section 5.4.2 and the detailed FEA modeling is described in Section 5.4.3.

5.4.1 Structural Models for Roadway Drop Scenarios

This modeling study is a three-dimensional impact analysis evaluating the effect of dropping a section of the I-580 roadway onto the SNF package, which has been subjected to a fully engulfing fire at 2012°F (1100°C). The structural impact models were developed using the LS-DYNA code (Livermore Software Technology Company 2007) to simulate the impact of the falling overhead I-580 span on the SNF package positioned beneath it on the lower I-880 roadway. This includes appropriate models of the roadway segments involved, and of the SNF package. These models were used to evaluate the potential for gross structural failure of the package, which could affect the containment boundary. The structural models of the roadway are described in Section 5.4.1.1, and the model of the SNF package is described in Section 5.4.1.2.

5.4.1.1 Modeling of Roadway Segments

The potential effects of the collapse of the overhead roadway onto the SNF package is investigated in this analysis by modeling a free-fall drop of the I-580 roadway span between Bent 19 and Bent 20 onto a structural model of the GA-4 package on the lower I-880 roadway. The partial collapse of the span between Bent 18 and Bent 19 was not modeled, as it would result in a much less severe impact on the SNF package. Based simply on the physical forces

involved, the slower partial collapse of the span between Bent 18 and Bent 19 could not impart as much energy to the SNF package as the rapid free-fall drop of the first span to collapse, and therefore would not have the potential to do as much damage.

For analysis of the drop scenario, the structural model in LS-DYNA consists of the upper I-580 roadway span between Bent 19 and Bent 20, the lower I-880 roadway segment beneath the overhead span, and the SNF package at rest on the I-880 roadway. Figure 5.13 shows a conceptual diagram of the impact model geometry. Each object is represented with a minimum amount of detail to make the calculation size manageable. The upper I-580 span and the I-880 span are modeled with similar components, but the upper I-580 span includes more detail, higher element resolution, and represents the steel girders with material properties that reflect the much higher temperature reached by the girders in the fire scenario.

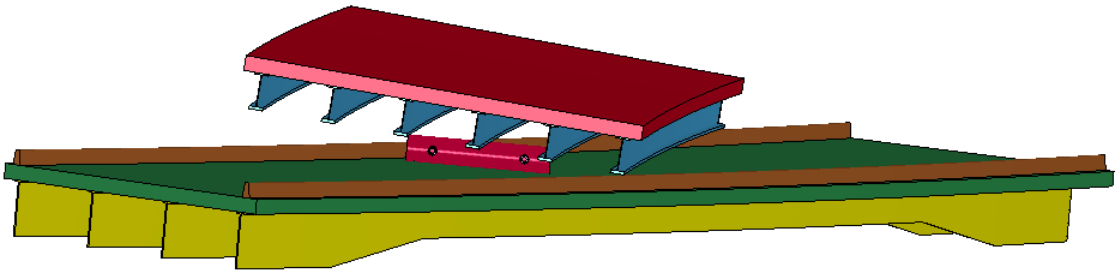

Figure 5.13. Impact Model Geometry

The level of detail in each component reflects its function in the model. The falling I-580 girders need greater element resolution because they impact and deform around the package and the roadway side barriers. The fine mesh is illustrated in Figure 5.14 and in Figure 5.15, which more clearly shows the increased mesh density in the two girders that impact directly on the SNF package. The girders of the I-880 roadway (also shown in Figure 5.14) are represented with a much coarser mesh, as they are needed only to provide a supporting surface with realistic stiffness beneath the package.

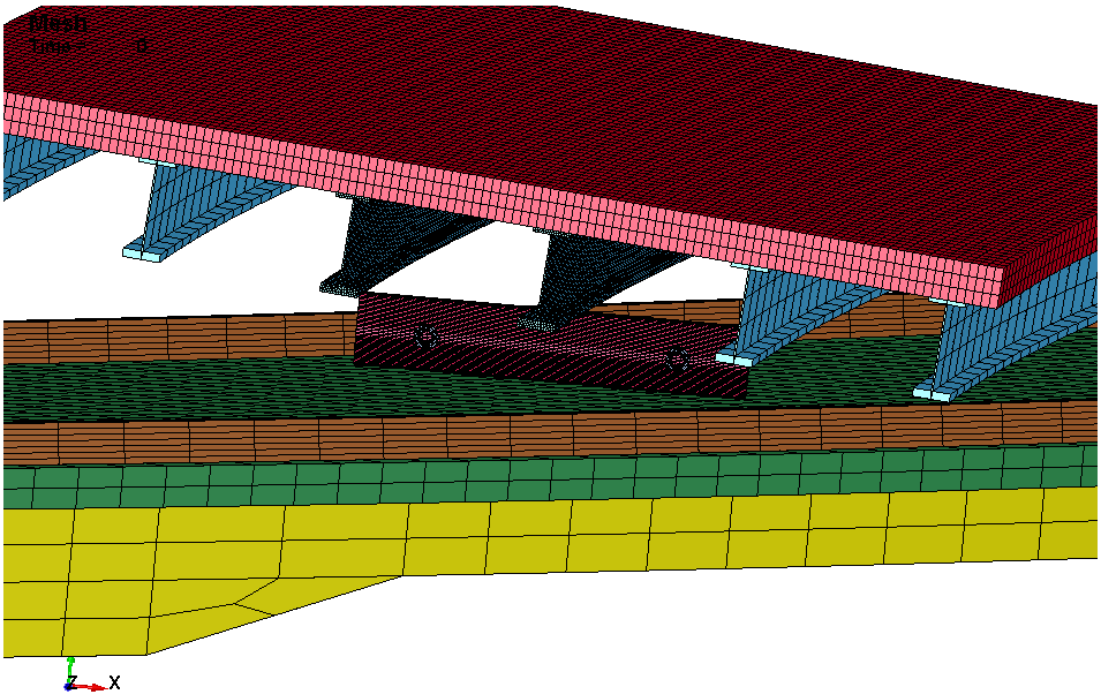

Figure 5.14. Impact Model Mesh

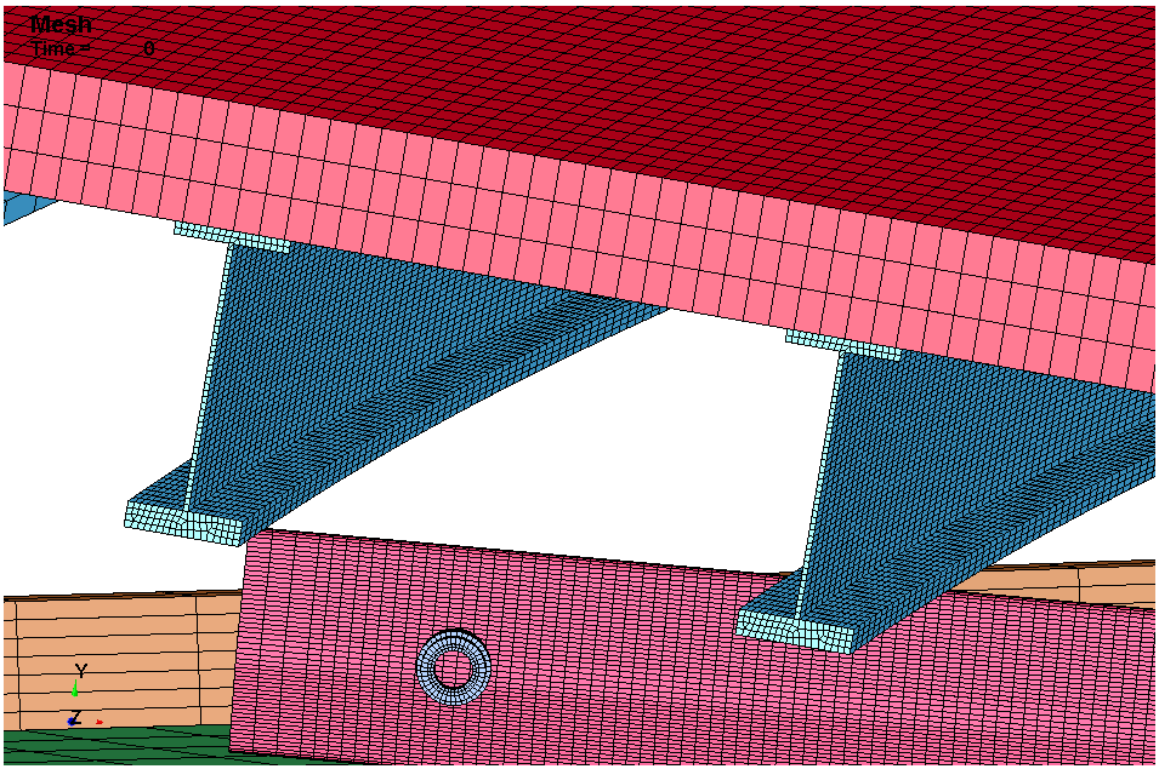

Figure 5.15. Impact Model Mesh Density in Impact Region

The upper I-580 roadway span between Bent 19 and Bent 20 is modeled as a deformable impact object, using geometry information from the original plate girder design drawings. The plate girders are the most important components of the overpass system for the impact modeling because these are the roadway structures that would contact the package directly in any potentially damaging drop scenario. The longitudinal girders are modeled with the major I-section plates connected as continuous material. Small lateral stiffening webs and the lateral plates and crossing members that connect to the longitudinal girders are neglected. This modeling approach is based on post-fire photographs (CHP 2007) showing that the main girder plates remained attached to the underside of the roadway but the stiffening ribs and cross members tended to fail or separate. Under localized impact, these components would be expected to fail without significantly influencing the impact response of the system.

Figure 5.16 shows a diagram of the mesh for the lower roadway (I-880) portion of the impact model. The finite element representation is similar to the upper roadway span, but with a coarse mesh density. A broad rigid surface (omitted from the diagram, for clarity) is also included in the model at ground level, to catch the end of the upper roadway that hangs over the edge of the lower roadway. In the impact analysis, the results show that one end of the falling roadway impacts the package while the other end continues falling until it hits the ground. This results in a significant bending of the falling span along the edge of the lower roadway. The purpose of this modeling effort does not extend to matching the final resting state of the fallen span, but it is a useful verification of the modeling fidelity that the overall behavior predicted with this model is consistent with the post-fire images of the fallen span, such as the one shown in Figure 1.1.

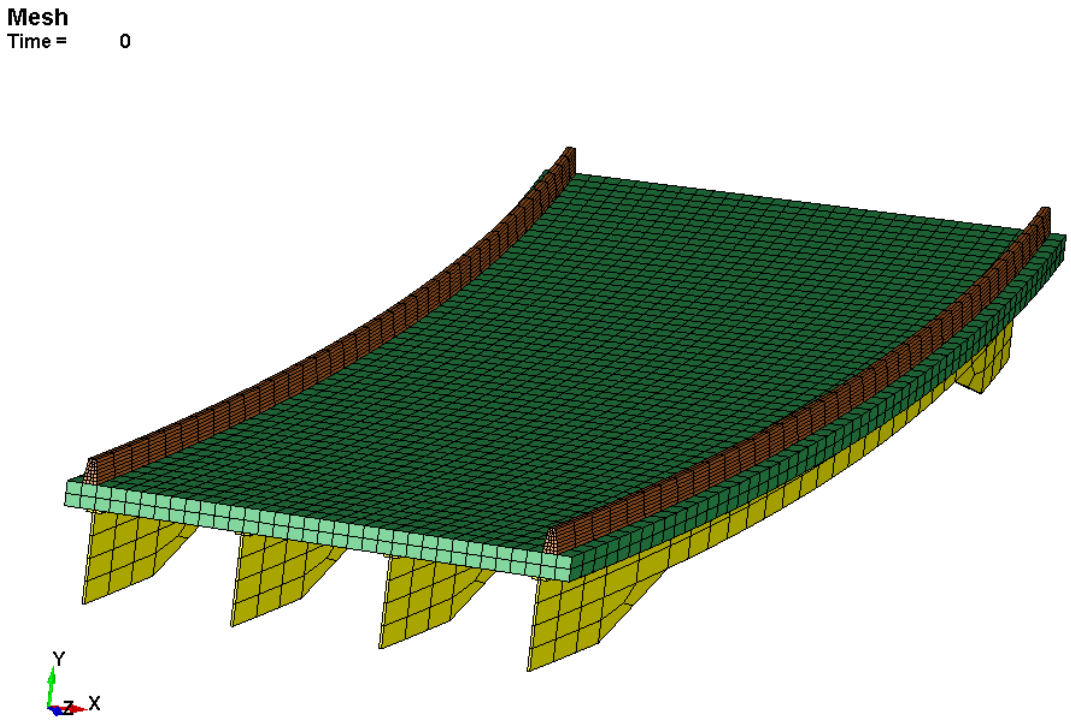

Figure 5.16. Model Mesh of Bottom Roadway (I-880) Segment

The concrete and rebar of the I-580 roadway is modeled as a homogenized linear-elastic material with an artificially low modulus of elasticity. Actual concrete behavior during the impact would be more complex, with concrete fracturing and breaking apart, but these nonlinear effects absorb energy and would reduce the amount of energy available to do damage to the package. The low elastic modulus for the upper roadway concrete results in the weight of the upper roadway acting on the plate girders through the full period of impact. Treatment of the roadway as a linear-elastic material is conservative in that it contributes to higher and more prolonged impact forces than would be obtained with a more physically realistic nonlinear model.

The steel girders of the upper I-580 roadway span are represented as elastic-plastic material, with temperature-dependent mechanical properties to account for effects of the elevated temperatures due to the fire. A uniform temperature distribution is assumed for the final set of analyses, so the material properties do not vary spatially. Tiebreak contact definitions are used in the model to attach the roadway to the plate girders. These are virtual links in the model that connect a node to a surface until a specified reaction force is exceeded, at which point the node is free to move away from the surface. However, even in cases when the tiebreaks fail due to excessive normal or shear force, the plate girders and roadway still detect contact with each other and all other components in the model through an all-inclusive general contact definition.

The falling span is subjected to constant acceleration due to gravity and a specified initial downward velocity that depends on the placement of the cask on the lower roadway. It is assumed that the overpass section falls straight down and the cask is resting on the I-880 roadway surface. Sagging of the girders before collapse is not considered, as it would reduce the potential freefall distance and associated impact velocity. The selected location and orientation of the cask dictates the distance the overpass can fall before it makes contact with the cask. That freefall distance and the initial location of the bridge span in the model dictates the initial velocity, which averages 30 ft/s (9.1 m/s) for the four impact scenarios considered.

If it were assumed that the package remained on the conveyance, the drop distance would be about 3.3 ft (1 m) less, resulting in a lower impact velocity (approximately 15 ft/s [4.41 m/s]), and therefore lower kinetic energy upon impact. In addition, the crushing of the conveyance would absorb some of the impact energy. The modeled drop assumes an uninterrupted fall onto the package on the roadway surface, neglecting all factors that might mitigate the force of the impact, including drag effects. These conservative assumptions result in a much more damaging drop scenario than could occur in reality in this accident scenario.

The support columns initially holding up the upper I-580 roadway span and the lateral box beam spanning the Bent 19 support columns are conservatively neglected in the model, since they have essentially no effect on the impact scenario. Based on post-fire photographs (CHP 2007), the box beam remained attached to the partially collapsed span between Bent 18 and Bent 19. As noted above, the partial collapse of that span was not analyzed in the impact model because the impact loads would be much smaller than in the case of the freefall of the span between Bent 19 and Bent 20.

The lower I-880 roadway is conservatively modeled to provide a foundation of appropriate stiffness beneath the package. It consists of a set of plate girders supporting the concrete roadway, with the ends of the plate girders fixed in space. The model also includes the concrete barriers on either side of the roadway deck. All materials of the lower roadway are treated as linear-elastic, and are represented with properties at 80°F (27°C) nominal temperature. This conservatively neglects temperature-dependence of the material properties of the lower roadway, which would be more compliant at higher temperatures. In the model, the

girders and side barriers are connected to the concrete roadway by tied surface definitions. Tied surface constraints effectively bond two surfaces by forcing the nodes of the “slave” side to maintain their relative spacing with the nodes of the “master” side. This type of connection persists throughout the analysis, unlike the tiebreak connections used in the upper roadway that allow the connection to end when the forces required to maintain the connection exceed a prescribed limit.

Conservative estimates of temperatures were obtained for the girders in the drop calculations, based on the results of thermal analyses to determine fire effects on the overhead girder temperatures. For the girders, a conservative temperature would be as low a temperature as can be reasonably postulated; at lower temperatures, the steel is stronger and therefore able to impart more energy to the package. Based on sensitivity studies of the effect of the fire on the overhead span prior to falling, a uniform temperature of 1800°F (982°C) was assumed for the girders and the upper I-580 roadway. The development of this important boundary condition is discussed in detail in Section 6.4.1. The peak temperature on the I-580 girders may have been higher than 1800°F (982°C), possibly as high as 2462°F (1350°C), but for the purposes of this analysis, the lower estimate of the girder temperatures is conservative, compared to assuming higher temperatures. Because of the temperature-dependent properties of steel (see Figure 2.10 for yield strength versus temperature), the lower temperature assumption results in a more rigid overhead span, and hence a more severe impact on the package.

5.4.1.2 GA-4 Package Model for Structural Analysis

The GA-4 package model is simplified to represent only the components that give it structural integrity. These are the steel package body, the DU gamma shield, and the lifting trunnions attached to the steel body. The fuel assemblies and FSS structure within the package cavity are neglected, as they would have limited effect on the package response to an external impact. The impact limiters and the fragile steel shell of the neutron shield tank are also ignored in this simulation, as a conservative simplifying assumption, since the effect of these structures would be to absorb energy as they crumpled under the impact of the overhead span.

The XM-19 stainless steel package body is a long rectangular box with rounded corners, with four lifting trunnions attached near either end, on the rounded corner edges. Figure 5.17 shows a diagram of the mesh used to represent the package for the calculations with LS-DYNA. The lid and flange region is treated as a solid volume of steel, without the physical interface between the two components, resulting in a fully enclosed package body. Realistic interaction between the lid, flange, and lid bolts is not captured in this model. The behavior of these components is investigated separately, using models described in Sections 5.4.2 and 5.4.3.

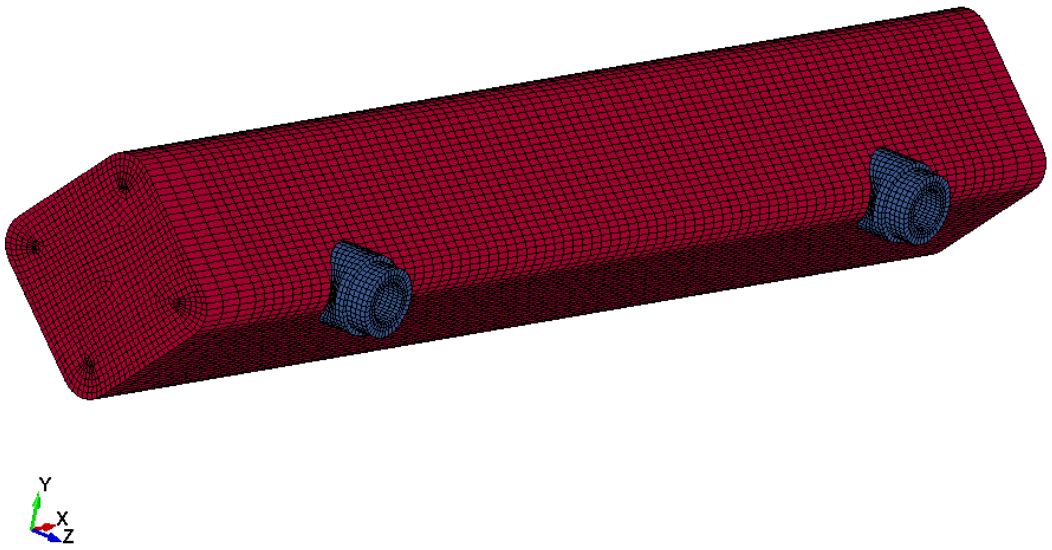

Figure 5.17. Model Mesh of the GA-4 Package Body

The DU gamma shield is modeled inside the package as a single free-moving body, since this component is enclosed within the XM-19 stainless steel cask body but is not physically attached to it. Figure 5.18 shows a diagram of the DU gamma shield mesh in the model. A small gap exists between the inner package wall and the gamma shield, on the order of 0.04 inches (1 mm), as represented in the design drawings from the SAR (General Atomics 1998). Dimensional changes in the package due to thermal expansion are neglected in this analysis, as their effect is minimal in a model with this level of detail.

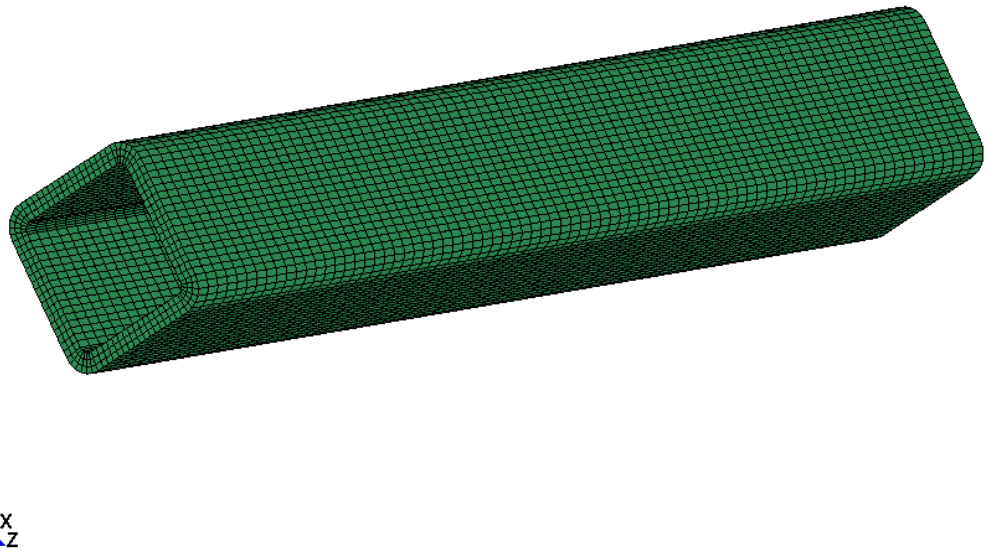

Figure 5.18. Model Mesh of the DU Gamma Shield

The connection between the trunnions and the package wall are represented with tied surface definitions. In the model evaluations, the outer faces of the trunnions are constrained to prevent the package from rolling under the impact of the overhead span. This forces the impact with the descending span to occur on the uppermost corner of the package cross-section, as a conservative assumption to localize the impact interaction.

Conservative estimates of temperatures of the GA-4 package were obtained for the drop calculations, based on the results of the thermal analyses of the package. For the package, a conservative temperature would be as high a temperature as can be reasonably estimated, as the material of the package will then be weaker, and therefore less able to absorb the force of the impact without damage. A temperature significantly above the hottest steel body temperatures calculated in the thermal analysis of the GA-4 package in the MacArthur Maze fire scenario was specified for the GA-4 package body, to obtain a conservative representation of the potential effect of the impact. A detail description of boundary conditions for the structural calculations is included in Section 6.4.

5.4.2 Preliminary Models for GA-4 Bolt Thermal Expansion Calculations

Preliminary models were developed to investigate the response of the package bolted connections to the extremely high temperatures of this fire scenario, since failure of these bolts could potentially affect containment integrity of the package. There are two critical concerns for the GA-4 package in this fire scenario; the retention of the impact limiters throughout the entire transient, and performance of the package closure lid bolts.

The impact limiter attachment bolts were evaluated to determine if these fasteners would be expected to hold at the elevated temperatures of this fire scenario. Failure of these bolts could potentially result in separation of the impact limiters from the package, which (for the top impact limiter) would subject the lid closure bolts to direct exposure to the engulfing fire. This would result in significantly higher temperatures for the lid closure and closure bolts than are predicted during the fire if the top impact limiter remains in place.

The evaluations of the behavior of the impact limiter connection bolts and of the package lid closure bolts consisted primarily of studies of the effect of differential thermal expansion on bolt loading. Temperatures for the bolts and surrounding structures were determined from results of the detailed transient simulations of the fire scenario with the ANSYS and COBRA-SFS thermal models. A diagram of the impact limiter geometry, with the locations of the attachment bolts indicated, is shown in Figure 5.19. (Note that this diagram is not to scale; the size of the bolts relative to the impact limiter is greatly exaggerated for clarity of illustration.) These bolts thread into an anchor plate that is attached to the steel body wall of the GA-4 package. Figure 5.20 shows a close-up view of the package closure lid and bolts, from the exploded view diagram of the entire package (shown in Figure 5.1).

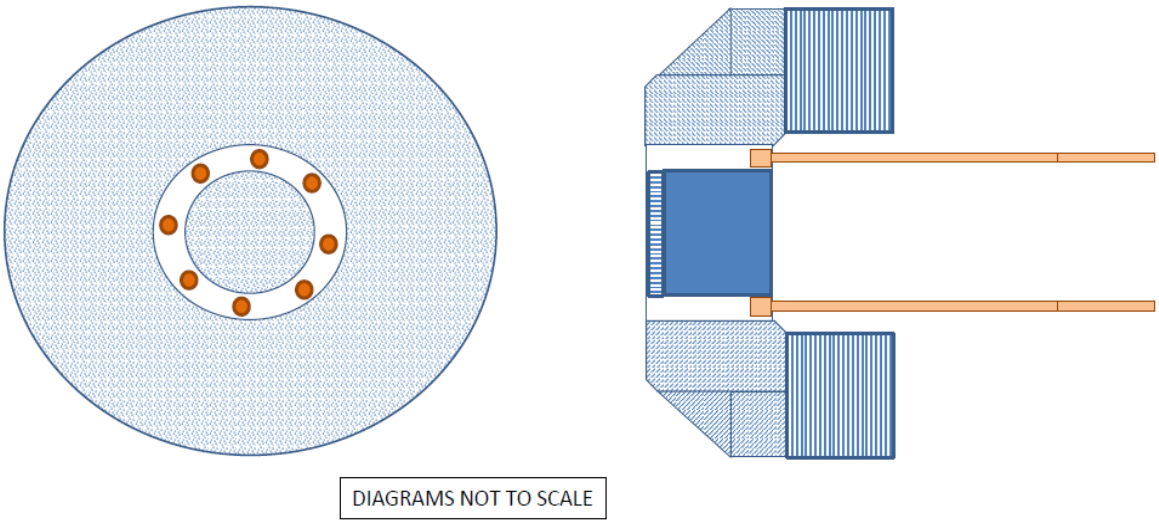

Figure 5.19. Diagram of Impact Limiter, Illustrating Attachment Bolts

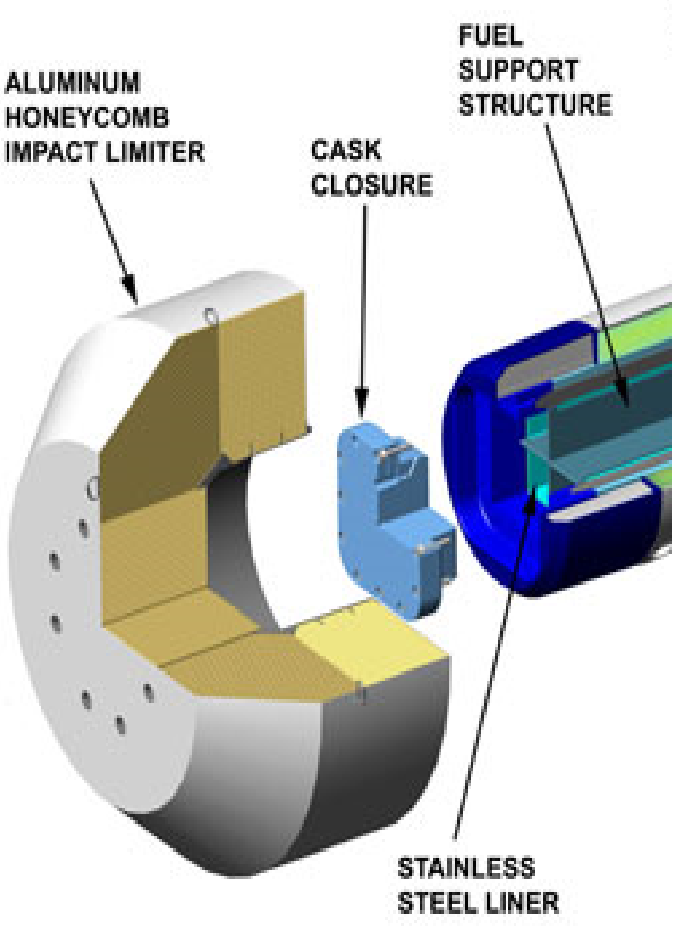

Figure 5.20. Package Closure Region, Showing Package Closure Lid and Bolts

The performance of the lid closure bolts was evaluated assuming that the impact limiters would be retained throughout the fire scenario, since the results of the evaluations of the performance of the impact limiter attachment bolts (as discussed in Section 7.0) shows conclusively and conservatively that the impact limiter attachment bolts would not fail in this fire scenario. The impact limiters therefore act as “friend and foe” to the closure lid during this fire scenario. During the fire, the impact limiters shield the package lid from the extreme temperatures of the fire, and therefore limit the temperature rise on this structure during the fire. In the post-fire cooldown, however, the impact limiter is an extremely effective insulator, and package temperatures in this region continue to rise for many hours after the end of the fire, as the extreme heat developed in the package body and internal structures during the fire naturally conducts toward the lower-temperature ends of the package. Evaluations of the closure bolts were undertaken to determine the response of the closure connection to the long exposure to elevated temperatures in the complete fire scenario, since the effect of the fire scenario on these bolts could potentially result in failure of package containment.

Both sets of attachment bolts are Inconel 718, a nickel alloy (General Atomics 1998). The closure lid is secured with 12 bolts; 3 per side of the square cross-section of the lid. The impact limiter is attached with 8 bolts, uniformly spaced in a circular ring. The package body flange that receives the lid closure bolts is XM-19 stainless steel, as are the anchor plates that the impact limiter bolts thread into. In both sets of connections, steel helical thread inserts are used to make the connection between the bolt threads and the matching threads of the package body flange (for the lid closure bolts) or anchor plate (for the impact limiter bolts).

The threaded inserts are ASTM Type 304 stainless steel. Inconel 718 and XM-19 stainless steel both retain their strength better than Type 304 stainless steel as temperature increases, which makes the threaded inserts a weak link in the threaded connection at elevated temperatures. In addition, the coefficient of thermal expansion for the nickel alloy of the bolts is significantly less than that of XM-19 stainless steel, so elevated temperatures will cause an increase in bolt tension and thread shear load. This issue is further complicated by the large thermal gradients predicted in the impact limiter attachment bolts, based on the results of the thermal analyses of the GA-4 package in the MacArthur Maze fire scenario.

For both the closure bolts and the impact limiter bolts, a preliminary evaluation was performed using classical mechanics equations to calculate bolt tension at a series of uniform temperature states. The coefficient of thermal expansion mismatch between the bolt material and the flange or anchor material results in an increase in tension in the bolt shank, which must be supported by an opposing shear force on the bolt threads. The strength of the materials is a function of temperature, so the yield and failure thresholds vary with time and changing temperature in this fire scenario. One concern in each case is the yield and failure limits of the bolt shank. The shear strength of the bolt threads are not a concern because the Type 304 thread inserts are weaker for all temperatures, and therefore would be expected to yield before the bolt threads. A classic thread-stripping equation is used to relate bolt tension to total shear force on the threaded interface.

The closure bolts and the impact limiter bolts can yield without actually failing in this scenario. Bolt materials are expected to have sufficient ductility to reduce the design-basis tensile load to zero without failing, as a general design criterion. Only if the tensile load could not be relieved sufficiently by yielding, and the residual load after yielding was still high enough to exceed the ultimate strength of the bolt material, would the bolt be expected to fail. For the closure bolts, a potential consequence of bolt failure is an unattached package closure lid. For the impact limiter bolts, potential consequences of bolt failure include detachment of the impact limiter from

the cask. In either case, failure of the bolts would indicate significant potential consequences in the overall evaluation of the MacArthur Maze fire scenario.

The preliminary evaluations provided an initial indication of the bolt response to the MacArthur Maze fire scenario, but additional evaluations were also undertaken using finite element models, to obtain a more complete understanding of the potential consequences of this fire scenario. For the impact limiter bolts, the uniform temperature assumption used in the initial evaluations was determined to be overly simplistic, due to large temperature gradients along the length of the bolt and surrounding material. To investigate the effect of these temperature gradients, a fully three-dimensional FEA model of the impact limiter bolt as it connects into the package was developed using ANSYS, to analyze the structural and thermal response of a bolt and the local surrounding material. Figure 5.21 shows meshing diagrams of the impact limiter bolt model developed for this analysis. Temperature distributions along the axial length of the bolts, obtained from the detailed ANSYS thermal model of the package, were incorporated into evaluations with this impact limiter bolt model.

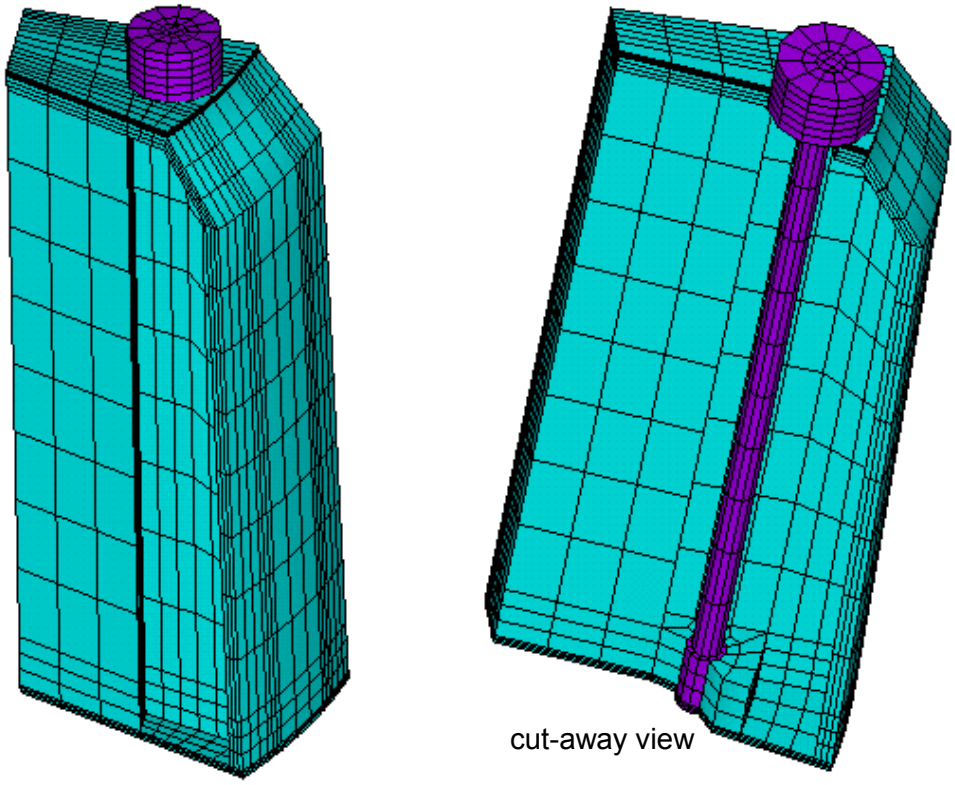

Figure 5.21. Model Mesh of Impact Limiter Bolt

In the evaluation of the results obtained with the preliminary models for the response of the closure bolts in the fire scenario, it was determined that the evaluation using mechanics equations was excessively conservative, and did not yield a sufficiently detailed picture of the consequences of the bolt response to this fire scenario. Therefore, additional, highly detailed FEA modeling was undertaken for the end region of the package, including the closure lid, steel body flange, and closure bolts. The modeling developed for this evaluation is described in Section 5.4.3.

5.4.3 Detailed Models for GA-4 Closure Lid Bolt Evaluations

The results of the preliminary models evaluating the behavior of the bolts attaching the impact limiters to the package show conclusively that the impact limiters would be expected to remain in place during the severe conditions of this fire scenario. In addition, the preliminary models show that even with extremely conservative assumptions, the bolts fastening the closure lid will not fail due to stresses related to differential thermal expansion of dissimilar materials. However, the simplifications and conservatisms in the preliminary models do not provide results with a sufficient level of detail to determine the detailed history of the clamping force the bolts impart to the lid/flange interface throughout the fire scenario. These analyses therefore cannot provide a means of obtaining a reliable estimate of the size of any potential leakage pathway for the contents of the package to escape to the environment.

This is crucial to determining the potential consequences of the MacArthur Maze fire scenario, and an additional detailed study was undertaken to develop a realistic evaluation of the closure bolt response over time. Evaluation of the closure force on the flange for the entire duration of the fire scenario, including the post-fire cooldown to a new ambient steady-state, can be used to determine a meaningful evaluation of the potential effect on package containment for the conditions postulated in this fire scenario.

Section 5.4.3.1 describes the modeling approach used in the preliminary evaluations. Section 5.4.3.2 presents the detailed FEA model developed for this most important evaluation in the overall study of the potential consequences to an SNF package of an accident of the magnitude of the MacArthur Maze fire scenario.

5.4.3.1 Modeling for Preliminary Closure Lid Bolt Evaluations

Classic bolt equations and analysis methods were applied to evaluate the response of the closure lid, bolts, and flange to the conditions of the MacArthur Maze fire scenario. In this context, “classic” refers to the set of equations that define bolt and flange loading, and can be found in any comprehensive engineering textbook on the subject, or as closed form equations generally used in the literature. The primary reference relied upon in this study was *Fundamentals of Machine Component Design* by Juvinall and Marshek (Juvinall and Marshek 1991).

The classic bolt calculations for the GA-4 closure bolts were used to determine estimates of the bolt tension and clamping force over time, extending from initial steady-state normal conditions of transport (NCT), through the fire transient, and on out through the long post-fire cooldown. These evaluations considered all three types of loads that these fasteners would be expected to experience in the MacArthur Maze scenario, which consist of the following:

- the preload caused by the initial torque on the bolts (as per the package manufacturer’s technical specifications),
- the external load caused by the internal gas pressure within the package cavity, and
- the thermal load due to the dissimilar coefficients of thermal expansion of the materials of the XM-19 stainless steel closure lid and flange, and the Inconel bolts.

The effect of the Type 304 stainless steel thread inserts was also taken into account, with sensitivity studies of the effect of this interfacing component on joint stiffness.

5.4.3.2 Modeling for Detailed FEA Evaluations of Closure Lid Bolt Response

In this evaluation, it is important to note a particular feature of the lid closure bolts of the GA-4 package. They are referred to as "bolts" in the SAR, and to avoid confusion this terminology is also used in the current study, but these fasteners are in fact used as ***screws***, since they are threaded into tapped holes in the steel flange of the package body. In order for these fasteners to function as ***bolts***, they would have to pass through the flange of the steel package body and thread into nuts on the other side. The design of the GA-4 package body does not allow this configuration for the fasteners holding the lid in place.

The distinction between "bolts" and "screws" for the GA-4 package closure lid is not particularly relevant to the preliminary evaluation using classic bolt equations. Both types of threaded fasteners generally perform the same function and are subject to the same family of equations for determining thread stripping, initial torque to a specified pre-load, and sizing to withstand an external load. The details of the physical configuration of the fasteners only becomes important in the FEA modeling undertaken to obtain a more accurate and detailed evaluation of the response of these fasteners to the extreme conditions of the MacArthur Maze fire scenario.

As with the FEA model of the impact limiter bolt, described in Section 5.4.2 above, radial symmetry was assumed in the loading of the closure lid bolts throughout the MacArthur Maze fire scenario. Significant gradients are present only in the axial direction, parallel to the axis of the bolt shank. This allowed the modeling simplification of representing only a single bolt. To reduce the model to a more tractable computational size, it was further assumed that an individual bolt was essentially radially symmetric, and could be appropriately modeled with a one-quarter section of symmetry, as shown in Figure 5.22, illustrating the model geometry of the bolt, lid and flange. This illustration also includes a close-up image of the modeling of the helical coil of the Type 304 stainless steel thread insert filling the thread patterns of the conjoined bolt and flange. The lid and flange are represented as an annulus with an outer diameter equal to 2.7 inches. This corresponds to a minimum annulus area of about 4.6 square inches, which is effectively equivalent to the estimate used in the classic bolt equations.

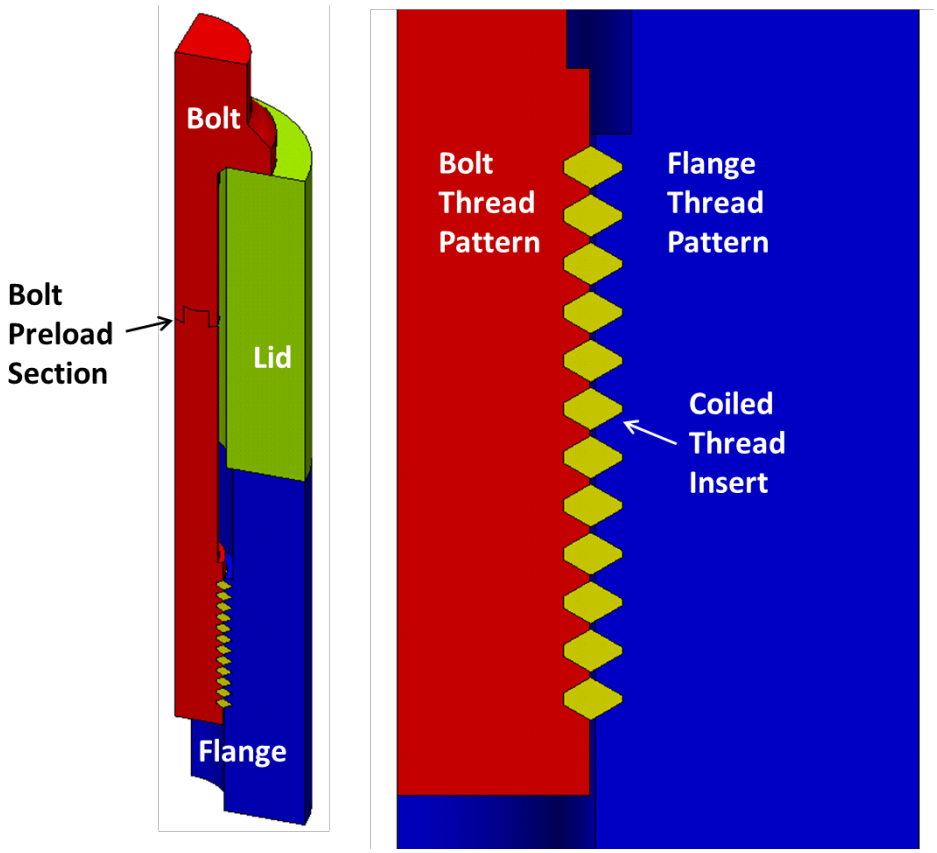

Figure 5.22. Finite Element Model Geometry for Closure Lid, Flange, and Bolt, including Thread Insert

The mesh density in the region of the threaded interface and thread insert is shown in detail in Figure 5.23. The yellow ovals indicate the surfaces where the threads and inserts are joined with degree-of-freedom couples. This forms a perfect bond between the materials (in all three directions) at the load-bearing surfaces and permits the other surfaces to separate. The use of more advanced contact surface behavior was considered to be unnecessary based on the results obtained using this simpler method. The octagonal shape of the thread inserts is primarily defined by the thread flanks, which are assumed to have spacing and angles defined by standard thread characteristics (Oberg et al. 2004). The thread flanks end at the minimum diameter of the external bolt thread and the maximum diameter of the internal flange thread. The bolt-side threads and flange-side threads are also assumed to be sized as per standard bolt threads, so the two sides have a mating geometry rather than an identical geometry. The bolt threads have a shear area that is proportional to 3/4-pitch. The flange threads have a shear area that is proportional to 7/8-pitch. This is consistent with the preliminary calculations using the classical equations for bolt modeling, in which it was assumed that the critical shear area for the insert occurs at the maximum diameter of the bolt thread and corresponds to 7/8-pitch.

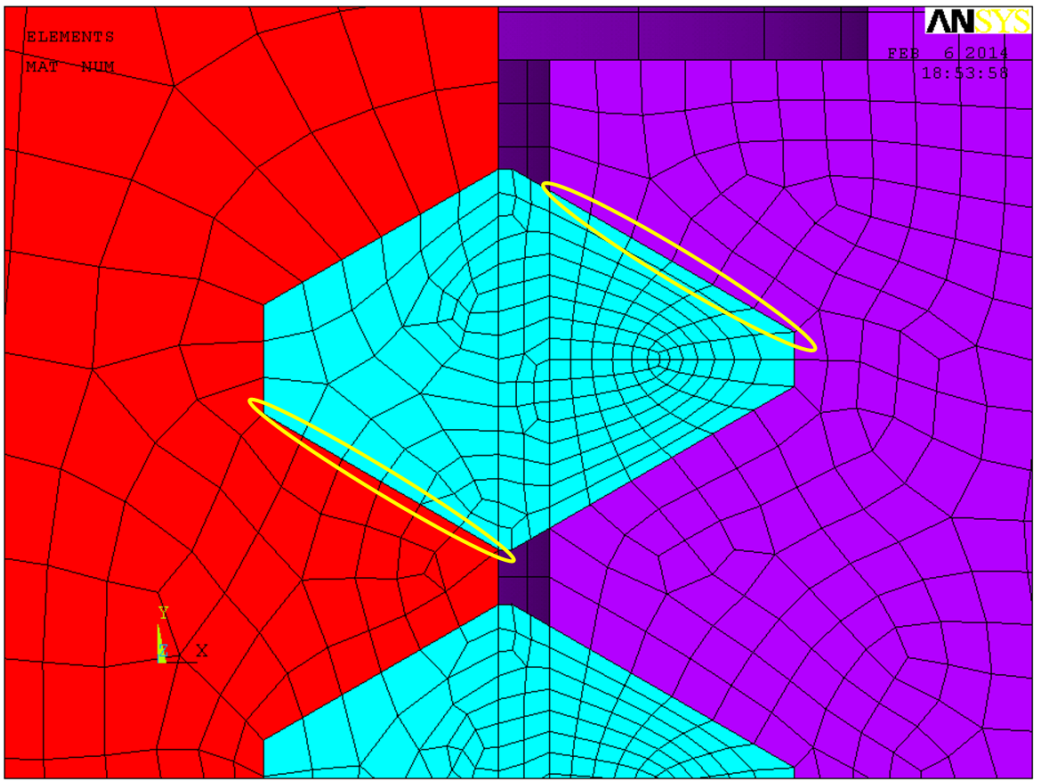

Figure 5.23. Detailed FEA Mesh in Thread Insert Region, Showing Bonded Surfaces

This detailed FEA model was used to perform evaluations to determine the effect of the MacArthur Maze fire scenario on the integrity of containment of the GA-4 package, as determined by the clamping force on the closure lid throughout the transient. Sensitivity studies were performed on the effect of assuming linear or non-linear material properties for the thread inserts. Additional cases were developed, to evaluate the causes of differences between results obtained with the detailed FEA model and those obtained with the classical bolt equations, to verify that differences were due to more realistic modeling, and assess the conservatism of the simpler modeling approach.

6.0 ANALYSIS METHOD

The detailed analysis models described in Section 5.0 were developed for evaluation of the GA-4 package performance if exposed to the severe conditions of the MacArthur Maze fire. For the thermal analyses, the models account for all significant heat transfer paths to and from the package by means of conduction, convection, and thermal radiation during the fire and in the post-fire cooldown. For the structural analysis, the models provide a conservative representation of the response of the package to the impact of the overhead roadway span that collapsed at 17 minutes into the fire. The structural analysis also includes evaluation of the effects of the thermal expansion mismatch between package closure flange and the closure bolts, and between the impact limiter anchor plates and the impact limiter bolts. The temperatures and temperature distributions in the bolts and associated package components are based on thermal model results. All of these various analyses using different analysis codes and physics regimes taken together provide an overall evaluation of the GA-4 package response to the Macarthur Maze fire scenario.

This section presents the initial conditions, modeling assumptions, and boundary conditions used to predict the response of the GA-4 package to the MacArthur Maze fire scenario. The first three sections focus on the package thermal model conditions. Section 6.1 presents the steady-state temperature results for NCT predicted with the ANSYS and COBRA-SFS models of the GA-4 package, with and without impact limiters, respectively. Section 6.2 describes the significant assumptions and simplifications used in developing the thermal models. Section 6.3 describes the fire scenarios assumed for the transient analyses, and the boundary conditions used for the calculations. The final sections deal with the assumptions, boundary conditions, and methodology particular to the structural modeling. Section 6.4 discusses the package impact analysis.

6.1 NCT and HAC Fire for GA-4 Package

Steady-state analyses for NCT with the ANSYS and COBRA-SFS models of the GA-4 package predict similar peak component temperatures for NCT, within the capabilities of their respective models for the fuel assemblies. The peak cladding temperature predicted with the ANSYS model is 306°F (152°C), and the COBRA-SFS model predicts 293°F (146°C). This is a difference of about 4 percent, and is consistent with the expected differences between the results obtained with a detailed thermal-hydraulic model of the fuel assemblies compared to the results obtained with the k-effective model for the fuel. The k-effective model for the homogenized fuel assembly is designed to yield results that are 5-15% conservative, compared to results obtained with a detailed CFD model of a fuel assembly (Bahney and Lotz 1996).

As a verification test of the accuracy of the geometry and material properties input and boundary condition specification logic, the ANSYS and COBRA-SFS models of the GA-4 package were exercised for the design-basis HAC fire transient defined in 10 CFR 71. This consists of an engulfing fire with uniform flame temperature of “1475°F (800°C)” and fire emissivity of 0.9, lasting 30 minutes. In the SAR analysis for the HAC fire, the initial steady-state assumes an ambient temperature of 100°F (38°C), which is the same as for NCT, but solar insolation is neglected. The solar heat flux is trivial in comparison to the heat input from the fire, and as a modeling convenience, it was included in the analyses with the ANSYS and COBRA-SFS models. The steady-state initial conditions for all transient calculations are NCT; i.e., assuming standard solar insolation (24-hr average solar heat flux) at an ambient temperature of 100°F (38°C).

Boundary conditions for the 30-minute HAC fire were specified for the ANSYS and COBRA-SFS models in essentially the same manner as in the SAR calculation. In general, the results obtained with the ANSYS and COBRA-SFS models are in very good agreement, with differences due mainly to the alternative fuel modeling approaches used in the two analyses. In addition, the omission of the impact limiters from the COBRA-SFS model and their inclusion in the ANSYS model affect the location of the maximum cladding temperature during the fire and influence the post-fire cooldown behavior.

The ANSYS model predicts 455°F (235°C) for the maximum peak clad temperature during the transient, and the COBRA-SFS model predicts 469°F (242°C) near the end of the hottest rod, since this model neglects the impact limiters. In the ANSYS model, the maximum temperature occurs near the axial center of the package. Both of these values are slightly higher than the maximum fuel cladding temperature of 442°F (228°C) reported the GA-4 SAR (General Atomics 1998) for the HAC analysis. The difference is due mainly to simplifications in the SAR analysis that tend to smear out temperature gradients, and thereby reduce the conservatism of the analysis somewhat. However, for this package, the temperatures are low enough in the HAC fire that the difference can be considered insignificant.

6.2 Thermal Modeling Assumptions

Computational modeling requires simplifying assumptions for even the most detailed representation of a physical system. The assumptions used in developing the detailed geometry models of the GA-4 package are discussed in Section 5.0 above. This section summarizes the major assumptions relevant to analysis of the response of this package if it were exposed to the conditions of the MacArthur Maze fire scenario. These assumptions apply to both the ANSYS and the COBRA-SFS models, unless specifically noted otherwise.

1. Initial conditions for the package are defined as steady-state NCT at 100°F (38°C) ambient with insolation, as defined in 10 CFR 71.71. This assumption conservatively neglects the effect of the actual conditions at the time of the MacArthur Maze accident (i.e., at night, with ambient temperature of 50°F [10°C]).

2. The decay heat load in the GA-4 package is assumed to be at its maximum design basis value of 2,105.4 Btu/hr (0.617 kW) per assembly, with a total package decay heat load of 8,423 Btu/hr (2.468 kW). This is a bounding assumption, as the actual decay heat load of an SNF package is typically lower than the design basis configuration.

3. Material properties of package components specified as inputs to the thermal models are listed in Appendix A. These were obtained from the GA-4 SAR (General Atomics 1998), with the following exceptions;

    a. The temperature-dependent thermal conductivity values used in the SAR for XM-19 stainless steel are lower-bounding values based on properties of high alloy steels[1]. At NCT, the thermal conductivity values from the SAR are approximately 20% below values published in material data sheets for XM-19 stainless steels. This is conservative for the NCT analysis, but is non-conservative for the fire analysis, since the lower bounding thermal conductivity would result in a lower rate of heating of the package during the fire.

[1] The SAR values used for thermal conductivity of XM-19 steel are from Material Group E “high alloy steels” in Table I-4.0 of the ASME code, 1986.

Therefore, thermal conductivity values specific to XM-19 steel[1] were used in the fire analyses.

b. The thermal conductivity for DU reported in the SAR is for a temperature of approximately 100°F (68°C), and does not take into account the significant increase in thermal conductivity with increasing temperature for this material. As with XM-19, this is a conservative approximation for NCT, but is non-conservative for fire analysis. Therefore, temperature-dependent thermal conductivity values were used for the DU in the thermal analyses, as documented in Appendix A.

4. Clearance gaps within the package (e.g., between the steel inner liner and the DU gamma shield, between poison rods and the steel plates of the cruciform basket) are modeled at "as built" values, based on design drawings.

   a. Gaps are assumed closed due to thermal expansion during the fire transient, to conservatively maximize heat transfer into the package.

   b. Gaps are assumed open, and at nominal "cold" values during the cooldown portion of the transient, to conservatively limit heat removal from the package.

5. The content of the neutron shield tank is conservatively represented to maximize heat transfer through this region during the fire, and minimize it during the post-fire cooldown.

   a. Initial steady-state is represented with the effective conductivity model from the SAR, to account for natural circulation of the neutron shield liquid. This model is used in the fire transient until the peak liquid temperature reaches 276°F (136°C), the saturation temperature corresponding to the maximum operating pressure for the tank.

   b. The liquid is assumed lost when the predicted peak temperature in the neutron shield region exceeds 276°F (136°C). Thermal energy absorbed in the vaporization of the liquid is conservatively neglected.

   c. After loss of the liquid, heat transfer between the inner surface of the NS tank outer shell and outer surface of the package body is assumed to consist of thermal radiation and conduction through air for the remainder of the fire and post-fire cooldown transient. The inner surfaces of the tank are assumed to be affected by soot, and the emissivity is conservatively specified at 0.9. Mainly because of the high thermal radiation heat flux at the elevated fire temperatures, this results in a higher heat transfer rate into the package through the neutron shield during the fire than would be achieved with only conduction and natural convection heat transfer through the neutron shield liquid, if it were assumed that the neutron shield tank did not rupture during the fire.

6. The exterior surface of the neutron shield tank is assumed to have an emissivity of 0.15, as specified in the SAR, for the initial pre-fire steady-state calculation. At the start of the fire, the package surface emissivity is set to 0.9, to represent the effect of sooting of the outer surface of the package and impact limiters. This value is also used throughout the post-fire cooldown. (This is slightly more conservative than the value of 0.8 to 0.85 documented in the SAR for the package surfaces in the HAC fire.)

7. Convection heat transfer during the fire is conservatively modeled assuming forced convection to the package from the hot external environment. (See Section 6.3.1 for discussion of the specific correlations used.)

[1] Values used are for Allegheny Ludlum ATI 50™ Alloy (UNS S20910), Type XM-19. See the Technical Data Sheet in Appendix A.

8. For the post-collapse configuration (after 37 minutes), the package is assumed to be fully covered by the fallen I-580 span between Bent 19 and Bent 20, while simultaneously exposed to a fully engulfing pool fire with an uniform temperature of 1652°F (900°C). This modeling approach conservatively places the GA-4 package in the most adverse configuration possible relative to the collapsed overhead spans, and at the same time yields a bounding fire exposure for the package.
9. Convection heat transfer from the upper surface of the fallen I-580 roadway in the post-collapse fire scenario is treated as free convection from a horizontal plate with heated surface facing upward. For the lower surface of the I-880 roadway beneath the package, heat transfer is treated as free convection from a horizontal plate with heated surface facing downward. (See Section 6.3.1 for discussion of the specific correlations used.)
10. For the post-fire cooldown portion of the transient, the air temperature is assumed to be 100°F (38°C) with insolation, to conservatively bound long-term ambient conditions.
11. During the fire, the aluminum impact limiters in the ANSYS model are assumed to remain intact within their stainless steel outer shells, and are represented with effective thermal material properties for the honeycomb material, based on bulk density and thermal conductivity of the component materials. This assumption maximizes heat input to the package during the fire by conduction through the impact limiters.
12. After the fire, the elements representing the honeycomb material of the impact limiters in the ANSYS model were modified to account for melting of the aluminum. This assumption maximizes the thermal resistance to heat removal from the package by conduction through the impact limiters. Unmelted portions were treated as a combination of aluminum honeycomb and air, and melted portions were assumed to have the thermal properties of aluminum alloy 5052. It was also assumed that the molten aluminum would settle to the bottom of the impact limiters. The effective thermal material properties of the various elements of the impact limiters affected by melting were calculated using a volume-averaging scheme. (Section 5.2 discusses this modeling approach in detail.)
13. The latent heat absorbed by the honeycomb material in the phase change due to melting was conservatively neglected.
14. The effect of the conveyance carrying the GA-4 package is conservatively neglected, both for the thermal analysis of the effects of the fire and the structural analysis of the effects of the collapse of the upper highway span. In the thermal analysis, the fire is assumed fully engulfing, and any shielding effect that the conveyance might have is neglected. In the structural analysis, the conveyance would tend to increase the compliance of the system, and would also decrease the drop distance between the falling roadway and the GA-4 package. Both factors would mitigate the effects of the impact of the upper roadway falling on the package. The impact is assumed to occur with the package lying on the lower roadway, to maximize the drop distance and the overall stiffness of the system.

6.3 Thermal Boundary Conditions for GA-4 Package Models

The boundary conditions for the thermal analysis define the external environment that the GA-4 package experiences during the fire and post-fire cooldown. These are specifically defined in Section 6.3.1. The boundary conditions for the structural analysis define the physical behavior of the overhead I-580 span that falls onto the SNF package, the temperature of the falling roadway and girders, and the temperature of the package at the time of impact. These boundary conditions are discussed in Section 6.4.

6.3.1 Thermal Boundary Conditions

As described in the detailed description of the fire in Section 2.0, the MacArthur Maze fire began as a large open pool fire that lasted for approximately 17 minutes, until the collapse of the overhead roadway span between Bent 19 and Bent 20. During the following 20 minutes (17 to 37 minutes of the total fire duration), the partial collapse of the span between Bent 18 and Bent 19 reduced the size and extent of the large open pool fire to a much smaller fire in the approximately 12-15 ft (3.7-4.6 m) gap between the collapsed spans at Bent 19. This smaller fire burned steadily until the end of the fire, at approximately 108 minutes.

This fire scenario is conservatively modeled as a fully engulfing fire lasting 108 minutes, with two different constant bounding fire temperatures, as shown in Figure 6.1. For the first 37 minutes, the fire is represented with a uniform flame temperature of 2012°F (1100°C). For the remaining 71 minutes, the fire is represented with a uniform flame temperature of 1652°F (900°C). The fire emissivity is specified at 0.9. This value is also applied to all external surfaces of the package and roadway exposed to the fire, including the inner surfaces of the failed neutron shield tank, to conservatively represent the effect of sooting.

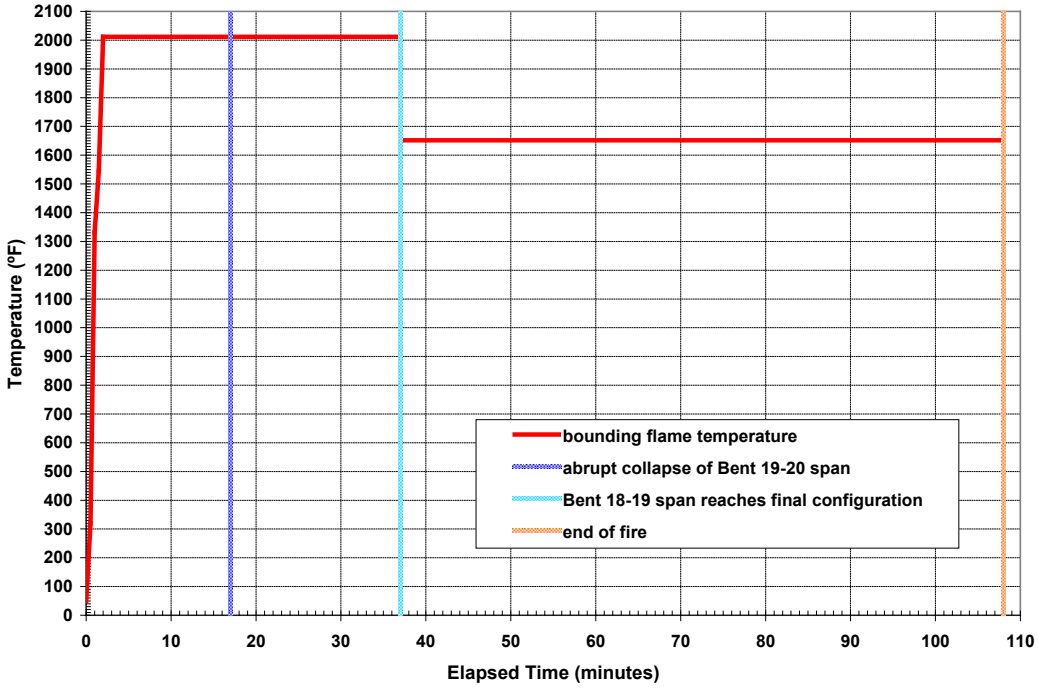

Figure 6.1. Fire Boundary Temperatures

As noted in Section 6.2 in the presentation of modeling assumptions, convection heat transfer at the SNF package surface during the fire was treated in both models as forced convection. Along the package body (for both the ANSYS and COBRA-SFS models) and the sides of the impact limiters (in the ANSYS model), the Nusselt number is defined using a correlation (Kreith and Bohn 2001)[1] for axial flow over a flat or slightly curved surface at zero angle of attack, and has the form

[1] Source reference for this correlation is Kreith; primary references cited in Kreith are Rohsenow, Patankar and Spalding, and Bejan.

$$Nu = a(\mathrm{Re}_L^b + c)\,\mathrm{Pr}^d \quad \text{(turbulent regime; } \mathrm{Re}_L > 5.0\text{x}(10^5),\ \mathrm{Pr} > 0.5) \qquad (6\text{-}1)$$

where

a = 0.036
b = 0.8
c = -23,200
d = 0.3333
L = characteristic length (in this case, the exposed package body or impact limiter side)
Pr = Prandtl Number
Re_L = $\rho U_\infty L / \mu$

where

ρ = fluid density
U_∞ = free-stream external velocity
μ = fluid viscosity

On the package ends (in the COBRA-SFS model), and on the flat ends of the impact limiters (in the ANSYS model), the Nusselt number is defined using a correlation for forced convection from an isothermal disk or circular plate with axis perpendicular to the flow direction (Kreith and Bohn 2001). The correlation has the form

$$Nu = a\,\mathrm{Re}_D^b\,\mathrm{Pr}^c \quad (900 < \mathrm{Re}_D < 30{,}000) \qquad (6\text{-}2)$$

where

a = 0.591
b = 0.564
c = 0.3333
Pr = Prandtl Number
Re_D = $\rho U_\infty D / \mu$

where

ρ = fluid density
U_∞ = free-stream external velocity
D = diameter of disk or plate
μ = fluid viscosity

In the above correlations, fluid properties are evaluated at the near-wall temperature, defined as the average of the wall surface temperature and the ambient temperature, which in this application is the fire temperature. The free-stream external velocity was specified at a bounding value of 12 ft/s (3.7 m/s), based on the velocities predicted in the FDS simulation of the open pool fire.

In the post-fire cooldown, with the package beneath the concrete "blanket" of the collapsed upper roadway span, the boundary conditions on the external roadway surfaces were specified as free convection to ambient still air. For the COBRA-SFS model, the boundary conditions on the SNF package were determined by solving for the flow and heat transfer within the irregular annulus between the package and the concrete roadway surfaces. The air velocity within the annulus was assumed to be essentially stagnant in the post-fire cooldown.

In typical open pool fires, it is conservative to assume free convection to ambient for the post-fire cooldown when evaluating heat transfer from an object such as an SNF package which had been engulfed in the fire. For a horizontal cylinder, correlations typically yield Nusselt number values on the order of 100-200, which for a cylindrical object the size of this SNF package produces heat transfer coefficient values on the order of 0.8 to 1.5 Btu/hr-ft^2-°F (4.5 to 8.5 W/m^2-°K). However, for the package beneath the concrete roadway, this assumption is neither conservative nor correct, since the presence of the roadway would severely inhibit the development of natural convection flow patterns around the package.

In the COBRA-SFS analysis, convection heat transfer in the annulus channel between the package outer surface and interior surfaces of the concrete was represented with a bounding value of Nu = 3.66 for laminar flow, based on experimental studies (Creer et al. 1987) of heat transfer in enclosed spaces within a horizontal package. This approach conservatively treats the "blanket" of the collapsed roadway as an enclosure. After the end of the fire, the hot air in the irregular annular flow channel is assumed to be optically transparent, allowing thermal radiation heat transfer via gray body exchange factors between the package surface and interior surfaces of the overlying upper roadway, side barrier, and lower roadway. The temperature of air trickling into the annulus due to the changing temperature and pressure gradients in the flow channel is assumed to be 100°F (38°C).

In the analysis with the ANSYS model, thermal radiation exchange between the package and the enclosing concrete was calculated directly, as described in Section 5.2.2 above. However, it was assumed that the impact limiters would effectively block air flow within the annulus, so convection heat transfer between the package exterior surfaces and the enclosing concrete surfaces was conservatively neglected. This was modeled by specifying Nu = 1.

The temperatures of the concrete surfaces surrounding the package at the beginning of the cooldown portion of the transient were determined assuming that these structures had also been exposed to the same fire boundary temperatures of 2012°F (1100°C) and 1652°F (900°C), for the same time intervals as the SNF package. This approach establishes bounding concrete surface temperatures for the post-fire cooldown portion of the transient. The effect of spalling of the concrete, which dissipates thermal energy and therefore would tend to result in lower concrete temperatures, was conservatively neglected.

Heat transfer to the external environment from the concrete surfaces of the upper and lower roadways was represented with free convection from these surfaces (Kreith and Bohn 2001)[1] and thermal radiation to ambient. For the upper surface of the fallen upper roadway span, the correlation used is for free convection from a horizontal heated surface facing upward, and is of the form

$$Nu = a\mathrm{Ra}_L^b \tag{6-3}$$

[1] Source reference is Kreith; primary references are MacAdams, plus Incropera and DeWitt.

where

Ra_L = Rayleigh Number ($Gr_L Pr$)

where

L = (surface area)/perimeter

For laminar flow ($10^5 < Ra_L < 10^7$), the coefficients are

a = 0.54
b = 0.25

For turbulent flow ($10^7 < Ra_L < 10^{12}$), the coefficients are

a = 0.15
b = 0.3333

For the lower surface of the lower roadway, the correlation is of the same form, but with coefficients for free convection from a horizontal heated surface facing downward

$$Nu = a\mathrm{Ra}_L^b \quad (10^5 < Ra_L < 10^{10}) \tag{6-4}$$

where

a = 0.27
b = 0.25

In the above correlations, fluid properties are evaluated at the near-wall temperature, defined as the average of the wall surface temperature and the ambient temperature. The ambient temperature external to the fire is conservatively assumed to be 100°F (38°C), as a convenient bounding value.

6.4 Structural Impact Model Assumptions and Analysis Method

Because of the complexity of the impact portion of the MacArthur Maze fire scenario, the structural model of the fallen overhead span was developed in progressive stages, starting with a simple approximation using only a truncated section of a single plate girder for scoping calculations, and evolved to include representation of the complete overpass section. The purpose of the preliminary structural modeling was to determine the level of complexity and sophistication in the final set of impact models needed to assure that all potentially significant structural consequences to the containment boundary were considered. The initial modeling work included mesh sensitivity studies and evaluation of the effects of including or neglecting the conveyance. A primary conclusion of the initial modeling phase was that the thin plate girders would tend to deform around the stronger package wall instead of causing significant local deformation to the package, making a failure of the containment boundary unlikely. The more realistic final impact models described in this report were carefully crafted to include the upper bound of potential package response without resorting to incredible conservatism. The basic features of the structural models are described in Section 5.4.1.

Fire exposure raises the package temperature, which lowers the structural material strength and makes the package more susceptible to damage from impact loading. Therefore, a conservative estimate of the maximum package temperature was obtained from the thermal analyses, to appropriately bound the package temperature at the time of the collapse of the overhead span. As described in Section 2.0, the collapse of the first span occurred at approximately 17 minutes, and the partial collapse of the second span was complete at about 37 minutes after the start of the fire. The thermal analysis (see Section 6.3) conservatively assumed that the large fully engulfing (pre-collapse) pool fire lasted for the full 37 minutes. For the purposes of the structural analysis, the peak temperature on the package surface predicted at 37 minutes was used to define the overall package temperature, conservatively assuming that the entire package was at the peak temperature. This approach results in an estimated bounding temperature of 1800°F (982°C) for the package in the structural analyses.

The results of the FDS model of the pre-collapse fire (see Section 3.0) and an additional ANSYS thermal model of the I-580 roadway were used to determine a reasonably conservative uniform temperature for the falling steel girders of the overpass structure. In the case of the falling girders, the conservative condition errs on the cool side, so the strength and stiffness in the girders is as high as possible, within the thermal constraints of the scenario. In this case, 1800°F (982°C) was chosen as the representative girder temperature for the drop scenario. Coincidentally, this value is the same as the assumed package temperature, which was chosen using a different rationale, as described in Section 6.4.1. The package temperature was chosen to be bounding with as high a value as possible; the girder temperature was chosen to be as conservatively low as possible, based on realistic package locations.

The temperature of the lower I-880 span at the location of the GA-4 package is assumed to be a nominal 80°F (27°C). This conservatively neglects elevated temperature effects on the material properties of the lower roadway. The roadway would have been much hotter during the fire, and would have been more compliant at a higher temperature than the assumed bounding value. Assuming higher, more realistic temperatures for the lower roadway would allow it to dissipate more of the energy of the impact, mitigating to some degree the effect of impact on the package. Similarly, air drag forces and reduction in fall distance resulting from sagging of the girders before collapse of the span are conservatively neglected in the impact analysis.

Yield strength and the plastic behavior of the materials are critical parameters in the impact model. The evaluation of the package containment is based on the amount of plastic strain developed in the XM-19 stainless steel package body. The significant capacity of the plate girders to deform during impact because of the elevated temperature, visible in the post-fire photographs of the girders (CHP 2007), is a fundamental physical phenomenon captured in the analysis with this model.

The DU gamma shield is not a structural component of the containment boundary, but it does offer potential support to the steel body wall. The DU is modeled as a bilinear (elastic/plastic) material with a near-zero tangent modulus. If the yield stress limit is exceeded, the material is allowed to deform with a negligible increase in load. This behavior results in the DU layer providing realistic support to the package as long as it remains in the elastic range, but the support drops off quickly if the stress in the material exceeds the elastic range. The tangent modulus is six orders of magnitude lower than the elastic modulus for this material, resulting in calculated plastic strains that are conservatively higher than they would be if a realistic stress-strain curve were implemented. However, the response of the DU gamma shield is not specifically evaluated for failure in this analysis, since it is not critical to the containment boundary.

In the calculations, contact between a falling girder and the package body or any other component of the model was defined with an automatic single surface contact definition. This contact rule prohibits the components from occupying the same space, and applies a coefficient of static and dynamic friction of 0.5. Dry steel-to-steel friction is typically reported in the range of 0.7-0.8 for static friction and 0.4-0.6 for dynamic friction, but there is significant variation and instances of data reported outside those ranges. The 0.5 was chosen as a middle range dynamic friction value, based on sensitivity studies that showed friction was not a major force in this scenario. The relative fraction of frictional energy to total system energy was in the range of 1-2%, while the fraction of frictional energy to internal energy (due to material deformation) was in the range of 1-5%.

Global mass damping of 5% was applied to the model as an additional source of energy dissipation. This level of damping is typically used in dynamic impact modeling for numerical stability and to account for natural sources of energy dissipation that are not specifically modeled. The amount of energy this damping dissipates in the model is comparable to the amount of energy dissipated by friction. Global damping does not have a significant effect on the results obtained in this analysis.

6.4.1 Overpass Temperature Evaluation

The temperature of the I-580 overpass at the time of impact is an important assumption that affects its material characteristics and the overall impact response. The elastic modulus and the yield strength of the girder material are two material properties that affect the force and energy transmission during impact, and both material properties decrease at elevated temperatures. As discussed in Section 2.2, evidence gathered from the post-collapse material indicated that the plate girders experienced temperatures at least as high as 1472-1652°F (800-900°C) at locations near the middle of the fire. Material data in the literature for this temperature range predict a reduction in the yield strength of steel to values roughly 10% of the room-temperature yield strength (see Figure 2.10), and a substantial increase in ductility.

To obtain a more detailed picture of the temperature distribution on the girders than could be determined from the relatively small range of sampling locations, additional analysis was performed with an ANSYS model of the I-580 upper roadway span between Bents 18 and 20. ASTs from the FDS model of the pre-collapse fire (discussed in Section 3.0), were used as boundary conditions for thermal analysis of the girders. The AST boundary values were applied as time-history thermal loads over the interval from initiation of the fire to 18 minutes, encompassing the time frame of the complete collapse of the overhead span between Bent 19 and Bent 20. The lower temperature corresponding to the actual time-frame of the collapse of this span is more conservative for the purposes of the structural analysis. However, a higher temperature is more conservative for the package temperature, and the package temperature for the impact analysis was based on a fire exposure time of 37 minutes, corresponding to the time of final collapse of both overhead spans.

The thermal model of the upper spans predicts a rapid heating of the steel girders directly above the fire. By 5 minutes into the fire, the peak girder temperature exceeds 2192°F (1200°C). At 18 minutes, the temperature distribution reaches the state shown in Figure 6.2, with peak temperatures up to 2462°F (1350°C). The left half of the thermograph shows the hotter side of the overpass, which is directly above most of the fire area, beneath the span between Bents 18 and 19. The right side is generally cooler, and represents the span that fell straight down and is modeled in the impact analyses. This is consistent with the physical distribution of the fire pool (as shown in the fire video images in Figure 2.2, Figure 2.3, and Figure 2.4). Over much of the

girder length exposed to the fire, the ANSYS results show girder temperatures that are in the range determined from the material analysis. (This corresponds to the light green to yellow segments of the color thermograph in Figure 6.2). However, this calculation also predicts much higher temperatures for the girders in locations that were not sampled for the material analysis.

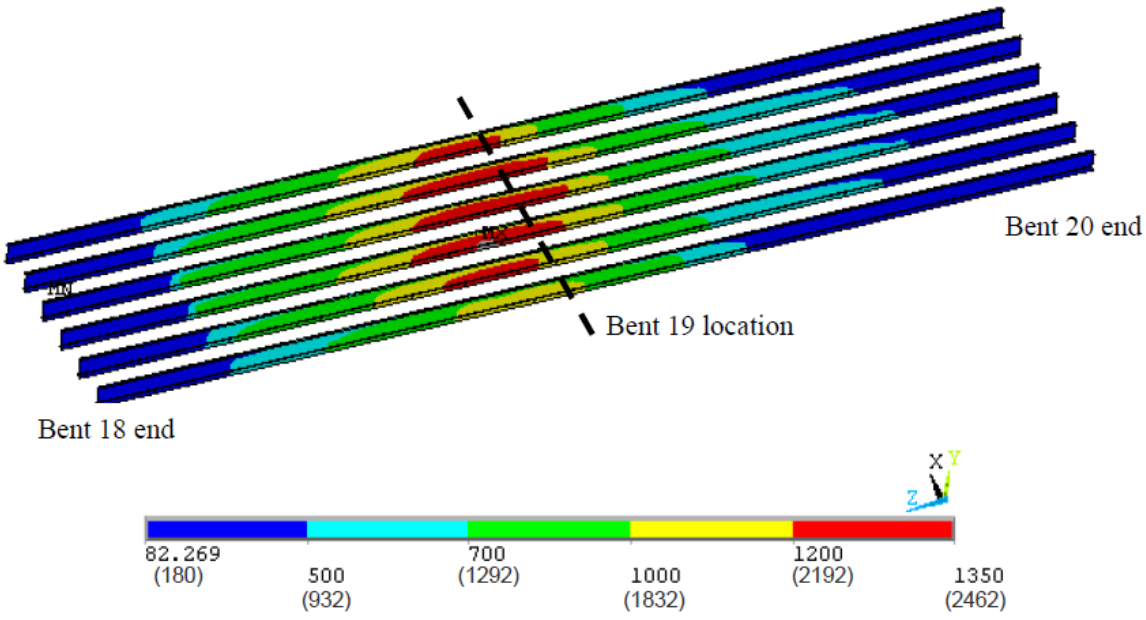

Figure 6.2. Girder Temperatures, (°C [°F]), at 18 Minutes Predicted with ANSYS Model

Sensitivity studies on thermal processes that would carry heat away from the girders, such as conduction heat transfer longitudinally down the girders and conduction into the concrete above the girders, showed that these processes do not play a major role in determining the girder temperature or temperature distributions. The local heat input to the girders due to the fire, as defined in the ANSYS model using the AST values from the FDS fire model, dominates all other thermal processes, even when conservatively high heat dissipation through the girders is assumed, by such means as enhanced convection coefficients between the upper roadway surface and the cool air above it.

As illustrated in Figure 6.2, the peak girder temperatures are predicted to be as high as 2462°F (1350°C). This very high temperature zone includes girder segments above potential impact locations for the SNF package. However, from the standpoint of the drop scenario, higher girder temperatures would result in a less severe impact, due to the greatly decreased yield strength of steel with increasing temperature. Using these very high temperatures to define the girder temperatures for the impact analysis would result in a less severe drop scenario than would be obtained by assuming lower temperatures for the girders. The goal in assigning a temperature to the girder structure was to ensure the temperature was conservatively low, giving the structural steel of the girders conservatively high strength and stiffness, but remaining consistent with the range of temperatures that could reasonably be expected from the accident conditions.

A uniform overpass girder temperature of 1800°F (982°C) was chosen as a conservatively low temperature estimate for the hot side of Bent 19. The geometry of overhead roadway for the impact models actually corresponds to the right half of Figure 6.2, which is the cooler side,

because that is the span that fell relatively cleanly onto the lower roadway in the MacArthur Maze accident (i.e., the span between Bents 19 and 20), and offers the potentially most damaging mechanical loading. The thermal state of the impact model is defined based on conditions from the hot side, to ensure the package is at its hottest and structurally weakest.

7.0 ANALYSIS RESULTS

This section presents the results of the structural and thermal analyses of the GA-4 package exposed to the conditions of the MacArthur Maze fire scenario. The thermal analysis of the fire portion of the transient is presented in Section 7.1, for both the ANSYS model and the COBRA-SFS model. The thermal analysis of the post-fire cooldown transient with these models, in which the package is covered by the concrete "blanket" of the collapsed upper roadway, is presented in Section 7.2. The results of the structural analysis are discussed in Section 7.3.

7.1 GA-4 Package: Thermal Results for Fire Transient

The starting point for the fire transient thermal modeling was assumed to be steady-state NCT. The initial temperature distribution in the package is summarized in Figure 7.1, which shows the peak component temperatures predicted with the ANSYS and COBRA-SFS models of the GA-4 at NCT. Figure 7.2 shows a color thermograph illustrating the ANSYS model temperature results for the package cross-section for this initial steady state evaluation. As discussed in Section 6.1 above, the peak fuel region temperature predicted with the ANSYS model is 306°F (152°C), and the peak cladding temperature predicted with the COBRA-SFS model is 293°F (146°C). This is consistent with the expected differences between the results obtained with a homogeneous representation of the fuel region using a k-effective model when compared to a detailed thermal-hydraulic model of the fuel assemblies. The two models give essentially the same results for NCT, within modeling uncertainty, and are in reasonable agreement with the results reported in the GA-4 SAR (General Atomics 1998).

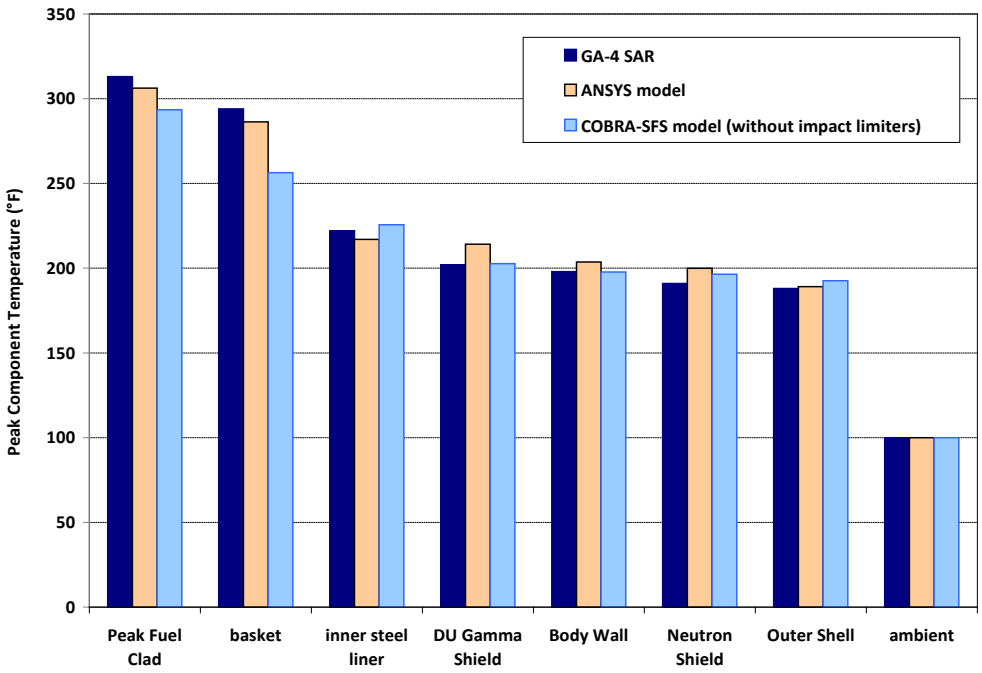

Figure 7.1. Initial Conditions for Fire Transient Analyses: GA-4 at NCT

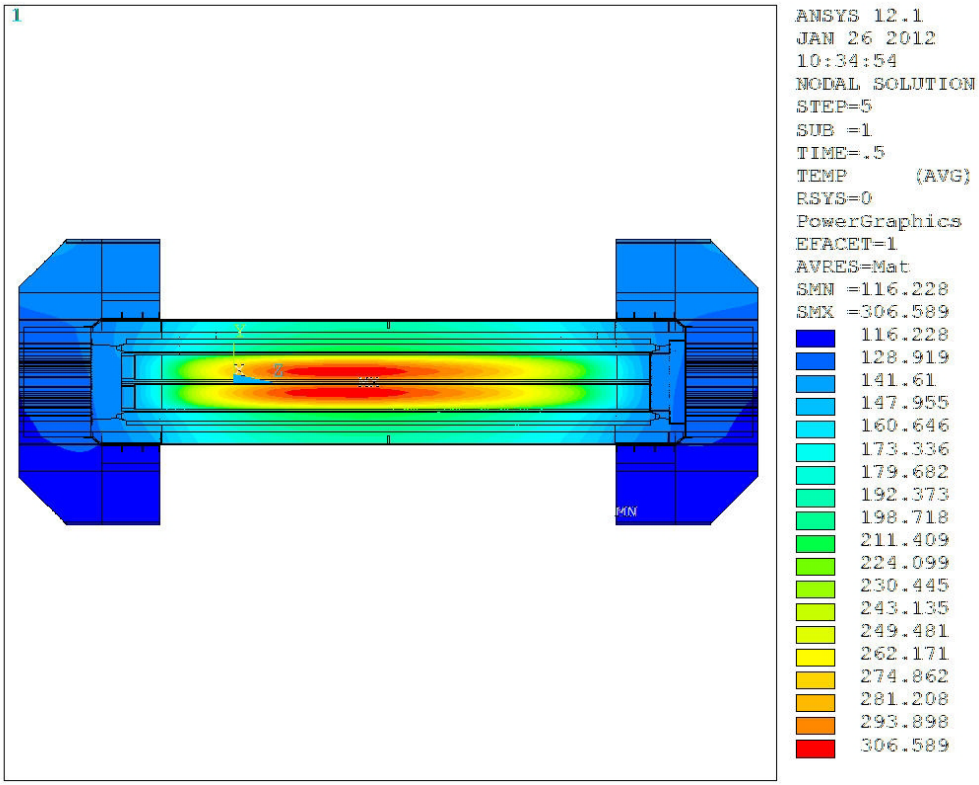

Figure 7.2. ANSYS Results[1]: Thermal Cross-section (°F) of GA-4 Package at NCT

The MacArthur Maze fire was simulated for the GA-4 package by imposing boundary conditions representing the large (pre-collapse) engulfing fire, followed by the smaller (post-collapse) engulfing fire. To simulate the pre-collapse fire, the package model was subjected to an ambient boundary temperature of 2012°F (1100°C) for 37 minutes. The detailed results for the fully engulfing fire at 2012°F (1100°C) are described in Section 7.1.1. To simulate the post-collapse fire, the fire boundary temperature was reduced to 1652°F (900°C) for the remaining 71 minutes of the fire portion of the transient. The results obtained for the post-collapse portion of the fire are described in Section 7.1.2.

7.1.1 Pre-collapse Fire (2012°F [1100°C])

The initial fully engulfing pool fire of the MacArthur Maze fire scenario at 2012°F (1100°C) was assumed to extend to 37 minutes of the total fire duration, to conservatively encompass the collapse of both of the upper roadway segments. Figure 7.3 shows a color thermograph of the package central cross-section illustrating the temperature results obtained with the ANSYS model at the end of this portion of the fire. (Note that the TIME reported on the plots includes the initial pre-fire pseudo-transient of 0.5 hr for NCT.)

[1] To ensure a smooth transition within the ANSYS calculation between the NCT steady-state analysis and the transient fire analysis, the NCT analysis was run as a transient solution with an arbitrary time-step, updating temperature-dependent material properties and external convection coefficients until the solution did not change significantly between time-steps. Time-stamps on graphics produced using ANSYS include the arbitrary 0.5 hrs of the NCT analysis, and therefore are off-set by 0.5 hr compared to other plots referenced to the start of the fire as time zero.

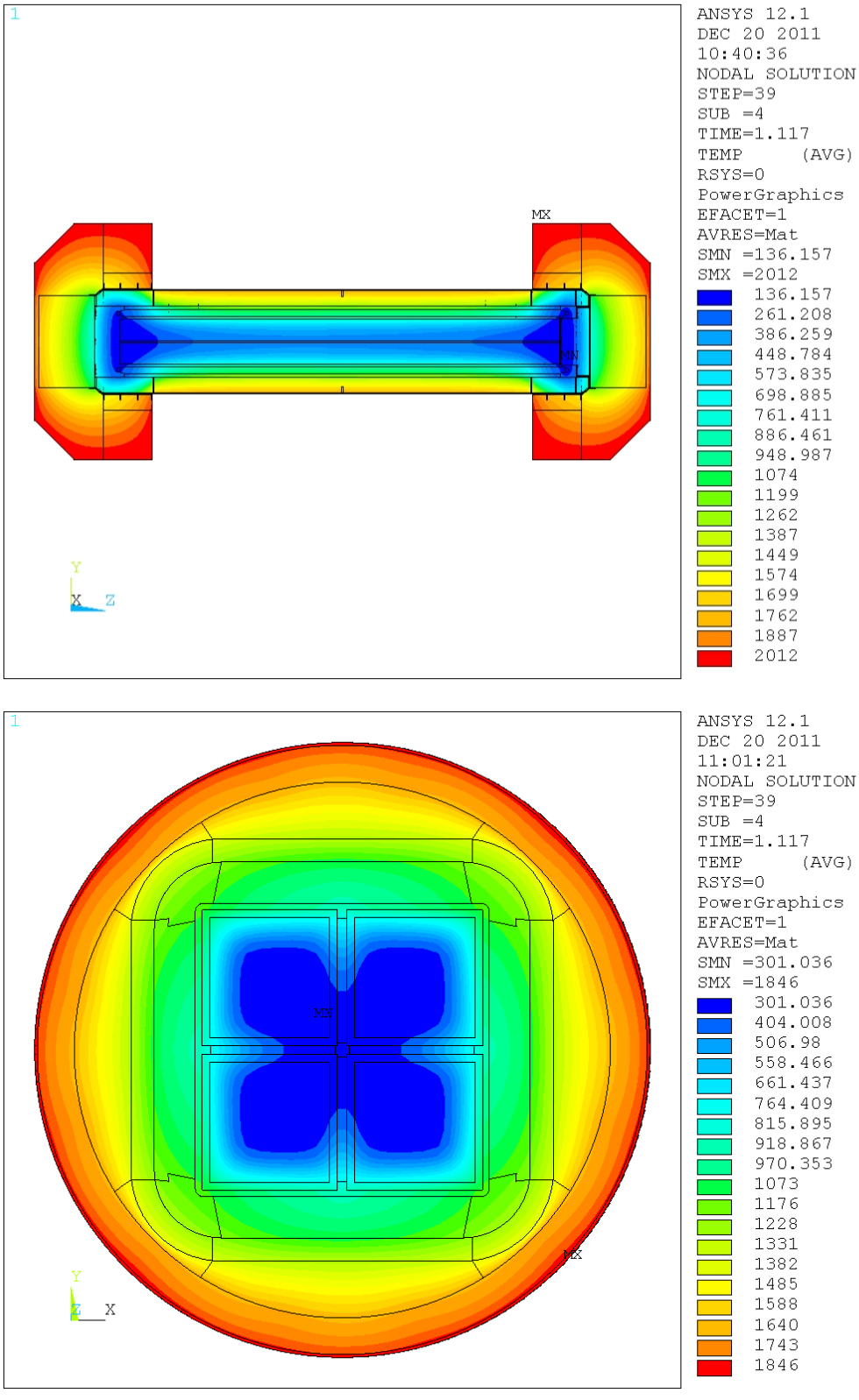

1

2

3 Figure 7.3. ANSYS Model Results: Axial and Central Radial Thermal Cross-sections (°F) of
4 GA-4 Package at End of 2012°F (1100°C) Fully Engulfing Fire (37 minutes)

Peak temperatures predicted with the ANSYS model for the main components of the GA-4 package are shown as a function of time in Figure 7.4. The peak temperature on the outer surface of the package, which consists of the thin stainless steel shell of the neutron shield tank, rises rapidly in the initial minutes of the fire, paralleling the rapid rise in the exterior ambient temperature. Within approximately 5 minutes, the surface temperature of the package is approaching the fire temperature on an asymptotic curve. In a similar manner, the peak temperature on the outer surface of the impact limiters very rapidly approaches the fire boundary temperature. This temperature occurs on the thin stainless steel outer surface of the impact limiter, which is effectively insulated on the inner side by the relatively low thermal conductivity of the honeycomb structure that the steel is there to protect. The temperature of the outer stainless steel surface therefore approximates an adiabatic surface temperature at the local fire boundary condition.

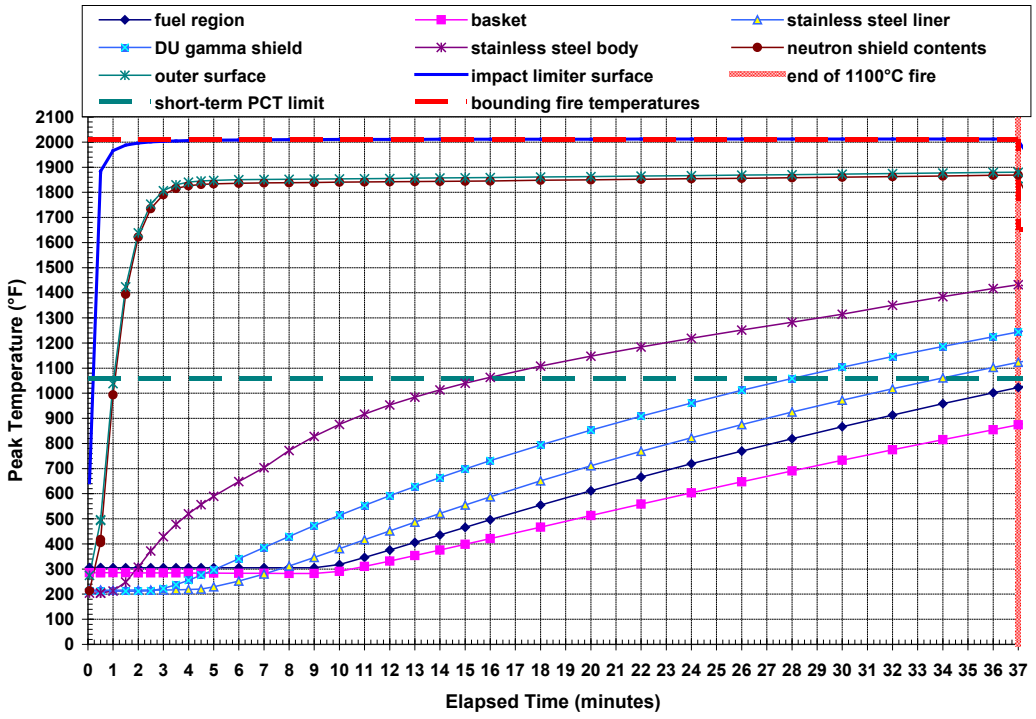

Figure 7.4. Peak Component Temperatures Predicted with ANSYS Model for 37-minute Fully Engulfing 2012°F (1100°C) Fire

The peak fuel region temperature does not begin to show any increase until about 9 minutes into the fire transient. Such a delay is typical of the peak fuel temperature response to a fire transient, because of the thermal inertia of the massive body of an SNF package. In addition, the location of the maximum temperature in the fuel region shifts toward the outer edge of the hottest fuel assembly as the fire transient progresses, and part of the delay is due to the time required to heat up the region of the fuel assembly that is initially cooler than the central region in the pre-fire steady state at NCT.

Peak temperatures predicted with the COBRA-SFS model for the major components of the GA-4 package in response to the fire conditions are shown in Figure 7.5. The plots in Figure 7.4 and Figure 7.5 show that the two models are predicting similar responses for the GA-4 package in this severe fire transient. The significant difference between them is in the response of the fuel region. The ANSYS model uses the homogeneous k-effective model for the fuel region,

which is a steady-state model that is by design a conservative representation of heat transfer within the rod array. The more detailed rod-and-subchannel representation of the fuel assembly in the COBRA-SFS model results in a more realistic prediction of the rate of fuel cladding temperature rise.

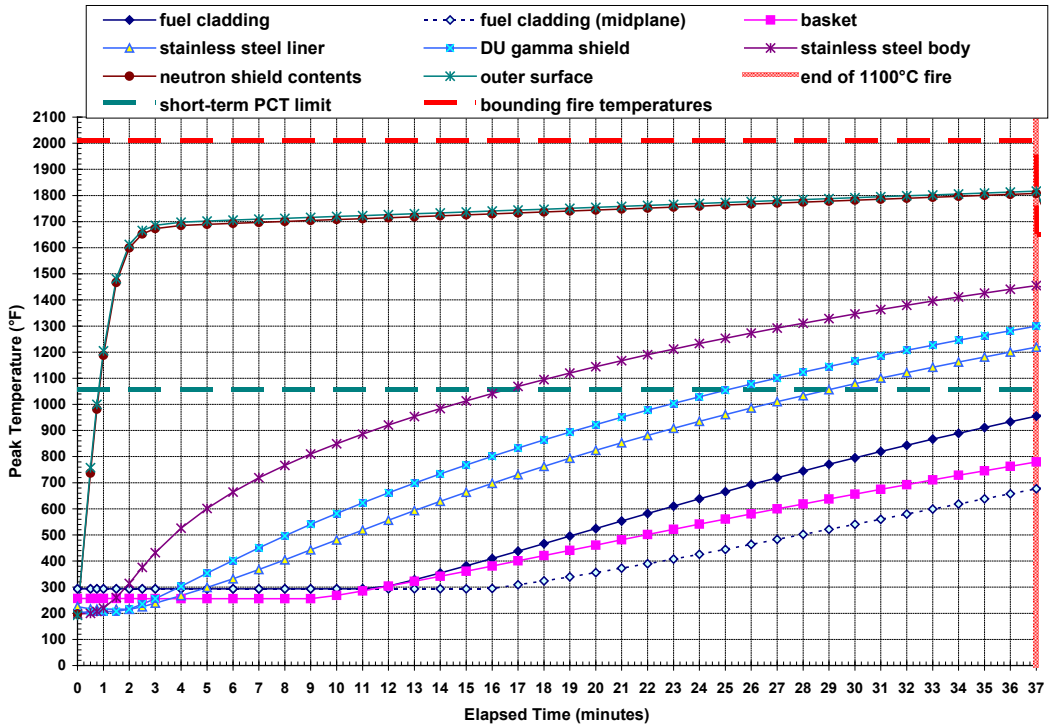

Figure 7.5. Peak Component Temperatures Predicted with COBRA-SFS Model for 37-minute Fully Engulfing 2012°F (1100°C) Fire

The COBRA-SFS model predicts that the peak cladding temperature near the ends of the rods, which in this model are not protected by the impact limiters, rises to 955°F (513°C) by 37 minutes. The COBRA-SFS model predicts 677°F (358°C) by this time for the peak cladding temperature at the midplane of the package, the location where the ANSYS model predicts the peak temperature in the fuel region. Because of the more conservative homogeneous k-effective model for the fuel region, the ANSYS model predicts a somewhat higher peak temperature of 1023°F (551°C) by 37 minutes. The cladding peak temperatures predicted with both of these models have not exceeded the limit of 1058°F (570°C) for short-term operations by the end of the 37-minute bounding representation of the pre-collapse fire. However, the total fire duration has 71 more minutes to run, at the lower fire temperature of 1652°F (900°C), simulating the post-collapse portion of the fire.

7.1.2 Post-Collapse Fire (1352°F [900°C])

The post-collapse portion of the MacArthur Maze fire, in which the physical extent of the fire was greatly reduced by the intrusion of the fallen upper roadway spans, was modeled as a fully engulfing fire at the lower boundary temperature of 1652°F (900°C). The temperatures predicted with the ANSYS model for the end of the fire, after 37 minutes of exposure to 2012°F (1100°C) followed by 71 minutes of exposure to 1652°F (900°C), are shown in Figure 7.6.

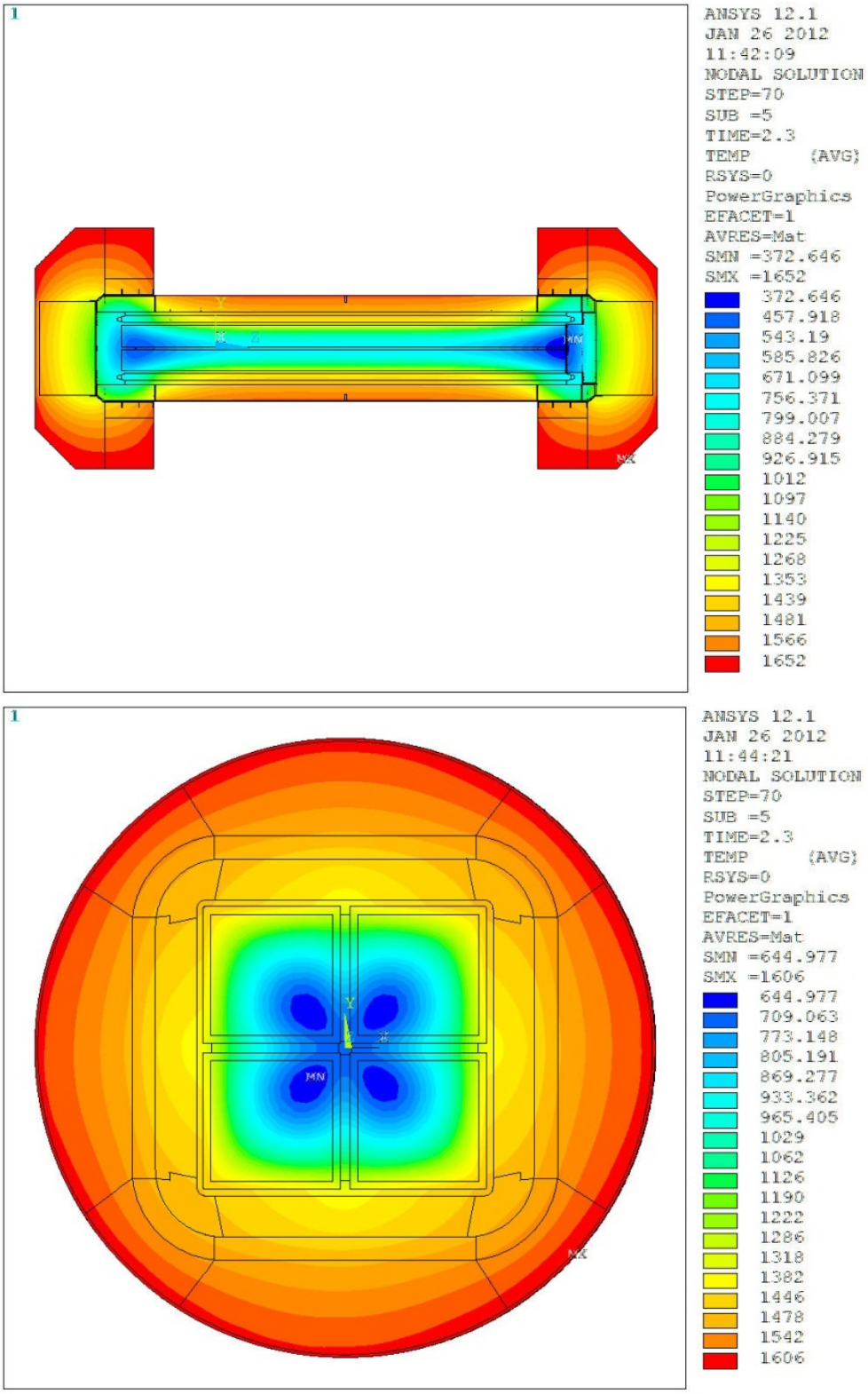

Figure 7.6. ANSYS Model Results: Axial and Central Radial Thermal Cross-sections (°F) of GA-4 Package at the End of the Fire at 108 Minutes

Peak temperatures predicted with the ANSYS model for the main components of the GA-4 package are shown as a function of time in Figure 7.7. Figure 7.8 shows the response of major components of the package to the fully engulfing post-collapse fire predicted with the COBRA-SFS model. By the end of the 37-minute fire at 2012°F (1100°C), both models predict peak temperatures on the outer surface of the package that are significantly above the post-collapse fire temperature of 1652°F (900°C). As a result, the initial response of these components during the post-collapse fire is to cool down toward the new ambient fire temperature. In the first 13 minutes of this portion of the transient, the peak temperatures on the outboard components drop rapidly in response to the sudden change in the boundary fire temperature, then stabilize to a slow asymptotic rise toward the new fire temperature.

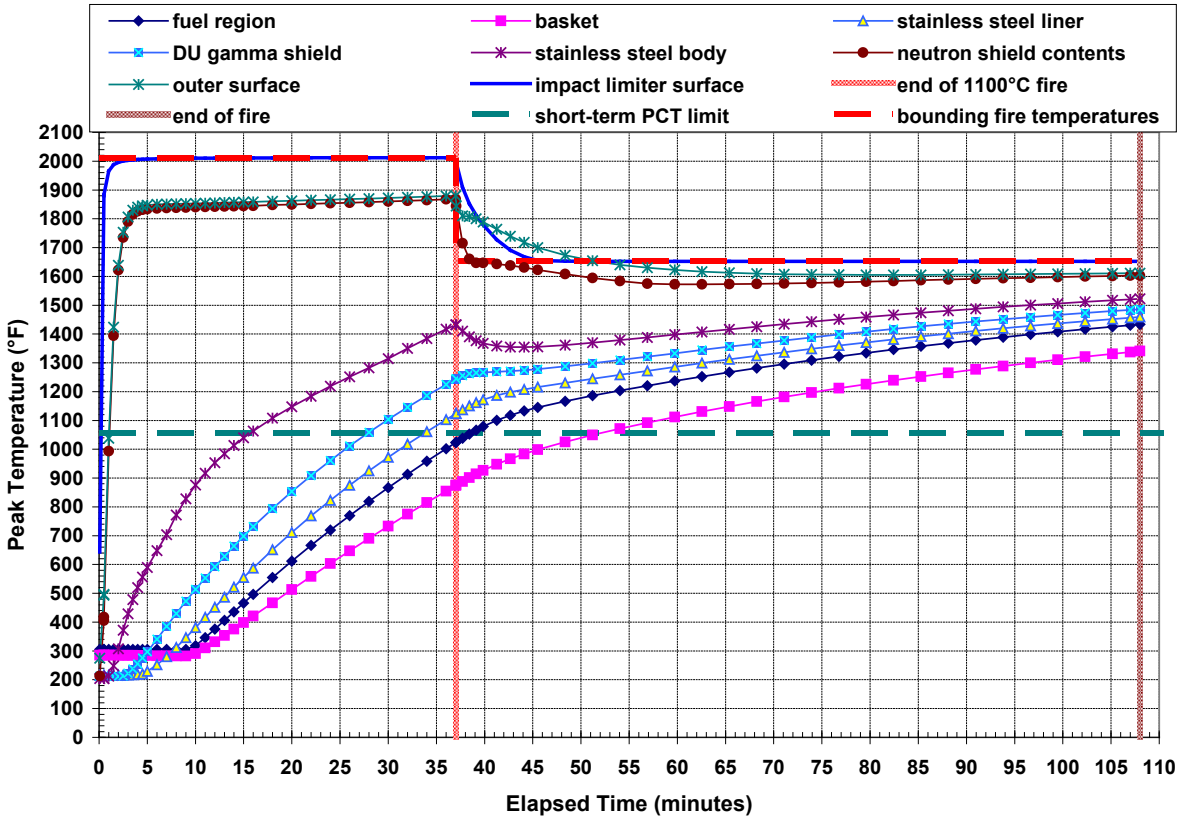

Figure 7.7. Peak Component Temperatures Predicted with ANSYS Model at 108 Minutes

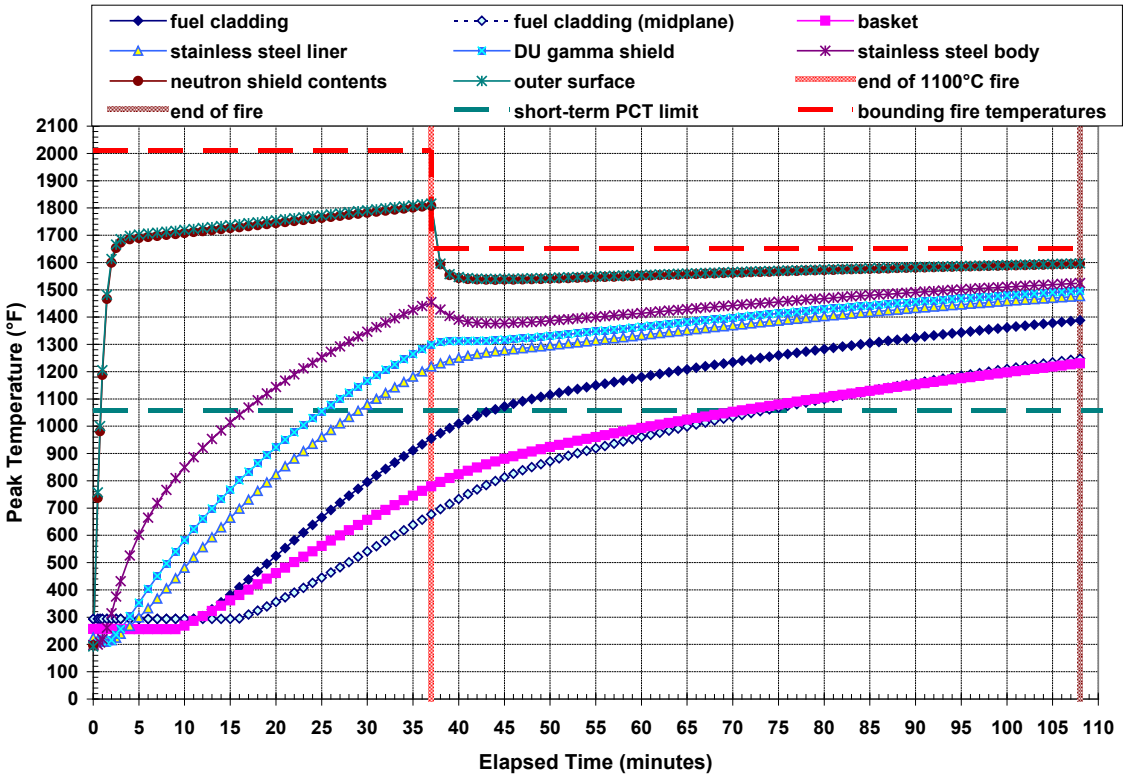

Figure 7.8. Peak Component Temperatures Predicted with COBRA-SFS Model at 108 Minutes

Similarly, the peak fuel temperatures respond to the lower boundary temperature by slightly slowing their rate of rise, but these components are also on an asymptote approaching the new fire temperature. By the end of the fire transient at 108 minutes, the peak fuel region temperature predicted with the ANSYS model has reached 1433°F (779°C), exceeding 1382°F (750°C), the temperature at which burst rupture of zircaloy cladding has been assumed in previous SNF package transportation studies (NUREG/CR-6672). The peak fuel cladding temperature predicted with the COBRA-SFS model also exceeds this temperature, reaching 1388°F (753°C) on the end of the hottest fuel rod. The mid-plane peak fuel cladding temperature predicted with this model is not far behind, at 1248°F (675°C).

These predicted peak temperatures are in response to a conservative and bounding representation of the MacArthur Maze fire. However, even after the fire is over, the transient is not finished, as the package is evaluated in the post-fire cooldown, with the conservative assumption that it is blanketed by the concrete structure of the fallen overhead roadway span. Experience with modeling of SNF packages in long-duration fires (NUREG/CR-6487; NUREG/CR-6886 2009) has shown that the maximum fuel cladding temperature can occur well after the end of the fire, during the post-fire cooldown of the package. In addition to the rise in temperature on the fuel rods in response to heat input from the fire, some portion of the temperature rise is due to the high ambient fire temperature preventing decay heat removal from the fuel rods during the fire and for some time after the fire while the outboard components of the package are above the maximum fuel temperature.

7.2 GA-4 Package: Thermal Results for Post-Fire Cooldown Transient

For the cooldown portion of the transient, in which the GA-4 package is enclosed by the fallen roadway, the roadway surface temperatures at the end of the fire were determined by a separate calculation with COBRA-SFS. This calculation represented the roadway as described in Section 5.2.2 above (see Figure 5.7), exposing the roadway surfaces to the same fire conditions as the GA-4 package. Figure 7.9 shows the peak temperatures predicted for the roadway concrete surfaces in response to the pre-collapse fire at 2012°F (1100°C) and the post-collapse fire at 1652°F (900°C). These temperatures exhibit the same asymptotic behavior as the outer surface of the SNF package.

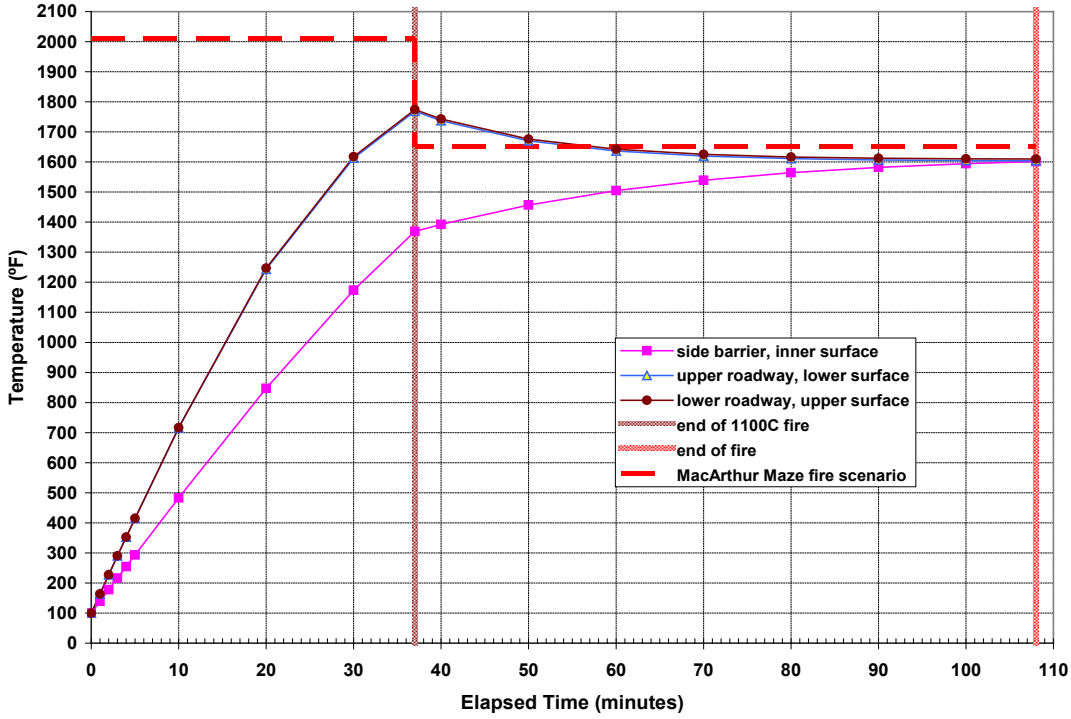

Figure 7.9. Peak Concrete Surface Temperatures Predicted with the COBRA-SFS Model for the 37-minute Fire at 2012°F (1100°C) and the 71-minute Fire at 1652°F (900°C)

In Figure 7.9, the upper roadway temperature is the peak temperature on the under surface of the upper roadway span that is assumed to cover the SNF package in the post-fire scenario. The lower roadway temperature shown in the plot is the peak temperature predicted on the surface of the lower roadway beneath the SNF package. The concrete barrier temperature is the peak temperature predicted for the inner surface of the lower roadway side barrier, which the SNF package is assumed to be lying beside. The peak temperature of 1774°F (968°C) predicted for the roadway surfaces occurs at the end of the 37-minute fully engulfing fire. The side barrier is predicted to reach approximately 1369°F (743°C) at this time. The temperatures on the roadway surfaces drop somewhat during the 71-minute interval of exposure to the lower temperature of the post-collapse fire, and by the end of the fire, all of the concrete surfaces exposed to the fire are at approximately the same temperature of 1609°F (876°C).

The results in Figure 7.9 show that it is extremely conservative to assume that the concrete structures would be exposed to the bounding fire temperatures for the full duration of the pre-collapse and post-collapse fires. As with all other components exposed to these extreme boundary conditions, the concrete temperatures begin to asymptotically approach the fire temperature. Post-fire evaluation of the damaged roadway, including detailed assessment of the lower roadway deck and side barriers (Wiss, Janney, Elstner Associates, Inc. 2007), found that the concrete surfaces were exposed to temperatures in the range 446°F (230°C) to 842°F (450°C). The maximum temperature exposure at the concrete surfaces was estimated as 1472°F (800°C), over a relatively small localized area. The bounding approach used in this model sets up an extremely conservative environment for the SNF package in the post-fire cooldown transient beneath the collapsed roadway.

The roadway temperatures at the end of the fire define the initial conditions for the cooldown transient calculated with the ANSYS and COBRA-SFS models for the GA-4 package beneath the concrete 'blanket' of the upper roadway. Figure 7.10 shows the response predicted with the COBRA-SFS model for the major components of the system in the post-fire cooldown in the first 5 hours after the end of the fire. Figure 7.11 shows the response predicted with the ANSYS model for this portion of the transient. In both models, all major components show an initial rapid decrease in peak temperature, followed by a more gradual decline as the temperature gradients flatten.

The results for the COBRA-SFS model show the effects of the rapid cooling of the ends of the package, where the peak temperatures are predicted during the fire transient. By about 2.3 hours, the ends have cooled sufficiently for the location of the peak temperatures to shift back toward the axial center of the package, and the effects of thermal inertia are seen in the peak fuel cladding temperature and the peak basket temperature. For these components, the temperatures near the center of the package continue to rise after the end of the fire, and eventually exceed the peak temperatures on the ends. This is illustrated in Figure 7.12, which shows the evolution of the axial temperature profile on the hottest rod in the package, as predicted with the COBRA-SFS model.

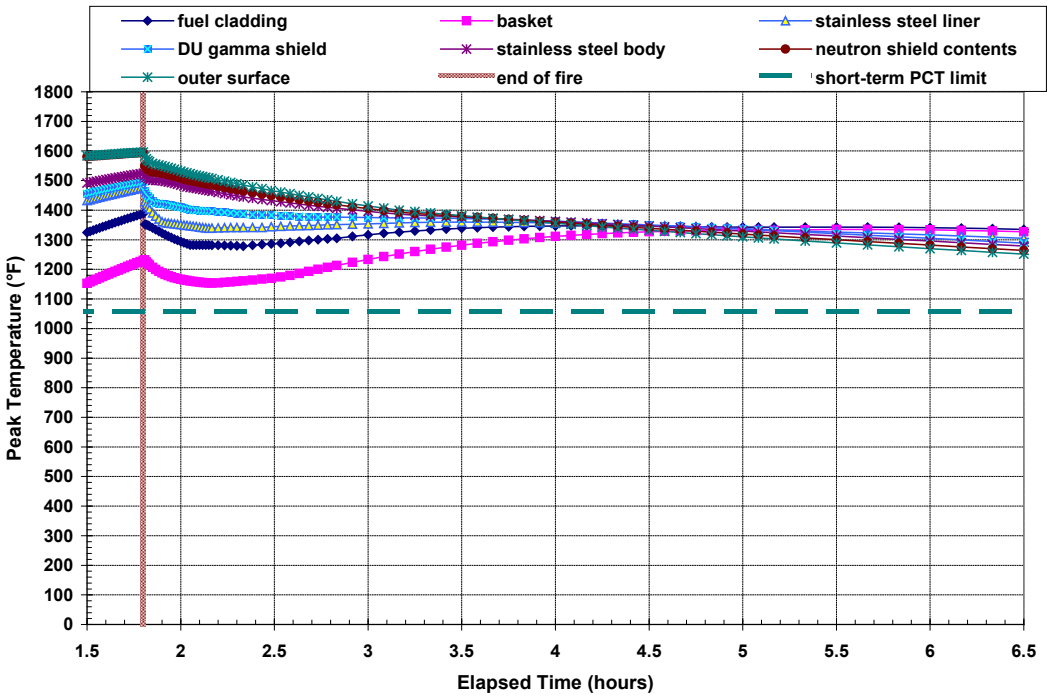

Figure 7.10. Peak Component Temperatures Predicted with COBRA-SFS Model for Post-fire Cooldown to 6.5 Hours

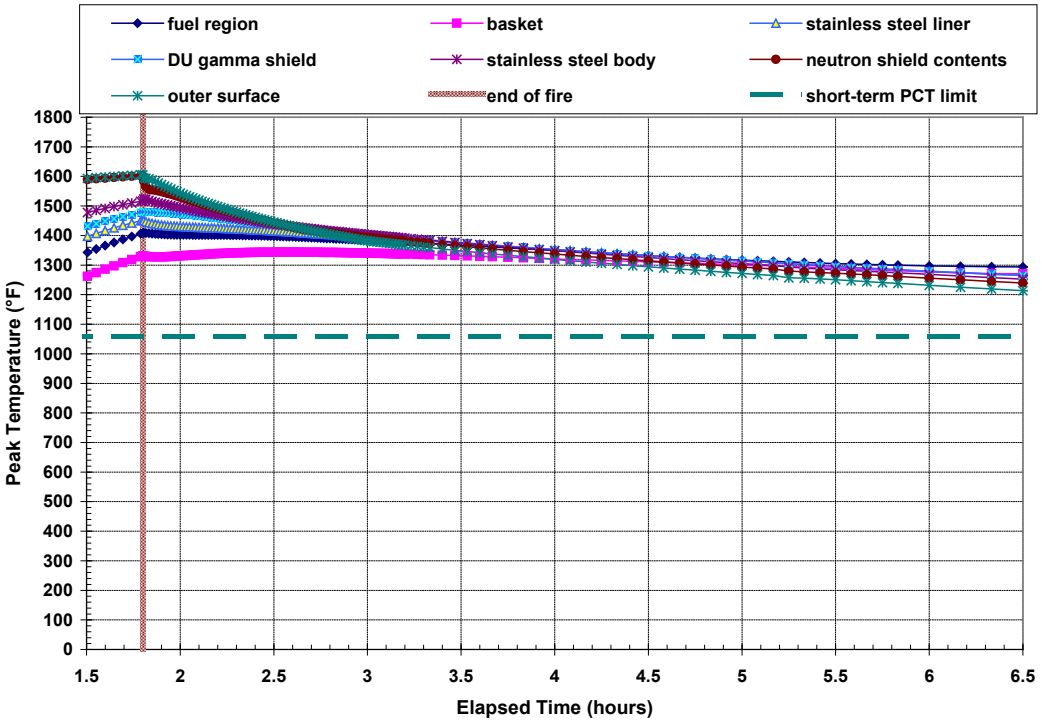

Figure 7.11. Peak Component Temperatures Predicted with ANSYS Model for Post-fire Cooldown to 6.5 Hours

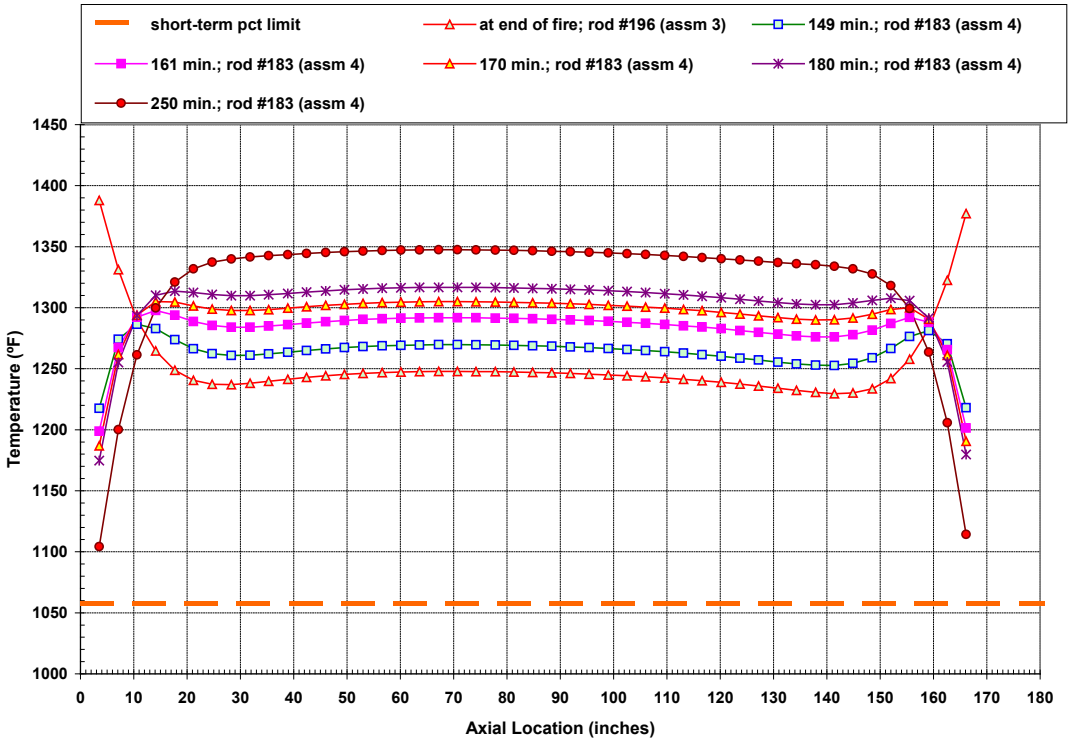

Figure 7.12. Axial Temperature Evolution on Hottest Fuel Rod Predicted with the COBRA-SFS Model for Post-fire Cooldown with the Package under Concrete

The peak fuel cladding temperature near the axial center of the hottest fuel rod is predicted to reach a maximum of 1347°F (731°C) at approximately 250 minutes, which is nearly 2.4 hours after the end of the fire. The results obtained with the ANSYS model also show the effect of thermal inertia for the fuel, sustaining a peak fuel region temperature of nearly 1400°F (760°C) for approximately 3 hours after the end of the fire, as shown in Figure 7.11.

Because the ANSYS model includes the impact limiters, the ends of the package do not experience the high temperatures predicted with the COBRA-SFS model, which omits the impact limiters. However, in the post-fire cooldown, the impact limiters act as insulators, slowing the rate of heat removal from the ends of the package. As the package cools, the steep temperature gradients within the package, due to the heat input from the fire and the decay heat trapped within the fuel region, result in the cooler ends of the package continuing to increase in temperature for some time after the fire, even as the peak temperatures near the center decrease. This is illustrated in Figure 7.13, with color thermographs of the package axial cross-section. In these thermographs, the scale of the color coding is held constant, to clearly illustrate the increasing temperature on the ends and interior components, while the peak temperatures steadily decrease.

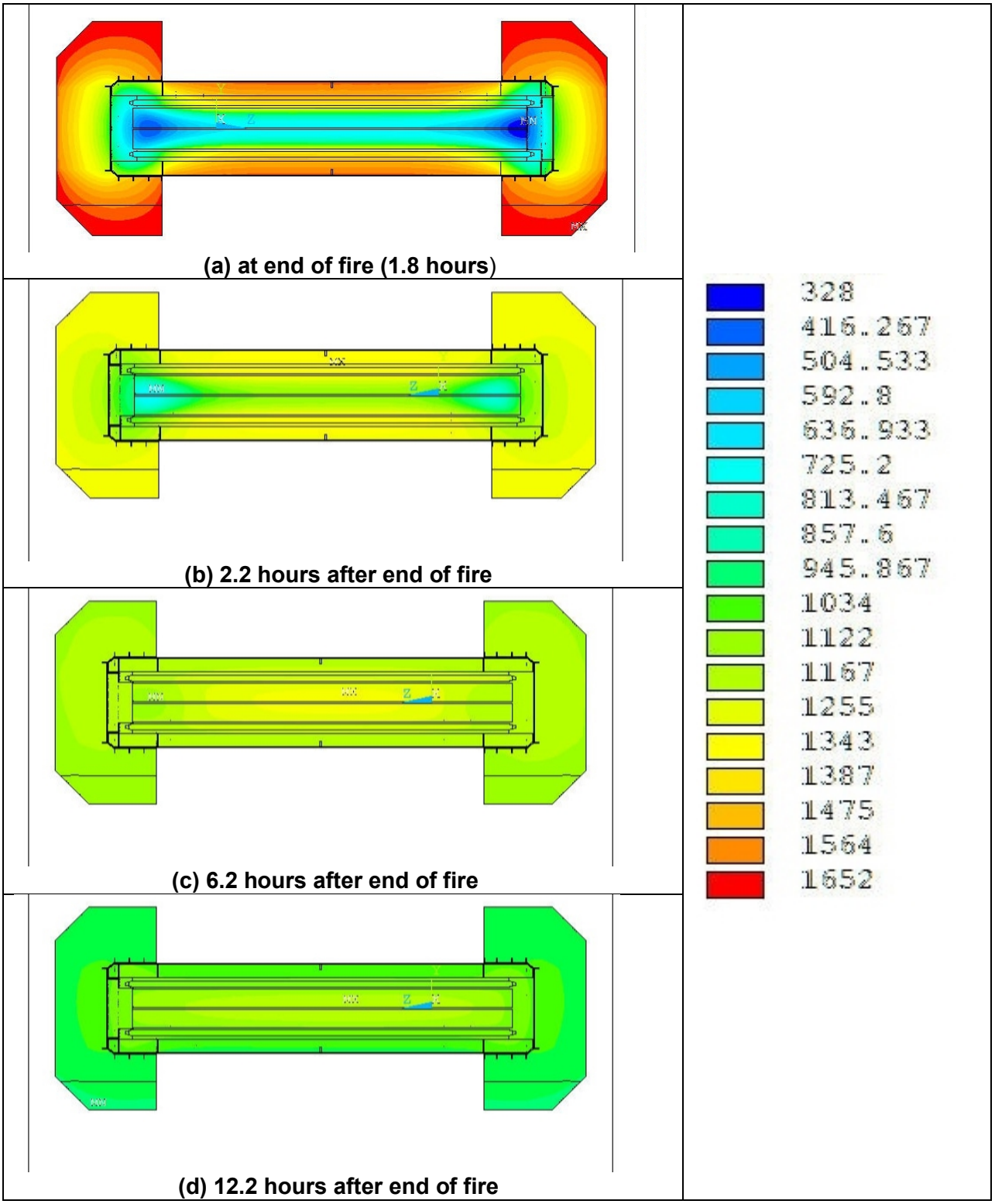

Figure 7.13. ANSYS Model Predictions of Temperature Distributions (°F) in GA-4 Package during Post-fire Cooldown

As shown in Figure 7.13, at the end of the fire the temperatures at the ends of the fuel region (beneath the impact limiters) are relatively cool, but continue to increase in temperature for many hours after the fire is over. The temperature increase in the end region of the fuel is summarized below.

Timeframe	Temperature Range at End of Fuel Region
end of fire (108 minutes)	328°F to 416°F (164°C to 213°C)
2.2 hours after end of fire	725°F to 1122°F (385°C to 606°C)
6.2 hours after end of fire	1122°F to 1255°F (606°C to 679°C)
12.2 hours after end of fire	1167°F to 1255°F (630°C to 680°C)

By 12.2 hours, the impact limiters and outer shell of the package are at temperatures in the range 1034°F to 1122°F (557°C to 606°C), slightly cooler than the end of the fuel region. The package begins to experience a uniformly decreasing temperature at all points, including the sheltered locations within the package beneath the impact limiters, only after about 12.5 hours beyond the end of the fire.

This behavior is more precisely illustrated with the temperature plot in Figure 7.14 for three specific locations beneath the top impact limiter in the ANSYS model of the package. This figure shows the temperature histories during the cooldown for a point in the fuel region near the lid end of the package, a point in the top impact limiter immediately adjacent to the package lid, and a point near the upper end of the DU gamma shield.

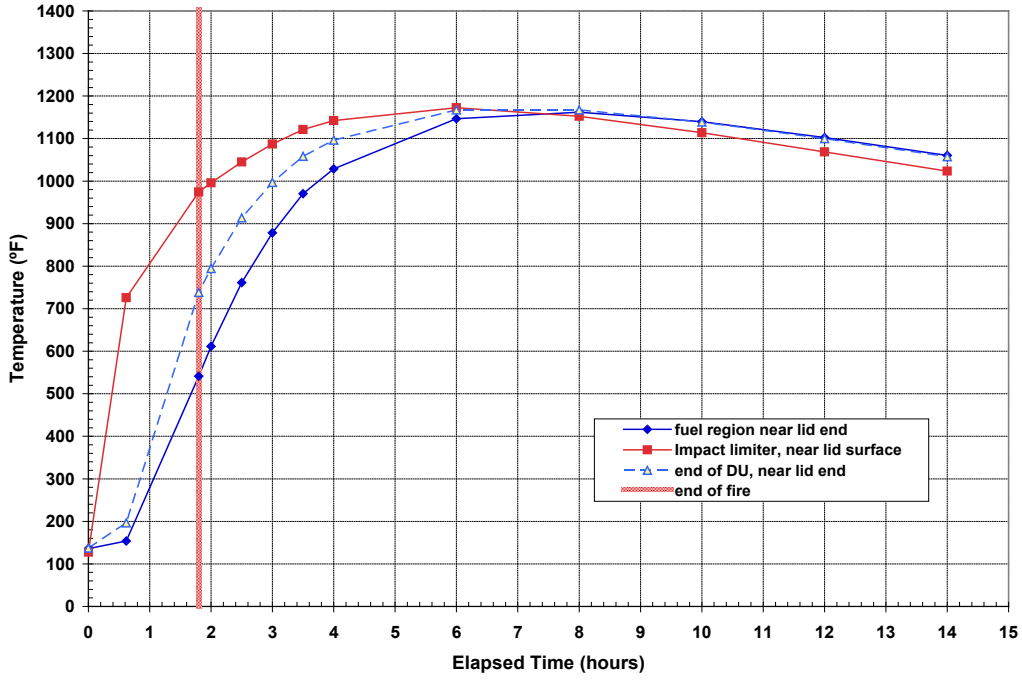

Figure 7.14. ANSYS Model Predictions of Temperature History during the Post-fire Cooldown at Locations in the GA-4 Package Shielded by the Top Impact Limiter

The overall results of the thermal analysis with the ANSYS and COBRA-SFS models show that a fire of the severity of the MacArthur Maze fire scenario would result in extremely high component temperatures on an SNF package such as the GA-4, and that those temperatures would be sustained over a long period of time. In particular, fuel cladding temperatures are predicted to exceed the short-term limit of 1058°F (570°C) for several hours, over essentially the full axial length of the fuel assemblies. In addition, the temperatures in the regions of the package seals exceed the seal material operating temperature limits for most of the fire transient and for many hours of the post-fire cooldown transient. The potential consequences of this extended period at elevated temperatures are discussed in Section 8.0.

7.3 GA-4 Package: Structural Evaluation

The positioning of the SNF package on the lower roadway has a significant effect on the potential consequences of the overpass collapse. It affects the freefall distance for the overhead span, and the location(s) at which the girder(s) can strike the package. In addition, the alignment of the center of gravity (CG) of the package and the CG of the falling span affect the total energy of impact imparted to the package. All other things being equal, the more closely the two CGs are to the same vertical line, the greater the amount of energy transmitted by the impact.

It is not obvious what impact orientation could do the most damage to the package, and in this analysis, four different configurations are considered, to cover a range of possible impact behavior and to explore the effects of the most significant variables. In all cases considered, the package location on the lower roadway is as close as possible to the center of gravity of the falling span, within the constraints of the geometry of the lower and upper roadway structure. The cases evaluated are summarized as follows:

- Case #1: a girder strikes directly across the center of the package (Figure 7.15)
- Case #2: a girder strikes along the axial length of the package (Figure 7.16; the package is barely visible beneath the third girder from the right)
- Case #3: a girder strikes directly on the package lid (Figure 7.17)
- Case #4: a girder strikes directly onto the package lifting trunnions, which are assumed to be oriented vertically, such that the impact applies a highly localized load to the package wall (Figure 7.18).

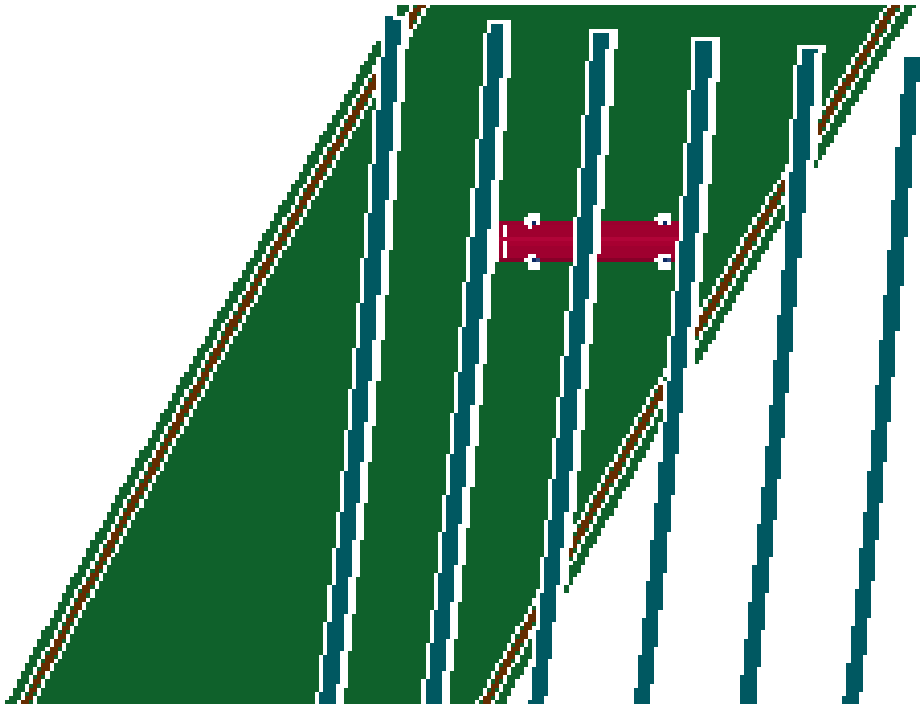

Figure 7.15. Impact Case #1: GA-4 Package Perpendicular to Upper Roadway Girders; Main Impact on Package Center

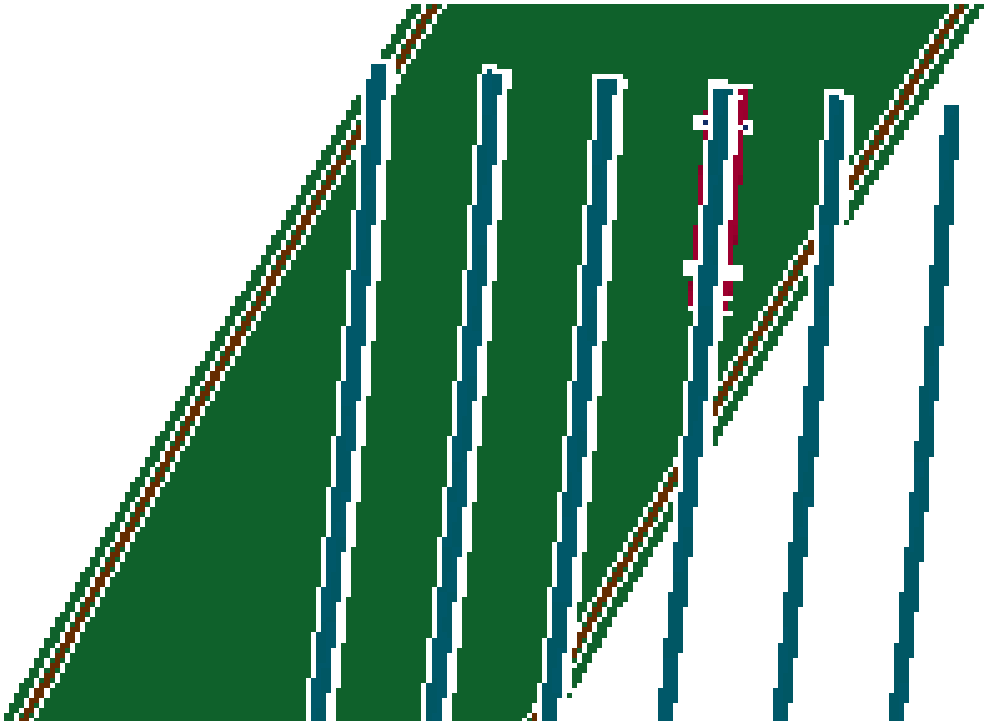

Figure 7.16. Impact Case #2: GA-4 Package Parallel to Upper Roadway Girders; Main Impact along Axial Length of Package

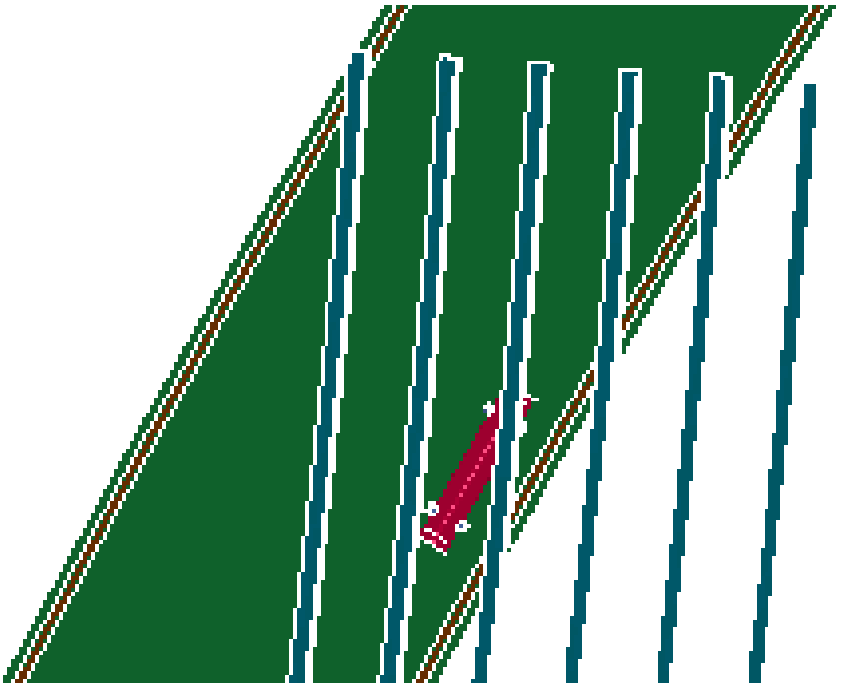

Figure 7.17. Impact Case #3: GA-4 Package Oriented to Yield Main Impact on Package Lid

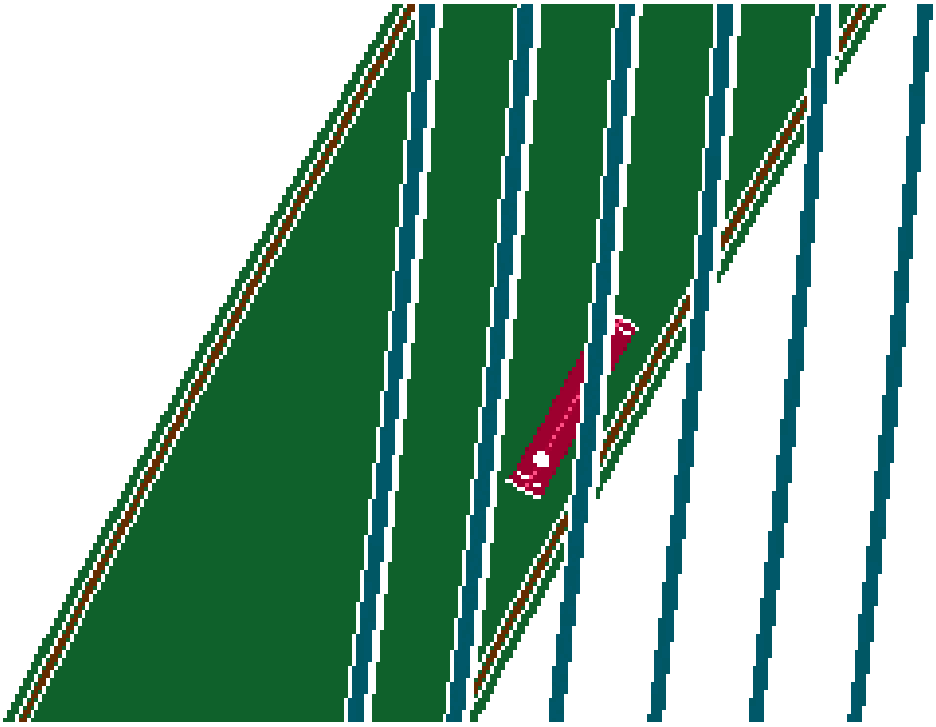

Figure 7.18. Impact Case #4: GA-4 Package Oriented for Trunnion Impact

The results of the analysis for all four of these cases show that the steel plate girders of the overhead roadway are more severely affected by the impact than the SNF package. The calculations show that the impact would cause significant plastic strains in the girders, such that the metal plates would deform under the impact, while the SNF package is relatively unaffected

by the impact force. Localized plastic strains are predicted in the package wall and the DU gamma shield, but these are much smaller than the strains predicted for the girders.

For the conditions of this scenario, it is expected that failure mode for the steel of the girders would be ductile fracture. Uniaxial tensile test data for A36 steel suggest that for conditions in the temperature range of the MacArthur Maze fire scenario, the elongation capacity for this material is over 50% and the reduction of area is over 95%. With this amount of available ductility, the calculated effective plastic strains below 20% appear to be well within the material's capacity. The girders would be severely deformed, but would be unlikely to fracture. This is illustrated conceptually in Figure 7.19, comparing a photo of a damaged girder from the actual roadway collapse following the fire to a graphic image from the LS-DYNA calculation for Case #1.

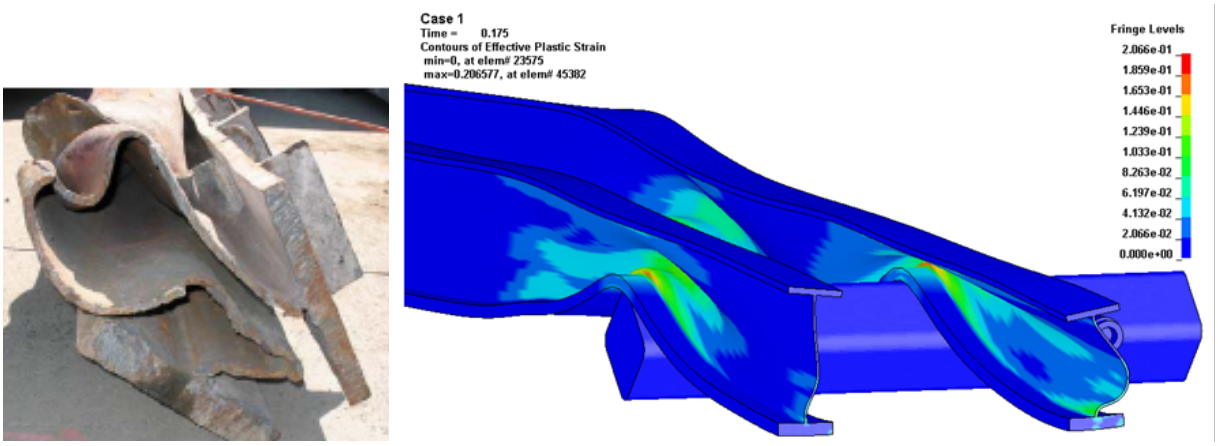

Figure 7.19. Illustration of Actual and Calculated Failure of Overhead Roadway Girders (photo from MAIT Report, CHP 2007, reprinted with permission.)

The maximum peak effective plastic strain in the XM-19 stainless steel of the package wall is calculated as 11 percent, and occurs in Case #2. An industry source lists short-term elevated temperature elongation data (*Nitronic 50 Product Data Bulletin*) for this material as having maximum elongation values between 41% and 59%t at 1500°F (816°C). Based on this data, the local plastic strains are not sufficient to cause structural failure of the steel components of the GA-4 package. In each impact orientation, the plastic strain regions are further evaluated based on relative size and penetration into the volume of the material or through the wall. In all cases, the localized plastic strains represent surface damage, not gross deformation of the steel package body.

The DU gamma shield is included in the model to give the steel package body realistic support. It is not considered a structural member in the GA-4 design, but the package SAR (General Atomics 1998, Section 2.1.2.2.2) notes that the DU may transfer compressive loads and provide backing for the containment wall. It is modeled to perform this function in a conservative manner. Since the DU is not a part of the containment boundary, it is not specifically evaluated for failure. Plastic deformations in the DU are reported and plotted to show the locations where the containment wall required maximum support from the DU structure.

7.3.1 Structural Case #1: Package Perpendicular to Upper Roadway Girders

The axial length of the GA-4 package and the spacing of the I-580 girders permit direct perpendicular impact on the package from only two of the girders simultaneously, with a narrow miss from a third. If one of the impacting girders strikes the package near its mid-point, the second one strikes on one end. Figure 7.20 shows a diagram of the pre-impact configuration for this scenario.

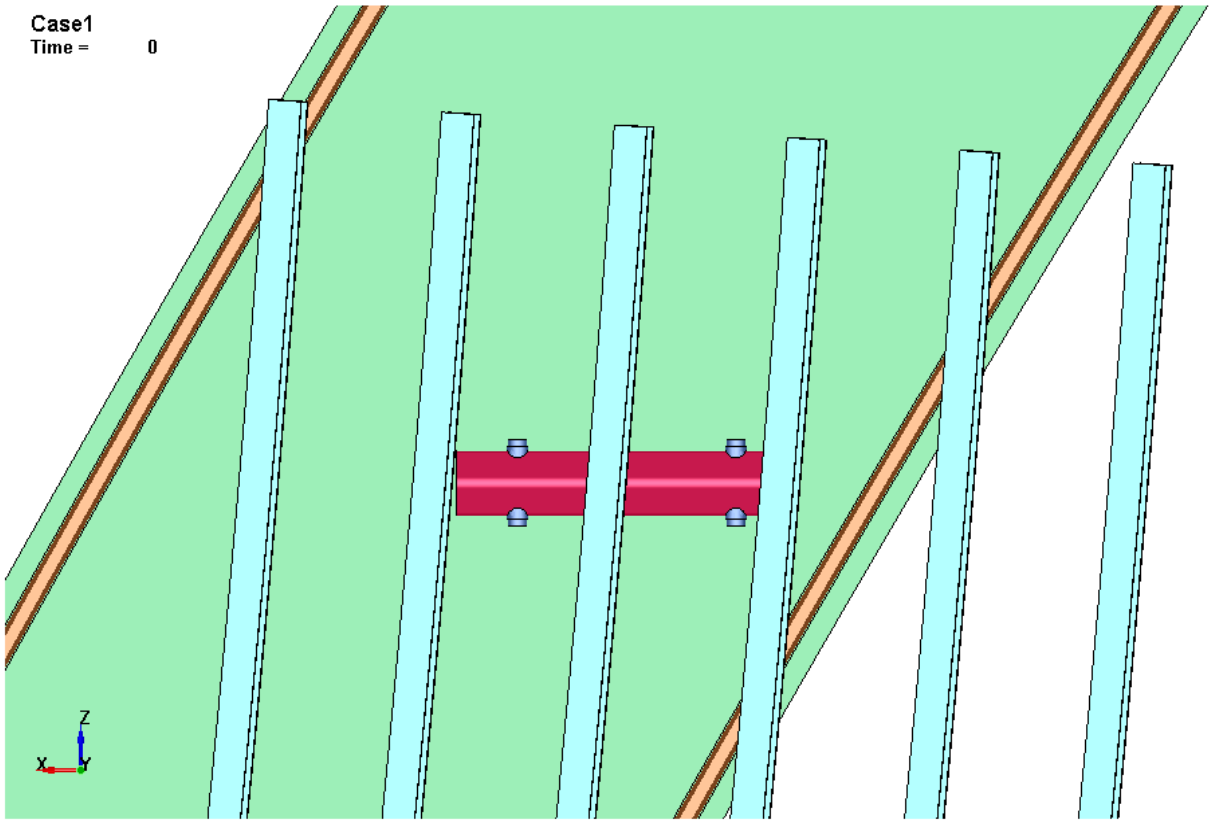

Figure 7.20. Case #1: Pre-impact Geometry—Girders Perpendicular to SNF Package

Figure 7.21 shows the deformation of the upper roadway girders after 0.205 s, which is after the maximum load has been transferred to the package. The calculation continues to 0.4 s, and the plastic strain in the package body at this time is shown in Figure 7.22. Plastic strain is localized at the contact points with the girders on the upper edge of the package, and with the lower roadway on the lower edge of the package. The maximum through-wall plastic strain is plotted in Figure 7.23. The maximum strain is predicted to be 2.4%. Plastic strain drops to zero on the inside surface.

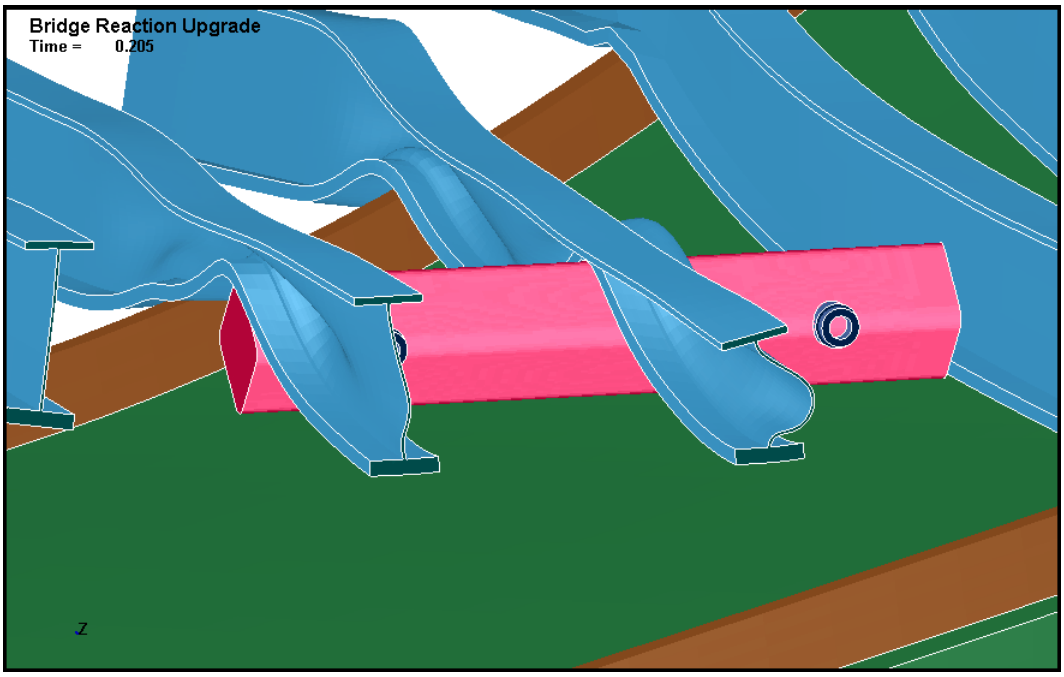

Figure 7.21. Case #1: Deformation of I-580 Span after Impact

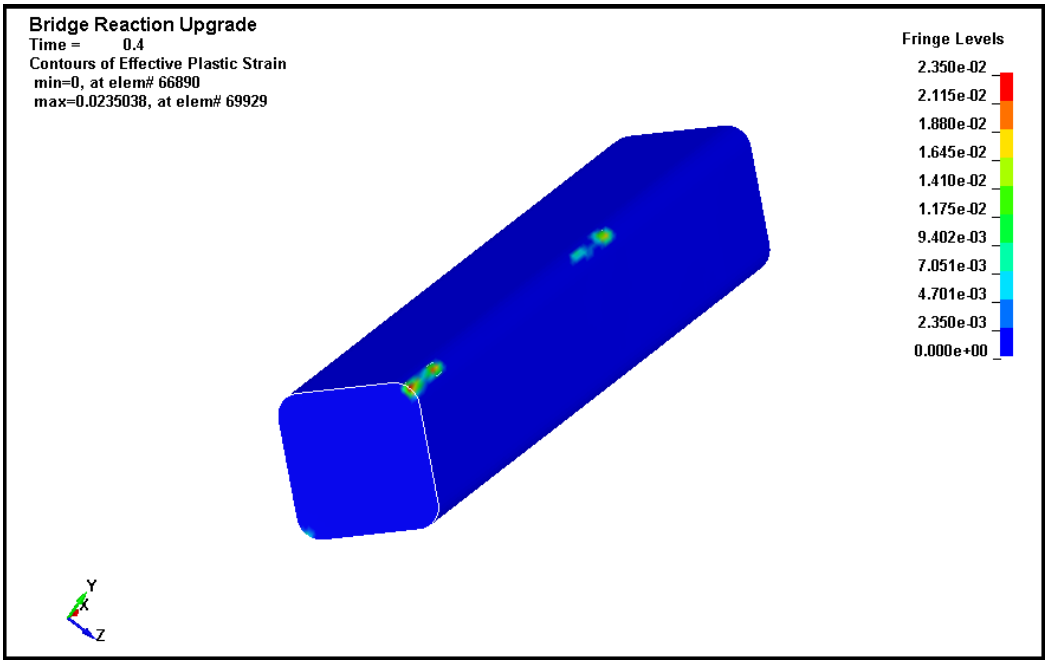

Figure 7.22. Case #1: Effective Plastic Strain in Package Body Wall

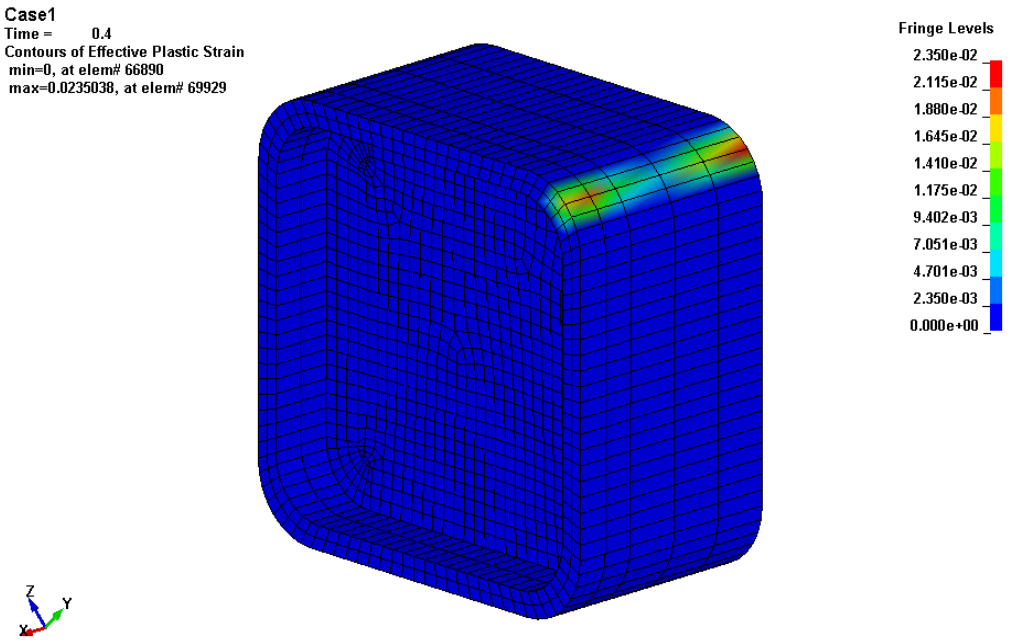

Figure 7.23. Case #1: Maximum Plastic Strain in Package Body Wall

Figure 7.24 shows the plastic strain in the DU gamma shield for this scenario. The steel shell wall deforms across the 1-mm gap between it and the DU, imparting to the DU material plastic strains up to 1.5%. The plastic strain region in the middle of the length shows where the containment boundary requires the most support in this impact scenario.

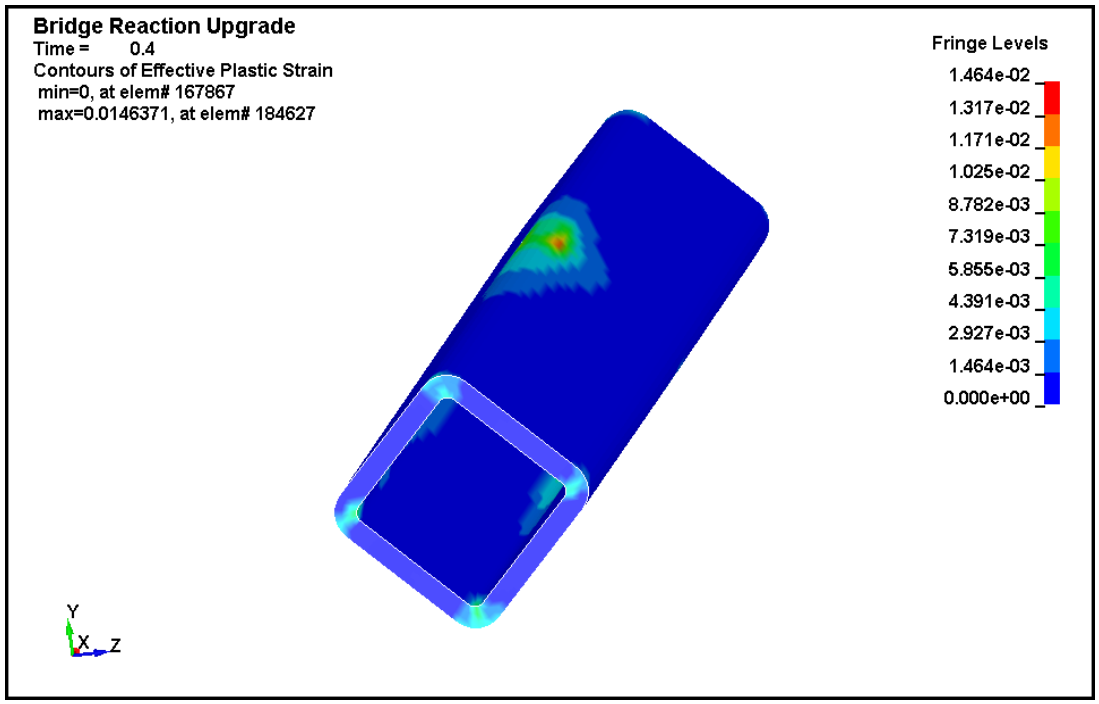

Figure 7.24. Case #1: Effective Plastic Strain in DU Gamma Shield

7.3.2 Structural Case #2: Package Parallel to Upper Roadway Girders

This case considers the effect of an impact with one of the upper roadway girders aligned along the spine of the GA-4 package. Figure 7.25 shows the positioning of the package and girders before impact. (The roadway concrete has been omitted from this image, for clarity.)

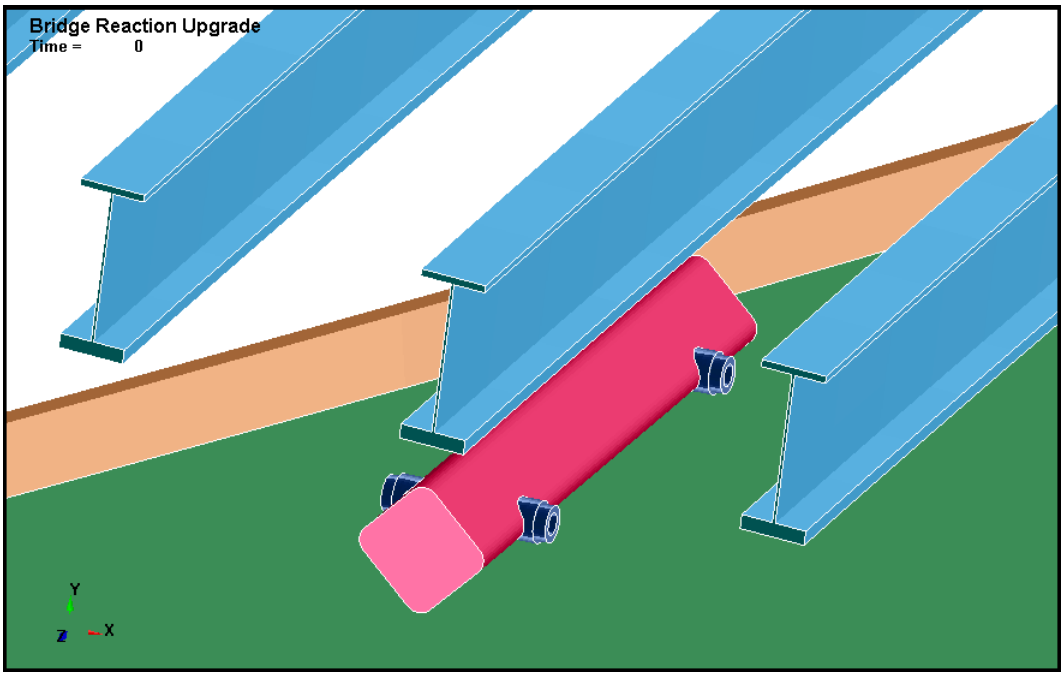

Figure 7.25. Case #2: SNF Package and Girder Orientation

Figure 7.26 shows that plastic strain in the package is below 1.1% for most of the axial length, with higher values occurring only near the end of the package. In this region, plastic strains are predicted to be up to 11%. This value is the highest predicted in the four cases. Figure 7.27 shows the plastic strain is localized, but it does penetrate into the third layer of elements with plastic strains below 1%. This is the end region, at either the base plate or closure end, and not through the package shell wall. While the closure plate and bolts are not modeled, the closure end is structurally robust because the thick closure plate extends into the flange for additional structural support. Figure 7.28 shows the predicted plastic strain in the DU gamma shield, within the steel body wall. Plastic strain in the DU is more widespread but also at a relatively low magnitude, up to about 3%.

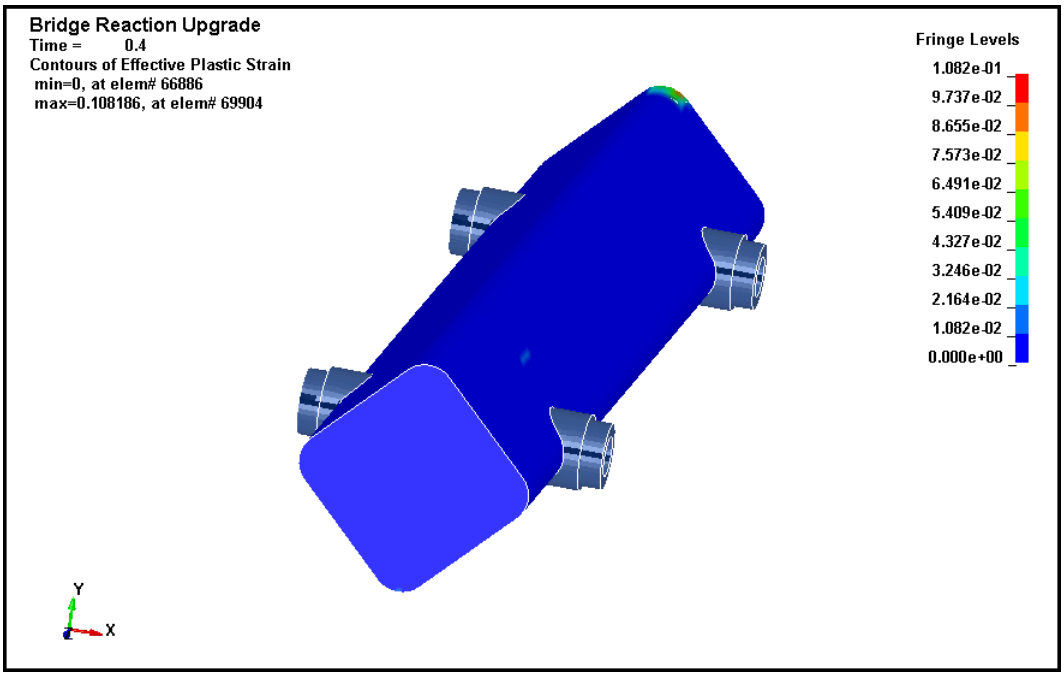

Figure 7.26. Case #2: Effective Plastic Strain in Steel Body Wall of SNF Package

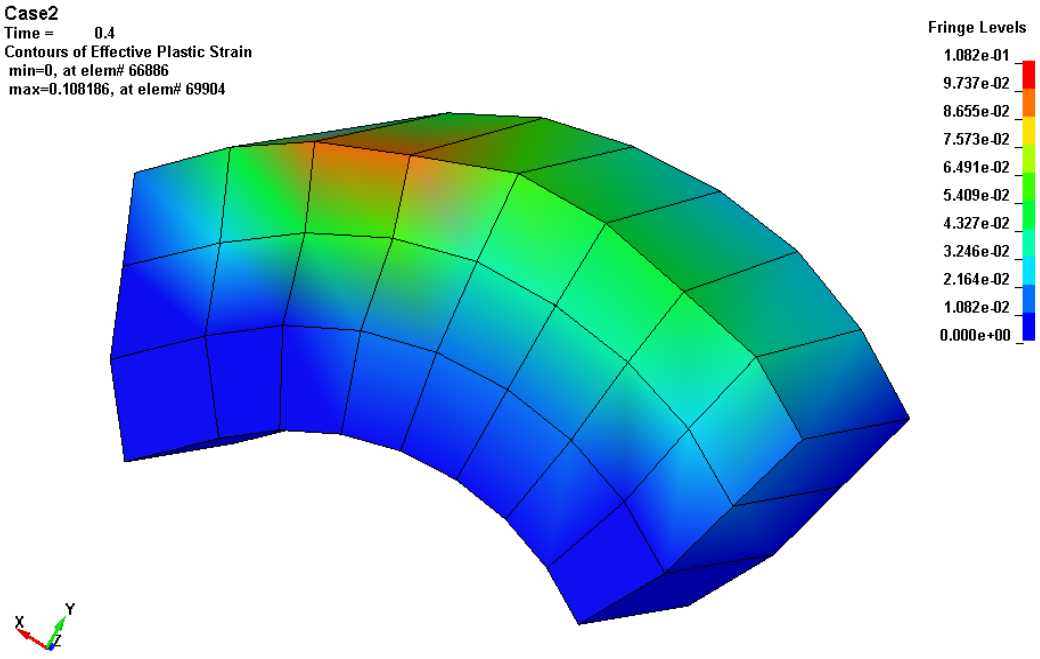

Figure 7.27. Case #2: Local Plastic Strain in Containment End

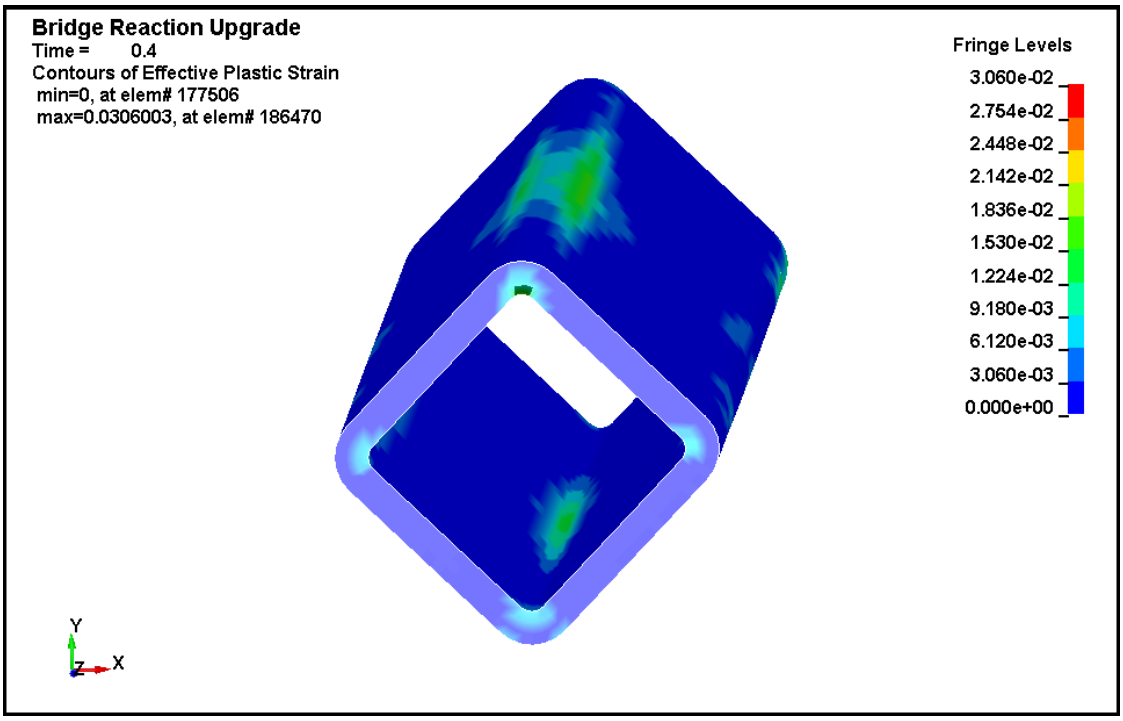

Figure 7.28. Case #2: Effective Plastic Strain in DU Gamma Shield

7.3.3 Structural Case #3: Impact Localized on the Package Lid

In this case, the package was positioned such that only one girder made contact with the end of the package. As in all the other cases, the simplified model of the GA-4 package does not include detailed representation of the closure bolts, but the purpose of this case is to investigate the amount of potential damage to the flange area. (See Section 7.3.6 for analysis and discussion of the effect of the fire scenario on the closure bolts.) Figure 7.29 shows the girder deformation around the package for this drop scenario.

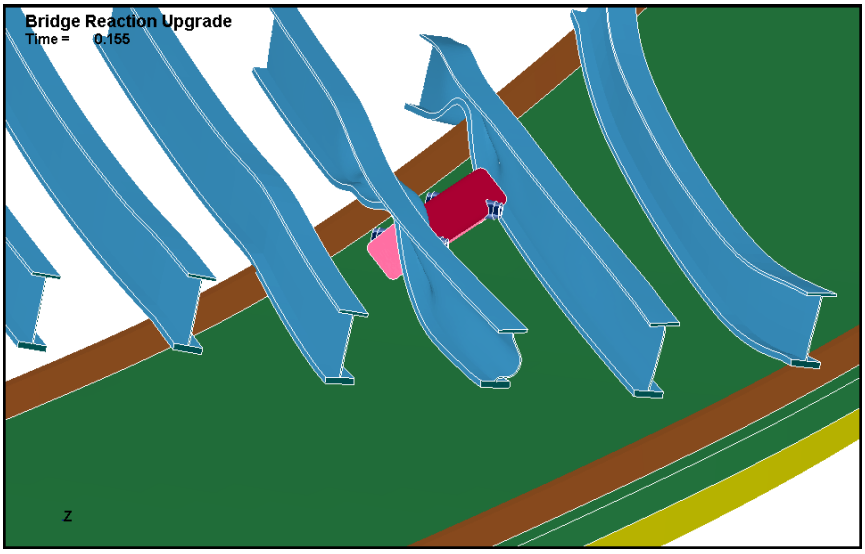

Figure 7.29. Case #3: Girder Deformation and Effective Plastic Strain

Figure 7.30 shows the plastic strain in the package wall for this drop scenario, which is localized at the impact area with a magnitude of about 5%. Figure 7.31 shows the extent of the plastic strain region. Plastic strains barely penetrate into the third layer of elements, with plastic strain magnitudes less than 0.1%. Figure 7.32 shows the plastic strain in the DU gamma shield, which remains below 3%.

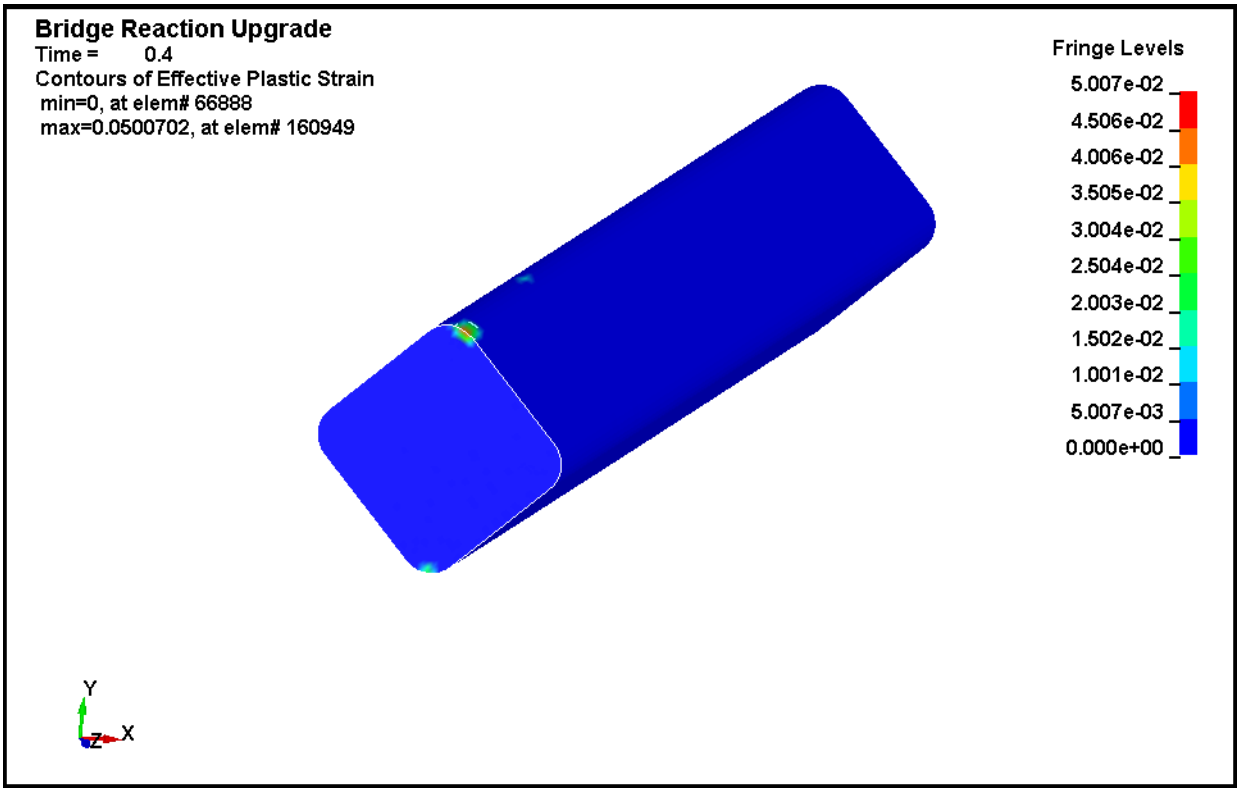

Figure 7.30. Case #3: Package Effective Plastic Deformation

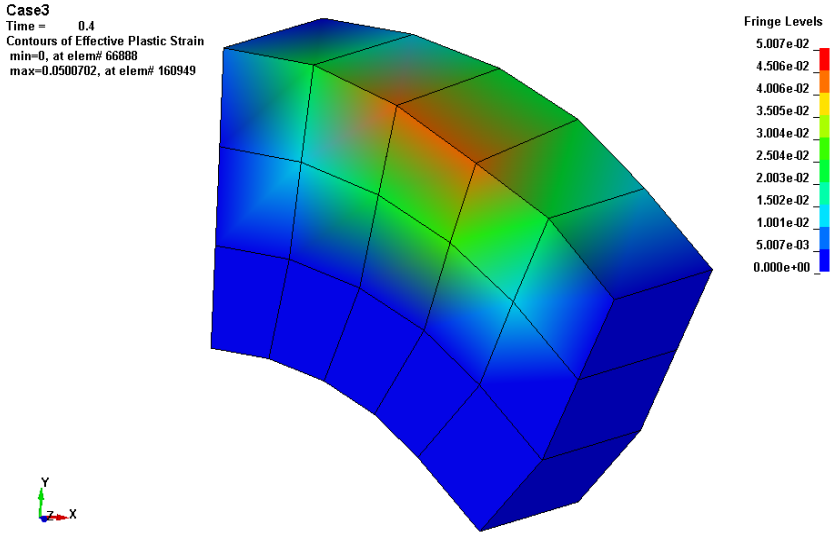

Figure 7.31. Case #3: Package End Plastic Strain

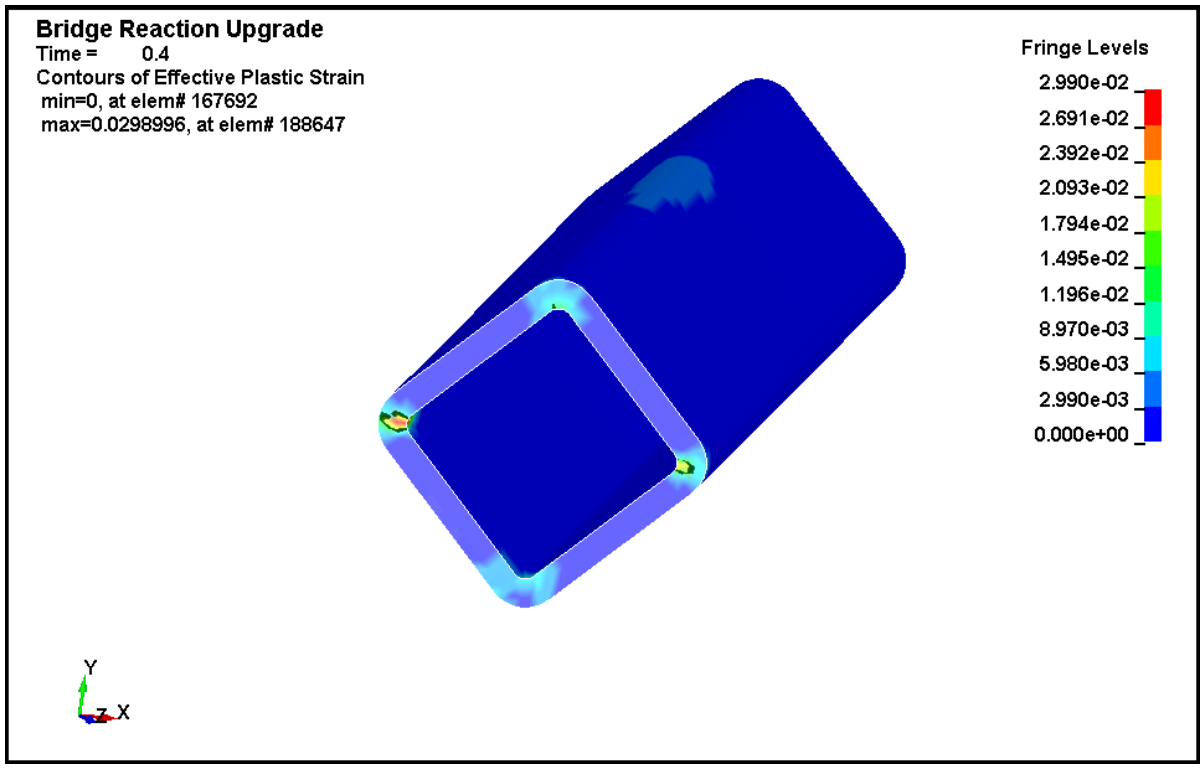

Figure 7.32. Case #3: DU Gamma Shield Effective Plastic Deformation

7.3.4 Structural Case #4: Impact Localized on the GA-4 Trunnions

This case investigates the potential for trunnion impact to localize the load on the package wall. Figure 7.33 shows the girder impact location and deformation. Figure 7.34 shows the plastic deformation in the package, which is very low and localized. Since peak plastic strains are below 1%, this case is the least damaging of the four considered here. Figure 7.35 shows the through-wall plastic strains in the maximum location. Figure 7.36 shows the plastic strain in the DU gamma shield, which is spread over a few areas but remains below 1.5%.

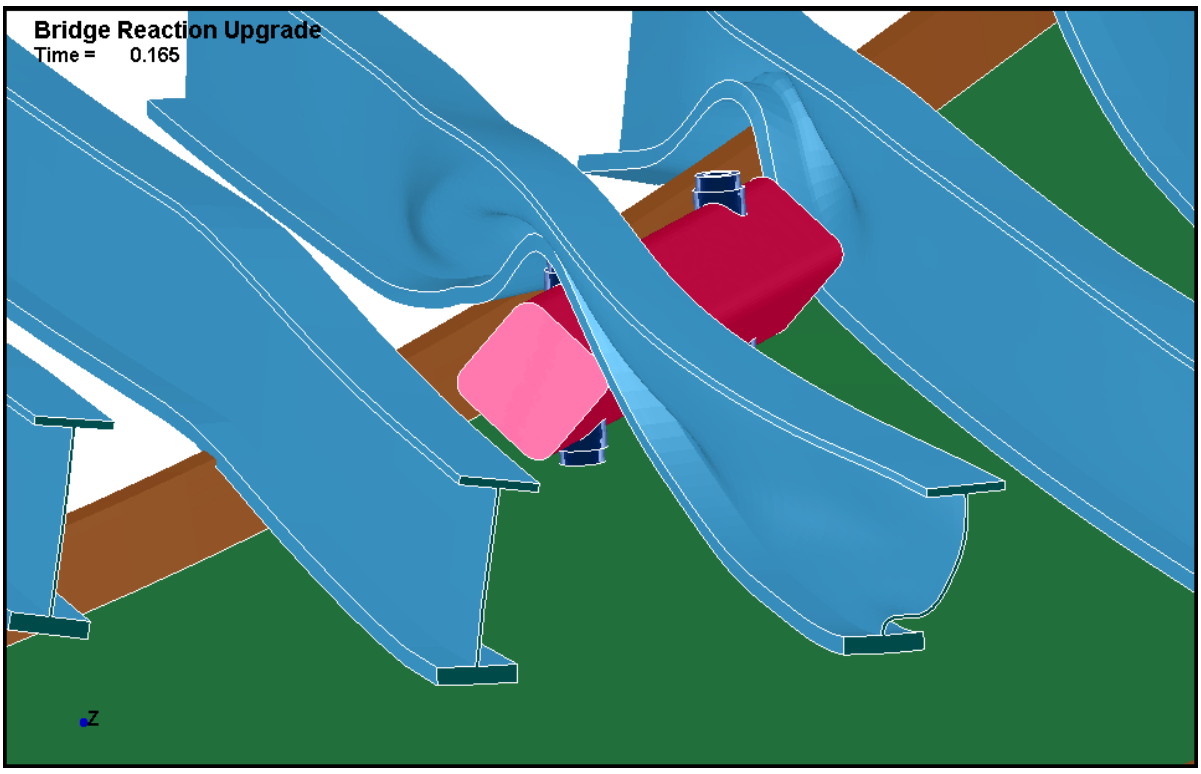

Figure 7.33. Case #4: Girder Deformation

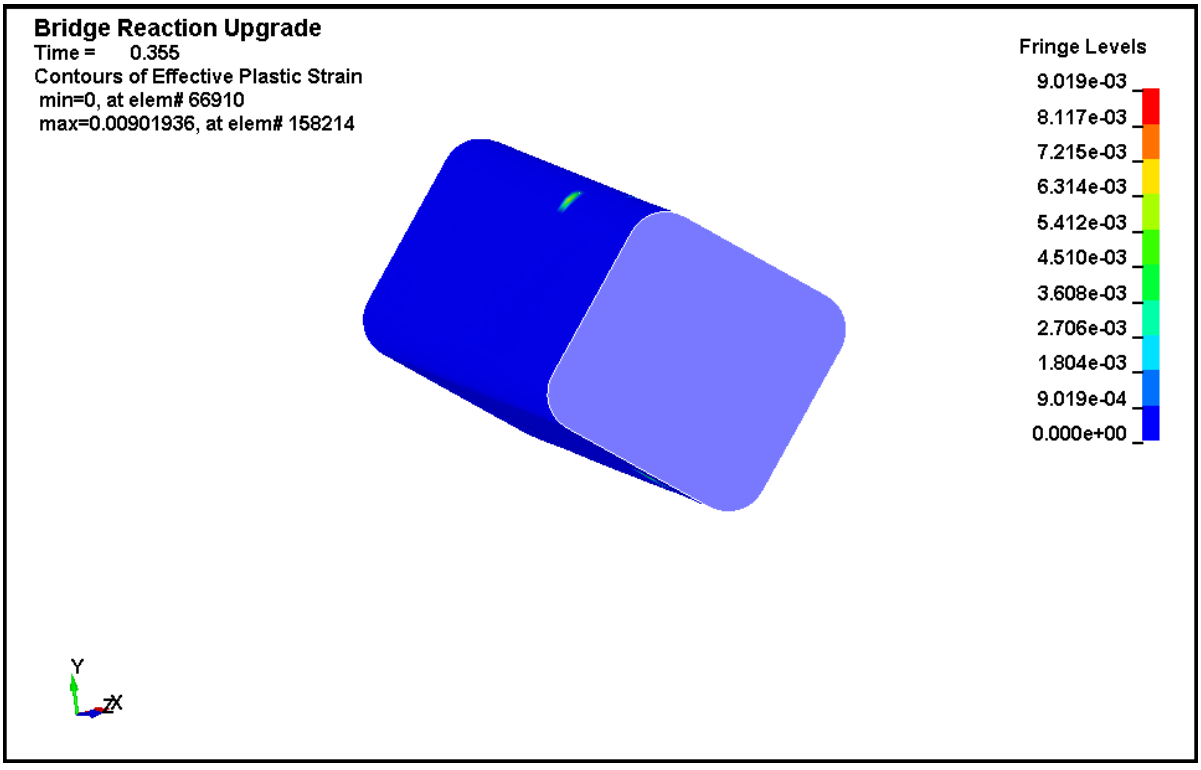

Figure 7.34. Case #4: Package Wall Plastic Strain

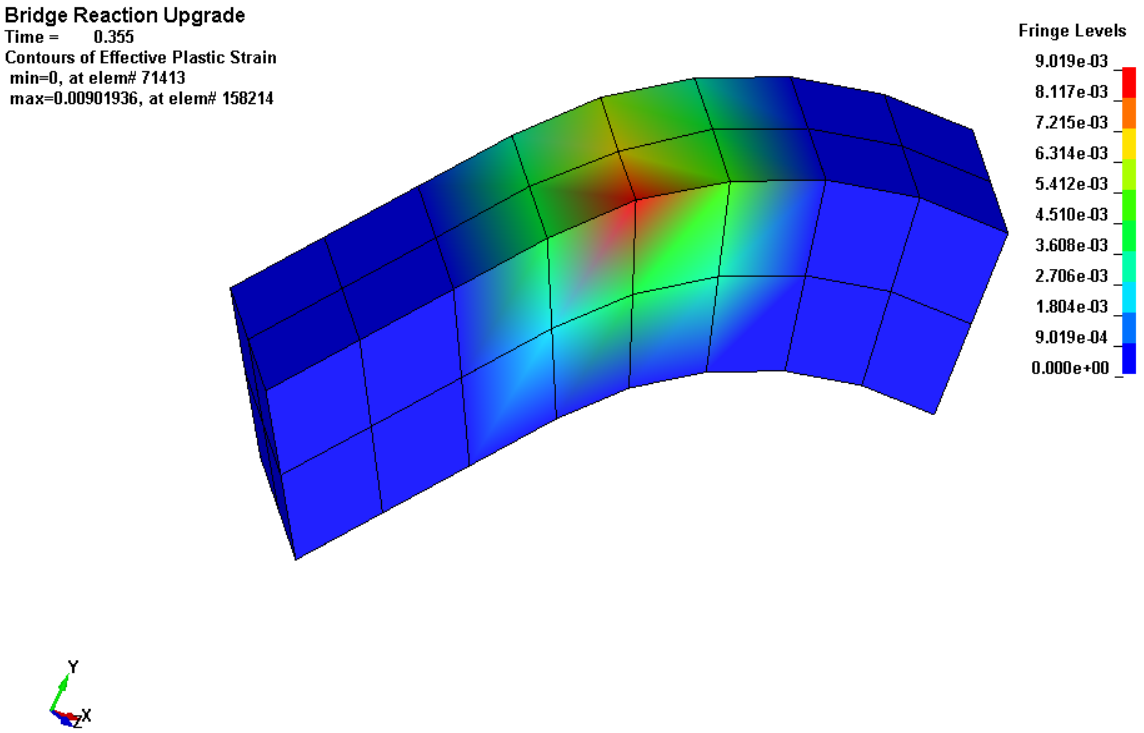

Figure 7.35. Case #4: Through-wall Plastic Strain

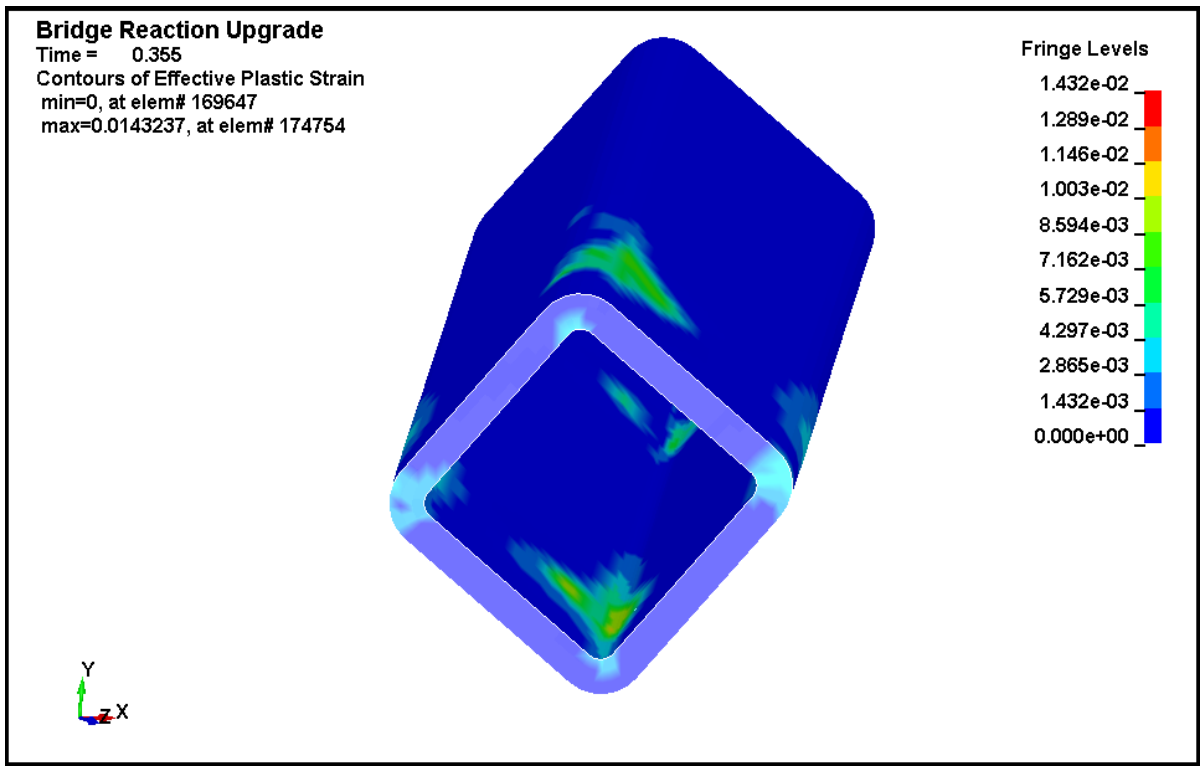

Figure 7.36. Case #4: Plastic Strain in DU Gamma Shield

7.3.5 Structural Impact Modeling Summary

The GA-4 package meets all regulatory requirements for over-the-road spent fuel transportation packages, and has a current Certificate of Compliance[1] issued by the NRC. Although the conditions of the MacArthur Maze fire, as conservatively modeled in these analyses, constitute conditions that are not specifically defined in the design basis for this package (as per 10 CFR 71), the results of the analyses with the structural models show that this package design is robust in this scenario. The structure of the GA-4 package wall is predicted to remain largely undamaged if subjected to this fire and roadway collapse scenario. The plastic strains imparted to the package wall by the girders are well within the expected ductility limit. Plastic strain tends to be localized on the outside surface, with through-wall plastic strains tapering off to zero or near zero on the inside surface. Some permanent deformation of the package wall would be expected, but there would be no gross failure or rupture of the package.

The most important mechanisms at work in this impact scenario appear to be the fundamental characteristics of the girder structure and the package structure. The girders are thin and comparatively weak at high temperatures, so tend to deform on impact instead of imparting energy to the stronger package. Based on the physics, minor variations in temperature or geometry are not likely to change the broad conclusion that the package would maintain its structural integrity during this scenario.

The results of Case #2 show the potential for localized plastic deformation of the cask if the impact were to occur in the closure region. The package model used in these impact analyses represents the closure lid and flange as a single undifferentiated structure. In reality, the closure lid is inset into the top flange, extending 11 inches into the package cavity. Approximating the region as a solid slab of material is reasonable for determining the general package response, but the individual response of the two components is not evaluated. In the cases with impact at the cask lid region, plastic strain predicted at the flange end could cause localized deformations that could potentially affect the seating and seal of the closure lid.

A complete representation of the impact response of this region would require more detailed modeling of the lid and top flange. However, the results of the thermal analyses of the package, as discussed in Section 7.1 and 7.2 above, show that the seals would be expected to fail in this fire scenario, so it is not necessary to examine additional potential modes of seal failure, such as the possibility of localized deformation due to impact loading. The issue of retaining the seating of the closure lid is investigated in Section 7.3.6, which reports the results of evaluations of the consequences of differential thermal expansion of the closure bolts, package lid, and top flange using a range of approaches, from classic bolt analysis to detailed FEA modeling of the components. These evaluations show that these crucial fasteners continue to perform their function, and would be expected to hold the closure lid in place even in the severe thermal environment of the MacArthur Maze fire scenario.

7.3.6 Structural Issues Related to Bolt Thermal Expansion

Evaluations with the thermal and structural models of GA-4 package have identified two critical sets of bolts that could potentially affect its performance under the conditions of the MacArthur Maze accident scenario. These are the closure bolts fastening the lid to the package body, and

[1] Docket No. 71-9226, Certificate No. 9226, originally issued in 1998. Updated with Revision 1 in 2003, Revision 2 in 2008, Revision 3 in 2009, and is currently licensed under Revision 4. Expiration date for Revision 4 is October 31, 2018.

the bolts fastening the top impact limiter to the anchor plate attached to the package body. Fire temperatures cause a significant amount of thermal expansion in the bolts and the package structure in general. The bolts are Inconel, and expand less than the XM-19 top flange and lid. The stresses caused by this thermal expansion mismatch are high, and add to the initial bolt tension. The closure bolts affect the containment boundary, while the impact limiter bolts affect the thermal response of the package, especially in the closure region, in that they determine whether or not the impact limiters would remain attached to the package in this accident scenario.

Inconel and XM-19 stainless steel are materials that retain high strength at elevated temperatures, but the Inconel experiences significantly less thermal expansion than the XM-19. This leads to increased tension in the bolt, beyond the initial tension due to the bolt torque applied at normal operating temperature. As the temperature increases during the fire scenario, the stresses from thermal expansion increase, and material strength begins to decline. There is a temperature limit for both sets of bolts, above which there could be failure of the connection, either through the tensile load on the bolt shank or the shear load on the threaded interface. This effect is independent of the postulated mechanical impulse load due to the overpass falling on the package, which occurs early in this transient scenario.

A critical feature of the GA-4 package design relative to its potential performance in this fire scenario is that the Inconel bolts are not threaded directly into the XM-19 structure of the package, either for the lid or the impact limiters. They are instead threaded into Heli-Coil threaded inserts, which protect the harder metals from galling. These inserts are made of Type 304 stainless steel, which decreases in strength much more rapidly with increasing temperature than does XM-19. As a result, the insert threads can become the weakest link in the fastener, which is not consistent with standard bolted fastener design practice[1]. The dissimilar materials involved in this design, coupled with the elevated temperatures resulting from the MacArthur Maze fire scenario, require detailed evaluation. The approach used in this analysis is based on calculations with engineering mechanics equations, using temperature results from the FEA thermal model. The effects of elevated temperature and forces due to differential thermal expansion are also evaluated with the structural and thermal FEA models of these components.

The radial symmetry in the package geometry and the time-varying but uniform ambient boundary temperature throughout the fire scenario result in a symmetrical temperature distribution around the ends of the package. The uniform boundary temperature, which during the fire portion of the transient is a bounding temperature based on the FDS analysis presented in Section 3.0, is a reasonable approximation for the actual conditions seen by a surface with an assumed bounding uniform view of ambient. The radial symmetry of the temperature distribution extends to the ring of closure bolts, and also to the ring of impact limiter attachment bolts. As a result, all of the bolts in a given ring would be expected to have essentially the same temperature distribution. The response of any given bolt or insert can be treated as representative of the response of all bolts and inserts of that ring.

One important unknown in the bolt thermal expansion evaluation is the post-yield behavior of the threaded inserts. The inserts carry a shear load that maintains the tension in the bolts due to initial bolt torque and differential thermal expansion. If the threaded interface were to yield, it

[1] Bolts are generally designed to fail (yield) in the shank before an unexpectedly high load damages the threads. Analyses reported in the GA-4 SAR (General Atomics 1998) show that this would not be an issue for the maximum temperatures and impact loadings predicted for the design basis of this SNF package (10 CFR 71).

would reduce tension in the bolt, and thereby reduce the potential for the bolt to yield. However, if the threaded interface were to fail, it could potentially result in a complete loss of bolt restraint and the possibility of detachment of the closure lid or impact limiter from the package. These possibilities are evaluated by considering two thresholds for the shear strength of the threaded inserts: shear yield, based on the material's yield strength, and shear failure, based on the material's ultimate tensile strength. The total shear force on the interface is compared to these thresholds over the effective thread shear area. It is assumed that the shear area remains constant between yield and failure, which is reasonable in this case, since the inserts fill the void between thread patterns and have little physical room to deform.

The presence of the impact limiters was treated as a variable in the thermal cask analyses by including them in the ANSYS thermal model but omitting them from the COBRA-SFS model. The thermal response of the package is affected by this variable, in that the location of the maximum fuel temperatures is different for the two cases, but the maximum fuel temperature values are not substantially different. In the context of the closure bolt evaluation, however, this becomes a critical issue.

The thermal models of this study consider two possibilities: the impact limiters detach before the fire or they remain attached through the fire duration and post-fire cooldown. A case where the fire or the bridge collapse causes the impact limiter to detach at some point during the fire is not explicitly modeled, but the thermal results of that case would be bounded by the assumption that the impact limiters are lost before the beginning of the fire. This treatment provides a bounding thermal evaluation for the package and the spent fuel assemblies contained within it (as discussed in Section 7.2), but carrying this uncertainty forward into the closure bolt evaluation is unnecessary. As discussed below in Section 7.3.6.1, loss of the impact limiters is not a credible consequence of the MacArthur Maze accident scenario. Therefore, the impact limiters are assumed to remain attached to the package for the evaluations of the closure lid bolts presented in Section 7.3.6.2 and Section 7.3.6.3.

7.3.6.1 Results of Impact Limiter Bolt Evaluations

A 3D structural and thermal finite element model of one impact limiter bolt and the surrounding material was developed, using the ANSYS thermal model results as a baseline temperature distribution. (See Section 5.4.2 for model description details.) This model considered the effects on bolt temperature of an additional heat transfer path for the bolts that was neglected in the ANSYS thermal model of the GA-4 package. The detailed single-bolt model was used to evaluate bolt thermal expansion at the predicted temperatures.

The GA-4 package impact limiter attachment bolt heads are located at the bottom of long holes extending the axial depth of the impact limiter cap. (See diagram in Figure 5.19.) The bolt heads are by design uncovered, for access when attaching or removing the impact limiters. This configuration results in the bolt heads being directly exposed to ambient conditions. The deep holes would essentially preclude convection heat transfer to the bolt heads, but they would be exposed to thermal radiation exchange with ambient conditions.

This pathway for heat to enter the system was not captured in the ANSYS thermal model of the GA-4 package, since it would not be expected to have a significant effect on the total package thermal response to the fire scenario. However, this omission could have an effect on the local temperature distribution and affect the thermal expansion calculations for the impact limiter bolts. Therefore, additional evaluations were performed with the impact limiter bolt model, to determine the potential effect of the additional thermal energy that could be entering the region

by means of thermal radiation. There are two possible ways the extra energy could affect the thermal response of the impact limiter bolts to the fire conditions. It could increase the temperature in the threaded interface, or it could increase tension in the bolt, due to changing the temperature distribution in the bolt shank. Both of these possibilities are explored using the ANSYS thermal model of the impact limiter bolt region.

The single bolt model used in the thermal expansion structural evaluation was extended to the thermal-physics environment by changing element types, degree of freedom constraints, and other ANSYS model parameters. The thermal radiation load was modeled with ideal heat transfer between the fire environment and the top bolt head surface, with all other surfaces adiabatic. The initial temperature was set to 124°F (51°C) throughout the bolt and local package region, which is the minimum initial temperature in the region, based on the ANSYS thermal model of the GA-4 package at NCT. The single bolt model was then subjected sequentially to the two phases of the MacArthur Maze fire scenario. As described above, the first phase consists of an ambient temperature of 2012°F (1100°C) lasting 37 minutes, and the second phase consists of an ambient fire temperature of 1652°F (900°C), lasting for another 71 minutes. Evaluation of the post-fire cooldown period was found to be unnecessary.

The results obtained with this thermal model show that including thermal radiation to the top of the bolt slightly increases the temperature of the bolt shank at the end closest to the fire, but has almost no effect on the temperature at the other end of the shank, in the threaded region of the bolt. This response is due to the relatively low thermal conductivity of the bolt nickel alloy, and the relatively small amount of radiant thermal energy that can be absorbed through the small cross-section of the bolt heads. The net effect of including thermal radiation at the bolt head is to slightly increase the bolt shank temperature relative to the package steel wall, which slightly reduces overall bolt tension, because of the corresponding small increase in thermal expansion. This is because thermal radiation helps reduce the component of bolt tension caused by the non-uniform temperature distribution in the bolt shank and box region. The results of this analysis show that it is appropriate and conservative to neglect the effect of thermal radiation on the bolt head in this analysis.

These evaluations show that the fire conditions defined to bound the MacArthur Maze fire could be damaging to the threaded inserts, but the potential for failure of the threaded interface is limited by the bolt shank's capacity to yield and relieve tension. The results of these analyses support the conclusion that the attachment of the impact limiters to the package would not fail due to thermal loads imposed by this fire scenario. The mechanical loads of the accident are within the regulatory realm and do not require additional evaluation. This fire scenario represents a more challenging fire accident than that required in the design basis for the GA-4 package, but a detailed thermal evaluation of the system shows that the connection formed by the impact limiter bolts would survive even under these conditions.

The baseline temperature history case evaluates the thermal expansion of the impact limiter bolt using a temperature history from the results obtained with the ANSYS thermal model of the GA-4 package. (See Section 7.2 for package thermal modeling results.) This model yields detailed nodal temperature predictions in the region of the bolts, but the mesh does not directly align with the nodal mesh of the bolt model. The predicted temperatures were mapped onto the bolt model mesh using a simple averaging scheme at locations along the axial length of the bolt. The appropriateness of this approach was verified by developing a mapping scheme based on the maximum temperatures at a given axial location. The temperature history considered here includes only the 108-minute fully engulfing fire transient. The results show that considering the post-fire cooldown period is not necessary.

Total force on the thread interface is extracted from the ANSYS model at each solution time step, and the tension due to the bolt preload is added to obtain the total shear force. The initial preload due to bolt torque is a tension of 21,657 lbs (96.3 kN) at room temperature (General Atomics 1998). To account for temperature-dependent material properties, the preload force is scaled by the modulus at the average shank temperature. For example, with an average shank temperature of 754°F (401°C), the preload is reduced to 88% of its initial value.

The bolt will yield wherever the temperature is hottest along its length, since yield strength decreases with temperature, but the force load on the cross section remains constant along the axial length. The shear yield behavior of the threaded inserts is not well quantified, but the tensile yield behavior of the bolt shank would closely resemble a typical tensile test. In the temperature range of the conditions predicted for the MacArthur Maze fire scenario, the elongation capacity of the bolt material is approximately 20% or greater. The amount of elongation required to relieve all tension in the bolt at these temperatures is less than 1%. This indicates that the bolt shank has enough ductility to accommodate the yield without failure.

For all temperatures in the range of interest, including post-fire temperatures, these evaluations show that bolt yield is reached before insert shear failure. Shear failure of the insert before the bolt shank yields and releases tension could occur only with the insert at a much higher temperature than the bolt shank. This is not physically possible in this scenario, because of package geometry considerations, and is therefore not of concern.

7.3.6.2 Results of Lid Closure Bolt Evaluations (Classical Approach)

The results of classical bolt calculations for the bolts securing the closure lid of the GA-4 package are presented in this section. The analysis considers the bolt preload (due to the initial torque on the bolts), the external load (due to the internal pressurization of the package cavity), and the thermal load (due to differential thermal expansion of the Inconel bolts and XM-19 stainless steel closure lid and flange of the package body). The bolt preload is defined based on the manufacturer's requirements (General Atomics 1998). The external load due to package pressurization is calculated based on the average gas temperature within the package cavity, as predicted with the ANSYS thermal model. The thermal load is determined in this analysis, based on the detailed temperature predictions from the ANSYS thermal model.

Many parameters in the classic bolt analysis are based on the geometry of the system, and therefore are straightforward to determine, such as the diameter of the bolt shank and its cross-sectional area. Less readily defined parameters include the effective joint area, which affects the representative stiffness of the lid and flange combined. One common method (Juvinall and Marshek 1991) uses the average area of a conical volume between clamped members. An alternative approach using bolt mechanics gives a more approximate estimate, based on bolt diameter. For the GA-4 geometry, the effective areas estimated from these two methods are 4.60 in^2 and 3.18 in^2, respectively. The difference in estimated area results in less than a 3% difference in predicted bolt tension, which is within the uncertainty in the overall approach, and therefore either estimate would be considered reasonable.

The thread inserts are a complicating feature for this analysis. Although thread inserts are commonly used to prevent thread galling, there is little information in the literature concerning their effect on the mechanics of a bolted joint. In typical applications, it can generally be assumed that the thread inserts have negligible effect on the bolt tension, particularly if the thread insert material is similar to the surrounding material. In the GA-4 package, however, the

bolts are nickel alloy (Inconel), the closure lid and flange is XM-19 stainless steel, and the inserts are Type 304 stainless steel thread inserts. At NCT, temperatures are in a range where the XM-19 and Type 304 stainless steels have similar mechanical and thermal properties. Potential problems arise in the fire scenario as the predicted temperatures on these components rise to ranges in which the yield strength of the Type 304 insert decreases much more than the XM-19. At high temperatures and high tensions, the classic bolt calculations demonstrate that the inserts could have a dramatic effect on the clamping force between the closure lid and the package body flange.

As part of an initial assessment of the bolt behavior due to the elevated thermal loads of the fire scenario, the effect of the thread insert was neglected. Classical bolt calculations were used to determine the bolt tension and clamping force over time, assuming the thread insert would have no effect on the bolt or joint stiffness. The joint effective area was assumed to be 4.5 square inches, which is near the high end of the area estimates described above. The key parameters in this calculation are listed in Table 7.1.

Table 7.1. Key Bolt Parameters

Parameter	**Specified Value**
Critical Bolt Cross Section (in^2)	0.605
Effective Bolt Shank Length (in)	4.62
Bolt Pitch Diameter (in)	0.9100 - 0.9168
Bolt Major Diameter (in)	0.9830 - 0.9980
Bolt Shank Diameter (in)	0.878
Lid Bolt Hole Diameter (in)	1.08
Flange Bolt Hole Maximum Diameter (in)	1.21
Bolt Head Diameter (in)	2.0
Effective Joint Area (in^2)	4.5

The significant loads on the bolt are determined from the initial tension specified by the design and the temperature and internal pressure response of the package to thermal conditions of the MacArthur Maze fire scenario, as determined from the thermal modeling. The ANSYS thermal model calculated the transient out to 14.5 hours, which is approximately an hour beyond the point at which all components of the package were decreasing in temperature. This is more than 12 hours after the end of the actual fire duration, but average component material temperatures within the package are still above 1000°F (538°C), and the average cavity pressure is more than 100 psi above the initial pressure at the start of the transient. Given the large thermal inertia of the GA-4 package, it would take a very long time for the system to cool back down to its starting conditions after exposure to a fire of the severity of this bounding model of the MacArthur Maze fire scenario.

Figure 7.37 shows the extrapolated cavity gas temperature calculated with a reasonable assumed power-law cooldown rate, based on the physical behavior of a large object with high thermal inertia cooling in air. The corresponding cavity pressure from the ideal gas law (conservatively assuming no leakage), is shown in Figure 7.38. Based on this extrapolated cooldown rate, the time required for the closure lid bolt region to drop from its peak temperature of 1223°F down to 500°F would be on the order of 50 hours. It would require approximately 400 hours for the system to return to its original temperature and pressure state. The long-term temperature response is important to this analysis, because it is in the cooldown phase that the clamping force has potentially the greatest challenge in this scenario.

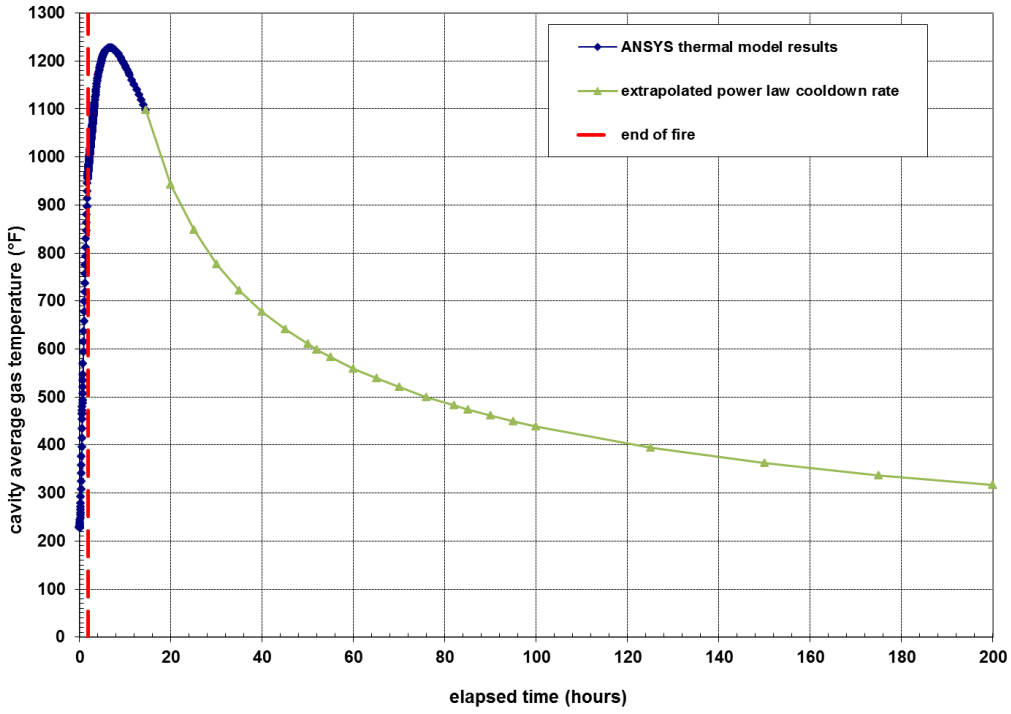

Figure 7.37. Average Cavity Gas Temperature from ANSYS Thermal Model Calculated to 14.5 Hours, with Power-law Extrapolation to 400 Hours

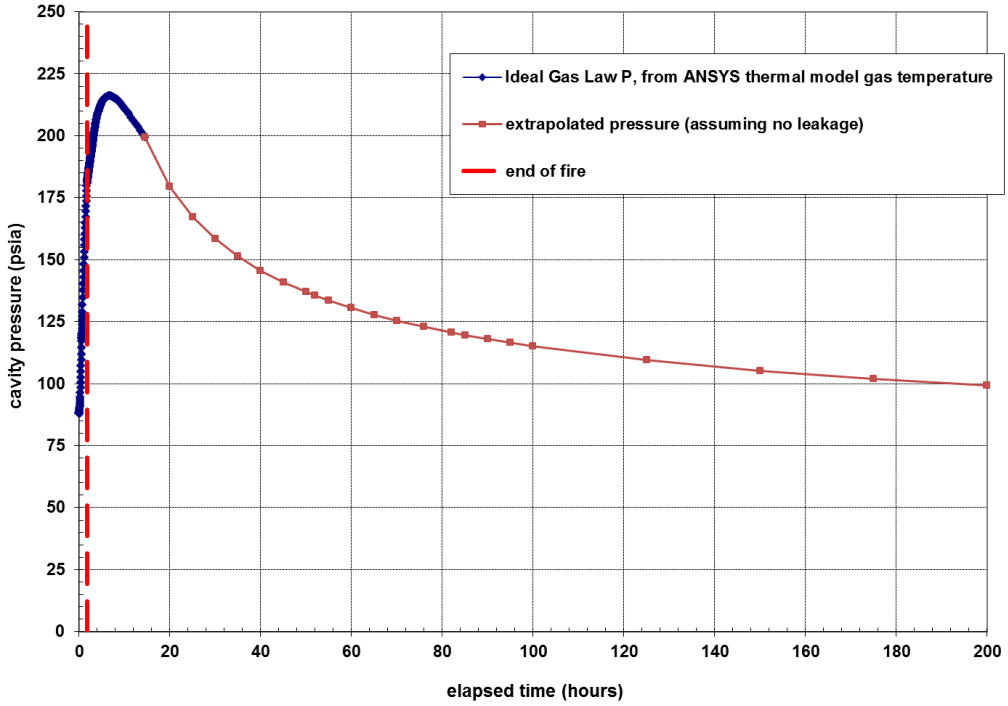

Figure 7.38. Cavity Pressure Calculated from Average Cavity Gas Temperature, Assuming No Leakage

The results of the classical bolt analysis are tabulated in Table 7.2, with the three components of bolt force separated for comparison. Bolt Force is the tension on each of the twelve bolts, considering all loads and the stiffness of the bolt and joint material. Clamp Force is expressed on a per-bolt basis, so the surfaces in contact would experience a total force that is twelve times the value given in the table. Figure 7.39 shows plots of these force values, on a per-bolt basis.

Table 7.2. Results of Classical Bolt Analysis

Time (hrs)	Temperature (°F)	Pressure (psi)	Components of Bolt Force			Bolt Force (lbs)	Clamp Force (lbs)
			Initial Bolt Preload Fi (lbs)	Elongation Fe (lbs)	Thermal Expansion Ft (lbs)		
0	129.9	73.7	20,655	2,806	0	20,998	18,192
0.17	153.4	75.7	20,655	5,297	13,356	34,612	29,314
2	857.3	169.9	20,655	6,470	18,779	40,424	33,953
5	1184.6	199.4	20,655	7,594	26,953	48,810	41,216
10	1199.9	197.3	20,655	7,512	27,262	49,103	41,590
14.5	1114.9	185.4	20,655	7,062	25,512	47,300	40,239
52	482.8	120.6	20,655	4,592	9,768	31,052	26,460
400	129.9	73.7	20,655	2,806	0	20,998	18,192

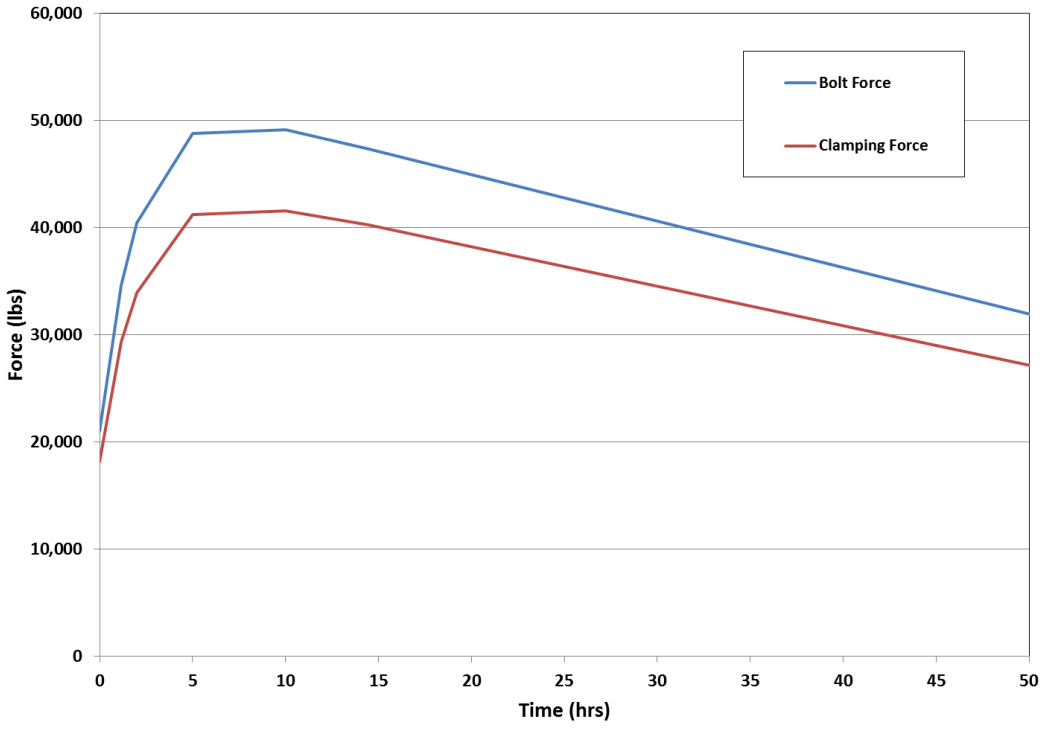

Figure 7.39. Bolt Force and Clamping Force Predicted using Classic Bolt Equations

The peak value of 49,103 lbs for the bolt force calculated from the classical bolt analysis is significantly high, considering the strength of materials involved. Figure 7.40 shows the predicted strength of the thread insert and bolt materials over time (in response to the temperature transient), compared to the predicted bolt force during this transient. The strengths are determined based on the thread insert minimum shear area, which is defined at the major diameter of the bolt thread. As the plot in Figure 7.40 shows, the bolt is not in any danger of yielding under the load of the predicted bolt force in this analysis. By contrast, the weaker thread insert is predicted to exceed its yield limit at approximately three hours into the transient. However, the ultimate shear strength of the insert is not exceeded at any time during the transient, which suggests that the insert would yield and release some tension without completely failing.

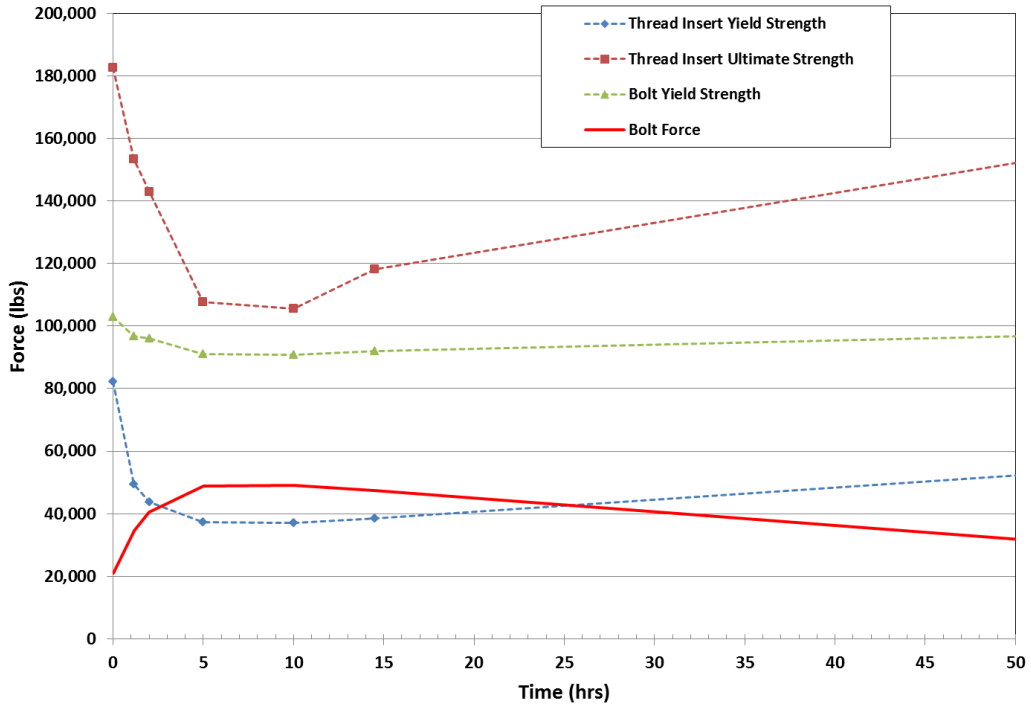

Figure 7.40. Strengths of Thread Inserts and Bolts Compared to Bolt Force Predicted using Classic Bolt Equations

This is an important conclusion for the release calculations, and provides some indication that the GA-4 package could withstand the MacArthur Maze fire scenario without significant failure of the containment boundary. However, the yielding in the inserts and the effect this would have on the clamping force needs to be more precisely quantified, so that it can be used in evaluations of potential consequences of subjecting an SNF package to this accident scenario. It is therefore necessary to expand this analysis with the classic bolt equations to include an estimate of the effect of insert yielding on the closure lid clamping history.

If the thread insert were to yield, this would be expected to result in a reduction of tension in the bolt. Furthermore, such yielding would be expected to cause a permanent reduction of the initial tension load, which would persist after the system returned to its starting temperature and pressure. This is truly a complex scenario, but a few simplifying assumptions can be made to adjust the classic bolt equations to estimate the potential reduction in clamping force.

The first assumption is that the force that can be carried by the thread insert is limited to the yield strength at each particular temperature. This is a conservative assumption because in reality the material would be expected to strain-harden, which means that the actual load that the insert can support would tend to increase as the material starts to yield. A second assumption is that the effect of plastic deformation in the thread insert corresponds to a pound-for-pound reduction in the initial bolt tension. In other words, the initial preload force (Fi in Table 7.2) is permanently reduced by the amount of bolt force that exceeds the thread insert yield limit. This is potentially a non-conservative assumption because the yielding occurs at elevated temperatures where the stiffness is lower than the starting condition. Yielding at high

temperatures might contribute to a proportionally higher reduction of bolt tension when the system cools. Both of these assumptions are made to simplify the problem enough to obtain an estimate of the potential effect on the clamping force.

Figure 7.41 shows the effect on bolt force and clamping force when yielding of the thread insert is taken into account in this analysis. The plot in this figure compares these results from the predicted forces shown in Figure 7.39, calculated assuming no yielding of the thread insert. The plot in Figure 7.41 shows that accounting for yielding of the thread insert results in a dramatic change in the overall results. By the time the system returns to its initial state, the clamping force is significantly reduced from its starting value. This is a very different outcome than is predicted in the elastic case, which assumes the bolt will ultimately return to its starting state of tension.

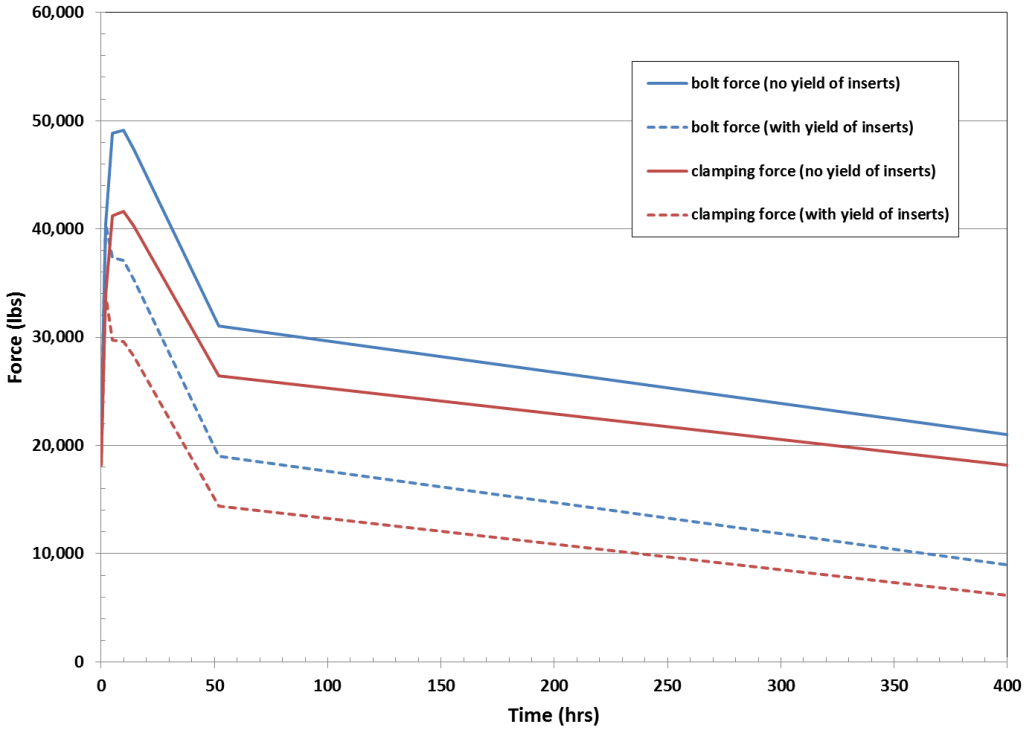

Figure 7.41. Estimated Effect of Yielding Thread Inserts Using Classic Bolt Equations

Since the package ethylene propylene seals are not expected to survive the MacArthur Maze fire temperatures, the clamping force on the metal-to-metal contact surfaces of the closure lid and package body flange is all that will be holding the pressurized contents inside the package cavity. In this configuration, the leak rate from the package cavity would be directly related to the clamping force. Basing estimates of leak rates on this type of simplified modeling evaluation would lead to large uncertainties in any estimate of potential release rate from the package. Because of the sensitive nature of the leak rate calculations, a more sophisticated estimate of the clamping force history is needed. This is provided by the results of the detailed FEA modeling approach, as described in Section 7.3.6.3.

7.3.6.3 Results of Lid Closure Bolt Evaluations (FEA Modeling Approach)

As described in Section 5.4.3.2, the FEA modeling of the lid closure bolt region consisted of a detailed representation of a single bolt, due to the radial symmetry of the package and assumed boundary conditions for the MacArthur Maze fire scenario. Figure 7.42 shows a diagram of the model, including a close-up of the detailed mesh in the thread insert region.

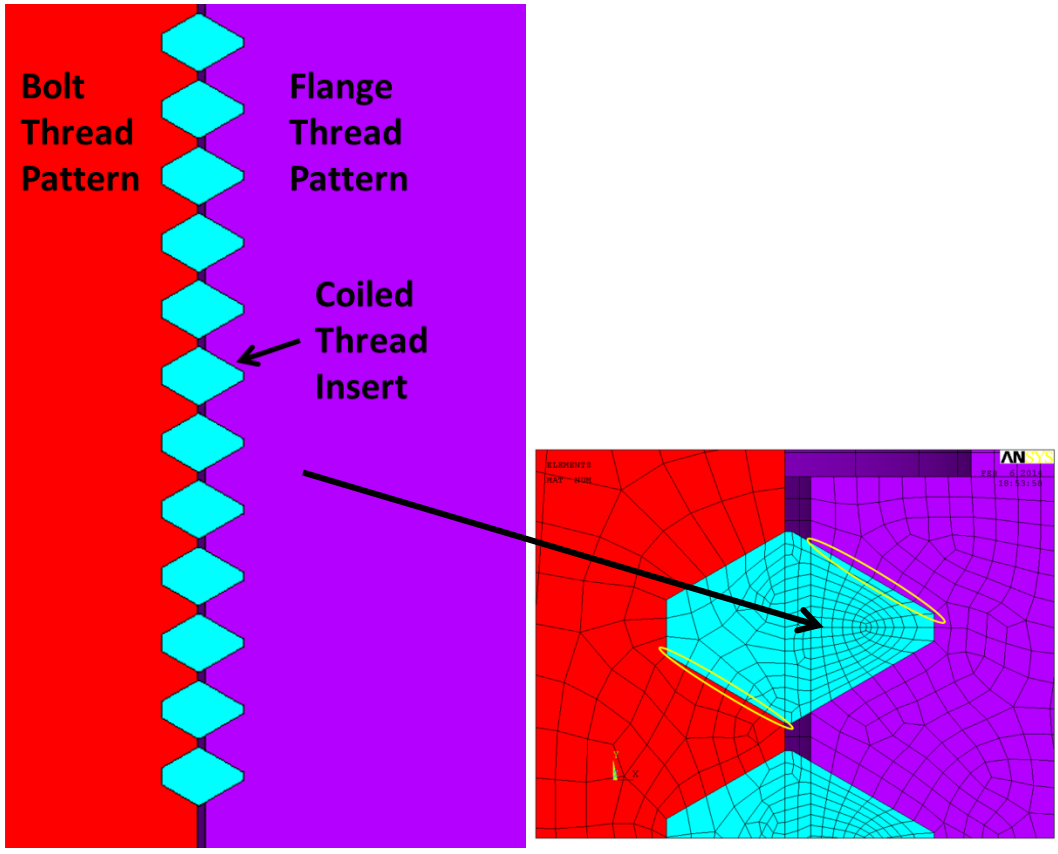

Figure 7.42. Diagram of Detailed Mesh in Thread Insert Region

In the classical bolt analysis presented in Section 7.3.6.2, the critical shear area for the thread insert was assumed to occur at the maximum diameter of the bolt thread, corresponding to 7/8-pitch. In reality, the critical shear area of the insert would be more likely to occur on the flange thread. However, in this geometry, the area of the two possible shear areas would not be significantly different. The finite element model shows that peak stress concentrations occur on the bolt side, but it is not obvious which shear plane would have the higher average stress. This is illustrated in Figure 7.43 which shows the peak von Mises stress (psi) state in the thread inserts at the peak temperature in the evaluation assuming elastic materials. The high stresses would certainly cause plastic strain to occur, with a corresponding redistribution of the stress. This is further evidence that the evaluation requires a multilinear elastic-plastic material model.

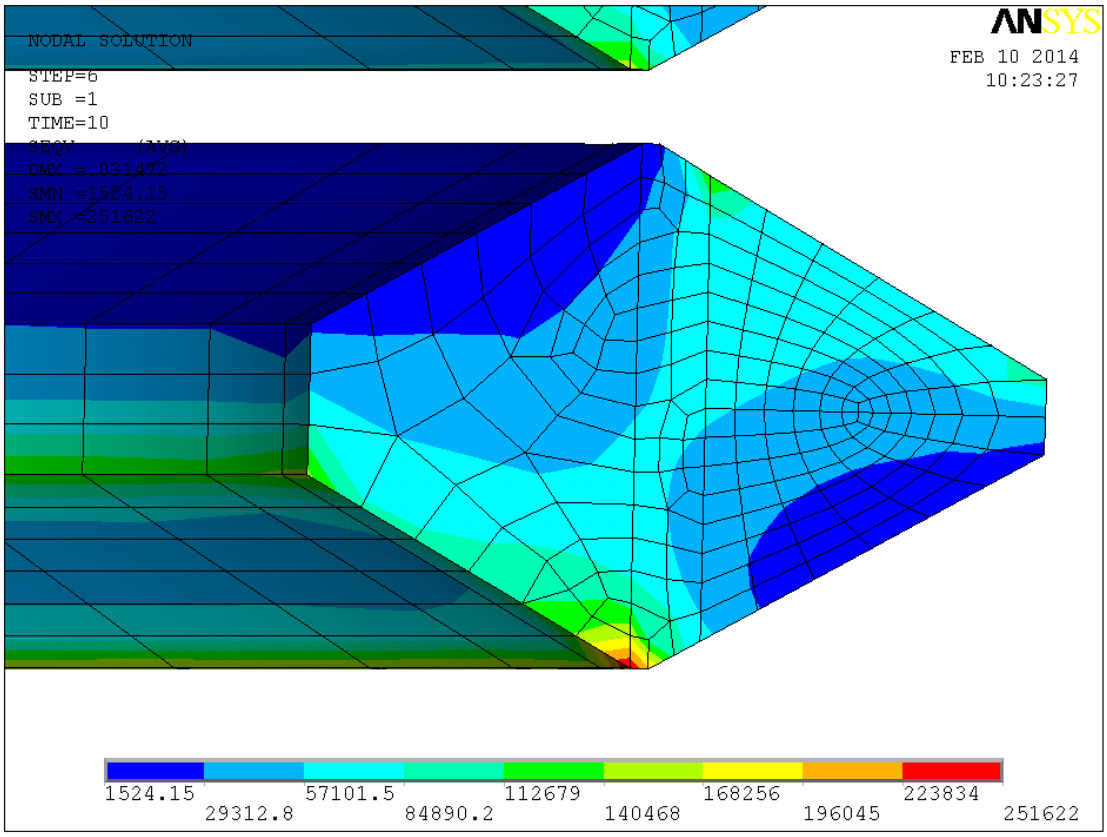

Figure 7.43. Stress Distribution Predicted with Elastic-only Assumptions in FEA Model

With elastic materials, the bolt force and clamping force agree with the classic bolt calculations to within 1% at the initial temperature and pressure. But as temperature and pressure increase in the transient, the bolt force and clamping force predicted with the FEA model are approximately 20% lower than the values predicted by the classic bolt calculations. Sensitivity evaluations comparing the FEA model results and the classic bolt calculations showed that the two can be brought in good agreement using assumptions and parameter adjustments that simplify the FEA model to approximate the level of detail captured in the classical approach. These evaluations demonstrated the significance of the stiffness of the thread insert material in determining the behavior of the system, and show that the classic hand calculations overestimate the bolt tension and clamping force, and would offer a conservative prediction of the amount of plastic deformation that would occur in the thread insert.

This is consistent with the distinction between a bolt and a screw, as was noted previously as an important factor in this evaluation. The nut-and-bolt configuration assumes the clamping force is applied by the head of the bolt on one side and the axial face of the nut on the other side of the joint. The clamping area estimate for a true bolt (Juvinal and Marshek 1991) assumes that the conical volume extends from the bolt head to the nut, as illustrated in Figure 7.44(a). The clamping area estimate for the corresponding screw configuration, as shown in Figure 7.44(b) would result in an effective clamped volume that would be smaller than in the bolt-and-nut configuration. The angle defining the volume for the screw fastener cannot readily be determined in the classical approach, and for this reason alone, the elastic FEA results would be expected to provide a better estimate of the effective joint area of this screw configuration (2.0 in^2) than the values obtained in the classic bolt estimates (3.18-4.60 in^2).

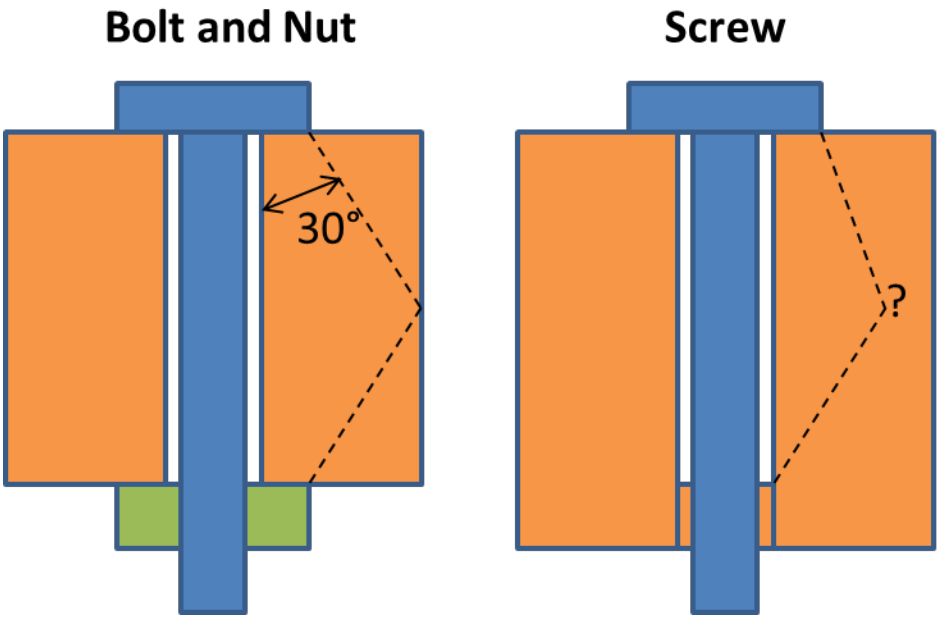

Figure 7.44. Diagram of Compression Volume for (a) Bolt and (b) Screw Fasteners

Even when considering only elastic behavior of the system, the FEA model provides a more realistic prediction than the classic bolt calculations. Further refining the FEA model to include multilinear temperature-dependent material properties for the thread insert material permits a best-estimate of bolt tension and clamping force for the conditions assumed in the MacArthur Maze fire scenario.

For the nonlinear analysis, the only change in the FEA model was in the definition of the material properties for the thread insert. The multi-linear kinematic hardening model was used to define stress-strain curves for a range of temperatures between 70°F (21°C) and 1200°F (649°C). Figure 7.45 shows the stress strain curves in units of psi versus strain (in/in). The bolt material and flange material were both defined as elastic material. The nickel alloy bolt retains such high strength that even localized yielding is not expected.

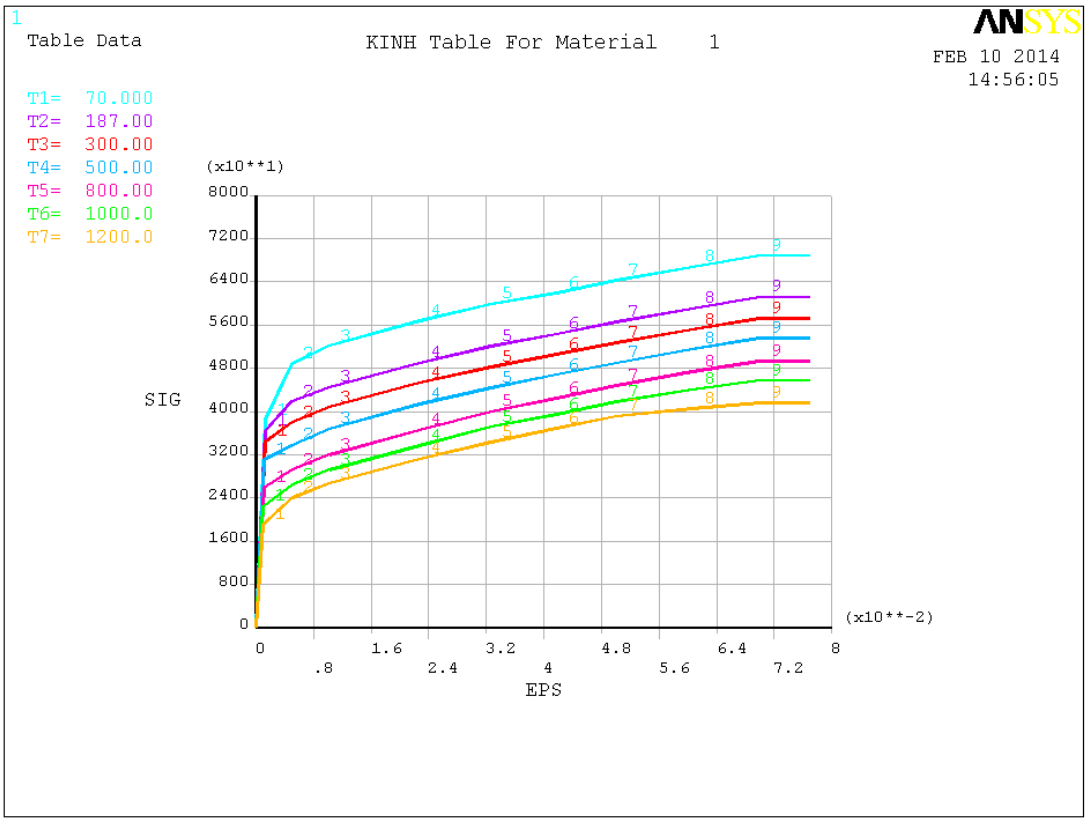

Figure 7.45. Stress-Strain Curves used for Thread Inserts in Multi-linear FEA Model

The model predicts small plastic strains throughout the thread inserts, particularly along a line from the bolt outer diameter to the flange inner diameter, crossing from one shear plane to the other. Figure 7.46 shows contours of equivalent plastic strain at the peak temperature and pressure. The peak localized plastic strain is about 5%, while the maximum average along a plane is roughly 2% in the bottom segment. At the top of the thread pattern, the plastic strain is generally much less, and the maximum average plane drops to less than 1%. However, even this relatively small plastic strain is significant when strain hardening is considered. Considering a plastic strain of 1% along the critical shear plane at 1200°F (649°C), strain hardening would increase the yield strength by roughly 50%. This suggests that the predictions obtained with the classic calculations are highly conservative, even when considering the effect of yielding thread inserts (as shown in Figure 7.41), since that approach does not consider the effect of strain hardening.

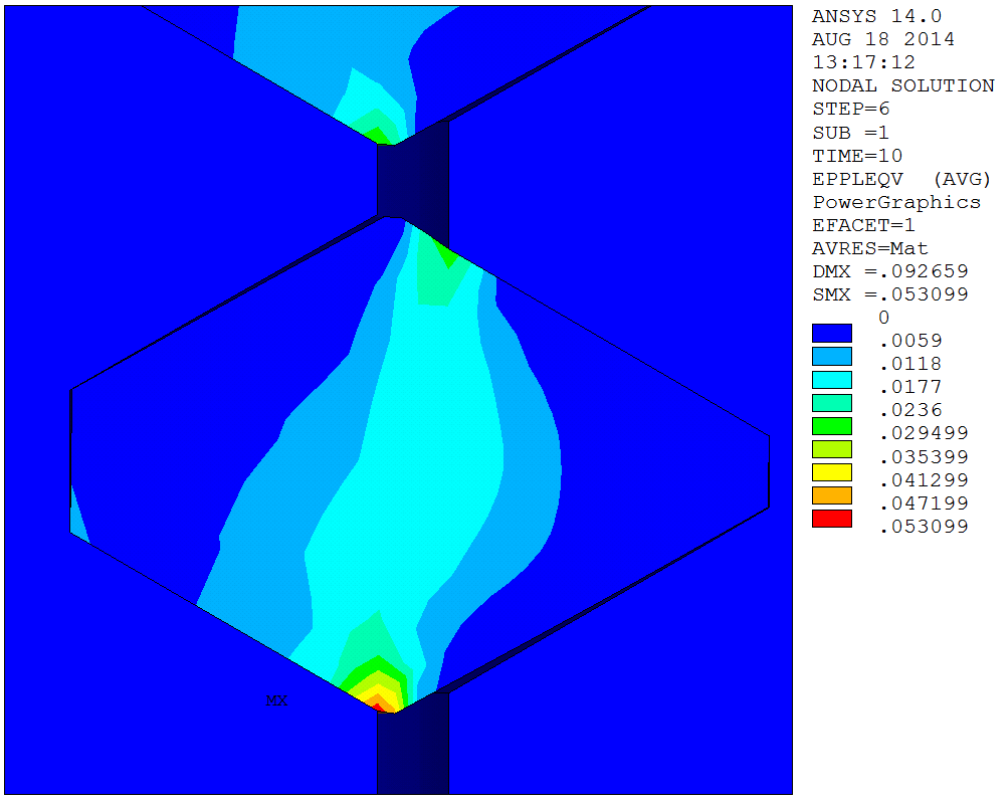

Figure 7.46. Plastic Strain in Thread Insert Predicted with Multi-linear FEA Model

The bolt tension and clamping force history, on a per-bolt basis predicted with the nonlinear finite element model is summarized in Table 7.3. These results can be considered a best estimate evaluation, within the conservative assumptions of the MacArthur Maze fire scenario. Comparing the initial conditions and final cooldown conditions at 400 hours, the ultimate reduction in clamping force due to plastic deformation of the thread inserts is predicted to be less than 8%. In absolute numbers, the loss of initial load (Fi from the classic bolt calculations) is only 1358 lbs.

Table 7.3. Best Estimate Results from Non-Linear FEA Model

Time (hrs)	Temperature (°F)	Pressure (psi)	Bolt Force (lbs)	Clamp Force (lbs)
0	129.9	73.7	20,920	18,191
0.167	153.4	75.7	29,995	24,876
2	857.3	169.9	33,923	27,680
5	1184.6	199.4	39,210	31,885
10	1199.9	197.3	39,399	32,149
14.5	1114.9	185.4	38,208	31,391
52	482.8	120.6	26,452	22,013
400	129.9	73.7	19,557	16,833

The nonlinear finite element model provides a reasonable best estimate prediction of the clamping force on the flange throughout the MacArthur Maze scenario and its eventual cooldown. These results are used as the basis for leak rate calculations for the GA-4 package, presented in Section 8.3.3.

8.0 POTENTIAL CONSEQUENCES

Potential adverse consequences of a severe accident involving an SNF transportation package fall into two general categories; a loss of shielding, which could pose an exposure risk to members of the public, and a failure of the containment boundary of the package, which could lead to a release of radioactive material to the environment.

Loss of either the neutron or gamma shielding of the package could potentially result in a direct radiation dose to an individual in close proximity to the package. Failure of any of the components (e.g., package seals) that make up the containment boundary could result in a release of radioactive material from inside the package, potentially resulting in a direct radioactive dose to first responders at the scene of an accident, or possibly to members of the public in the surrounding area. Loss of shielding as a potential consequence of the MacArthur Maze fire scenario is discussed in Section 8.1. Section 8.2 discusses the performance of package seals in this fire scenario. Section 8.3 presents detailed evaluations of the potential for a release from the GA-4 package as a result of the severe conditions predicted for this extremely conservative representation of the MacArthur Maze fire scenario.

8.1 Potential for Loss of Shielding

The potential for increased neutron and gamma radiation dose rates from the GA-4 as a result of exposure to the MacArthur Maze fire scenario was evaluated. Direct radioactive dose rate limits are specified in 10 CFR 71 for NCT and HAC conditions. As a licensed transportation package, the design basis of the GA-4 complies with the regulatory limits for all conditions of transport.

Section 8.1.1 describes the consequences of loss of neutron shielding for the GA-4 in the MacArthur Maze fire scenario. Section 8.1.2 discusses the potential for loss of gamma shielding.

8.1.1 Neutron Shielding

Neutron shielding for the GA-4 package is provided by neutron-absorbing liquid in an annular tank surrounding the steel body of the package (see Sections 5.1 and 5.2 for details of package geometry). The neutron shielding material is a mixture of 56% propylene glycol and water, with 1% dissolved boron. The neutron shield tank is not generally expected to survive the hypothetical accident conditions prescribed in 10 CFR 71 for SNF transportation packages, which include a 30-minute fully engulfing fire at “1475°F (800°C).”

The GA-4 package is designed to be in compliance with the regulatory limits for all conditions of transport. Loss of the neutron shield tank contents is a design-basis assumption for HAC, and analyses presented in the SAR (General Atomics 1998) for this package assume loss of the neutron shield in all accident scenarios, including the HAC fire. The conditions of the MacArthur Maze fire, although more severe than the HAC fire, can do no more damage to the neutron shield of the GA-4 than is assumed *a priori* in the HAC fire. Therefore, the GA-4 package would be expected to remain below the regulatory dose limits after loss of neutron shielding in the MacArthur Maze fire scenario.

8.1.2 Gamma Shielding

Gamma shielding for the GA-4 is provided by a 2.64-inch-thick (6.7 cm) layer of DU encased within the stainless steel body of the package. The DU layer extends a few inches beyond the full axial length of the package inner cavity to assure complete coverage of the active fuel length, and is positioned between the stainless steel inner liner and the 1.5-inch-thick (3.81 cm) stainless steel body of the package.

The DU material experiences a significant increase in temperature, but the performance of the DU gamma shield is unaffected by the MacArthur Maze fire scenario. As discussed in Section 7.3, structural analysis of a range of postulated scenarios in which the overhead I-580 highway span is assumed to impact the GA-4 package shows that the package would be expected to survive without structural failure. The thermal analyses of the package response to the fire scenario show that the peak temperature in the DU material could reach up to about 1480°F (805°C). This is significantly below this material's melting temperature of 2070°F (1132°C).

These results show that the gamma shielding of the GA-4 can be expected to remain intact and functional even if subjected to the severe conditions of the MacArthur Maze fire scenario. Therefore, the GA-4 package would be expected to remain below the limits specified in 10 CFR 71 for accident conditions.

8.2 Performance of Package Containment Seals

Based on the results of the thermal analysis (as discussed in Sections 7.1 and 7.2), there is a possibility of a release from the package because of failure of components that make up the containment boundary of the package. Calculated temperatures in the region of the lid closure seal, drain valve/port, and gas sample valve/port seals during the transient far exceed the continuous use temperature limits for the seal material. Therefore, the potential exists for the release of contents from the package in this fire scenario.

Section 8.2.1 provides a detailed discussion of seal temperatures predicted for the GA-4 package in the MacArthur Maze fire scenario. Section 8.2.2 presents a discussion of seal performance at elevated temperatures, based on experimental data relevant to the conditions of the MacArthur Maze fire.

8.2.1 Seal Temperatures in the MacArthur Maze Fire Scenario

The containment boundary for the GA-4 package is maintained by the seals on the package lid, drain valve and port, and gas sample valve and port. The package lid seal consists of primary and secondary O-rings at the interface of the lid and the package stainless steel body. The gas sample valve is located within the package lid, and the drain valve is located in the steel base of the package. The gas sample valve is sealed with primary and secondary O-rings, and for transport conditions, the outer face of the port is fitted with a steel plug that is threaded to a specified torque of 20 ft-lb. The drain valve is sealed within its access port with primary, secondary, and tertiary O-rings. The drain valve cover and drain port plug are also sealed with O-rings, in addition to being threaded, and are torqued to 20 ft-lb.

The O-ring seals at all locations are ethylene propylene, which has a continuous-use temperature limit of 302°F (150°C). Figure 8.1 shows a graph of the temperature limit on this

material as a function of exposure time. As exposure temperature increases, the time limit for allowed exposure decreases. (Note that the horizontal axis, Exposure Time, in this plot is on a logarithmic scale.) The maximum temperature this material is rated to withstand without effectively immediate failure is 790°F (421°C), but it will tolerate this exposure for only six minutes.

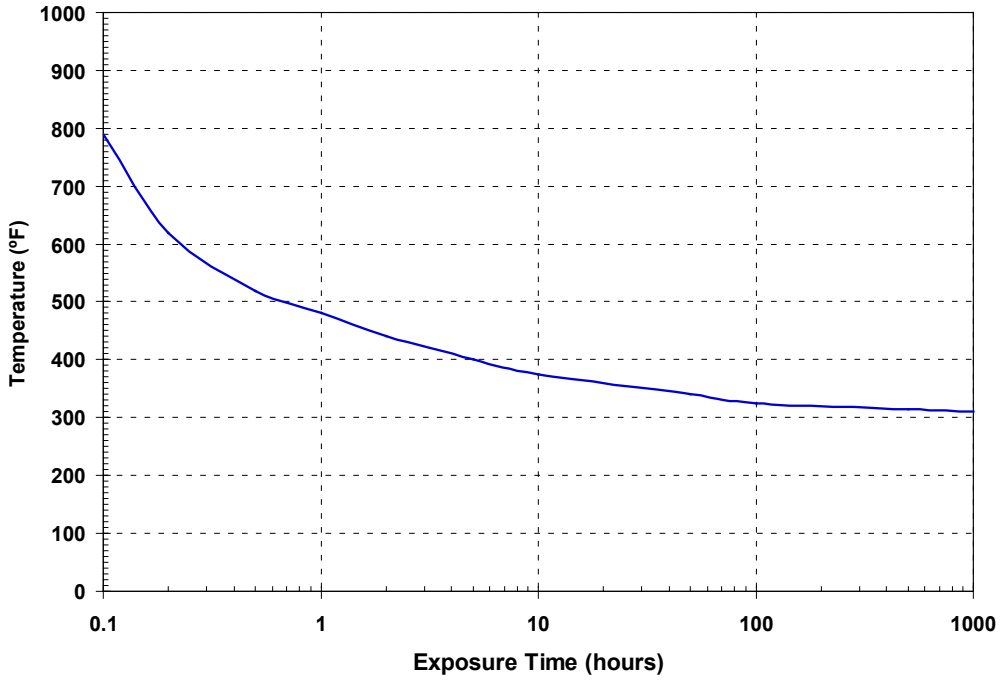

Figure 8.1. Operating Temperature Limit as a Function of Exposure Time for Ethylene Propylene Seal Material (Based on Data Presented in the GA-4 SAR [General Atomics 1998])

All of the containment boundary seals in the GA-4 package are in locations that are covered by either the top or bottom impact limiter assembly. Without the impact limiters in place, the seal locations are directly exposed to the fire conditions, and as a result, exceed all operating temperature limits within minutes, and high temperatures persist at these locations throughout the fire transient and into the post-fire cooldown. However, as discussed above in Section 7.0, structural and thermal evaluations show that loss of the impact limiters is not a credible consequence of this fire scenario. Therefore, the seal performance evaluations consider only the case with the impact limiters in place.

In the HAC fire analysis (30 minutes at 800°C) presented in the package SAR, the predicted peak temperatures on the seal components do not exceed the bounds of the operating temperature limit curve shown in Figure 8.1. This is verified by results obtained for this transient with the ANSYS and COBRA-SFS models, as noted in Section 6.1. It is therefore justifiable to assume that the seals would survive intact in the HAC fire. In the conditions of the MacArthur Maze fire scenario, however, the higher fire temperatures and longer duration of the fire exposure result in temperatures that far exceed the rated temperatures of this hydrocarbon seal material. Figure 8.2 shows the temperature predicted with the ANSYS model (with impact limiters in place) for the closure lid seal location during the fire scenario.

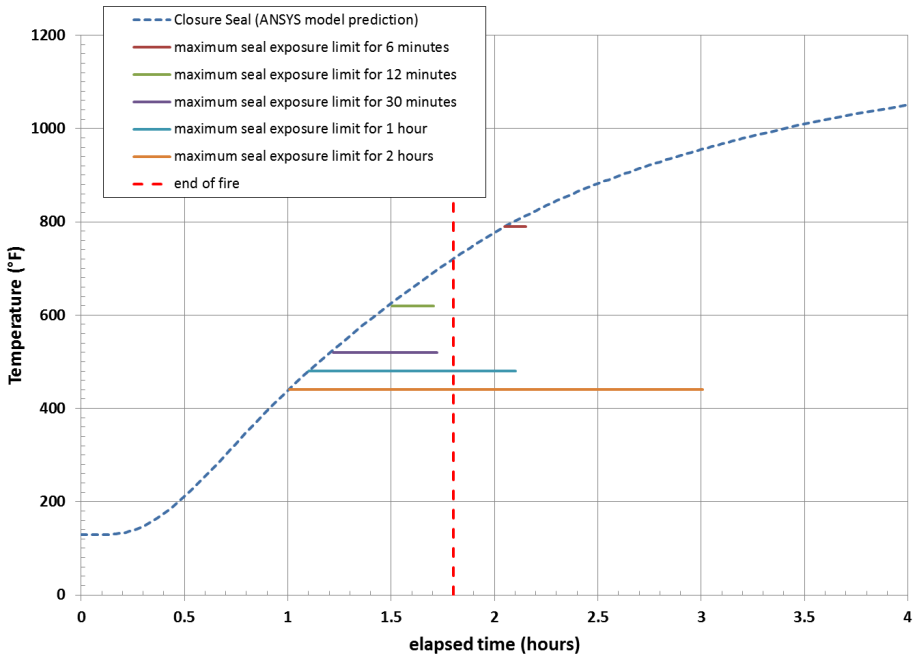

Figure 8.2. Closure Lid Seal Temperatures Predicted with the ANSYS Mode (with Impact Limiters) for the MacArthur Maze Fire Scenario

The plot in Figure 8.2 also shows the time in the transient when the closure lid seal location is predicted to exceed specific exposure temperature limits for the seal material. This plot indicates that the seal material could survive these conditions for possibly as long as 1.7 hours; almost the entire duration of the fire portion of the transient. However, temperatures in the seal location continue to rise for many hours after that point, and by approximately 2 hours into the transient, exceed all operating temperature limits defined by the graph in Figure 8.1. Similar plots in Figure 8.3 for the gas sample valve/port seals and in Figure 8.4 for the drain valve/port seals show that all operating temperature limits for these seals are exceeded, in approximately the same time-frame.

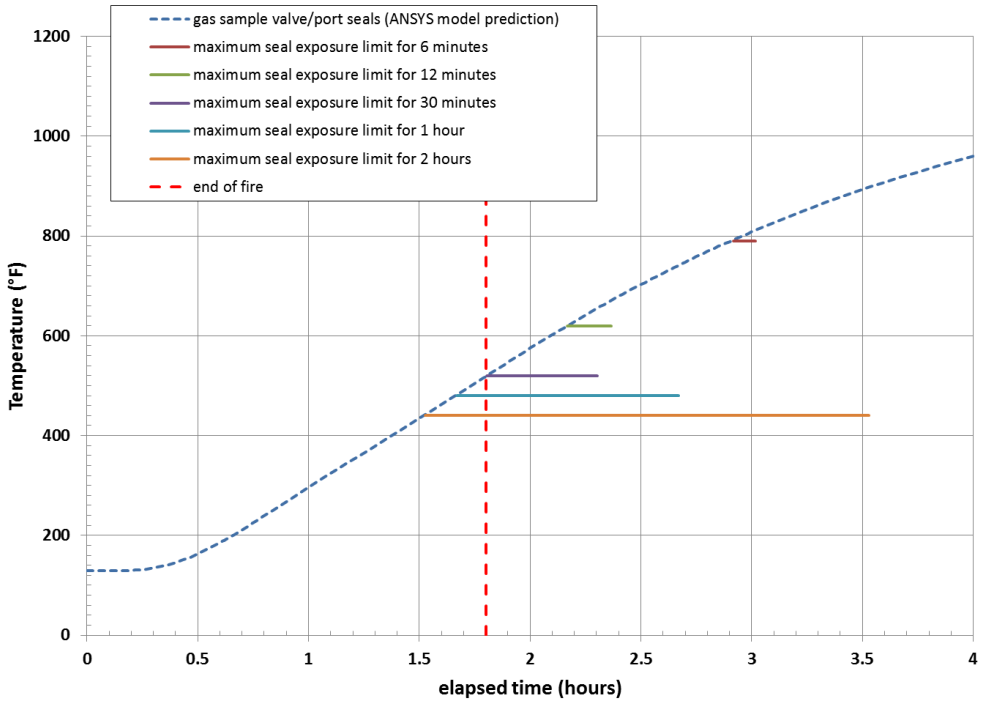

Figure 8.3. Gas Sample Valve/Port Seal Temperatures Predicted with the ANSYS Model (with Impact Limiters) for the MacArthur Maze Fire Scenario

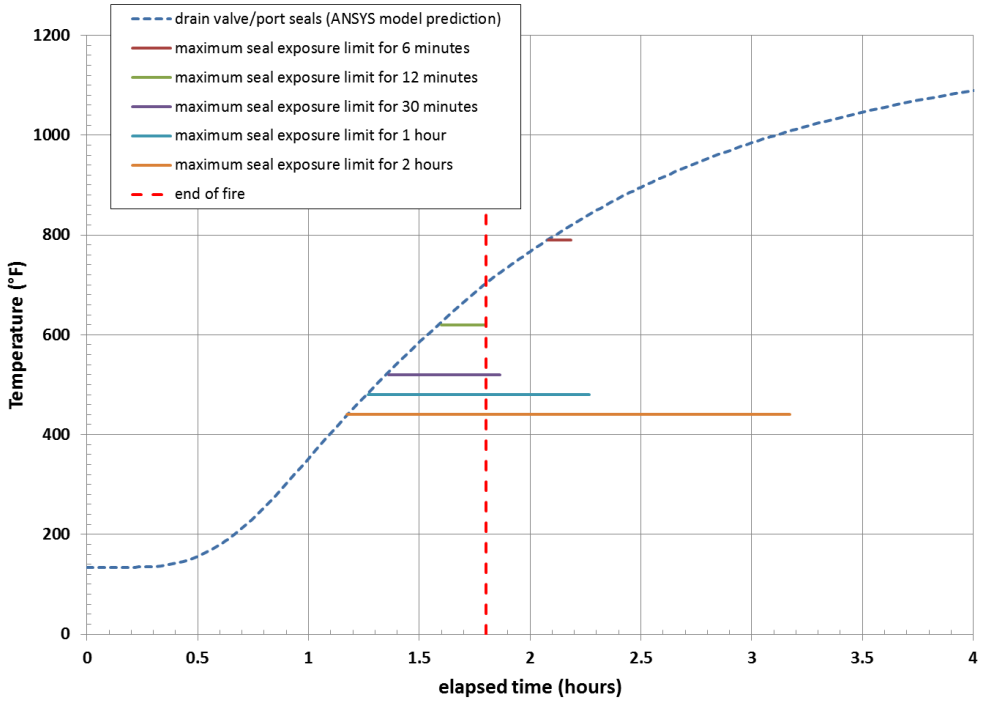

Figure 8.4. Drain Valve/Port Seal Temperatures Predicted with the ANSYS Model (with Impact Limiters) for the MacArthur Maze Fire Scenario

The plots in Figure 8.2, Figure 8.3, and Figure 8.4 incidentally confirm the SAR prediction, showing that these seals could probably survive a fire lasting only 30 minutes, followed by a cooldown at normal ambient conditions. However, if exposed to the conditions of the MacArthur Maze fire scenario, the seal material would exceed its rated long-term temperature limit within 1.5 to 2.5 hours at all locations. Complete evaluation of the effect of the fire scenario on the seal region requires evaluating the seal region temperatures during the post-fire cooldown transient, as well as during the fire itself. As discussed in Section 7.2, the insulating effect of the impact limiters results in the temperatures of components near the ends of the package continuing to increase long after the end of the fire. Figure 8.5 shows that the peak temperatures in the seal region locations continue to increase for more than 4 hours after the fire, reaching approximately 1150°F (621°C), and after 14.5 hours are still above 1000°F (538°C).

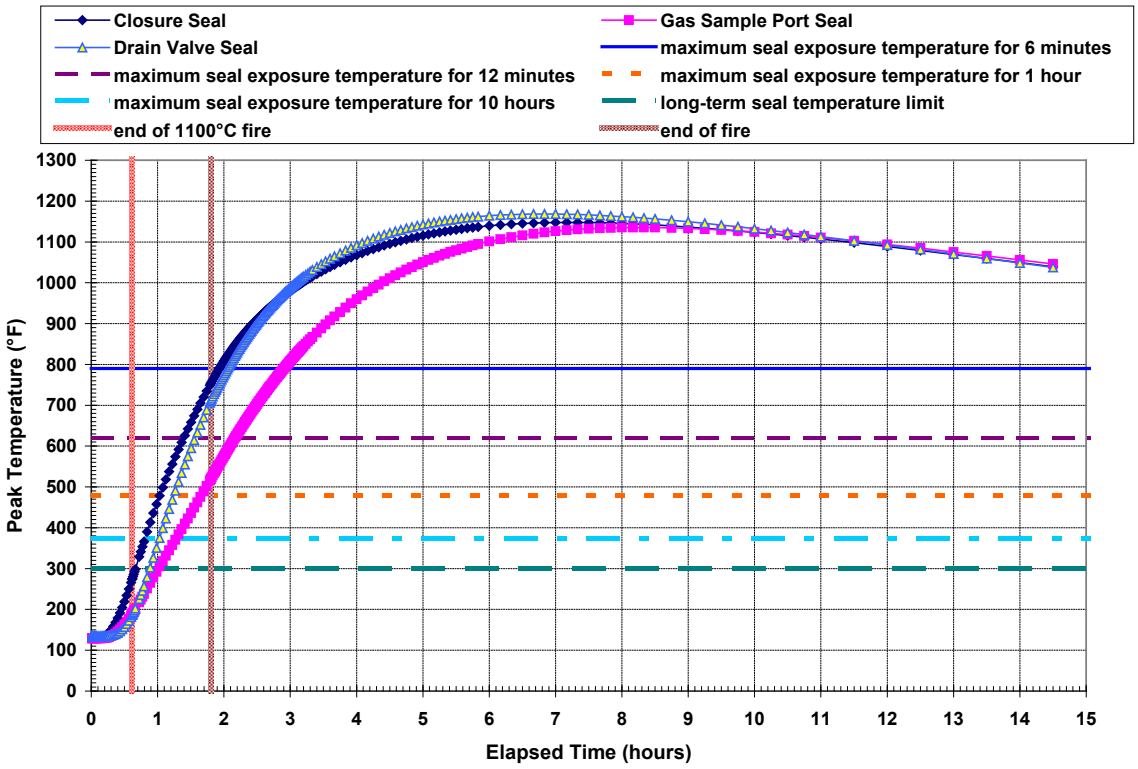

Figure 8.5. Seal Temperatures Predicted with ANSYS Model (with Impact Limiters) for MacArthur Maze Fire Scenario and Post-fire Cooldown

The results in Figure 8.2 through Figure 8.5 show that the seal region temperatures would exceed all exposure temperature limits for a long period of time during the post-fire cooldown. Seal failure, which is defined as the inability of the seal material to maintain a stable differential between the internal pressure within the package cavity and the external ambient pressure, seems inevitable under these conditions. In general, if seal materials exceed their rated temperature limits, they are treated for safety evaluation purposes as having failed entirely. However, this is a bounding assumption, since it does not attempt to quantify the degree of seal failure or resulting leak rate as a function of temperature or time-at-temperature. Section 8.2.2 summarizes results of experimental measurements of the performance of elastomer seals at elevated temperatures, which show that seal failure is a complex process, not a simple pass/fail test.

8.2.2 Seal Performance Testing

The NRC and NIST conducted testing of seals in thermal conditions simulating fire environments that exceeded the rated temperatures for the seals tested (NUREG/CR-7115 2012). These tests evaluated the performance of one type of metallic seal and two different polymeric compound seals typically used in SNF transportation packages, using a small stainless steel cylinder with a single O-ring seal. The test vessel was pressurized at 75°F (24°C) with helium to 73.5 psia (5 bar) for the tests with metallic seals, and to 29.4 psia (2 bar) for the tests with polymeric seals. The fire was simulated using an electric furnace that could maintain a controlled thermal environment for a specified duration, which was varied in different tests from several hours to 24 hours, and in some cases up to 72 hours. (These tests were designed to simulate accident conditions. Typical seal tests for long-term normal operating conditions are performed for a minimum of 1000 hours.) Following the simulated fire exposure duration, the test vessel was cooled to room temperature within the electric furnace.

A total of 15 tests were conducted in this study, including the initial shake-down test for which results were not recorded, due to instrumentation failure. Of the 14 tests for which measurements were recorded, 11 tests were with a metallic seal, 2 tests were with an ethylene propylene seal, and 1 test was with a polytetraflouroethylene (PTFE) seal. In terms of the applicability of this testing to the evaluation of the GA-4 package in the MacArthur Maze fire scenario, the two tests with ethylene propylene seals are of significance, since this is the seal material used in the GA-4 package for the lid closure and the gas sampling port valve and the drain valve.

The most severe exposure for ethylene propylene seals in the testing was at 842°F (450°C). Based on the performance curve in Figure 8.1, the exposure time limit for this seal material at this temperature is less than 6 minutes. The seal material failed in this test within the first three hours of the simulated fire transient, but exhibited a much slower leak rate than would be expected for the test vessel with no seals at the test conditions. The second test with ethylene propylene seals reached a much lower peak temperature, and simulated a fire environment with incremental heating from 302°F (150°C) to 572°F (300°C). Based on the performance curve in Figure 8.1, the exposure time limit at the maximum heating temperature in this test is less than 30 minutes. The total duration of the simulated fire was more than 20 hours, but in this test, the seal held with no measurable leakage.

The results of two tests in a small (not-to-scale) test vessel are not sufficient data on which to base a general evaluation of ethylene propylene seal material at temperatures above rated performance values. However, this testing does show that even when exposed to temperatures above rated time-at-temperature exposure limits, the seal material may retain sealing capability. Additional testing is needed to obtain a broader technical basis for determining the performance of seal materials at elevated temperatures, to evaluate the influence of such variables as the size of pressure vessel, the magnitude of the pressure differential at the high temperature exposure, and the effectiveness of double versus single O-ring seals. (SNF packages typically use double O-ring seals, and this testing used only a single O-ring in the test vessels.) These seal tests demonstrate that ethylene propylene seals such as those that are used for the GA-4 package may have a performance envelope that far exceeds the conservative temperature limits indicated in the ratings for long-term performance provided by the seal manufacturer. Seals will not necessarily exhibit catastrophic leakage when exposed to temperatures beyond design basis, even at the extreme thermal exposure postulated for the MacArthur Maze fire scenario.

The results of the thermal analysis indicate that for the GA-4 package in the MacArthur Maze fire scenario, all seals would be significantly challenged. Based on the seal testing conducted by NRC discussed here, it is remotely possible that some sealing capability would remain for the seals even after exposure to excursion temperatures well above their rated temperatures. However, for the purposes of determining the potential release from the GA-4 package in this fire scenario, a simple pass/fail criterion is used to evaluate potential seal performance. If the temperatures predicted in the transient exceed the maximum recommended service temperature for the seal material, the seal is assumed to fail. This evaluation shows that the assumption of complete seal failure is bounding for the performance of the GA-4 package seals, and may be quite conservative. Nevertheless, this assumption is the basis for determining that a release is possible from the GA-4 package in this fire scenario due to package containment boundary leakage. The analyses presented in the following sections determine the character and amount of material that could be released.

8.3 Potential Release Issues

NRC staff evaluated the potential for release of radioactive material from the GA-4 package as a consequence of the MacArthur Maze fire scenario. Based on the results of the thermal analysis (as discussed in Sections 7.1 and 7.2), there is a possibility of a release from the package because of failure of components that make up the containment boundary of the package. Calculated temperatures in the region of the lid, drain valve/port, and gas sample valve/port seals during the transient far exceed the continuous use temperature limits for the seal material, as discussed in Section 8.2 above. In addition, the peak temperatures predicted for all fuel rods in the package reach the range where burst rupture of zircaloy cladding can occur, as discussed in the presentation of results of the thermal analyses in Sections 7.1 and 7.2. Therefore, the potential exists for the release of fission products and spent fuel particles, as well as particulate resulting from CRUD[1] detaching from the fuel rod surfaces.

Results of analysis of fuel performance for the conditions encountered in this fire scenario are presented in Section 8.3.1. Evaluations of the potential for release from fuel rods to the GA-4 package cavity are presented in Section 8.3.2. Evaluations of the potential for release from the GA-4 package to the surrounding environment are presented in Section 8.3.3.

8.3.1 Fuel Rod Cladding Performance

Spent fuel has two potential sources of radioactive material that could serve as source terms for a release from an SNF transportation package; the CRUD on the rod outer surface, and the radioactive material (fission products and fuel fragments) confined within the metal cladding. The Standard Review Plan (NUREG-1617 2000) specifies the assumption of 100% spallation of CRUD from fuel rod surfaces for HAC analyses. For consistency, this assumption is also applied to the MacArthur Maze scenario. Determining the amount of material that could potentially be released from within the rods, however, requires additional analysis of fuel rod behavior for the conditions of the fire scenario. If it can be shown that the fuel rods remain intact throughout the fire scenario, there would be no release of material from within the rods. If

[1] **C**halk **R**iver **U**nknown **D**eposit; generic term for material deposited on the rod surface from the coolant during reactor operations. The significant activated element is Cobalt-60. Regulatory guidance specifies a bounding value of 140 μCi/cm^2 for spent fuel rods in PWR assemblies. A bounding estimate for total activity due to CRUD can be calculated from the total fuel rod surface area and the age of the fuel (i.e., time out of the reactor).

conditions are such that the fuel rods could fail, the nature and severity of the potential failure must be determined.

The predicted fuel cladding temperatures obtained with the COBRA-SFS model of the GA-4 were used to evaluate the potential for rod failure in the severe conditions of the MacArthur Maze fire scenario. The results obtained with the ANSYS model are more conservative, as discussed in Section 7.1 and 7.2, due to the more conservative representation of the fuel using the homogeneous k-effective model. The COBRA-SFS model, with a more detailed representation of the fuel region using the rod-and-subchannel approach, produces predictions of fuel and cladding temperatures with a more accurate evaluation of thermal radiation and the transient thermal inertia of the fuel and cladding. However, the many conservatisms in the modeling approach and fire scenario definition that apply equally to the ANSYS model and the COBRA-SFS model ensure that the cladding temperature results obtained with this code are also very conservative, even though they do not include the specific conservative effect of the effective conductivity model in the representation of the fuel assemblies.

Based on the predicted fuel cladding temperatures from the COBRA-SFS modeling results for the MacArthur Maze fire scenario, fuel performance was evaluated using the burst rupture model in the FRAPTRAN-1.4 code (NUREG/CR-7023 2011). In the FRAPTRAN code, cladding rupture is evaluated with a burst stress/strain model developed from test data obtained for loss of coolant accident (LOCA) analysis and reactivity insertion accident (RIA) evaluations. Burst rupture is the expected mechanism of failure for fuel rods in the reactor core when subjected to severe accident conditions, and is a potential failure mode for spent fuel at high temperatures.

Creep rupture is considered a possible alternative mechanism of failure for spent fuel rods. To evaluate this possibility, a separate analysis was performed with a creep rupture model, using the FRAPCON-3.4 code (NUREG/CR-7022 2011) in conjunction with the DATING code (Simonen and Gilbert 1988). The version of the code used in this analysis has been updated with creep coefficients from creep tests on irradiated cladding (Gilbert et al. 2002), for the temperatures in the range predicted for the hottest rod in the MacArthur Maze fire scenario.

Fuel performance evaluations used the same design basis fuel configuration assumed in the thermal analysis. The fuel rod cladding initial conditions and cladding temperatures assumed during the fire scenario are summarized as follows:

- Westinghouse 14x4 fuel design operating at a rod average linear power rating of 5.7 kW/ft, up to 33 GWd/MTU rod average burnup in-reactor prior to discharge
- Initial as-fabricated rod pressure of 460 psig at room temperature
- Rod pressure at room temperature after irradiation to 33 GWd/MTU is 651 psig.
  - The increase in pressure from the as-fabricated pressure of 460 psig is due mainly to a reduction in rod void volume because of fuel swelling and cladding creepdown. There is also a small increase in pressure due to release of fission gas (0.0024 release fraction) from the pellets to the fuel rod void space. Fission gas release fractions and consequently rod pressure would be significantly higher (between 0.05 to 0.20) for a peak power rod operating rod in the core. A release fraction of 0.002 to 0.005 would be representative of the majority of rods (but not the peak operating rods) in a core at this discharge burnup.
- Initial conditions at the start of the fire are assumed to be NCT, which results in an initial steady-state peak cladding temperature of 293°F (145°C) with a rod pressure of 922 psig (hoop stress approximately 50 MPa)

- Cladding temperature as a function of time for the hottest rod in the package, as predicted in the COBRA-SFS thermal analysis for the fire conditions (see Figure 7.8, which shows the peak cladding temperatures; however, the complete axial temperature distribution as a function of time was provided as input to the burst rupture calculations, not simply the peak temperature)

The cladding temperatures from the fire, as calculated with COBRA-SFS, and rod pressures calculated by FRAPCON-3.4 (NUREG/CR-7022 2011) assuming the spent fuel had been subjected to normal reactor operation at 5.7 kW/ft, were input into FRAPTRAN-1.4 to calculate the cladding stresses. The FRAPTRAN-1.4 cladding burst model was also used to calculate the rupture temperature during the fire. The calculated cladding temperatures during the fire from the COBRA-SFS analysis, and the calculated hoop stresses obtained from FRAPTRAN-1.4 for the fire conditions were input into FRAPCON-DATING to calculate cladding rupture based on the out-of-reactor creep relationship in the DATING subroutine.

8.3.1.1 Fuel Rod Cladding Performance: FRAPTRAN Evaluation

The peak cladding temperatures calculated with COBRA-SFS for the MacArthur fire were 293°F (145°C) at the start of the fire and reached a peak cladding temperature of 1388°F (753°C) in the fire transient. Based on these temperatures, the calculated cladding hoop stress is 50 MPa at the start of the fire and reaches a peak of 121 MPa just prior to predicted cladding rupture at 1098°F (592°C), as predicted with the burst strain model in FRAPTRAN-1.4. This relatively low rupture temperature reflects the conservatism in the cladding temperature history predicted in the thermal analysis, and the uncertainty in the FRAPTRAN predictions at the relatively low heating rate for the cladding in this fire scenario.

The FRAPTRAN code was designed to predict nuclear fuel behavior during reactor accidents. In particular, failure models have been developed to provide reasonably accurate predictions for Reactivity Initiated Accident (RIA) and Loss-Of-Coolant Accident (LOCA) failures. For the case of a fire accident scenario in transportation of spent nuclear fuel, potential cladding failure can occur as a result of temperature increase and the associated rod internal pressure increase. These concurrent temperature and pressure increases can result in sufficient stress to cause ballooning and rupture of the cladding due to rapid high temperature creep. In a FRAPTRAN calculation of such an event, if the temperature and stress in the cladding are such that the cladding deforms to its uniform elongation in the hoop/circumferential direction, fuel rod ballooning is predicted. If the stress exceeds a correlated temperature-dependent level, cladding rupture will be predicted. In the less severe conditions of the HAC fire, the stress in the cladding is not expected to exceed the elastic limit, and therefore burst rupture would not be predicted with the models in the FRAPTRAN code.

Ballooning and rupture models such as those in the FRAPTRAN code have been developed with the specific intent to accurately predict cladding failures during a LOCA, where the temperature increase rate is typically much higher (on the order of 10°C/s or higher) than in the case of fire scenarios (typically on the order of 0.2°C/s for the HAC fire, and for the MacArthur Maze fire scenario, conservatively estimated to be 0.27°C/s). For a given stress level, a slower heatup rate will generally tend to result in a lower rupture temperature, but there is very little data in the FRAPTRAN validation database that has heatup rates below 1°C/s. There is much more data at higher heating rates, ranging from 5°C/s to >30°C/s, as fully documented in the FRAPTRAN code manual (NUREG/CR-7023 2011). Figure 8.6 shows a summary of burst temperature data in the FRAPTRAN modeling database that are from tests with heating rates in the range 0.08 to 5°C/s. (This data set is from NUREG/CR-0344.) The lowest burst (i.e.,

rupture) temperatures observed in this limited subset of the validation database are around 667°C (1232°F). Due to the sparseness of the data in this low temperature range, burst rupture temperatures predicted with FRAPTRAN for heatup rates below 1°C/s have a greater uncertainty than predictions obtained for higher heating rates, where the database is more fully populated. In particular, predictions of burst rupture temperatures lower than 667°C (1232°F) should be evaluated as indicative of the possibility of rupture, rather than absolute indicators of rupture, since these results are outside the available validation database.

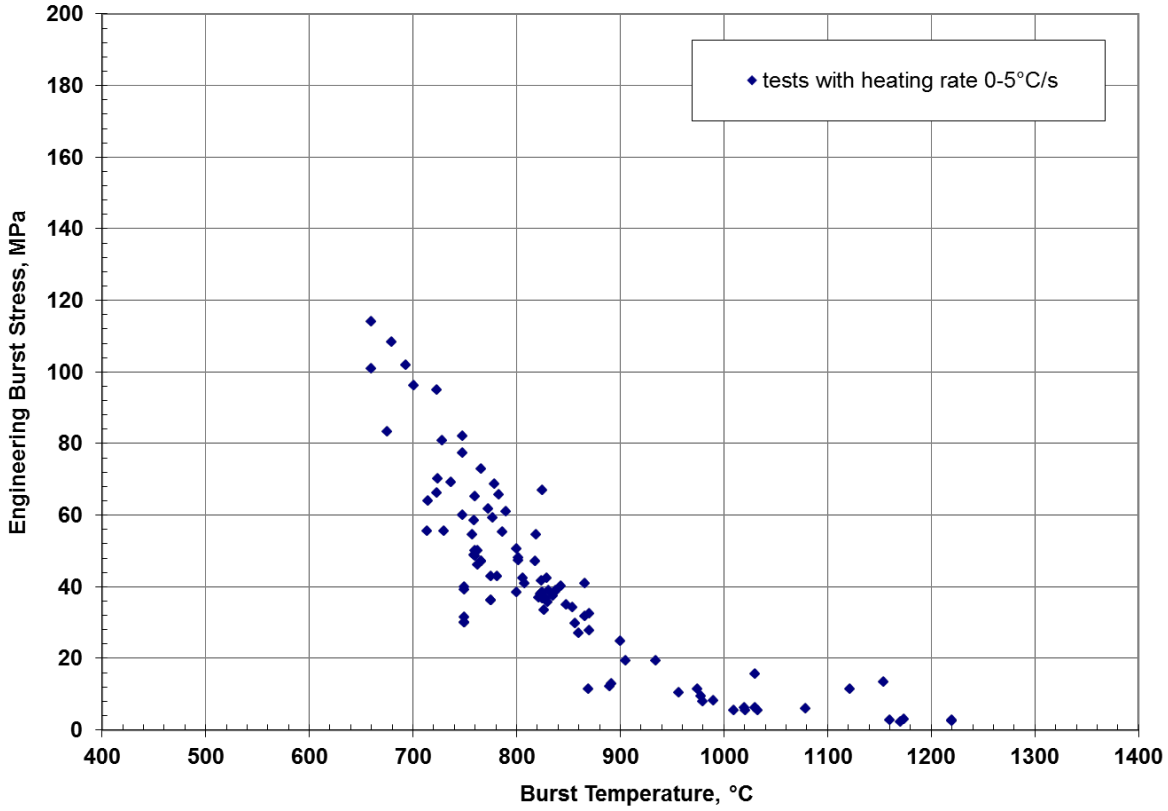

Figure 8.6. Experimental Results for Rod Burst Rupture Testing at Low Heating Rates (data from NUREG/CR-0344)

Based on the validation range of the models in FRAPTRAN, and the conservative assumptions in the thermal modeling that impose an extraordinarily severe temperature transient on the fuel rods within the GA-4 package in this fire scenario, the predicted cladding rupture at 1098°F (592°C) obtained in the FRAPTRAN analysis can be considered an extremely conservative result. However, the predicted peak cladding temperature obtained in the thermal modeling is 1388°F (753°C) in this fire scenario, and this temperature is well within the range where the data in Figure 8.6 shows burst rupture temperatures at low heating rates. The specific temperature value for burst rupture predicted with FRAPTRAN for these conditions may be quite conservative, and may have a fairly large uncertainty, but there is little uncertainty that the cladding would at some point fail by burst rupture if subjected to the severe conditions predicted for the fuel in the GA-4 package in the MacArthur Maze fire scenario.

8.3.1.2 Fuel Rod Cladding Performance: FRAPCON/DATING Evaluation

The cladding failure temperature predicted with the creep model in the DATING code is 1229°F (665°C), which is significantly higher than the burst rupture temperature of 1098°F (592°C) obtained in the FRAPTRAN analysis. The DATING code was designed to predict creep failures and temperature limits for dry storage of spent fuel, based on creep failures of the cladding. The range of applicability of the DATING code is for lower temperatures, resulting in much longer times to failure, when compared to the FRAPTRAN ballooning models. The databases used to develop creep rate correlations and creep rupture models for the DATING code span temperature ranges that are in general lower than the temperatures and heating rates typically encountered in fire scenarios.

The DATING code is a more general creep prediction tool than FRAPTRAN, with its ballooning and rupture models, which are effectively high temperature creep models. However, it must be noted that, as with FRAPTRAN, the DATING code is being applied outside its validation databases when used to evaluate cladding response to the conditions of the MacArthur Maze fire scenario. However, the results obtained with both modeling tools show that although there might be some uncertainty as to the exact temperature at which it would occur, fuel cladding could and probably would fail, if subjected to the severe conditions postulated for the MacArthur Maze fire scenario. For the purposes of this evaluation, the predicted temperatures from these codes are taken at face value, and treated as conservative estimates of rupture temperature in the evaluation of potential consequences of this fire scenario.

Table 8.1 summarizes the results of the fuel performance modeling analyses for temperatures on the hottest rod in the MacArthur Maze fire scenario, as predicted with the COBRA-SFS model. The burst rupture and creep rupture models both predict that the hottest fuel rod would rupture if subjected to the temperatures predicted in this fire scenario. Furthermore, the peak temperature on the hottest rod at the time of rupture is eventually exceeded by all rods in the package during the transient, which suggests that there is the potential for all rods in the package to rupture in this fire scenario.

Table 8.1. Results of Fuel Performance Analyses in the MacArthur Maze Fire Scenario

LOCA Burst Strain Model (FRAPTRAN)		**Creep Rupture Model (FRAPCON/DATING)**	
Cladding Temperature	**Rupture Conditions**	**Cladding Temperature**	**Rupture Conditions**
1097°F (592°C)	rod rupture in end region	1229°F (665°C)	rod rupture near end

The burst rupture and creep rupture models predict cladding failure at a single location along the axial length of a fuel rod. Based on the temperature predictions obtained with the COBRA-SFS model, which omits the impact limiters, the fuel performance models predict rod rupture in the end region of the rod. Temperature distributions obtained with the ANSYS model, which assumes the impact limiters remain in place throughout the transient, result in the highest temperatures occurring near the axial center of the fuel region, and rod rupture would be expected near the middle of the rod for this package configuration. Since the design basis fuel for the GA-4 is low burnup (i.e., no more than 45 GWd/MTU), the degree of pellet-clad interaction would be relatively limited, and a single rod breach would be expected to effectively depressurize the fuel rod. Therefore, no additional ruptures are predicted on a given rod, and potential release calculations are based on the assumption of one rupture per rod.

The peak fuel cladding temperatures predicted with the ANSYS model are somewhat higher than the peak temperatures on the rod ends predicted with COBRA-SFS (see Sections 7.1 and 7.2). Furthermore, the rod temperatures in both analyses remain much higher than the predicted rupture temperatures for an extended period of time. It is therefore reasonable to conclude that for the temperature distribution predicted with the ANSYS model (with the impact limiters in place), rod ballooning and rupture would also be expected to occur, but in the central region of the rod, rather than at an end. Table 8.2 summarizes the elapsed time and time duration that the hottest rod peak temperatures are predicted to exceed the calculated burst rupture temperatures.

Table 8.2. Time above Predicted Rod Rupture Temperatures in the MacArthur Maze Fire Scenario

		COBRA-SFS model		**ANSYS model**	
		Max PCT in fire transient	1388°F (753°C)	**Max PCT in fire transient**	1433°F (779°C)
Rod Condition	**PCT at time of rupture**	**Elapsed Time (hours)**	**Time Above Rupture Temperature (hours)**	**Elapsed Time (hours)**	**Time Above Rupture Temperature (hours)**
rod rupture (burst strain model)	1097°F (592°C)	0.8	16	0.69	>14.5
rod rupture (creep model)	1229°F (665°C)	1.15	10.5	0.97	11.5
PCT = Peak Cladding Temperature					

Based on the burst strain model, the fuel rods are expected to rupture before the end of the fire. Based on the creep rupture model, the fuel rods would also be expected to begin rupturing before the end of the fire, but slightly later in the transient. Furthermore, the peak temperatures remain significantly above these predicted rupture temperatures for more than 10 hours. The results presented in Sections 7.1 and 7.2 show that the fuel rod temperatures continue to increase even after the end of the fire, because of thermal inertia and build-up of decay heat that is not removed from the package during and immediately after the fire.

By the time of the secondary peak of 1348°F (731°C) in cladding temperature predicted with the COBRA-SFS model, which occurs at 250 minutes elapsed time (142 minutes after the end of the fire), the peak temperature on every rod in the package exceeds the highest temperature predicted for rod rupture (1229°F [665°C]). The peak temperature of 1343°F (728°C) predicted with the ANSYS model is at essentially the same value as that predicted with the COBRA-SFS model at this point in the cooldown transient. More significantly, at this time the lowest peak rod temperature is 1285°F (696°C) in the COBRA-SFS model results, and the lowest axial peak temperature predicted in the fuel region in the ANSYS model is approximately 1134°F (612°C). Based on these results, it is assumed that all of the rods in each of the four assemblies within this package would rupture in the MacArthur Maze fire scenario.

8.3.2 Potential Release to GA-4 Package Cavity

Determining potential release quantities from an SNF package involves first determining the amount of material that is available for release from the fuel rods, and then determining the amount of this material that can be released from the package. This section presents analyses

performed by NRC staff to determine the total amount of activity that could be released from the four assemblies defining the design-basis payload for the package, as described in the GA-4 SAR. Analyses to determine the potential for release from the package to the environment are presented in Section 8.3.3.

Typically, release quantities are expressed in terms of *release fractions*, a ratio calculated as the amount of material actually released divided by the total amount available for release. Regulatory guidance for determining the releasable source term for SNF transportation packages is provided in the *Standard Review Plan for Transportation Packages for Spent Nuclear Fuel: Final Report*, NUREG-1617 and in *Containment Analysis for Type B Packages Used to Transport Various Contents*, NUREG/CR-6487. The release fractions specified in these documents are listed in Table 8.3. These release fractions define bounding values for the fraction of material that is assumed to be released from the fuel rods to the package under NCT and HAC.

Table 8.3. Bounding Values of Release Fractions from Ruptured Fuel Rods

Radionuclide Group	Release Fraction	
	(NCT)	(HAC)
non-reactive gases (e.g., Kr-85)	0.3	0.3
volatile gases (e.g., cesium and iodine compounds)	0.0002	0.0002
particulate (fuel fragments or fines)	0.00003	0.00003
CRUD spallation fraction	0.15	1.0

The potential release from the GA-4 package corresponding to the release fractions in Table 8.3 is a function of the contents of the package. The radionuclide inventories for the two design basis fuel configurations for the GA-4 package were obtained using ORIGEN-ARP (Gauld et al. 2009). The source term inventories obtained in these calculations are listed in Table 8.4. Consistent with the criticality and shielding calculations in the GA-4 package SAR (General Atomics 1998), WE14x14 fuel at 35 GWd/MTU burnup and 10-years cooling is bounded by WE15x15 at 35 GWd/MTU and 10-years cooling. Therefore, all source term and potential release calculations are performed assuming 10-year-old WE 15x15 fuel at 35 GWd/MTU, even though the thermal analysis is based on WE 14x14 fuel geometry. This is a conservative assumption, since the temperatures obtained with WE 14x14 fuel would be slightly higher than those predicted for WE 15x15 fuel for the same design basis decay heat loading. Table 8.4 lists the calculated source terms for a single assembly. The total inventory within the GA-4 is four times the quantities listed in this table, since this package can carry up to four fuel assemblies.

Table 8.4. Radionuclide Inventory for a Single Assembly in the GA-4 Package

Nuclide	Activity (Ci)	
	WE 15x15 (45 GWD/MTU; 15 yrs cooled)	WE 15x15 (35 GWD/MTU; 10 yrs cooled)
Ag-110m	2.44E-03	2.42E-01
Am-241	5.56E+03	3.54E+03
Am-242		1.59E+01
Am-242m	2.15E+01	1.60E+01
Am-243	9.68E+01	4.74E+01

Table 8.4. (continued)

Nuclide	Activity (Ci)	
	WE 15x15 (45 GWD/MTU; 15 yrs cooled)	**WE 15x15 (35 GWD/MTU; 10 yrs cooled)**
Ba-137m	1.78E+05	1.57E+05
Ce-144	3.21E+00	2.84E+02
Cm-242	1.77E+01	1.32E+01
Cm-243	5.71E+01	3.22E+01
Cm-244	9.37E+03	3.99E+03
Cm-245	1.64E+00	
Cs-134	2.78E+03	1.01E+04
Cs-137	1.88E+05	1.66E+05
Eu-152	6.17E+00	7.38E+00
Eu-154	5.41E+03	5.54E+03
Eu-155	8.50E+02	1.23E+03
H-3	6.42E+02	6.37E+02
Kr-85	8.28E+03	9.80E+03
Np-239	9.68E+01	4.74E+01
Pm-147	6.01E+03	2.27E+04
Pr-144		2.84E+02
Pr-144m		3.97E+00
Pu-238	8.78E+03	5.31E+03
Pu-239	6.51E+02	6.41E+02
Pu-240	1.26E+03	1.04E+03
Pu-241	1.50E+05	1.60E+05
Pu-242	6.98E+00	4.22E+00
Rh-106		1.17E+03
Ru-106	4.74E+01	1.17E+03
Sb-125	4.41E+02	1.28E+03
Sm-151	7.47E+02	7.02E+02
Sn-119m		2.47E-02
Sn-121		1.80E+01
Sn-121m	2.94E+01	2.32E+01
Sr-90	1.19E+05	1.14E+05
Tc-99	3.38E+01	2.74E+01
Te-125m	1.08E+02	3.13E+02
U-234	1.91E+00	1.98E+00
U-237		3.84E+00
Y-90	1.19E+05	1.14E+05
Zr-93	4.26E+00	3.46E+00

1

The bounding values for release fractions defined in Table 8.3 were applied to the source terms listed in Table 8.4 to determine a bounding estimate of the activity that could be released from the four fuel assemblies to the GA-4 package interior in the MacArthur Maze fire scenario. Figure 8.7 shows the activity released to the package for the source term inventory from Table 8.4 for the bounding configuration of 10-year-cooled WE 15x15 fuel at 35 GWd/MTU. Figure 8.8 shows the activity released to the package for the source term inventory from Table 8.4 for 15-year-cooled WE 15x15 fuel at 45 GWd/MTU.

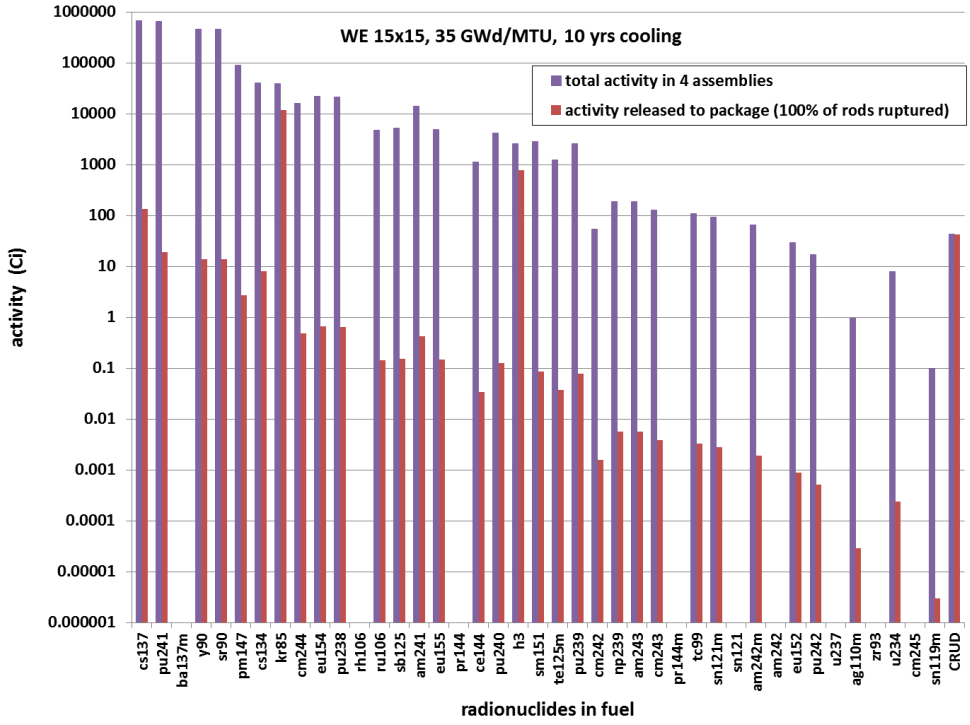

Figure 8.7. Summary of Activity in Radionuclides Released to GA-4 Package Cavity from WE 15x15 (35GWd/MTU, 10-yrs-cooled fuel) for Bounding Release Fractions Specified in NUREG-1617

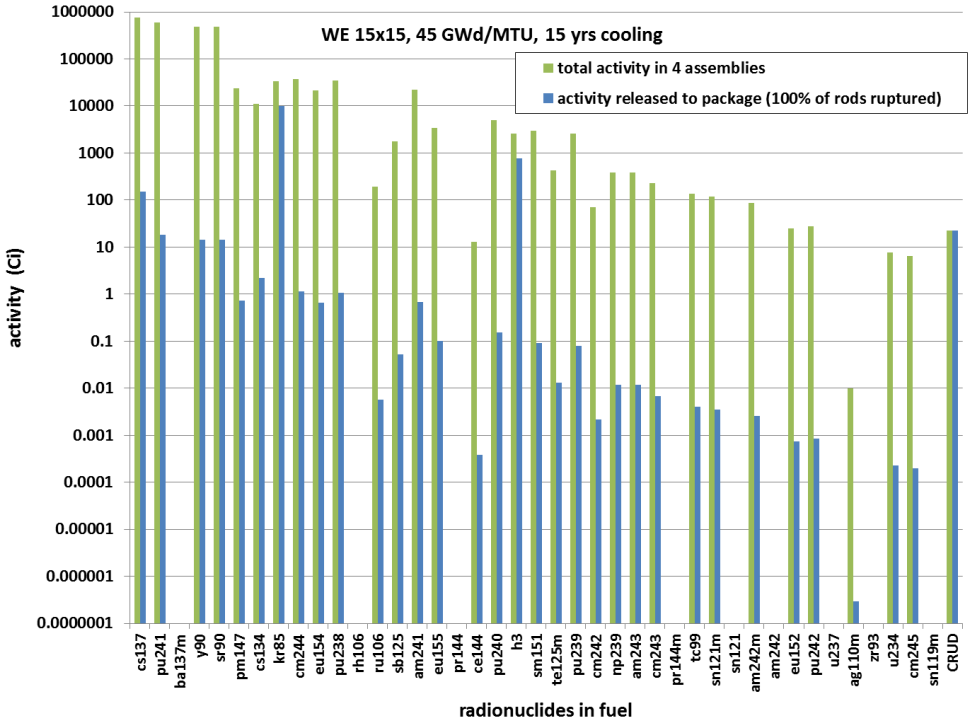

Figure 8.8. Summary of Activity in Radionuclides Released to GA-4 Package Cavity from WE 15x15 (45GWd/MTU, 15-yrs-cooled fuel) for Bounding Release Fractions Specified in NUREG-1617

8.3.3 Potential Release from GA-4 Package in MacArthur Maze Fire Scenario

Release rates from SNF packages are typically calculated for NCT and HAC using models based on guidance in NUREG/CR-6487, which contains models that reference ANSI standards for leakage tests on packages for shipment of radioactive materials (ANSI N14.5 1997). The analyses presented in the GA-4 SAR show that as long as the package seals remain intact, the package can be expected to meet all containment requirements, and potential releases from the package would be well below regulatory limits. However, as discussed in Section 8.2.1, the GA-4 package seals are predicted to exceed operational temperature limits after approximately 1.5 to 2.5 hours of exposure to the thermal conditions of the MacArthur Maze fire scenario. In addition, as discussed in Section 8.3.1, all fuel rods in all four assemblies contained within the GA-4 package are predicted to exceed temperatures at which burst rupture or creep rupture of the zircaloy cladding would be expected to occur. Therefore, there is the potential for leakage of radioactive material from the GA-4 package after this point in the fire transient.

Determining an appropriate leak rate for the package in the conditions predicted for the MacArthur Maze fire scenario presents an interesting challenge. The models for leak rates derived from the ANSI standard ANSI N14.5 are not based on the assumed seal conditions in this fire scenario, and there is very little information in the literature on leak rates associated with *failed* seals. In typical engineering applications, the leak rates of failed seals are unacceptable by definition, and their potential magnitude is of no practical interest. What little information to be found tends to focus rather narrowly on special applications where time-to-failure could be a critical design parameter (e.g., equipment that will be sent into orbit). In these types of studies,

the focus is on the time interval to the point where the seal begins to leak, not on the leak rate itself, and the work is mainly interested in modes of seal failure or seal behavior prior to failure.

It was therefore necessary to develop a modeling approach to determine a reasonable bounding leak rate for the GA-4 package for the long portion of the transient following the time after assumed seal failure due to exceeding thermal operating limits. Section 8.3.3.1 presents the model developed for this analysis, and describes its application to the GA-4 package in the MacArthur Maze fire scenario. Section 8.3.3.2 presents the potential release calculations for the GA-4 package, based on the leak rate determined with this model.

8.3.3.1 Leak Rate Model for GA-4 Package without Seals

For leak rate modeling, the interface between the closure lid and end flange of the package body is of greatest significance. (There is also the potential for leakage paths through the gas sample valve/port and the drain valve/port; this is discussed in Section 8.3.3.2.) Failure of the seals in the fire scenario is conservatively treated in this evaluation as if the seals simply cease to exist after one hour of the fire duration. This timeframe conservatively bounds the interval of the estimated time when all seals are predicted to have exceeded operating temperature limits. The possibility of damaged seal material affecting the geometry of the leakage path is ignored. If it is assumed that there is no O-ring seal material remaining in the seal grooves of the lid and flange, and the only barrier to flow through the interface is the actual physical contact between these two components.

The closure lid and body flange both have smooth metal surfaces where the two components are in contact, and the closure bolts are torqued to a specified pre-load, such that there is a positive and essentially uniform clamping force at the interface. The evaluations presented in Section 7.3, investigating the response of the lid closure bolts to the extreme thermal environment of the MacArthur Maze fire scenario, show definitively that the bolts maintain a positive clamping force throughout the fire transient, including the long cooldown back to ambient conditions.

Flow of gas through the very narrow space between the closure lid and body flange can be treated as analogous to fluid flow through fractured material in which the local scale of motion can be approximated by the cubic law for flow between parallel plates. This is a simplified form of the momentum conservation equation, and is a function of the geometry of the flow path and the driving pressure difference between the package interior and the external environment (Brown 1987). A formulation of this relationship, expressed in cylindrical coordinates, is given by

$$Q_{LR} = 2\pi\left(\frac{d_e^3}{12\mu}\right)\left(\frac{\Delta P}{\ln(r_o/r_i)}\right)$$

where:

- Q_{LR} = volumetric flowrate through the leakage path
- d_e = equivalent gap between surfaces in contact
- μ = viscosity of flowing gas
- ΔP = driving pressure difference
- r_o = outer radius
- r_i = inner radius

The equivalent gap between the surfaces in contact is the critical unknown in the above equation, since all other parameters can be readily determined from the geometry of the GA-4 package closure lid and flange, and the conditions calculated for the MacArthur Maze fire scenario with the thermal models. The actual gap is a function of the surface roughness of the components in contact and the clamping force holding them together. This gap cannot readily be estimated with any degree of certainty without knowing the exact microscale geometry of the surfaces involved.

Therefore, an alternative approach was developed by considering another much simpler physical process in which the gap between two surfaces in direct contact has an important effect on physical behavior; the flow of heat between two surfaces in direct or very close contact. The thermal resistance between two such components is a strong function of the contact pressure and surface texture of the two surfaces, and is typically expressed in terms of the overall thermal contact resistance, as

$$R_{tc} = \frac{d_e}{k}$$

where:

R_{tc} = thermal contact resistance (m^2-K/W) as a function of contact pressure and surface texture for two surfaces in direct contact
d_e = equivalent gap between surfaces in contact
k = thermal conductivity of gas in spaces between contacting surfaces

Using thermal contact resistance data for stainless steel surfaces (Shajaefard and Goudarzi 1987) as a function of contact pressure and surface roughness at the interface, and assuming helium gas in the very constrained spaces between the contacting surfaces, the above relationship can be used to determine an equivalent gap for the closure lid and package flange in the MacArthur Maze fire scenario.

The results presented in Section 7.3 for evaluations of the lid closure bolt response to the MacArthur Maze fire scenario using detailed FEA modeling provide a history of the clamping force between the closure lid and package body flange. Figure 8.9 shows the estimated equivalent gap after seal failure, based on the contact resistance as a function of the lid/flange contact pressure due to the clamping force, and the thermal conductivity of helium gas.

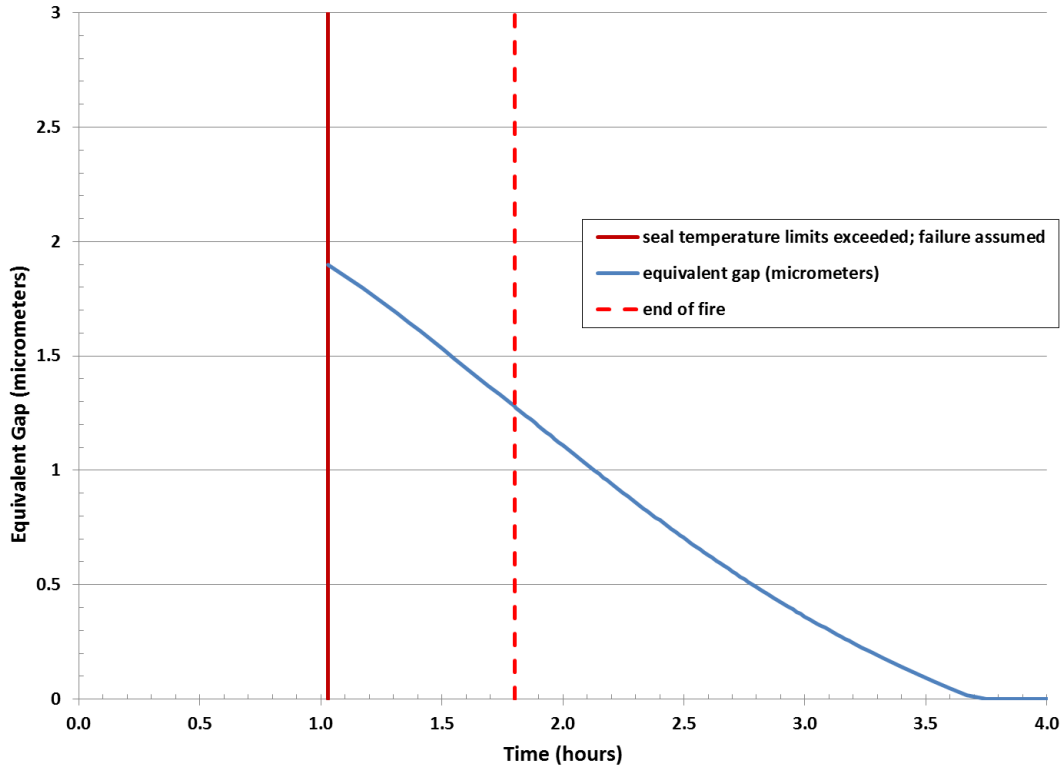

Figure 8.9. Equivalent Gap between Closure Lid and Package Body Flange after Seal Failure

As discussed in Section 7.3, the clamping force on the lid increases during the post-fire cooldown, due to differential thermal contraction between the nickel alloy closure bolts and the stainless steel lid and package body. The effect is to essentially close the gap entirely, for all practical purposes, by about 3.75 hours into the fire transient. This effectively limits the "window" of time in which material could leak out of the package to less than 3 hours. This has the effect of greatly reducing the potential for a substantial release of radioactive material from the package, as shown by the release evaluations in Section 8.3.3.2.

8.3.3.2 Bounding Estimate of Potential Release from GA-4 Package

Using the leak rate model and equivalent gap width relationship presented in Section 8.3.3.1, a conservative bounding estimate was obtained for potential release of radioactive material from the GA-4 package in the MacArthur Maze fire scenario. The fluid viscosity of pure helium was used for this calculation, rather than attempting to quantify the viscosity of the mixture of helium and fission gases that would actually be in the package following the rod ruptures. This is a conservative assumption, since the viscosity of the mixture would be higher than the viscosity of pure helium. The difference between the mixture property and that of pure helium would in any case be expected to be small, since the gas released from the fuel rods would consist mainly of helium.

The pressure difference driving the volumetric flow through the interface between the package cavity and ambient was calculated assuming a constant external ambient pressure of 1 atm. The internal cavity pressure was calculated using the ideal gas law, based on the average gas temperature predicted with the ANSYS thermal model. The initial pressure in the cavity was assumed to be at the Maximum Normal Operating Pressure (MNOP) for the GA-4 package.

This is a conservative initial pressure, as it corresponds to the pressure effect of 100% of the fuel rods in the package having ruptured, and the density change is determined for B&W 15x15 fuel[1], which is the most limiting fuel configuration for the maximum operating pressure. This approach provides a bounding estimate of the cavity internal pressure throughout the fire transient, and avoids the complication of changing the gas density in the package at the predicted time of rod rupture in this analysis.

Figure 8.10 shows the predicted leak rate as a volumetric flow of helium gas through the equivalent gap. Two leak rate calculations were performed; a bounding case in which the package gas density was assumed to remain constant throughout the transient, and a more realistic case in which the change in gas density (and hence pressure) due to outflow of gas from the package was accounted for. The difference between the two cases is relatively small, due to the small leak rates predicted for this configuration with the closure lid clamped tightly to the package body flange throughout the transient.

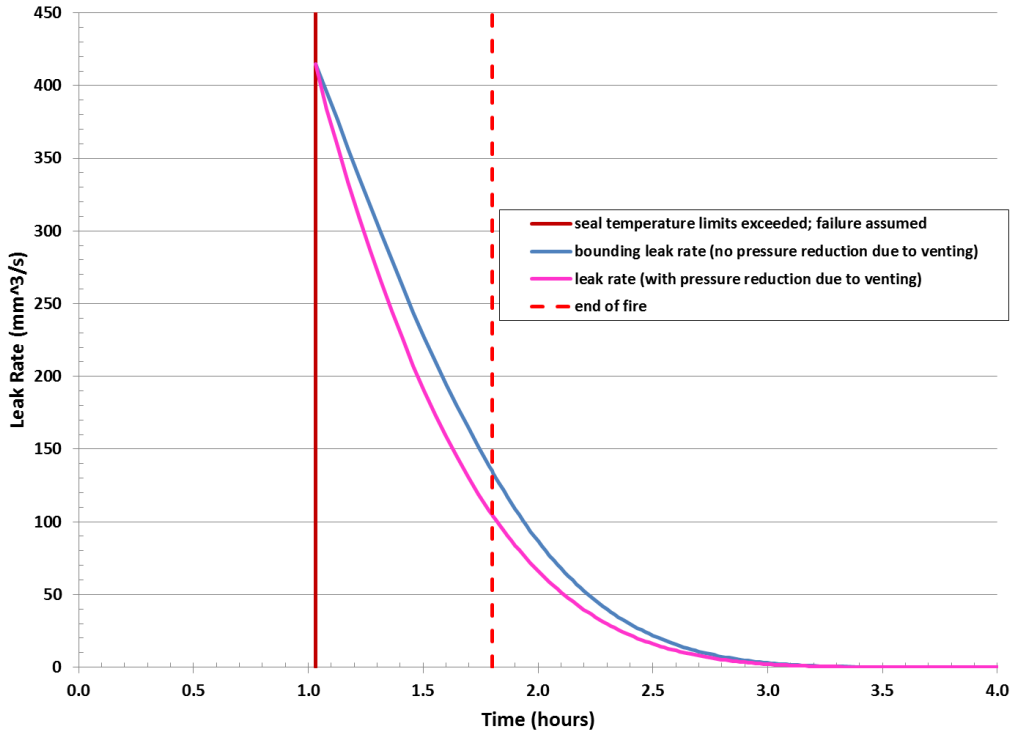

Figure 8.10. Volumetric Leak Rate for GA-4 Package after Seal Failure

The release calculations were performed assuming the bounding leak rate over time (as shown in Figure 8.10), providing a bounding estimate of potential release from the package. The activity within the package cavity was assumed to be uniformly distributed within the gas, with all particulate (i.e., fuel fines and spalled CRUD) suspended in the gas as an aerosol. It is

[1] For the thermal analysis, the most limiting fuel is WE 14x14, and this is the fuel configuration represented in the thermal models, as described in Sections 5 and 6. However, for maximum cavity pressure evaluations, as presented in the SAR, B&W 15x15 is the limiting configuration, due to the fuel rod design of this fuel assembly. Therefore, the cavity pressure obtained assuming 100% rod rupture (for four assemblies) with this fuel design was used, as a conservatism in the leak rate evaluations.

assumed that all solid particles remain suspended in the gas. The total release of each component was calculated simply as the activity of that component times the volumetric fraction of gas escaping from the package.

A number of additional conservatisms were incorporated into the release calculation, including the following assumptions

- the entire quantity of fuel and CRUD particulate was assumed to remain suspended in the gas within the cavity; the possibility of particulate settling or plating out on internal package structures was ignored

- the filtering effect of the equivalent gap size was neglected; the maximum size of the equivalent gap is only about 2 micrometers, and the release calculations do not consider that a large percentage of the fuel and CRUD particulate simply could not escape from the package, due to the small size of the gap

These assumptions result in a very conservative estimate of the amount of activity that could escape from the package in the approximately 2.7 hours that the package could sustain a significant leakage.

The activity of the large number of radionuclides comprising the estimated release can be more conveniently expressed in combined form, as a function of their combined isotopic A_2 limit[1] values from 10 CRF 71, Appendix A.

The A_2 value for a mixture of normal form material can be determined using the following relationship from 10 CFR 71, (Appendix A, Section IV.d), as

$$A_2 \; for \; mixture = \frac{1}{\left[\sum_{i=1}^{n} \frac{f(i)}{A_2(i)}\right]}$$

where

n = number of radionuclides in mixture
$f(i)$ = fraction of total mixture activity due to the i^{th} component
$A_2(i)$ = A_2 value for the i^{th} component

[1] An A_2 quantity is defined in 49 CFR 173.403 as the maximum activity of a Class 7 (radioactive) material permitted in a Type A package, which does not require an accident resistant design. The amount of material that constitutes an A_2 quantity depends on its specific activity and other radiological properties. Appendix A of 10 CFR 71 specifies the specific A_2 quantities for a large number of radioactive materials, and defines methods for calculating values for materials not listed in the table. Spent nuclear fuel requires a Type B package, which can carry more than an A_2 quantity of radioactive material, but must retain the integrity of containment and shielding under normal conditions of transport (as per 49 CFR 173) and meet the release limits of less than an A_2 per week for hypothetical accident conditions.

Using this approach, the A_2 for the mixture of radionuclides in the estimated potential release from the GA-4 package is calculated as 88 Ci (3.25 TBq) for WE 15x15 fuel at 45 GWd/MTU, 15 yrs cooling. The corresponding result for WE 15x15 fuel at 35 GWd/MTU, 10-yrs cooling is a mixture A_2 of 143 Ci (5.3 TBq). The calculation of the mixture A_2 for each fuel configuration includes all fission gas and particulate released from the fuel, plus the CRUD assumed to spall from the exterior surfaces of the rods.

Based on the leak rate model, the total release from the package is estimated as 21 Ci (0.78 TBq) for the higher burnup fuel, and as 24.5 Ci (0.91 TBq) for the lower burnup fuel. Expressed as an A_2 fraction, relative to the mixture A_2 for each configuration, these release rates are 0.24 and 0.17, respectively. Therefore, the bounding estimate of the total release from the package is 0.24 of the mixture A_2 calculated assuming WE 15x15 fuel at 45 GWd/MTU, 15 yrs cooling. As mentioned above, if the effect of particulate settling and the restriction of large particulate from passing through a small gap were taken into account, the release estimate would be significantly reduced.

The evaluations of potential release from the GA-4 package assume that the estimated release by way of the closure lid is sufficiently conservative to be bounding on the possible contribution of leakage through the drain valve/port and gas sampling valve/port, which form part of the containment boundary of the GA-4 package. These components also contain seals that would be expected to exceed their operating temperature limits in this fire scenario, as discussed in Section 8.2 above. However, these penetrations of the package are less than an inch in diameter, compared to the approximately 2-ft diameter of the closure lid rim, and therefore do not provide a significant increase in the area available for potential leakage. In addition, the ports consist of long and convoluted flow paths that would tend to filter any particulate that might be carried through them to the ambient environment. The gas sample port is effectively blocked by the sample valve itself, which in addition to having primary and secondary O-ring seals, is threaded into place over a length of several inches. Also, for transport conditions, the outer face of the gas sample port is plugged with a threaded cover that extends to a depth of more than an inch. Similarly, the drain port is plugged by the drain valve, and capped with a threaded drain valve cover and port plug.

Based on the geometry of the valve/ports in this package, it is reasonable to assume that leakage from the package at these locations due to failed seals would be much less likely to be significant compared to leakage through for the much larger area and more direct flow path of the closure lid seal region. The conservative assumptions regarding the amount of material that could be transported out of the package through the lid closure/flange equivalent gap are sufficient to bound any possible contribution of the valve/port leakage paths. It is therefore justifiable to neglect the effect of the valve/ports, without compromising the conservatism of the estimated leak rate and total package release calculations.

9.0 OVERALL SUMMARY AND CONCLUSIONS

The U.S. Nuclear Regulatory Commission has established requirements for packaging and transportation of spent nuclear fuel assemblies under NCT and for HAC. These requirements (10 CFR 71) conservatively bound the expected range of conditions that an SNF package might be subjected to in the course of its service life. However, real-world accidents of greater severity are certainly possible, and rare as they may be, the NRC has proactively undertaken the examination of such accidents, to determine what the potential consequences might be, were such an accident ever to involve an SNF package.

Two previous studies of transportation accidents, one resulting in a fire in a railroad tunnel (NUREG/CR-6886 2009) and one in a highway tunnel (NUREG/CR-6894 2007) were undertaken with three different SNF package designs. Based on conservative scenarios constructed from these real-world fire conditions, the results of these studies have shown that the design basis for SNF packages is sufficiently robust for them to survive such beyond-design-basis conditions without adverse consequences to public safety. In all cases evaluated, the modeling results showed that the various SNF packages would be expected to maintain required shielding for ionizing radiation, and also would maintain the integrity of the containment boundary sufficiently to limit potential release of radioactive material from the packages to within regulatory bounds for accident conditions.

The MacArthur Maze accident of April 29, 2007 was selected as a third study in this series of evaluations of real-world accidents because of the severity of the fire and the unusual structural consequences, in which the heat from the fire caused the overhead roadway segments to collapse onto the roadway where the fire was burning. Since this was a highway accident, the only type of SNF package that could potentially be involved would be a LWT package. The General Atomics GA-4 LWT transportation package was selected for this investigation, mainly because it can carry a relatively large payload for an over-the-road transportation package, and therefore the potential consequences of package failure could be more severe than for packages with smaller payload capacities. The GA-4 package is designed to transport up to four intact PWR spent fuel assemblies, with a maximum total package decay heat load of 2.5 kW.

Bounding Scenario for the MacArthur Maze Accident

The MacArthur Maze accident involved a gasoline tanker truck and trailer that overturned and caught fire on the I-880 connector of the MacArthur Maze interchange in Oakland, CA. The fire lasted approximately 108 minutes, consuming the entire load of gasoline fuel. The heat from the fire caused two sections of the overhead I-580 freeway to collapse onto the lower roadway, the first falling at approximately 17 minutes into the fire, the second collapsing on only one end, and reaching its final configuration by about 37 minutes. (Refer to Figure 1.1, which shows the configuration of the collapsed roadway, in an image taken in daylight the next day, after the fire was out. See Section 2.0 for a detailed discussion of the fire scenario, with images from a video of the fire.)

Based on fire modeling with the FDS code, and physical examination of material samples obtained from the damaged highway girders and the remnants of the tanker truck, a bounding fire scenario was defined for the thermal and structural evaluations of the potential effects of this fire on an SNF package. The complex and dynamic fire conditions are represented as a fully engulfing pool fire at 2012°F (1100°C) prior to the overhead roadway collapse, and as a slightly smaller and less severe fully engulfing pool fire at 1652°F (900°C) after the roadway collapse.

These temperatures represent conservative bounding values for open pool hydrocarbon fires for any possible configuration of both the pre-collapse and post-collapse fire pools in this accident.

As an additional simplifying conservatism in the definition of the scenario, it is assumed that the pre-collapse pool fire (at 2012°F [1100°C]) lasts for the full 37 minutes required for the completion of the collapse of the overhead segments. The smaller fire size is assumed as a step change to 1652°F (900°C), after 37 minutes, and this smaller pool fire is assumed to persist unchanged until the end of the fire, at 108 minutes. The fire scenario for modeling purposes also assumes that in the post-fire configuration, the fallen overhead roadway segment completely covers the SNF package, resulting in an additional barrier to heat transfer from the package during the cooldown phase of the transient.

Thermal and Structural Modeling Approach and Summary of Results

Detailed thermal models of the GA-4 package were constructed for the ANSYS and COBRA-SFS codes, for transient evaluations to determine the temperature response of the package to the fire scenario, including the long post-fire cooldown transient. The initial condition of the package at the start of the fire scenario was defined as steady-state NCT. Additional detailed structural and thermal-structural models were also developed using ANSYS and LS-DYNA for the roadway and package, for evaluation of the package response to the effect of the roadway falling on it.

Considerable effort was given to defining bounding and conservative estimates of the possible configurations of the package on the roadway that could produce the “worst case” structural loading of the SNF package due to the overhead roadway segment falling on it. These evaluations showed that the worst that the overhead spans could do to the package imposed relatively innocuous loads on the stainless steel body and DU gamma shield compared to the HAC structural loading that the package is designed to withstand. At a nominal fully loaded weight of approximately 55,000 lb (nearly 28 tons), the package itself falling from a height of 30 ft (9 meters) – the HAC package drop scenario – would be expected to do far more damage than the roadway falling on it, even with the added impact of the projecting “blades” of the steel girders. The only real challenge of the overhead roadway drop in the fire scenario is that the impact is postulated to occur with the package at higher temperatures than are typically assumed in the structural analyses for HAC scenarios. This could potentially make the package more vulnerable to structural damage, due to the reduction in the strength of steel with increasing temperatures. However, the steel girders of the overhead span suffer more from this problem, and the weight of the overhead roadway concrete is not sufficient to impart significant loading to damage the package in any way.

Much more interesting structural analyses were undertaken to investigate in detail the response of the bolts attaching the impact limiters to the package, and the package lid closure bolts. Issues of bolt performance were further complicated by the use of thread inserts in all bolt attachments in the package, in which helical coils of Type 304 stainless steel fill the interface between the bolt threads and the threaded holes in the package body. Differential thermal expansion of the Inconel bolts relative to the XM-19 stainless steel package body, and different strength-versus-temperature properties of the three metals involved, results in a time-and-temperature dependent history of force on the bolts that raised the possibility that the impact limiters might detach from the package. These material issues also raised the possibility that there could be a loss of clamping force between the lid and the package body during the post-fire cooldown.

Detailed evaluations of the structural and thermal response of the impact limiter bolts to the conditions of the MacArthur Maze fire scenario with FEA modeling using ANSYS show definitively that the impact limiter bolts will not fail under these conservative and bounding thermal and structural loading conditions. Loss of the impact limiters is not a credible consequence of this fire scenario for the GA-4 package. Additional detailed evaluations of the response of the lid closure bolts to the fire scenario were undertaken with LS DYNA, and the modeling accuracy was verified with classic bolt equation methods. These evaluations show unambiguously that the lid closure bolts maintain a positive clamping force between the package lid and body flange during all phases of the fire scenario, including the fire duration (108 minutes) and the very long cooldown period of approximately 400 hours, back to post-fire steady-state ambient conditions. This means that there is at all times forced metal-to-metal contact between the lid and the package body. This is particularly important to assessing the response of the GA-4 package to this fire scenario, because the thermal evaluation shows that the seals exceed their rated temperature limits within the first hour or so of the transient, and this metal-to-metal contact becomes the containment boundary of the package.

Thermal evaluations of the package response to this fire scenario predict that the peak cladding temperature would be expected to exceed the short-term limit of 1058°F (570°C) long before the end of the fire. Maximum cladding temperatures on all rods in the package are predicted to exceed this temperature limit in the course of the transient, and remain above this limit for several hours. In addition, the thermal inertia of the package and the insulating effect of the fallen overhead roadway, which is assumed to blanket the package during the post-fire cooldown, means that fuel cladding temperatures continue to rise for many hours after the end of the fire. The insulating effect of the impact limiters, which shield the package ends from direct heating by the fire, results in the cooler ends of the rods continuing to heat up for several hours after the end of the fire, as heat in the hot central region of the rods redistributes throughout the package.

The maximum peak cladding temperature in the transient is predicted to be in the range of 1350-1400°F (732-760°C), and occurs approximately 3 hours after the end of the fire. In addition, temperatures in the regions of the package seals exceed the seal material operating temperature limits for most of the fire transient and for several hours of the post-fire cooldown transient.

Fuel Rod Performance Evaluation

Based on the predicted fuel cladding temperatures from the COBRA-SFS modeling, fuel performance was evaluated by direct comparison to fuel rod burst data as a function of cladding hoop stress and temperature. In addition to comparison to relevant data, predicted fuel rod rupture temperatures were obtained using the burst rupture model in the FRAPTRAN-1.4 code (NUREG/CR-7023 2011). Creep rupture is considered a possible alternative mechanism of failure for spent fuel rods. To evaluate this possibility, a separate analysis was performed with a creep rupture model for the temperatures predicted for the hottest rod in the MacArthur Maze fire scenario, using the FRAPCON-3.4 code (NUREG/CR-7022 2011) in conjunction with the DATING code (Simonen and Gilbert 1988), which has been updated with creep coefficients from creep tests on irradiated cladding (Gilbert et al. 2002).

Fuel performance analyses for peak temperatures on the hottest rod in the MacArthur Maze fire scenario, as predicted with the COBRA-SFS model, predict cladding rupture temperatures of 1097°F (592°C) using LOCA burst strain modeling (FRAPTRAN) and 1229°F (665°C) using creep rupture modeling (FRAPCON/DATING). Applicable experimental data (NUREG/CR-

0344) yields measured rupture temperatures in the range 1205-1256°F (652-680°C). The burst rupture and creep rupture models both predict that the hottest fuel rod would rupture if subjected to the temperatures predicted in this fire scenario. Furthermore, the peak temperature on the hottest rod at the time of rupture is eventually exceeded by all rods in the package during the transient, which suggests that there is the potential for all rods in the package to rupture in this fire scenario.

Potential Radiological Consequences

Neutron and gamma radiation dose rates from the GA-4 package as a result of the postulated conditions of the MacArthur Maze fire scenario will not exceed the design basis of the package, which is well within the regulatory limits for hypothetical accident conditions. The neutron shielding is lost very early in the transient, but loss of the neutron shield tank is a design-basis assumption for this package in all HAC analyses. The more severe conditions of the MacArthur Maze fire can do no more damage to the GA-4 package neutron shield than is assumed *a priori* in the HAC analyses. The gamma shielding for the GA-4 is provided by a layer of DU within the stainless steel package body. The shielding function of this material is not affected by the higher temperature it is predicted to reach in the MacArthur Maze fire scenario. There is no credible scenario in this fire accident that could result in neutron and gamma dose rates from the design-basis GA-4 package exceeding the regulatory limits for accident conditions.

Loss of the package seals due to exceeding seal material thermal limits means that there is the potential for radioactive material to escape from the package. Rupture of all rods in the package, as is predicted by the fuel performance analyses, based on the calculated thermal response of the fuel, means that fission gas and fuel particulate would be released to the package cavity. In addition, 100% spalling of CRUD from the external surfaces of the fuel rods is an assumed for all accident analyses for SNF packages, per NRC guidance. Therefore, it must be assumed that there is material available in the package cavity that could be released through the failed seals. But because the lid closure bolts maintain positive clamping force throughout the transient, it is not physically possible for very much of it to actually escape. Conservative and bounding modeling assumptions show that the maximum possible release total release is 0.24 of the A_2 quantity calculated for total activity of the mixture of radionuclides (comprised of fission gases, fuel particulate and CRUD) released from the package. The regulatory limit specifies a maximum allowable release rate of an A_2/week. The predicted total release estimate of approximately one-fourth of a mixture A_2 is below the prescribed limit for safety, and indicates that the potential release from this package in the MacArthur Maze fire scenario would not pose a risk to public health and safety.

10.0 REFERENCES

10 CFR 71. 2003. "Packaging and Transportation of Radioactive Material." *Code of Federal Regulations*, U.S. Nuclear Regulatory Commission, Washington, D.C.

49 CFR 713.403. 2011. "Subpart 1 – Class 7 (Radioactive) Materials - Definitions." *Code of Federal Regulations*, U.S. Nuclear Regulatory Commission.

ANSYS, Inc. 2003. *ANSYS Users Guide for Revision 8.0*. ANSYS, Inc., Canonsburg, Pennsylvania.

ANSI N14.5. 1997. *American National Standard for Radioactive Materials—Leakage Tests on Packages for Shipment.* American National Standards Institute.

Bahney RH III and TL Lotz. 1996. *Spent Nuclear Fuel Effective Thermal Conductivity Report*, BBA000000-01717-5705-00010 Rev. 00, TRW Environmental Safety Systems, Inc., Fairfax, Virginia.

Brekelmans J, R ven den Bosch, and K Both. 2008. *Summary of Large Scale Fire Tests in the Runehamar Tunnel in Norway.* UPTUN Research Program, official deliverable, Workpackage 2 Fire development and mitigation measures, D213. Available from http://www.vegvesen.no/_attachment/61890/binary/15101.

Brockenbrough RL and FS Merritt, eds. 1999. *Structural Steel Designer's Handbook*. 3rd edition, MacGraw-Hill, Inc., New York.

Brown R. 1987. "Fluid Flow through Rock Joints: The Effect of Surface Roughness." *Journal of Geophysical Research*, 92(B2):1337-1347.

Burian RJ. 1985. *Response of Spent LWR Fuel to Extreme Environments*. SAND85-7213. Sandia National Laboratory, Albuquerque, New Mexico.

CHP - California Highway Patrol. 2007. *California Highway Patrol Multi-Disciplinary Accident Investigation Team Report, MacArthur Maze Accident, April 29, 2007*. CHP 558D (REV 6-84) OPI 065, Oakland, California.

Creer JM, TE Michener, MA McKinnon, JE Tanner, ER Gilbert, and RL Goodman. 1987. *The TN-24P PWR Spent-Fuel Storage Cask: Testing and Analysis*. EPRI-NP-5128/PNL-6054, Electric Power Research Institute, Palo Alto, California.

Dow Chemical Company. 2003. *A Guide to Glycols*. Available at http://www.dow.com/webapps/lit/litorder.asp?filepath=propyleneglycol/pdfs/noreg/117-01682.pdf. The Dow Chemical Company, Midland, Michigan.

Einziger RE, SD Atkin, DE Stellrecht, and V Pasupathi. 1982. "High Temperature Post-Irradiation Materials Performance Spent Pressurized Water Reactor Fuel Rods Under Dry Storage Conditions." *Nuclear Technology* 57(1):65 – 80.

Gauld IC, SM Bowman, and JE Horwedel. 2009. *ORIGEN-ARP: Automatic Rapid Processing for Spent Fuel Depletion, Decay, and Source Term Analysis*. ORNL/TM-2005/39, Oak Ridge National Laboratory, Oak Ridge, Tennessee.

General Atomics. 1998. *GA-4 Legal Weight Truck Spent Fuel Shipping Cask Safety Analysis Report for Packaging (SARP).* Document No. 910469, Revision G, General Atomics. (Public version available in ADAMS: ML070020004, ML070020006, and ML070020007.)

Gilbert ER, CE Beyer, EP Simonen, and PG Medvedev. 2002. "Update of CSFM Creep and Creep Rupture Models for Determining Temperature Limits for Dry Storage of Spent Fuel." International Congress on Advanced Nuclear Power Plants (ICAPP) ANS Embedded Topical Meeting, June 9-13, Hollywood, Florida.

Guyer EC and DL Brownell, eds. 1989. *Handbook of Applied Thermal Design.* McGraw-Hill, Inc., New York.

HEXCEL Composites. 1999. HexWeb™ Honeycomb Attributes and Properties. Available at http://www.hexcel.com/Resources/DataSheets/Brochure-Data-Sheets/Honeycomb_Attributes_and_Properties.pdf.

Johnson AB and ER Gilbert. 1983. *Technical Basis for Storage of Zircaloy-clad Spent Fuel in Inert Gases.* PNL-4835. Battelle Pacific Northwest Laboratory, Richland, Washington.

Johnson AB, ER Gilbert, and RJ Guenther. 1983. *Behavior of Spent Nuclear Fuel and Components in Dry Interim Storage*. PNL-4189. Pacific Northwest Laboratory, Richland, Washington.

Juvinall RC and KM Marshek. 1991. *Fundamentals of Machine Component Design*, 2nd Edition. John Wiley & Sons, New York.

Kreith F and MS Bohn. 2001. *Principles of Heat Transfer.*6th ed. Brooks/Cole, Forest Grove, California.

Livermore Software Technology Company. 2007. *LS-DYNA Keyword User's Manual, Version 971*. Livermore Software Technology Company, Troy, Michigan.

McGrattan KB, B Klein, S Hostikka, and J Floyd. 2008. *Fire Dynamics Simulator (Version 5), User's Guide*. Special Publication 1019-5, National Institute of Standards and Technology, U.S. Department of Commerce, Washington, D.C.

Michener TE, DR Rector, JM Cuta, RE Dodge, and CW Enderlin. 1995. *COBRA-SFS: A Thermal-Hydraulic Code for Spent Fuel Storage and Transportation Casks*. PNL-10782. Pacific Northwest Laboratory, Richland, Washington.

NFPA - National Fire Protection Association. 2008. *NFPA 502: Standard for Road Tunnels, Bridges, and Other Limited Access Highways.* National Fire Protection Association. Nitronic 50 Product Data Bulletin[1]. High Performance Alloys, 444 Wilson St. Tipton, IN 46072. Available at http://www.hpalloy.com/Alloys/brochures/Nitronic50book.pdf.

NRC – U.S. Nuclear Regulatory Commission. 2008. *Analysis of Structural Material Exposed to a Severe Fire Environment – Final Letter Report*, Contract NRC-02-07-006, prepared by Southwest Research Institute and Center for Nuclear Waste Regulatory Analyses, San Antonio, Texas, published by U.S. Nuclear Regulatory Commission, Washington, D.C.

NUREG-0170. 1977. Final Environmental Statement on the Transportation of Radioactive Material by Air and Other Modes. U.S. Nuclear Regulatory Commission, Washington, D.C.

NUREG-1617. 2000. *Standard Review Plan for Transportation Packages for Spent Nuclear Fuel: Final Report*. U.S. Nuclear Regulatory Commission, Washington, D.C.

NUREG/CR-0344. 1980. *Embrittlement Criteria for Zircaloy Cladding Applicable to Accident Situations in Light-Water Reactors: Summary Report.* U.S. Nuclear Regulatory Commission, Washington, D.C.

NUREG-0630. 1980. *Cladding Swelling and Rupture Models for LOCA Analysis.* U.S. Nuclear Regulatory Commission, Washington, D.C.

NUREG/CR-0772. 1980. *Fission Product Release from Highly Irradiated LWR Fuel.* U.S. Nuclear Regulatory Commission, Washington, D.C.

NUREG/CR-4829. 1987. *Shipping Container Response to Severe Highway and Railway Accident Conditions*. U.S. Nuclear Regulatory Commission, Washington, D.C.

NUREG/CR-6487. 1996. *Containment Analysis for Type B Packages Used to Transport Various Contents.* BL Anderson, RW Carlson, and LE Fischer. U.S. Nuclear Regulatory Commission, Washington, D.C.

NUREG/CR-6672. 2000. *Re-examination of Spent Fuel Shipment Risk Estimates*. U.S. Nuclear Regulatory Commission, Washington, D.C.

NUREG/CR-6886, Rev 2. 2009. *Spent Fuel Transportation Package Response to the Baltimore Tunnel Fire Scenario.* U.S. Nuclear Regulatory Commission, Washington, D.C.

NUREG/CR-6894, Rev. 1. 2007. *Spent Fuel Transportation Package Response to the Caldecott Tunnel Fire Scenario.* U.S. Nuclear Regulatory Commission, Washington, D.C.

NUREG/CR-7022, Vol. 1. 2011. *FRAPCON-3.4: A Computer Code for the Calculation of Steady-State Thermal-Mechanical Behavior of Oxide Fuel Rods for High Burnup.* U.S. Nuclear Regulatory Commission, Washington, D.C.

[1] This bulletin has no specific publication date documented. The pdf file was downloaded March 26, 2014, and verified to be the same document as used in the work performed here.

NUREG/CR-7023, Vol. 1. 2011. *FRAPTRAN 1.4: A Computer Code for the Transient Analysis of Oxide Fuel Rods*. U.S. Nuclear Regulatory Commission, Washington, D.C.

NUREG/CR-7115. 2012. *Performance of Metal and Polymeric O-Ring Seals in Beyond-Design-Basis Temperature Excursions*. U.S. Nuclear Regulatory Commission, Washington, D.C.

Oberg E, FD Jones, HL Horton, and HH Ryffel. 2004. *Machinery's Handbook*, 27th Edition, and *Guide to Machinery's Handbook*. Industrial Press. On-line version at http://app.knovel.com/hotlink/toc/id:kpMHEGMH0B/machinerys-handbook-27th.

Sanders TL, KD Seager, YR Rashid, PR Barrett, AP Malinauskas, RE Einziger, H Jordan, TA Duffey, SH Sutherland, and PC Reardon. 1992. *A Method for Determining the Spent-Fuel Contribution to Transport Cask Containment Requirements*, *Appendix III, Spent Fuel Response to Transport Environments*. SAND2000-0324. Sandia National Laboratory, Albuquerque, New Mexico. Accessed on http://pbadupws.nrc.gov/docs/ML0427/ML042710347.pdf.

Shajaefard ML and K. Goudarzi. 2008. "The Numerical Estimation of Thermal Contact Resistance in Contacting Surfaces." *American Journal of Applied Sciences* 5(11):1566-1571.

Simonen EP and ER Gilbert. 1988. *DATING – A Computer Code for Determining Allowable Temperatures for Dry Storage of Spent Fuel in Inert and Nitrogen Gases.* PNL-6639, UC-85, Pacific Northwest Laboratory, Richland, Washington.

Society of Fire Protection Engineers. 2002. *SFPE Handbook of Fire Protection Engineering.* 2nd ed., National Fire Protection Association, Quincy, Massachusetts. (Specifically, the chapter *Fire Hazard Calculations for Large, Open Hydrocarbon Fires*, by Beyler, in *SFPE Handbook of Fire Protection Engineering,* 2nd ed.)

Society of Fire Protection Engineers. 2008. *SFPE Handbook of Fire Protection Engineering.* 4th ed. National Fire Protection Association, Quincy, Massachusetts. (Specifically, the chapter Liquid Fuel Fires, by DT Gottuk and DA White, in *SFPE Handbook of Fire Protection Engineering*, 4th ed.)

Wilmot EL. 1981. *Transportation Accident Scenarios for Commercial Spent Fuel.* SAND80-2124. Sandia National Laboratory, Albuquerque, New Mexico.

Wiss, Janney, Elstner Associates, Inc. 2007. *Route 580/880 Fire and Collapse: Evaluation of Concrete.* Prepared by Wiss, Janney, Elstner Associates, Inc., for the Office of Rigid Pavement Materials and Structural Concrete, Caltrans, 4 May 2007. WJE No. 2005.2002.3.3.

APPENDIX A

MATERIAL PROPERTIES FOR COBRA-SFS MODEL OF GA4 PACKAGE

APPENDIX A

MATERIAL PROPERTIES FOR COBRA-SFS MODEL OF GA4 PACKAGE

Table A.1. Internal Fill Gas—Helium at Atmospheric Pressure

Temperature (°F)	Enthalpy (Btu/lbm)	Thermal Conductivity (Btu/hr-ft-°F)	Specific Heat (Btu/lbm-°F)	Specific Volume (ft^3/lbm)	Viscosity (lbm/hr-ft)
0	100	0.078	1.24	83.33	0.0410
200	348	0.097	1.24	119.76	0.0533
400	596	0.115	1.24	156.25	0.0641
600	844	0.129	1.24	192.31	0.0727
800	1092	0.138	1.24	229.36	0.0823
1000	1340	0.138	1.24	265.25	0.0907
2552	3264	0.138	1.24	549.00	0.1138

Table A.2. External Ambient Air at Atmospheric Pressure

Temperature (°F)	Enthalpy (Btu/lbm)	Thermal Conductivity (Btu/hr-ft-°F)	Specific Heat (Btu/lbm-°F)	Specific Volume (ft^3/lbm)	Viscosity (lbm/hr-ft)
60	124.5	0.0146	0.24	13.5669	0.0434
300	182.1	0.0193	0.243	19.8325	0.058
400	206.5	0.0212	0.245	22.4432	0.063
500	231.1	0.0231	0.247	25.0539	0.068
600	256	0.025	0.25	27.6645	0.072
700	281.1	0.0268	0.253	30.2752	0.077
800	306.7	0.0286	0.256	32.8859	0.081
900	332.5	0.0303	0.259	35.4966	0.085
1000	358.6	0.0319	0.262	38.1072	0.0889
2000	617.2	0.0471	0.2586	64.214	0.1242
4000	1522	0.0671	0.4524	116.428	0.1242

Table A.3. Material Properties

Specific Heat (Btu/lbm-°F)	Density (lbm/ft^3)	Thermal Conductivity (Btu/hr-ft-°F)	Emissivity	Description	Source
0. 11	492.5	see Eq. (A-1)	see Table A.4	SA-240, Type XM-19 stainless steel, for basket plates, inner liner, package body, and neutron shield tank outer shell	Density and specific heat from GA-4 SAR (General Atomics1998); thermal conductivity from ATI 50™ Technical Data Sheet (see below)
0.065	1185.4	14.8	0.5	Depleted uranium for gamma shielding	Specific heat from Table 3.2-1 of GA-4 SAR; density from SAR Section 2.3, p. 2.3-1; Thermal conductivity from W21 SAR (see Appendix B)
0.29	151	15.0	0.8	Boron carbide rods within basket plates	Table 3.2-1 of GA-4 SAR, p. 3.2-2
0.787	61.72	$k_{Nsliq.}$ = 0.186 k_{eff} = 5.92	N/A	60% propylene glycol and water mixture (neutron shield)	Table 3.2-2 of GA-4 SAR (selected value at 194°F), and correlation for k_{eff} of liquid (see Eq. [A-3])
0.210	150	1.0	0.63 (pre-fire) 0.90 (fire and post-fire)	Concrete roadways and side barrier	From material exposure analysis report (NRC 2008)

Emissivity values for thermal radiation exchange were obtained from Table 3.2-3 of the GA-4 SAR (General Atomics 1998). However, the emissivity of package surfaces exposed to the fire was conservatively represented with a value of 0.9, rather than the “0.8 or 0.85” listed in the SAR. Table A.4 summarizes the emissivity values used for the XM-19 stainless steel components during the various phases of the fire scenario.

Table A.4. Emissivity Values for XM-19 Stainless Steel Components

Emissivity	Component	Transient Conditions
0.20	steel inner liner basket plates package body inner surface	pre-fire steady state, fire, and post-fire cooldown
0.20	package body outer surface NS tank shell inner surface	pre-fire steady state
0.15	NS tank shell outer surface	pre-fire steady state
0.9	package body outer surface NS tank shell inner surface NS tank shell outer surface	fire and post-fire cooldown

Temperature-dependent thermal conductivity (in units Btu/hr-ft^2-°R) for XM-19 stainless steel was evaluated in the COBRA-SFS model using a linear regression fit to ATI 50 thermal conductivity data (see Appendix B for the material data sheet). The relationship from this fit is

$$k_{XM-19} = a_0 + a_1 T \quad \text{(A-1)}$$

where

a_0 = 5.4446
a_1 = 0.0047
T = material temperature (°R)

The relationship in Eq. (A-1) is a polynomial curve fit to the same data used to derive the linear equation presented in the GA-4 SAR, which has the form

$$k_s = a_0 + a_1 T \quad \text{(A-2)}$$

where

a_0 = 3.6 (empirical coefficient)
a_1 = 0.00532 (empirical coefficient)
T = material temperature (°R)

These two equations give essentially identical results for temperatures below about 1000°F (538°C), but Equation (A-1) is more conservative by 15-20% at the high temperatures encountered in the MacArthur Maze fire scenario.

The formula for the effective conductivity used to model natural convection in the liquid neutron shield is documented in the GA-4 SAR as

$$k_{eff} = \frac{a_0 k_{NSliq.} \, \mathrm{Pr} \, Gr_D}{\left(a_1 + \mathrm{Pr}\right)^{a_2}} \quad \text{(A-3)}$$

where

a_0 = 0.135 (empirical coefficient)
a_1 = 1.36 (empirical coefficient)
a_2 = 0.278 (empirical coefficient)
$k_{NSliq.}$ = thermal conductivity of NS liquid (propylene glycol/water mixture)
Pr = Prandtl Number
Gr_D = Grashoff number, using thickness of neutron shield tank as characteristic length

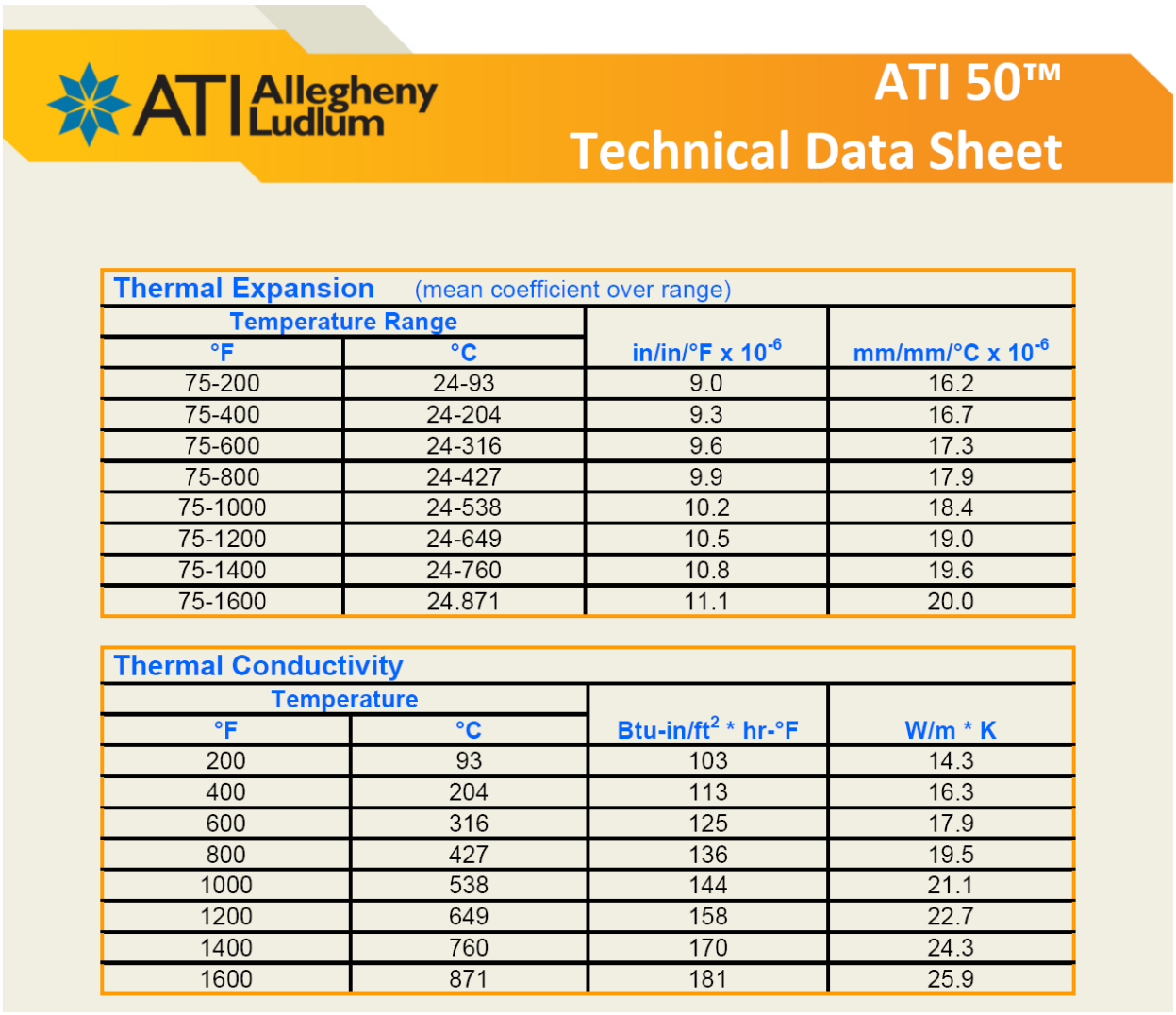

ATI Allegheny Ludlum

ATI 50™

Technical Data Sheet

Thermal Expansion (mean coefficient over range)

Temperature Range			
°F	°C	in/in/°F x 10^{-6}	mm/mm/°C x 10^{-6}
75-200	24-93	9.0	16.2
75-400	24-204	9.3	16.7
75-600	24-316	9.6	17.3
75-800	24-427	9.9	17.9
75-1000	24-538	10.2	18.4
75-1200	24-649	10.5	19.0
75-1400	24-760	10.8	19.6
75-1600	24.871	11.1	20.0

Thermal Conductivity

Temperature			
°F	°C	Btu-in/ft^2 * hr-°F	W/m * K
200	93	103	14.3
400	204	113	16.3
600	316	125	17.9
800	427	136	19.5
1000	538	144	21.1
1200	649	158	22.7
1400	760	170	24.3
1600	871	181	25.9

© 2009 ATI Allegheny Ludlum

Figure A.1. Source for Thermal Conductivity of XM-19 Stainless Steel

Table 3.2-1 - W21 Canister Homogenous Material Properties (3 pages)

Material	Temperature (°F)	Thermal Conductivity (BTU/hr-ft-°F)		Density[1] (lb/ft³)	Specific Heat (BTU/lb-°F)
Lead[3]	-58	21. 7		708	0.030
	32	20.4			0.030
	81	20.0			
	158	19.9			0.031
	248				0.032
	261	19.4			
	338				0.032
	428	18.4			0.033
	608				0.033
	621	16.4			
	698				0.051
	833	10.1			
BORAL®[4]		Through	Axial		
	-40	59.7[6]	63.2[6]	160	0.191[6]
	77	59.0	64.2		0.217
	212	58.1	65.3		0.246
	392	58.5	66.8		0.271
	482	58.3	67.1		0.280
	572	58.1	67.4		0.288
	662	57.7	67.4		0.293
	752	57.3	67.3		0.298
	842	56.2	66.4		0.304
	932	55.2	65.5		0.308
	1472	48.9[6]	60.1[6]		0.329[6]
Depleted Uranium[5]	68	14.6		1183	0.028
	140	15.0			0.028
	437	17.5			0.031
	824	19.3			0.038

Table 3.2-1 Notes:

(1) Single values are shown for homogeneous material density since this material property does not vary significantly with temperature.

(2) Material properties are obtained from ASME Boiler and Pressure Vessel Code, Section II, Part D, 1998 Edition.

(3) Touloukian, Y.S., *Thermal Conductivity - Metallic Elements and Alloys*, Thermophysical Properties of Matter, the TPRC Data Series, Vol. 1, 1970.

(4) AAR, Standard Specification for BORAL® Composite Sheet, AAR Advanced Structures.

(5) General Electric, *Properties of Solids, Thermal Conductivity, Metallic Materials*, Heat Transfer Division, July 1974.

(6) Extrapolated value.

1

2 Figure A.2. Source for Thermal Conductivity of Depleted Uranium

APPENDIX B

MATERIAL PROPERTIES FOR ANSYS MODEL OF GA4 PACKAGE

APPENDIX B

MATERIAL PROPERTIES FOR ANSYS MODEL OF GA4 PACKAGE

Table B.1. ASME SA-240 Grade XM-19

Temperature (°F)	Thermal Conductivity (Btu/hr-in-°F)	Density (lbm/in^3)	Specific Heat (Btu/lbm-°F)	Description
50	0.65333	0.2850	0.1150	Used for FSS liner, package body, ILSS, bottom plate, outer shell, trunnions, closure
100	0.67333			
300	0.75167			
500	0.83000			
700	0.90833			
900	0.98667			
1100	1.0650			
1300	1.1433			
1500	1.2217			
1700	1.3000			
1900	1.3783			
2100	1.4567			

Table B.2. FSS Inner Frame (XM-19, Helium, and Boron Carbide Composite)

Temperature (°F)	Thermal Conductivity (Btu/hr-in-°F)			Density (lbm/in^3)	Specific Heat (Btu/lbm-°F)	Description
	Kxx	Kyy	Kzz			
0	0.32494	0.40625	0.33828	0.19272	0.19893	Calculated composite properties of XM-19 steel, helium, and boron carbide pellets
100	0.33972	0.42913	0.35146	0.19272	0.19893	
200	0.36773	0.46354	0.38037	0.19272	0.19893	
300	0.39439	0.49628	0.40806	0.19272	0.19893	
400	0.42001	0.52716	0.43482	0.19272	0.19893	
500	0.44263	0.55498	0.45892	0.19272	0.19893	
600	0.46443	0.58131	0.48228	0.19272	0.19893	
700	0.48302	0.60502	0.50280	0.19272	0.20954	
800	0.50101	0.62760	0.52280	0.19272	0.22016	
900	0.51884	0.65034	0.54269	0.19272	0.22494	
1000	0.53611	0.67167	0.56210	0.19272	0.22971	
1100	0.55338	0.69302	0.58153	0.19272	0.23821	

Table B.3. Homogeneous Fuel Region for Westinghouse 14x14 OFA

Temperature (°F)	Thermal Conductivity (Btu/hr-in-°F)			Density (lbm/in^3)	Specific Heat (Btu/lbm-°F)	Description
	Kxx	Kyy	Kzz			
0	-	-	0.05923	0.1446	0.0747	Used for active fuel assembly region (WE 14x14)
75	0.01688	0.01688	-			
100	0.01815	0.01815	0.05923			
150	0.02069	0.02069	-			
200	0.02323	0.02323	0.05923			
250	0.02576	0.02576	-			
300	0.02865	0.02865	0.06163			
350	0.03173	0.03173	-			
400	0.03498	0.03498	0.06436			
450	0.03848	0.03848	-			
500	0.04220	0.04220	0.06706			
550	0.04628	0.04628	-			
600	0.05061	0.05061	0.06998			
650	0.05525	0.05525	-			
675	0.05768	0.05768	-			
700	0.06011	0.06011	0.07344			
725	0.06266	0.06266	-			
750	0.06545	0.06545	-			
800	-	-	0.07689			
900	-	-	0.08033			
1000	-	-	0.08143			

Table B.4. Helium

Temperature (°F)	Thermal Conductivity (Btu/hr-in-°F)	Density (lbm/in^3)	Specific Heat (Btu/lbm-°F)	Description
0	0.00650	0.6900 E-5	1.240	Used for gaps within package assembly
200	0.00808	0.4810 E-5		
400	0.00958	0.3690 E-5		
600	0.01075	0.2990 E-5		
800	0.01150	0.2520 E-5		
1400	0.01370	0.1710 E-5		

Table B.5. Air

Temperature (°F)	Thermal Conductivity (Btu/hr-in-°F)	Density (lbm/in^3)	Specific Heat (Btu/lbm-°F)	Description
0	0.001092	0.4994 E-4	0.2396	Used for trunnion air pockets, outer closure assembly gap, and the impact limiter to outer shell gap
32	0.001159	0.5039 E-4	0.2398	
100	0.001297	0.4103 E-4	0.2400	
200	0.001483	0.3484 E-4	0.2411	
300	0.001661	0.3021 E-4	0.2427	
400	0.001833	0.2674 E-4	0.2448	
500	0.002001	0.2390 E-4	0.2473	
600	0.002163	0.2164 E-4	0.2504	
800	0.002469	0.1823 E-4	0.2567	
1000	0.002769	0.1574 E-4	0.2631	
1200	0.003060	0.1383 E-4	0.2688	
1400	0.003331	0.1233 E-4	0.2740	

Table B.6. ASME SA-479 S21800, Nitonic 60

Temperature (°F)	Thermal Conductivity (Btu/hr-in-°F)	Density (lbm/in^3)	Specific Heat (Btu/lbm-°F)	Description
-	1.00	0.2750	0.1150	Used for trunnion sleeves

Table B.7. ASTM A-276 GR 304

Temperature (°F)	Thermal Conductivity (Btu/hr-in-°F)	Density (lbm/in^3)	Specific Heat (Btu/lbm-°F)	Description
-	0.8333	0.2836	0.1100	Used for stiffener ring

Table B.8. Aluminum Honeycomb 220 psi

Temperature (°F)	Thermal Conductivity (Btu/hr-in-°F)	Density (lbm/in^3)	Specific Heat (Btu/lbm-°F)	Description
0	0.22856	0.0024	0.210	Used for honeycomb Section 2 of impact limiters
100	0.28238			
200	0.34957			
300	0.40339			

Table B.9. Aluminum Honeycomb 725 psi

Temperature (°F)	Thermal Conductivity (Btu/hr-in-°F)	Density (lbm/in^3)	Specific Heat (Btu/lbm-°F)	Description
0	0.59172	0.0046	0.210	Used for honeycomb Section 3 of impact limiters
100	0.73086			
200	0.90488			
300	1.04410			

Table B.10. Aluminum Honeycomb 1400 psi

Temperature (°F)	Thermal Conductivity (Btu/hr-in-°F)	Density (lbm/in^3)	Specific Heat (Btu/lbm-°F)	Description
0	1.0322	0.0061	0.210	Used for honeycomb Section 1 of impact limiters
100	1.2751			
200	1.5787			
300	1.8216			

Table B.11. Stainless Steel 304L

Temperature (°F)	Thermal Conductivity (Btu/hr-in-°F)	Density (lbm/in^3)	Specific Heat (Btu/lbm-°F)	Description
-	0.8333	0.2836	0.110	Used for fuel spacer tube

Table B.12. ASTM A-412 Grade XM-11

Temperature (°F)	Thermal Conductivity (Btu/hr-in-°F)	Density (lbm/in^3)	Specific Heat (Btu/lbm-°F)	Description
-99.4	0.52500	0.2830	0.1150	Used for impact limiter shell
203.0	0.65777			
401.0	0.77777			
599.0	0.87500			
797.0	0.97223			
1200.0	1.18750			
1600.0	1.39580			

Table B.13. SB-637 Alloy N07718

Temperature (°F)	Thermal Conductivity (Btu/hr-in-°F)	Density (lbm/in^3)	Specific Heat (Btu/lbm-°F)	Description
-	0.5493	0.2960	0.1040	Used for assembly bolts

Table B.14. Emissivity Values for Thermal radiation Heat Transfer

Component	Material	Emissivity Before Fire	Emissivity During/After Fire	Solar Absorptivity
Inner Steel Surfaces	stainless steel	0.35	0.35	-
Outer Cask Skin	stainless steel	0.15	0.9	0.4
Outer Impact Limiter Shell	steel	0.85	0.9	0.6
Depleted Uranium	depleted uranium	0.5	0.5	-
Fuel Assembly	-	0.7	0.7	-
Boron Carbide Pellets	boron carbide	0.8	0.8	-
Surface Exposed to Fire	-	0.9	0.9	-
Ambient Environment	-	0.9	0.9	-
Inside of Cask Skin	stainless steel	0.9	0.9	-
Outer Surface of Package Body	stainless steel	0.9	0.9	-

Depleted Uranium – See Figure A.2 in Appendix A

Neutron Shield – Effective Conductivity Calculations:

An empirical relationship for effective conductivity incorporating the effects of both conduction and convection was used to determine heat exchange through the liquid neutron shield. The effective conductivity of the fluid within the tank is based on heat transfer between two concentric cylinders. Sensitivity studies were performed on this correlation to verify that it is applicable to the neutron shield tank geometry, in which the inner surface of the tank has a square cross-section with rounded corners, rather than a circular cross-section. This correlation produces reasonable values of k_{eff}, and the transient conditions are generally within its applicable range. The correlation relates the Nusselt number to the ratio of the effective conductivity over the actual conductivity, and is expressed as

$$\frac{k_{eff}}{k_c} = Nu = 0.386\left(\frac{\mathrm{Pr}}{0.861+\mathrm{Pr}}\right)^{0.25} Ra_c^{0.25} \qquad \text{(B-1)}$$

where

k_{eff} = effective thermal conductivity of material in node
k_c = thermal conductivity of motionless fluid in node
Nu = Nusselt number
Pr = Prandtl number
Ra_c = modified Rayleigh number

The modified Rayleigh number is defined as:

$$Ra_c = \frac{\left[\ln\left(D_o/D_i\right)\right]^4}{L^3\left[D_i^{-0.6} + D_o^{-0.6}\right]^5} Ra \qquad \text{(B-2)}$$

where

D_o = annulus outer diameter
D_i = annulus inner diameter
Ra = Rayleigh number
L = $\left(D_o - D_i\right)/2$

The Rayleigh number is based on the temperature difference across the annular gap and is expressed as:

$$Ra = \frac{g\beta\left(T_i - T_o\right)L^3}{\nu\alpha} \qquad \text{(B-3)}$$

where

g = acceleration of gravity
T_i = inner surface temperature
T_o = outer surface temperature
β = thermal expansion coefficient
α = thermal diffusivity of fluid
ν = kinematic viscosity of fluid

Using the correlations listed above, a macro was written to calculate the effective conductivity after each solution step within the transient model. For conditions below 276°F, the properties of 56% propylene glycol and water were used to calculate the effective conductivity. Once the maximum temperature within the tank exceeded 276°F, the properties of air were used to determine the thermal conductivity.

Verification of Effective Conductivity Model for GA-4 Neutron Shield Configuration

The effective conductivity model described above is based on experimental data for natural convection mixing of fluid between horizontal concentric cylinders. The neutron shield tank of the GA-4 package consists of an inner surface formed by the package body, which is a square with rounded corners, and an outer cylindrical shell. To verify that this empirical model could be applied to the GA-4 package neutron shield geometry, the correlation predictions were compared to results from a computational fluid dynamics model.

Calculations were performed with Star-CD[1], for a 2-D "slice" model at the midplane of the package, using two basic configurations to model the GA-4 neutron shield tank. In one model, the neutron shield fluid region is represented as a solid material with thermal conductivity

[1] **STAR-CD, *Version 4.14 Methodology***, Computational Dynamics Ltd. 2010.

determined using the relationship for the effective thermal conductivity, as defined in Eq. (B-1) above. In the other model, the neutron shield fluid region is represented as a liquid, with the fluid properties of the propylene-glycol/water mixture reported in the GA-4 SAR [11].

The results of this evaluation are summarized in Table B.15, with comparisons of the maximum and minimum predicted temperatures obtained with the Star-CD model for all cases considered. All calculations in this evaluation were performed at NCT. The maximum temperature is the peak temperature in the fuel region[1], and the minimum temperature is the minimum temperature on the package outer shell surface. As shown by the results in Table B.15, a computation mesh that was appropriate for the neutron shield represented as a solid was not sufficient resolution for the CFD model. The number of computational elements required was approximately two orders of magnitude larger.

Star-CD results for the case with the neutron shield represented as a solid material and for the case with the neutron shield represented as a fluid (with an appropriately refined mesh) are shown graphically with color thermographs in Figure B.1. Overall, this evaluation has shown that the effective conductivity model predicts temperatures that are results are consistent with the CFD model results. There is also some indication that the effective conductivity model may yield results that are slightly conservative.

Table B.1. Summary of STAR-CD Model Results

Case Description	Peak Fuel Region Temperature, °F (°C)	Minimum Outer Shell Temperature, °F (°C)	Number of Computational Elements	Number of Fluid Elements
Effective conductivity model	302 (150)	194 (90)	3,664	0
Baseline CFD model	312 (156)	194 (90)	3,664	1232
CFD model (2x2 refine, all)	307 (153)	194 (90)	14,596	4928
CFD model (4x4 refine, all)	303 (151)	192 (89)	58,384	19,712
CFD model (5x5 refine) 2x solids	301 (149)	189 (87)	46,936	30,800
CFD model (8x8 refine, all)	300 (149)	189 (87)	233,536	78,848

[1] Note that the 2-D “slice” model used in this study oversimplifies features captured in the fully 3-D ANSYS model used for the MacArthur Maze fire calculations. As a result, temperatures predicted for NCT with the fully 3-D ANSYS model differ slightly from the temperatures reported in this study with Star-CD. With the ANSYS model, the peak fuel region temperature is 306°F (152°C) and the minimum outer shell temperature is 188°F (87°C).

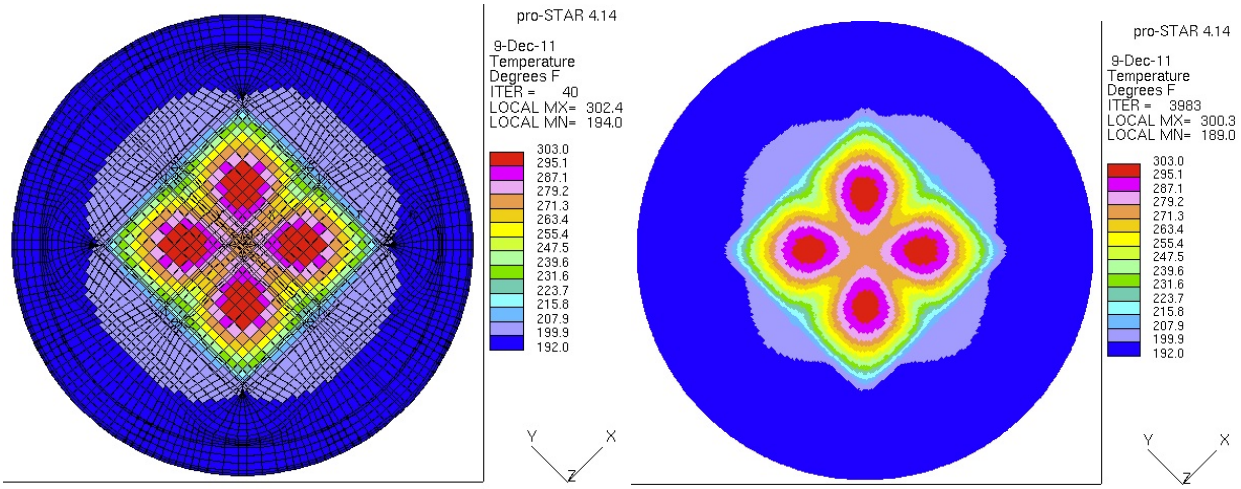

(a) **(b)**

Figure B.1. Mid-plane Temperature Distributions Predicted with Star-CD Model of GA-4 Package at NCT: (a) solid material neutron shield with effective conductivity model, and (b) liquid neutron shield with (8x8) refined mesh

NRC FORM 335 (12-2010) NRCMD 3 7

U.S. NUCLEAR REGULATORY COMMISSION

BIBLIOGRAPHIC DATA SHEET

(See instructions on the reverse)

1 REPORT NUMBER (Assigned by NRC, Add Vol., Supp., Rev., and Addendum Numbers, If any)

NUREG/CR-7206
Draft

2 TITLE AND SUBTITLE

Spent Fuel Transportation Package Response to the MacArthur Maze Fire Scenario

3 DATE REPORT PUBLISHED

MONTH	YEAR
December	2015

4 FIN OR GRANT NUMBER

5 AUTHOR(S)

H.E. Adkins, Jr., J.M. Cuta, N.A. Klymyshyn. S.R. Suffield, C.S. Bajwa, K.B. McGrattan, C.E. Beyer, A. Sotomayor-Rivera

6 TYPE OF REPORT

Technical

7 PERIOD COVERED (Inclusive Dates)

8 PERFORMING ORGANIZATION - NAME AND ADDRESS (If NRC, provide Division, Office or Region, U. S Nuclear Regulatory Commission, and mailing address, if contractor, provide name and mailing address.)

Pacific Northwest National Laboratory
P.O. Box 999
Richland, WA 99352

9 SPONSORING ORGANIZATION - NAME AND ADDRESS (If NRC, type "Same as above", if contractor, provide NRC Division, Office or Region, U S Nuclear Regulatory Commission, and mailing address.)

Division of Spent Fuel Management
Office of Nuclear Material Safety and Safeguards
U.S. Nuclear Regulatory Commission
Washington, D.C. 20555-0001

10 SUPPLEMENTARY NOTES

J. Piotter, NRC Project Manager

11 ABSTRACT (200 words or less)

The U.S. Nuclear Regulatory Commission has undertaken the examination of specific transportation accidents (of non-radioactive materials) to determine potential consequences on a spent fuel transportation package. The MacArthur Maze accident was selected as a third study in the evaluation series.

Analyses undertaken included FDS fire modeling, physical examination of material samples from the accident, ANSYS and COBRA-SFS code thermal modeling of a GA-4 package, ANSYS and LS-DYNA structural and thermal-structural modeling of the roadway and package, and fuel performance modeling using the FRAPTRAN-1.4, FRAPCON-3.4, and DATING codes. These analyses suggest that there is the potential for rods in the package to rupture, indicating fission gases and fuel particulate would be released to the package cavity. Loss of the package seals due to exceeding seal material thermal limits means there is the potential for radioactive material to escape from the package; however, because lid closure bolts maintain a positive clamping force it is not physically possible for very much of this material to escape. Using conservative and bounding modeling assumptions, the total possible release from the package, as a mixture of fission gases, fuel particulate, and CRUD particles, is estimated as approximately one-fourth of the mixture A2 quantity. Since the regulatory limit is specified as an A2 quantity per week for accident conditions, the estimated release from the hypothetical scenario is below the prescribed limit for safety.

12 KEY WORDS/DESCRIPTORS (List words or phrases that will assist researchers in locating the report.)

MacArthur Maze
Spent Nuclear Fuel
Accident
Transportation Package
Fire

13 AVAILABILITY STATEMENT

unlimited

14 SECURITY CLASSIFICATION

(This Page) unclassified

(This Report) unclassified

15 NUMBER OF PAGES

16 PRICE

NRC FORM 335 (12-2010)

Federal Recycling Program

UNITED STATES
NUCLEAR REGULATORY COMMISSION
WASHINGTON, DC 20555-0001

OFFICIAL BUSINESS

Spent Fuel Transportation Package Response to the MacArthur Maze Fire Scenario